Evaluation of Slope Bottom Tuned Liquid Dampers in Reduction of Earthquake Vibrations of Structure

A thesis submitted for the degree of

Doctor of Philosophy

by

G. R. Patil

Department of Civil Engineering
Indian Institute of Technology Guwahati
Guwahati – 781 039, India

January 2020

DECLARATION

I hereby certify that the work embodied in this thesis entitled '***Evaluation of Slope Bottom Tuned Liquid Dampers in Reduction of Earthquake Vibrations of Structure'*** in partial fulfilment of the requirements for the award of the Degree of **Doctor of Philosophy** and submitted in the Department of Civil Engineering, Indian Institute of Technology Guwahati, India, is an authentic record of my own work carried out during a period from Dec, 2010 to Jan, 2020 under the supervision of **Prof. Konjengbam Darunkumar Singh,** Professor, Department of Civil Engineering, Indian Institute of Technology Guwahati, India.

The matter presented in the thesis has not been submitted by me for the award of any other degree of this or any other institute.

Date: **(Mr. G. R. Patil)**

Place: IIT Guwahati Reg. No.: 10610421

CERTIFICATE

This is to certify that the thesis entitled '***Evaluation of Slope Bottom Tuned Liquid Dampers in Reduction of Earthquake Vibrations of Structure'*** being submitted by Mr. Gundopant Rajaram Patil to the Indian Institute of Technology Guwahati, India, for the award of degree of ***Doctor of Philosophy*** is a record of genuine research work carried out by him under my supervision.

The thesis work, in my opinion is worthy of considering for the award of degree of ***Doctor of Philosophy*** in accordance with the regulation of the Institute.

(Konjengbam Darunkumar Singh)

Professor

Department of Civil Engineering

Indian Institute of Technology Guwahati

Date:

Place: IIT Guwahati

To the Lord

To my family members:

Rajaram G Patil
Anandi R Patil
Dattatray D Patade
Vijaya D Patade
Rajni G Patil
Nivedita Patil

ABSTRACT

Earthquakes are one of the nature's main hazards to life on the earth and have destroyed cities and villages. They are one of man's most feared natural phenomena, producing almost instantaneous destruction of buildings and other constructed facilities. Hence it is important to minimize or mitigate such effects of earthquakes on building structures, by adopting appropriate designs and control measures. Structural control devices can enhance the integrity of structures without increasing the dimensions of structural members. These are found to be attractive alternatives for retrofitting or for upgrading performance of civil engineering structures. Because of these reasons, structural control is receiving increasing attention in civil engineering applications. Tuned Liquid Dampers (TLDs) are one such passive dampers, wherein dissipation of the structural vibrational energy is achieved by tuning the sloshing frequency of the liquid with that of the structure. TLD has several merits over other damping systems e.g. low installation and maintenance cost, less mechanical problems, no fail-safe device required, activated even at low excitation level, bidirectional effectiveness and easy adjustment of damper parameters even after installation (e.g. Xin 2006). However, TLD with flat bottom, exhibits a beating (e.g. Fujino *et. al*., 1992) phenomenon, wherein dynamic energy is transferred back to structure after cessation of external excitation. To mitigate the phenomenon of beating, a slope at the bottom of TLD has been introduced and investigated by limited researchers (e.g. Gardarsson *et. al.*, 2001, Reed and Olson 2001, Xin 2006 etc.) which acts as energy dissipator due to amplification of wave height.

Thus, in this study, an attempt has been made to systematically investigate the performance of slope bottom TLD for controlling the dynamic response of reinforced concrete (RC) frame structure, subjected to both harmonic and earthquake input base excitations; using finite element analysis. Slope bottom TLD analysis have been carried out based on the equivalent flat bottom approaches of Gardarsson (2001) and Xin (2006). Various types slope such as central (or single triangular) slope, dual triangular slopes, end slope, combination of central slope

and end slope and combination of dual triangular slopes and end slope; with a wide range of slope angles at bottom of TLD, have been considered for the study.

Dynamic analysis of a 10 story RC frame structure with both flat and slope bottom rectangular TLDs, subjected to harmonic and five earthquake time histories (*viz*., El Centro, 1940, Loma Prieta, 1989, Northridge, 1994, San Fernando, 1971, and Indian Standard (IS), 1893 (Kumar 2004) compatible time history) have been assessed, and key results have been presented in the form of tuning ratio, mass reduction and displacement response reduction.

For the case of TLDs with central slope, the analyses have been performed for slope angle ranging from 5-14º. The slope bottom TLDs have been studied by converting into equivalent flat bottom tanks, using 'wetting length' concept of Xin (2006). Based on the study, it has been observed that tuning ratio of TLD decreases with increase of central slope at the bottom of TLD and the variation of tuning ratio with slope, is observed to be nonlinear. With the increase of central slope, tuning ratio is found to change from over-tuned to a value close to 1. Reduction in displacement of the structure increased with increase in central slope angle. Maximum reduction in displacement of the structure, of ~53.73 % and ~26.00 % have been observed at 14º central slope TLD for input motions of El Centro earthquake (1940) and IS time histories respectively. For other inputs, maximum displacement reductions are with in range of El Centro earthquake and IS time history. The variation of liquid mass reduction with slope angle has been observed to be linear and liquid mass reduction for central slope of 14º is observed to be ~ 47.93 %. With the application of dual triangular slope in the range 5-25º, it has been observed that TLD is over-tuned and under tuned, showing tuning ratio range of 1.04-0.97. Displacement reduction has been observed to increase with dual triangular slopes and at an optimum angle of 20º, maximum reductions in displacement of about 59.27 % and 29.00 % have been observed for the input motions of El Centro earthquake and IS time history, respectively. Liquid mass reduction has been observed to increase

linearly with dual triangular slope with a reduction of about 35.01 % at an optimum slope (i.e. 20º).

The study has been extended further, by considering end slope bottom TLDs. The performance has been investigated considering end slope angle in the range 15–50º, considering Gardarsson's (2001) and Xin's (2006) approaches of equivalent flat bottom approximations. Based on the study, it has been seen that results of dynamic analysis by the two approaches have been seen to be near similar. For example, for the harmonic input, an optimum slope angle of 30.5º with displacement reductions of ~37.72 % and an optimum angle of slope ~29.5º with displacement reduction of 35.65 % have been observed by Gardarsson's and Xin's approaches respectively. However, for the case of earthquake excitations, Gardarsson's approach gave maximum reduction in displacement for slope of around ~30º, whereas it is about 30-35º following Xin's approach. Liquid mass reduction at the optimum slope angle of 30.5º and 29.5º is observed to be ~22 % and ~23 % respectively.

For the combined end slope and central slope, it has been seen that the tuning ratio decreases with increase in central slope angle, for a constant end slope. Liquid mass is found to decrease with increase in central slope. Rate of reduction in liquid mass has been seen to increase with increase of end slope. Maximum liquid mass reduction of around 49.47 % has been observed for the TLD with end slope of 30º and central slope of 25º. In case of TLD with combined end and dual triangular slopes, it has been seen that tuning ratio of TLD decreases with the amount of dual triangular slopes, for the constant end slope. It has also been observed that for the only case of combination of 25º end slope and 5º dual triangular slopes, the performance of TLD is marginally improved. The liquid mass has been seen to decrease with increase in dual triangular slope. Maximum liquid mass reduction (~39.38%) has been observed, due to application of 25º dual triangular slopes and 20º end slope.

ACKNOWLEDGEMENT

The acknowledgements are an account of the indebtedness towards those who have been a guiding light and source of inspiration during the completion of this research work.

I express my deep sense of gratitude to my supervisor *Prof. Konjengbam Darunkumar Singh* for his consistent valuable guidance, enthusiastic support and cooperation throughout this research work. He has been a constant source of motivation. I shall forever remain indebted to him for his untiring efforts and help, extended to me for resolving difficulties beyond academics. The experience of working with him would be remembered throughout my life.

I am thankful to Prof. S Talukdar, Dr. Arunasis Chakraborty and Dr. Kaustubh Dasgupta, my doctoral committee members, who have contributed in this work with valuable remarks and suggestions from time to time towards successful completion.

I would like to thank the Department of Civil Engineering for the provision of necessary facilities during this research work. Cooperation extended by the head of the Department and Office Staff deserve special thanks. I would like to express my sincere thanks to all faculty members who have helped me directly or indirectly during this research work. I also would like to thank the authorities of Hostel Affairs Board and particularly to Shri. Narayan Kalita, for having cooperated during the stay.

I wish to express my sincere gratitude to Dr. Nanda, for sharing the basic fluid structure interaction code, and for the helpful discussions I had with him.

I would like to express my sincere thanks for the privilege of having associated with friends, Sachidananda, Gishan, Narendra, Sonu, Kumar, Suman, Jyothirmoy, Mishraji, Ricky, Vipej and others.

The episode of acknowledgement will remain incomplete without the care, cooperation and support of my parents, brothers, sisters, uncles, aunts, relatives and all in-laws who are inseparable part of my life. I sincerely woe my gratitude to all of them. Special thanks to my wife Rajni and daughter Nivedita for their patience. Thanks to brother Sanjay, Shravan and sister Girija for moral support.

I would express my deepest sense of gratitude to all my well-wishers. Thanks, are also due to my friends, Prof. Awari, Prof. Atal and Colleagues for encouraging me towards completing this work.

Last but not the least, I express thanks to God Almighty for the blessings and for giving me the strength and wisdom for completion of this work.

G R Patil

CONTENTS

LIST OF FIGURES

LIST OF TABLES

NOTATIONS

B	Width of tank / TLD
B_b	Boundary condition at bottom of TLD
B_f	Boundary conditions on liquid free surface area
B_s	Boundary conditions at liquid interface
B'	Modified width of equivalent flat bottom TLD
C	Damping matric of structure
$\hat{C}$	Modal damping matrix
D	Strain displacement matrix
D_1	Absolute difference between undamped and damped displacement at a time
d_1	Undamped displacement of structure at a time
D_2	Absolute undamped displacement
d_2	Damped displacement of structure with application of TLD at a time
DR	Reduction in displacement of structure in percent
DS_1	Sum of all absolute differences between undamped displacements and damped displacements
DS_2	Sum of all absolute undamped displacements
$\ddot{d}n$	Acceleration of structure
F_{ef}	Element load vector
f_b	Sloshing frequency in box shaped TLD
F_{el}	External load vector
F_f	Liquid load vector
F_{TLD}	Resisting force to structure from TLD
F_w	Liquid sloshing frequency

H_T	Liquid sloshing surface level at edge
J_s	Jacobian matrix
K	Stiffness matric of structure
k	Element stiffness matrix of structure
K_e	Stiffness matrix in global coordinate system
K_f	Stiffness matrix of liquid domain
K_s	Element stiffness matrix of liquid domain
$\widehat{K}$	Modal stiffness matrix
L	Length of TLD
l_e	Element length
l_x, m_x, l_y, m_y	Direction cosines
L'	Total wetting length of TLD / Modified length of TLD
M	Mass matrix of structure
m	Element mass matrix of structure
M_e	Mass matrix in global coordinate system
M_{ef}	Element mass matrix of liquid
M_f	Liquid free surface mass matrix
$\widehat{M}$	Modal mass matrix
n	Outwardly drawn normal to liquid surface
N_j	Shape functions
NK	Number of liquid elements
P	Dynamic liquid pressure
P_j	Time dependent nodal pressure
$P_{(t)}$	Modal force vector
$\ddot{P}$	Acceleration vector of liquid
s	Shape parameter
T	Transformation matrix
T_s	Derivatives of shape function

$V_{(t)}$	Velocity at time t
X	Displacement vector of structure
$\ddot{X}$	Acceleration vector of structure
$\ddot{x}$	Harmonic acceleration
$\ddot{Xg}$	Ground acceleration vector
y	Wetting length of TLD with central slope on one side of centre of TLD
y_1	Wetting length of TLD on one side of dual triangular slope
y'	Wetting length of TLD with end slope at one end
α	End slope of TLD
θ	Central slope at bottom of TLD
θ_1	Dual triangular slope at bottom of TLD
ρ	Density of material
ρ_f	Density of fluid
η	Wave height in TLD
∇	Operator

CHAPTER 1

INTRODUCTION

1.1. BACKGROUND

Earthquakes are one of the nature's main hazards to life on the earth and have destroyed cities and villages. They are one of man's most feared natural phenomena, producing almost instantaneous destruction of buildings and other constructed facilities. Major earthquakes, greater than magnitude 7, happen more than once per month (Incorporated Research Institutions for Seismology (IRIS, 2019)). When such earthquakes hit highly populated areas like cities and towns, damages to structures and life can be substantial. Hence it is important to minimize or mitigate such effects of earthquakes on building structures, by adopting appropriate designs and control measures. With the advancement in high strength and lightweight construction materials, it has become possible to construct flexible tall (or slender) structures. However, such structures can lead to reduction in damping, thereby enhancing the structural vibrational response. Structural control devices can enhance the integrity of structures without increasing the dimensions of structural members. These are found to be attractive alternatives for retrofitting or for upgrading performance of civil engineering structures. Because of these reasons, structural control is receiving increasing attention in civil engineering applications. To control structural vibration, several vibration control devices have been suggested in the literature *viz.,* a) passive (e.g. Buckle 2000) e.g. base isolation, viscoelastic damper, friction pendulum, tuned mass damper (TMD) and tuned liquid damper (TLD), b) active (e.g. Soong 2000) e.g. active TMD, active brace system and active tendon system, c) hybrid (e.g. Soong 2000) e.g. hybrid mass damper system, and d) semi-active (e.g. Soong 2000) e.g. electrorheological damper, magnetorheological damper and friction control devices etc. Passive control requires no external energy for operation, and control mechanism moves with the main structure i.e. control forces are generated due to movement of control

device. Active control device uses external energy to mitigate the dynamic response of structure. Hybrid control device is generally the combination of passive and active control devices and requires less external energy as compared to active control. Semi-active devices provide adaptability of active device without large external power requirements (Xin 2006).

Compared to other (active, semi-active and hybrid) control systems, passive systems are simple in design and implementation and are reported to be more reliable in performance (e.g. Xin (2006)). Passive controls are widely used to control the response of structure because of their simplicity, reliability, stability and low-cost (Tait 2004). However passive device like base isolation can only be used for structures / buildings with time period in the neighborhood of 2 sec. and TMDs are effective within narrow frequency band, close to structure's natural frequency Xin (2006). TLD (wherein dissipation of the structural vibrational energy is achieved by tuning) on the other hand, has several merits over other damping systems e.g. low installation and maintenance cost, less mechanical problems, no fail-safe device required, activated even at low excitation level, bidirectional effectiveness and easy adjustment of damper parameters even after installation (Xin 2006). Hence, TLDs are a competitive option for the control of vibrations in civil engineering structures such as buildings.

1.2.. CONCEPT OF TUNED LIQUID DAMPERS

Tuned Liquid Dampers (TLDs) are passive mechanical dampers that rely on liquid motion in rigid containers, for changing the dynamic characteristics of structure and dissipation of vibration energy. Tuned Liquid Dampers (TLD) system represents an efficient and simple technique to increase the damping of a structure and relies on the sloshing wave developed at the free surface of the liquid to dissipate a portion of the dynamic energy. When TLDs are excited, the liquid inside sloshes and energy

is dissipated from the viscous action and wave breaking. TLD's origin could be traced back to 1950s (Winden 2009) where dampers utilizing liquid were used for stabilizing marine vessels against rocking and rolling motions. In 1960s (Miles 1963) this concept was used to control wobbling motion of satellite in space. The idea of applying TLD to reduce structural vibration due to dynamic loading in civil engineering structures began by Bauer (1984) proposing rectangular tank completely filled by two immiscible liquids. In essence, TLDs are tanks partially filled (i.e. shallow) usually with water, attached to the structures. The structures are generally high-rise buildings which are subjected to wind and earthquake vibrations. Figure 1.1 shows a schematic illustration of a TLD installation in One Rincon Hill, San Francisco. By installing TLDs at the top of building, the vibrations of building can be controlled. Due to vibration of structure the water in a tank sloshes in opposite direction as that of vibration of structure, which counteracts the motion of structure based on Fluid-Structure interaction phenomenon. The efficiency of damper (tank with water) depends on:

i) depth ratio (i.e. depth of liquid/length of tank)
ii) mass ratio (i.e. damper mass/structure mass)
iii) frequency ratio (i.e. frequency of sloshing of liquid/structure's frequency).

The liquid depth in tank is adjusted such that frequency of damper is close to the frequency of structure. The tanks are generally rectangular in plan but other shapes can also be employed. Many researchers have investigated the TLD, experimentally and numerically with flat bottom (Reed *et. al.*, 1997, Ikeda 2003, Sheng and Hua 2000 etc.), flat bottom with screens/baffles (Biswal et.al., 2003, Faltinsen *et.al.*, 2011) and adding surface contaminants/floats in the liquid (Xin 2006). Some examples of structure with TLDs are Yokohama Marine Tower (Tamura *et. al.*, 1995), Shin Yokohama Prince Hotel (Tamura *et. al.*, 1995), Tokyo International

Airport Tower (Tamura *et. al*., 1995), Nagasaki Airport Tower (Tamura *et. al*., 1995), and are shown in Figures 1.2-1.5.

1.3.OBJECTIVES OF STUDY

Slopped bottom tuned liquid damper is a tank with the slope at the bottom, partially filled with water. During forced excitation, water / liquid wave motion in TLD is established quickly in one or two sloshing periods. However, established wave motion does not stop immediately after the end of excitation, which is called 'beating' (Chaiseri *et. al.*, 1989) phenomenon. This is because a fraction of energy absorbed by TLD is being transferred back to the structure (Fujino *et. al.*, 1988). In order to mitigate beating, many alternates have been tried to stop wave motion after cessation of excitation. These attempts are like: a) using liquid, that is more viscous than water, b) improvement of roughness to bottom of tank, c) placing solid floats in water and d) placing screens in water etc. (Faltinsen *et. al.*, 2011) An idea of using slope bottom tank has its origin in sloping beach (Gardarsson *et. al.*, 2001), which is an effective energy dissipater due to wave breaking. Further, as wave run up, height amplification has been found to be greater for sloping beach than vertical wall, with wave motion in sloped bottom TLD becomes more nonlinear resulting in greater horizontal force with lesser liquid mass (as compared to flat TLDs). As per literature review, very few studies have been reported on sloped bottom TLD. Therefore, detailed parametric study for determining effectiveness of sloped bottom TLD has been proposed as under:

- To evaluate dynamic response of (a reinforced concrete frame) structure subjected to base motion, with flat bottom TLD and to investigate influence of tuning ratio and depth ratio of TLD, on the response of structure. To extend this study to evaluate performance central slope and dual triangular slope TLDs.

- To evaluate the effect of end slope TLD on the dynamic response of structure, subjected to base motion.

- To extend the previous study to investigate the effect of slope angle variation on the end-slope TLD with central-slope and dual triangular slopes, on the dynamic response of structure, when subjected with base motion.

Above studies are proposed with input motions as harmonic excitation and accelerograms of few major earthquakes e. g. EL Centro 1940, North Ridge 1994, San Fernando 1971, Loma Prieta 1989 and IS 1893 compatible time history.

1.4. REPORT ORGANISATION

Chapter 1 chapter provides a brief introduction about development of control methods of dynamic response of structure. The classification of these control methods is discussed in brief. Examples of some prominent structures with application of TLDs are mentioned in this chapter. Based on detailed literature review presented in chapter 2, the objectives of present study are mentioned.

Chapter 2 provides a detailed literature review on related work, carried out by researchers. Most of the studies are related to the evaluation of performance of flat bottom TLD. The gap area in the study has been identified from the literature review. It is proposed to carry a detailed study on evaluation of performance of TLD with bottom slope for mitigating dynamic response of structure.

Chapter 3 presents finite element (FE) based dynamic analysis of 2D reinforced concrete (RC) frame structure with flat TLD, TLD with central slope and TLD with dual triangular slopes at bottom, considering both harmonic and various earthquake

excitations (e.g. El Centro (1940), Loma Prieta (1989), Northridge (1994), San Fernando (1971), and design spectrum compatible Indian Standard (IS) 1893 compatible time history). FE analysis has been performed based on basic code developed by Nanda (2010) but modified suitably for the current work. For all the analyses, a two bay, ten story RC frame building with TLD, attached at roof level has been considered for dynamic analysis.

Chapter 4 presents the investigation on the performance of end slope TLD, considering slope angles from 15º - 50º. For the end slope case, both Xin's (2006) approach and Gardarsson's (2001) approach (applicable only for modelling end slope of TLD where frequency of the tank is determined form the geometric parameters) have been compared. Analysis is performed for input motion of harmonic loading and earthquake excitations mentioned above. The range of slope angles for which performance of slope bottom of TLD over flat bottom TLD is seen to improve has been investigated. The optimum slope angle of TLD for reduction of displacement of structure has been determined based on harmonic input.

Chapter 5 presents, evaluation of performances of TLD with i) end slope and central slope and ii) end slope and dual triangular slopes at bottom following Xin's (2006) approach. The results of the analyses have been presented considering end slopes, and central slopes, in the range 20º to 50º, and 2.5º to 25º, respectively.

Results are summarized and some important conclusions are drawn from the present study which are mentioned in **Chapter 6**. Suggestions for the future work on tuned liquid dampers are also mentioned in this chapter.

Appendices are provided for the things, supportive for the present study. Mathematical modelling of fluid structure interaction problem is given in **Appendix A**.

Appendix B represents an extract of free vibration analysis of 2D structural frame with STADD Pro software. Sample calculations for equivalent flat bottom TLD are also shown in this appendix.

Appendix C presents typical time history plots of undamped response structure and damped response of structure with application of TLD.

Appendix D presents results of dynamic analysis of structure with TLD having end slope at bottom, subjected to harmonic excitation.

Appendix E presents the formulation of liquid motion equations

Appendix F presents the list of abbreviations

Figure 1.1. Application of TLD for mitigating dynamic response; One Rincon Hill South Tower, San Francisco. https://media.techeblog.com/images/Tuned massdamper.jpg

Figure 1.2. Application of TLD for mitigating dynamic response; Yokohama marine tower: Assembly of 39 multi-layered cylindrical vessels with height 0.5m and diameter 0.49m. Tamura Y et. al. (1995). https://media.Timeout.com/images/103583958/630/472/image.jpg

Figure 1.3. Application of TLD for mitigating dynamic response; Shin Yokohama Prince Hotel: Assembly of 30 cylindrical multi-layered vessels with 2 m diameter and 2 m height. Tamura Y et. al. (1995) http://pix10.agoda.net/hotelImages/63293/1/a75fffec886f2c8489a59bc999d43fa1.jpg?s=1024x768

Figure 1.4. Application of TLD for mitigating dynamic response; Tokyo international airport tower. 1400 shallow cylindrical vessels of 60 cm diameter, 12.5 cm height have been installed (2001). Tamura Y et. al. (1995)https://upload.wikimedia.org/wikipedia/commons/8/8d/Tokyo_International_Airport_01.jpg

Figure 1.5. Application of TLD for mitigating dynamic response; Nagasaki airport tower: TLD consists of 25 cylindrical vesseles with height of 0.5 m and diameter 0.38 mm Tamura Y et. al. (1995)https://upload.wikimedia.org/wikipedia/Commons/3/38/Nagasaki_Airport_Omura_Nagasaki_pref_Jap

CHAPTER 2

LITERATURE REVIEW

2.1. INTRODUCTION

Tuned liquid dampers (TLDs) are being used for controlling the dynamic response (such as displacement, acceleration etc.) of structures subjected to high wind velocities and strong earthquake ground motions. Researchers (e.g. Fujino *et. al.*, 1988, Fujii *et. al.*, 1990, Banerji *et. al.*, 2000 etc.) have investigated the performance of TLD and have worked on measures to improve the effectiveness of TLD. Various shapes of TLDs *viz.*, flat bottom (Murudi and Banerji 2012) and slope bottom (Gardarsson *et. al.*, 2001) TLDs have been proposed to reduce the vibrational effects, especially the displacement response of structures. Studies have also been reported on TLDs with circular (Sun and Fujino 1992), rectangular etc. in plan. The use of baffles (Biswal et. al. 2003), screens (Faltinsen *et. al.*, 2011) floating roof (Ruiz *et. al.*, 2014) etc. in TLDs to dissipate vibrational energy have also been studied.

A detailed literature review of previous research work, reported on TLDs with respect to parameters influencing the performance of TLD such as shape of TLD, use of baffles and screens, application of slope at the bottom of TLD are presented in this chapter, are grouped into sub-headings: a) flat bottom TLDs and b) slope bottom TLDs.

2.2. FLAT BOTTOM TLD

Baur (1984) proposed initially, a damping device consisting of liquid container filled with two immiscible liquids. The motion at interface of two liquids has been found to dampen the structural response effectively, owing due to different viscosities of liquids at their interface. To assess the effectiveness of damper, a

rectangular container mounted at the end of cantilever beam has been considered. The sloshing frequency has been found to decrease with increasing density ratio (density of upper liquid/density of lower liquid). However, the sloshing frequency increased with increasing height ratio (height of upper liquid/height of lower liquid). It has been mentioned that the liquid vibration absorber with two immiscible liquids needs no servicing. Further, it has been also suggested that these dampers can be used for all kind of structures including satellite booms and space stations. A necessary liquid theory of linear sloshing has been derived for presenting mathematical model.

Fujino *et. al.,* (1988) experimentally studied circular TLD attached to single degree of freedom structural model with natural period of 2 sec. Effect of TLD on mitigation of free vibration of the structure has been evaluated. The damper effect was measured in terms of increase in the logarithmic rate of decrement of free oscillations of structure. It has been observed that breaking of surface waves, which was dependent on structural vibration amplitude, seems to be major mechanism of energy dissipation in the range of considered displacements. Based on the study, it has been seen that, for large damping effect at small amplitude of excitation, it is necessary to tune the fundamental sloshing period of liquid to the natural period of structure. Effect of enhanced bottom roughness has also been studied by attaching hemispheres (of height around 0.2 times depth of liquid in tank) at the bottom of TLD and found almost no improvement in TLD's effectiveness, as energy dissipation has been observed to occur primarily on the free surface of liquid.

Sun *et. al.,* (1989) simulated the liquid motion in rectangular tanks using a mathematical model based on nonlinear shallow water wave theory. Liquid damping was evaluated semi-analytically and was included in the formulation. The mechanical properties of TLD were also investigated by experiments conducted on shaking table. The model developed was able to predict the liquid free surface elevation and horizontal pressure due to liquid motion in the tank subjected to horizontal harmonic excitation. The model results were validated against shaking

table test results. It has been observed that for shallow (depth of liquid/length of tank < **0.15**) depth of liquid in TLD, the liquid motion developed strong nonlinearity behavior.

Modi *et.al.*, (1990) studied analytically, nonlinearities and viscous effects of sloshing liquid in torus shaped dampers and validity was assessed through experimental work. Experiments on steady state forced excitation with the damper undergoing a translational motion were designed for assessing the effect of TLD parameters (viz. h/d (depth of liquid/length of TLD) ratio, frequency of oscillation etc.) on energy dissipation. A horizontal frame, free to slide over the supporting bearing was used to provide smooth harmonic excitation. It has been seen that damping ratio and energy dissipation rate were largely dependent on liquid height. Energy dissipation rate has been found to have a tendency to be maximum for low values of *h/d* (liquid depth / diameter of TLD or side of square TLD) around 1/8 or **0.125**. It has been seen that TLDs / dampers with low liquid heights and large diameter ratios, operating at the liquid sloshing, led to increased damping at resonance. It has been suggested that the dampers can successfully control both vortex and galloping types of instabilities in earthquake and ocean engineering problems.

Fujii *et. al.*, (1990) installed circular tuned sloshing dampers on two actual tall towers *viz.* Nagasaki Airport and Yokohama Marine Towers. In case of Nagasaki airport tower, 25 cylindrical TLDs with 4.8 cm depth of water and 38 cm diameter (**h/d = 0.126**) were used. Sloshing in each TLD was almost tuned to natural frequency of the fundamental mode of tower. In case of Yokohama marine tower, 39 TLDs with liquid depth of 5 cm each and diameter of 49 cm were used **(h/d = 0.102**). It has been found that the reduced wind vibration levels after installation of dampers were in the acceptable limits from serviceability point of view. Also, the dynamic force frequency response function of tuned sloshing damper was determined experimentally. The frequency response function of damper has been found to be dependent on the amplitude of excitation.

Fujino. *et. al.,* (1992) developed a nonlinear model of 2D (two-dimensional) liquid motion in rectangular TLD, on the basis of shallow water wave theory. A single degree of freedom (SDOF) platform (with TLD) vibrating horizontally in a shear type motion, under the influence of harmonic base motion, was analyzed. Based on the analyses, it has been observed that at the region of resonance (tuning ratio = ~1.00), the vibration amplitude of the SDOF structure was found to reduce drastically (approximately from 3.00 cm to 0.60 cm) upon attachment of TLD. The experimental results were observed to be in good agreement with the numerical results

Chen *et. al.,* (1995) conducted a test on a pendulum like models with rectangular TLD (with water as liquid) in order to simulate the long period motion of a high-rise building. Both free and harmonic vibration tests have been carried out to assess the effectiveness of TLD to mitigate vibrations. It has been concluded that TLD system was more effective compared to optimal Tune Mass Damper (TMD) system.

Sun *et. al.,* (1995) investigated the performance of rectangular, circular and annular TLDs through experiments on shaking table, under sinusoidal base motion. Based on the study, it has been observed that the effective damping increases as the base excitation amplitude increases and exceeded 10 % when breaking of waves occurred. The wave motions in circular TLD were found to be more complicated than those in the rectangular TLD. For the TLD using an annular tank, wave motions were in general simpler than in the TLD using rectangular tank. No significant differences in energy dissipation (at least for engineering applications) could be seen, for the TLD shapes considered.

Reed *et al.* (1998) studied experimentally and numerically the behavior of rectangular TLD under large amplitude sinusoidal excitation. The normalized amplitude (amplitude / length of TLD) was varied from 0.011 to 0.11. The results suggest that the developed numerical model of random choice method was capable of capturing phenomenon of wave breaking for most of the frequency range of

interest. The results suggested that TLDs were robust in dissipating energy over a wide frequency range, particularly for large amplitude excitation. The maximum energy dissipation per cycle was observed experimentally at excitation frequency ratio (excitation frequency / sloshing frequency) of 1.

Chang and Gu (1999) studied experimentally, the control effects of rectangular TLDs installed on tall buildings subjected to vortex excitation. Wind tunnel experiments on scaled down building model attached with TLD of various sizes were performed. The liquid depths in TLDs were changed to determine an optimal frequency range of TLDs. Tests corresponding to different rectangular tank sizes of were performed for wind speeds ranging from 1.5 m/s to 4.2 m/s. Based on the study, rectangular TLD has been found to be quite effective in reducing the vortex excited vibrations of buildings, especially when its frequency was tuned within the optimal range. The top displacement root mean square (RMS) value has been seen to reduce to one-sixth of that of the original building i.e. without TLD.

Koneko and Ishikawa (1999) conducted an analytical study on TLD with submerged nets using a liquid model based on shallow water wave theory. Dissipation of energy due to liquid motion subjected to harmonic excitation was found out. It has been found that TLDs with submerged nets were more effective in reducing structural vibration as compared to TLDs without nets because of loss of energy of liquid while passing through net.

Yu *et. al.,* (1999) presented numerically modelled TLDs as equivalent tuned mass dampers with non-linear stiffness and damping (NSD). Models were observed to be able to capture the behavior of the TLD system adequately, under harmonic and seismic loading conditions. The stiffness and damping parameters of model derived from tests of rectangular tank subjected to large amplitude excitation, they were considered to be more representative of behavior of earthquake excitation.

Yung *et. al.,* (2000) presented a numerical simulation of three dimensional (3D) nonlinear sloshing phenomenon by boundary element method (BEM) for both

rectangular and cylindrical containers / TLDs. The analyses showed that both, rectangular and cylindrical TLDs produced excellent vibration reduction capabilities. The base shear force ratio of cylindrical tank / rectangular tank observed to be around 1.3.

Banerji *et. al.,* (2000) investigated numerically, single degree of freedom system (SDOF) structures with rectangular TLDs subjected to artificial and real ground motions. It has been observed that the TLD were more effective in mitigating structural response with increased ground motion excitation levels, because of more energy dissipation by wave breaking. A large water depth to tank length ratio was suggested based on shallow water theory, for improved performance. A large water mass to structure mass ratio of 1-4 % was shown to be required for the TLD to remain equally effective as more TLD force is developed. Also, it has been seen that reduction in structural response was fairly insensitive to the band width of ground motion and was dependent on structure's natural frequency relative to significant ground motion frequencies.

Sheng and Hua (2001) investigated the characteristics of rectangular TLDs both experimentally and numerically, using harmonic excitations. From the given structural period and within the range of parameters (*viz*. tuning ratio, liquid depth ratio, excitation wave period etc.) considered, the larger TLD was found to be more effective. Maximum reduction in the structural response was seen when the liquid sloshing frequency was tuned to structural frequency.

El Damatty (2002) studied the behavior of rectangular TLD to upgrade seismic resistance of existing and new structures, experimentally and numerically using Long Beach California (1993) earthquake time history. Study proceeded by considering equivalent tuned mass damper by simulating the TLD that was investigated experimentally. The TLD was simulated using a rigid mass attached to the structure using spring and dashpot. An attachment of a TLD system to eight

story steel building resulted in 60% reduction in vibration of building when subjected to real pre-recorded earthquake.

Modi and Akinturk (2002) worked on enhancing the energy dissipation efficiency of rectangular liquid damper through introduction of two-dimensional wedge-shaped obstacles at the bottom of the tank; as well as floating particles. It has been concluded that wedging increased the effectiveness of TLD by enhancing the damping factor (due to increase in bottom roughness). It has also been found that the wedge angle has considerable effect on the performance of damper. In this study, an optimum wedge angle of around 4º was observed. Presence of floating particles and wedging improved the damper performance by around 40%. Further, it has been observed that surface roughness of TLD promotes the boundary layer separation and increased the damping factor.

Ikeda (2003) investigated theoretically, the nonlinear coupled vibrations of system in which a rigid rectangular tank partially filled with liquid, attached to a structure subjected to vertical harmonic motion. Model equations were derived by taking nonlinear fluid force into account. Influence of depth of liquid and detuning parameter on the resonance curves for this system were investigated. It has been found that the shapes of resonance curves changed depending on the liquid's depth.

Biswal *et. al.*, (2003) introduced baffles in liquid and investigated numerically, their influence on performance of rectangular TLD subjected to harmonic excitation. The effects of baffle parameters such as position, dimensions and numbers on the non-linear sloshing response were examined. It has been seen from the study that baffles have appreciable effect on slosh frequency parameters of liquid when placed very close to the liquid free surface. It has been also seen that first baffle was very effective in reducing the slosh response of liquid and baffles placed below the first baffle had very little contribution in reducing the slosh response of liquid. The effect of baffle was found to be negligible when placed very close to the bottom (within 0.2 times depth of liquid) of TLD.

Banerji (2004) investigated numerically, rectangular TLDs subjected to broad band excitations. Based on the study, it has been found that, TLD to structure mass ratio and depth ratio have a significant effect on the ability of TLD to control response of large amplitude base excitation. The response of a typical single degree-of-freedom structure was observed to reduce by about 30% using a TLD with a depth ratio of 0.15 and mass ratio of 4%.

Frandsen (2005) developed a 2-D sigma transformed finite difference solver based on inviscid flow equations for the analysis of rectangular TLDs. From the investigation, it has been found that nonlinear free surface behavior plays an important role in describing the performance (e.g. system displacement) accurately. Further, it has been observed that the response of the structure-TLD system to be extremely sensitive to small changes in forcing frequency. It has also been seen that for a fixed mass ratio, maximum efficiency could be obtained for a relatively small water depth (when depth ratios are 0.125, 0.25 etc. i.e. depth of liquid / length of TLD) decreases.

Corbi (2006) studied the possibility of coupling 'sloshing water dampers / TLD' with rigid blocks moving on foundation base subjected to horizontal ground motion. Tests were performed by varying excitation frequency between 1Hz and 10 Hz, corresponding to most significant frequency range for seismic motion. It has been observed that even if the benefit of using liquid damper is not homogeneous on the frequency range, it was found to be strongly dependent on the frequency at which the power of excitation was lumped.

Jin *et. al.*, (2007) studied the effectiveness of cylindrical TLD in controlling earthquake response of jacket platform. Lumped mass method was employed to analyze numerically, the controlling earthquake effect on TLD. It has been concluded that the ratio of fundamental sloshing frequency of liquid to the natural frequency of platform was the key factor that controls earthquake response. Also, increase in mass ratio of TLD was found to be useful in reduction of vibration.

Tait *et. al.,* (2007) presented the results of bidirectional 2D structure-TLD test, over a range of excitation amplitude values covering the practical range of serviceability accelerations (10g $x10^{-3}$ - $30gx10^{-3}$) for buildings excited by wind. Based on the investigation, it has been seen that the response of the structure-TLD system excited bidirectionally was found to correspond to the linear superposition of responses of 1D structure-TLD system.

Sung *et. al.,* (2007) implemented experimentally 'Real Time Hybrid Sloshing Table Testing Method' (RHSTTM) to evaluate performance of TLD for controlling seismic response of buildings. The structural responses with TLD were calculated numerically in real time, using an analytical building model, a given earthquake excitation and shear force generated by TLD and the shaking table. Comparison between structural responses obtained by RHSTTM and the conventional shaking table test of single story steel frame with TLD indicated that the performance of TLD can be accurately evaluated using RHSTTM without physical model.

Falco and Campos (2008) developed, single degree-of-freedom transmission system with an adjustable dynamic characteristics to validate TLD properties with natural frequencies between 0.7 Hz and 2 Hz. Based on the study. It has been found that hydrodynamic component did not significantly effect the shear force in the TLD.

Marivani and Hamid (2009) developed fluid-structure interaction numerical model to simulate the response of single degree-of-freedom system, outfitted with TLD. The structure was subjected to random external excitation and nonlinear two-dimensional flow model of TLD was developed using finite difference method. Numerical results of this model have been compared with results of equivalent model of tuned mass damper (TMD). It has been shown that the model was capable of capturing about 70 % damping effect of the TLD on the structure response.

Eswaran *et. al.,* (2009) numerically analyzed the sloshing waves for baffled and un-baffled cubic tanks. Study was carried out by using different types of baffle in tank

viz. horizontal cum vertical baffles and ring baffles. It has been seen that ring baffles reduced pressure on tank wall effectively than other types of baffle.

Love and Tait (2010) investigated the use of TLD to reduce wind induced vibrations of base isolated structures. Based on the study, it has been seen that, TLD with a mass ratio of 2.4% was found to be capable of reducing the (root mean square) RMS response of the structure to below 9.5 milli.g. from 17.1 milli.g. where g is acceleration due to gravity.

Gabriele *et. al.,* (2010) assessed the capacities of smoothened particle hydrodynamics (SPH) to treat the coupling problem of TLD and structure, by describing the fluid as particles. In order to characterize the wave breaking of liquid on the response curves, tests have been conducted with liquids of different viscosities, and observed that increased viscosity could prevent the onset of breaking waves.

Marsh *et. al.,* (2010) used SPH to demonstrate the effectiveness of employing liquid sloshing (in TLDs) as a structural control mechanism. Predictions of fluid-structure interaction, identified the ability of the SPH method to accurately model the forces between structure and sloshing absorber, when liquid depth of 5.5 mm was employed. Based on the study tit has been seen that, control performance of TLD in terms of settling time (time taken from the instant of the structure's release to when its motion is ceased) was found to be independent of liquid level for a significantly wide range of depths of 2.75–22 mm.

Samantha and Banerji (2010) presented a modified TLD, where TLD rests on an elevated platform that was connected to the top of building through rigid rod with flexible rotating spring at its bottom, under harmonic and earthquake excitations. Modified TLD has been found to increase the base acceleration and also introduced additional in phase rotational motion, which increased the sloshing of liquid. For broad band earthquake motions, modified TLD configuration was found to be robust (in terms of reducing peak acceleration) compared to that of the standard

TLD configuration. It has been concluded that the modified TLD configuration with optimal design of rotational spring required half the water as compared to standard configuration.

Morsy (2010) investigated TLD with and without screens under harmonic excitations. It has been observed that the sway of structure (with TLD) was reduced by 71% and 80% for TLD without screens and TLD with screens respectively. Different screen locations and solidities ware also investigated for input motion of nonharmonic type. The case with screen placed in the middle with a solidity of 0.40 was found to be the best. The study also investigated the effect of fluid height under wide range of excitation amplitudes. The harmonic excitations, with amplitudes up to 3% of length of TLD and fluid heights up to 40% of length of TLD were used. It has been seen that TLD showed better performance with lower fluid heights in case of low excitation amplitudes. For high excitation amplitudes, TLD performance was better with higher fluid heights.

Nanda *et al.*, (2010, 2011) studied the effectiveness of TLD for controlling seismic vibration of structure. A ten story two bay framed structure was analyzed using various ground motions (e. g. El Centro (1940), Loma Prieta (1989), Northridge (1994), San Fernando (1971) and Indian Standard (IS) 1893 time history). It has been observed that TLD was more effective in reducing the dynamic response of structure when placed at the top of the building. TLDs, which were properly tuned to natural frequency of structure has seen to have more damping effect on the structure.

Faltinsen *et. al.*, (2011) studied theoretically / analytically and experimentally the behavior of rectangular TLD, equipped with central slat-type screen, subjected to horizontal harmonic motion. Theoretical analysis was based on multimodal method with linear free surface conditions and quadratic pressure drop condition at the screen, expressing an effect of screen induced cross flow separation. Very good agreement between theoretical and experimental studies has been seen for the

smallest frequency amplitudes considered (forcing amplitude-to tank width ratio ~0.001– 0.01).

Love and Tait (2011) developed a nonlinear mathematical model, describing sloshing behavior of a fluid in a flat bottom of an arbitrary geometry tank. It was observed that in an arbitrary geometry tank, the waveforms at two locations differ significantly due to two-dimensional nature of mode shapes. At frequency ratio of one, it has been observed that small out-of-plane sloshing force was present due to tank shape effect and sloshing force in the transverse direction was approximately 20% of sloshing force in the forcing direction.

Bhattacharya and Ghosh (2012) investigated the response of elevated water tank with multiple tuned liquid dampers (MTLD) subjected to earthquake. Variation of mass ratio and tuning criteria of dampers have been examined to investigate performance and robustness of dampers. The effect of detuning due to change in structural frequencies resulting from variation of water level in tank has been analyzed. The displacement response reductions of structure with MTLD have been found to be 21 % and 29 % for, full and half filled tank respectively which were significantly greater than single TLD.

Murudi and Banerji (2012) reported a comprehensive study of the effects of ground motion parameters (viz. frequency content, band width, intensity etc.) on the ability of TLD to mitigate response of structure, to input of both near-field and far-field ground motions. It has been seen that the frequency content and bandwidth of the ground motion do not significantly influence the performance of TLD. Also, it has been observed that TLD was more effective for the far field ground motions, where the strong motion phase and the peak response of structure after the first few cycles of vibration were observed.

Syed *et. al.,* (2013) have performed numerical study on RC frame buildings with rectangular TLDs, using El Centro 1940 earthquake and Kashmir 2005 earthquake time histories. Three multi story building models namely two, five and seven story

were chosen for the analysis. Analysis was performed by varying the location of rectangular tank on roof, and the depth of water in a tank. Based on the analysis, it has been seen that most suitable location of tank is the center of mass of building. It has also been concluded that for level of water in a tank between 0.32h (h: height of tank) to 0.81h, mitigation of response was more.

Hossein *et.al.,* (2013) have analyzed single degree of freedom (SDOF) structures with rectangular TLD, experimentally and numerically. The structural models were excited by harmonic and earthquake (recorded earthquake of Malaysia) inputs. It has been observed that TLD decreases the response of structure effectively. Also, it has been found that a tuned structure-TLD system was observed to be more effective when excited by harmonic input rather than earthquake input.

Ali *et. al.,* (2014) studied the use of multiple TLDs for controlling vibrations of MDOF (multi degree of freedom) system. Multiple shallow water tanks were designed to suppress the vibrations of a multiple degree of freedom structure. The equivalent tuned mass damper (TMD) approach of Yu (1997) was used to model the behavior of TLDs. Numerical simulations of the multiple TLD structure assembly was analyzed considering both harmonic and earthquake time histories. It has been observed that by introducing multiple TLDs to the MDOF structures and tuning them with respect to modal properties of structure, resulted in improved control of vibrations in comparison to the cases where only single TLD was employed.

Mondal *et. al.,* (2014) experimentally investigated the use of TLD for damping vibrations of structure. Frequency range around the first mode of resonant frequency was considered for excitation. From theoretical and experimental results, it has been confirmed that TLD is most effective when structure was excited to resonant frequency. Over 80 percent reduction in response was observed in the investigation.

Ruiz *et. al.,* (2014) introduced a new type of tuned sloshing damper consisting of traditional TLD with floating roof (TLD-FR). It has been seen that structures with TLD-FR can achieve significant reductions in their seismic response. Under harmonic excitations, the behavior of TLD-FR was observed to be amplitude independent.

Bang-Fuh and Shih-Ming (2015) have studied the dynamic response of small and large structures with TLD. Vibration control was investigated in terms of reduction of dynamic response of structure and reduction in maximum energy development in the interaction during excitation. It has been concluded that the response of tank-structure system was sensitive to the excitation frequency and water depth in the tank.

Chang (2015) investigated modified tuned liquid damper (MTLD) system. subjected to both harmonic and seismic excitations. Effect of parameters like mass ratio, tuning ratio, damping ratio and excitation conditions were considered in the investigation. Based on the study, tuning ratio other than one (preferably 0.8), has been suggested for improved performance of TLD. Also, the effectiveness of TLD in vibration control has been seen to increase with increasing mass ratio.

Ahmad *et. al.* (2016) investigated experimentally, 4-storey RC framed structural models with water tank as a TLD, using El Centro 1940 earthquake time history. It has been observed that when water tank was filled with water corresponding to tuned condition, it was very effective in reducing the acceleration and displacement response. With 2 to 2.5% of water mass the response acceleration and displacement were reduced by 2 and 1.8 times respectively.

Turner (2016) has presented a numerical study of free-surface elevation in a two-dimensional rectangular vessel with inhomogeneous (other than flat) bottom topography. He used, time dependent conformal numerical mapping to map physical fluid domain to rectangle, in computational domain with time dependent aspect ratio. Step and hump topography with free and forced vibrations were used

for the simulations. For forced periodic oscillations, it has been shown that the hump profile is the most effective topography for minimizing the nonlinear response of liquid and this topography found to reduce the stresses generated by liquid on the vessel walls. It was observed that by varying the width of step or hump, has less significant effect than varying its magnitude.

Ali *et. al.,* (2016) developed an experimental testing method of real-time hybrid simulation (RTHS) to investigate effectiveness of TLDs. TLD response was obtained experimentally and structure was modelled numerically, capturing the interaction in real time. Effects of parameters like mass ratio, frequency ratio etc. were investigated. Based on the study, sloshing frequency of around 1.2 times the fundamental frequency of structure has been suggested for maximization of the efficiency of TLD.

2.3. SLOPED BOTTOM TLD

Gardarsson *et. al.,* (2001) experimentally studied sloped bottom TLD with 30º end slope, on shaking table, considering harmonic excitation. For the frequency ratio (excitation frequency / sloshing frequency) of around 0.96, maximum sloshing force has been observed in the sloped bottom TLD. Further it has also been concluded that sloped bottom TLD can result in a greater sloshing force (more dissipation of dynamic energy) than that of box shaped TLD for the same water mass. Additionally, a relationship between sloshing frequency in box shaped TLD and sloshing frequency in sloped bottom TLD has been proposed, based on geometric parameter (horizontally projected sloping length / length of tank).

Olson and Reed (2001) studied numerically, sloped bottom TLD with end slope of 30º, subjected to harmonic excitation, employing an energy dissipation matching scheme. From the study, it has been reported that initial tuning of sloped bottom tank should be at a value greater than fundamental frequency of structure, to obtain maximum effectiveness under large amplitude excitation. Also, it has been

suggested that equation to determine sloshing frequency in flat bottom tank (Lamb's equation) may be used to estimate sloshing frequency of liquid in sloped bottom tank with modified length parameter representing wetted perimeter.

Xin (2006) investigated experimentally, a density variable sloped bottom TLD (DVTLD), using water and sand particles. Effectiveness of mitigating seismic response of structure was evaluated through a shaking table tests on ¼ scale, three story building. Further, a semi-analytical model was proposed based on the concept of equivalent flat bottom wherein, the length of flat bottom tank is made equal to the total length of sloping bottom, keeping maximum water depth constant. Four earthquakes *viz.* El Centro 1940, Taft 1952, Northridge 1994 and Kobe 1995 were used as input motions. Based on the experimental study, it has been seen that DVTLD with W shaped bottom was observed to be more effective in mitigating structural response than DVTLD as compared with V shaped bottom. Also, it has been observed that density variable strategy can mitigate structural response by 2 to 3 times more than the traditional TLD.

Gardarsson and Yeh (2007) experimentally explored hysteresis in sloshing of shallow water in flat bottom and sloped bottom tanks. In the sloping beach case, a softening spring behavior hysteresis was observed. It has been found that during the process of incrementally increasing the forcing frequency, the sloshing wave amplitude increased and formed wave breaking until it reached the jump frequency; and once the jump frequency was passed, the response abruptly subsided with no wave breaking. When the process was reversed i.e. incrementally decreasing the forcing frequency, the calm response was suddenly changed and returned to the active state at the jump frequency. When the investigation was extended to sloped bottom, a softening spring hysteresis was observed.

Idir and Ding (2009) investigated numerically, the performance of rectangular tank with various shapes of bottom slope *viz.* V shape, W shape and arc shape bottom, by converting into equivalent flat bottom TLDs. The deepest water depth was

taken as the water depth in the natural frequency formula of a flat bottom tank. The calculated natural frequency was validated with experimental data. It has been also found that free oscillations of water in a rectangular tank, after excitations are over, attenuated rapidly when its bottom is provided with various slope shapes such as. Based on shake table tests, simplified frequency formula derived from linear wave theory, proved to be accurate for excitations (up to 1.2 Hz).

Thus, it is seen from the literature review that limited studies (considering two types of bottom slopes and few slope angles e.g. 30) have been reported on slope bottom TLD and hence, an attempt has been made in this thesis, to conduct a systematic finite element (FE) based study, on the effects of slope location, amount of slope at the bottom of TLD, with an aim to get an efficient TLD, for controlling structural vibrations of framed building, caused by earthquake excitations.

2.4. SIGNIFICANCE OF THE STUDY

Tuned liquid dampers (TLDs) have found to have several advantages over other vibration control devices (e.g. TMD etc.), such as low cost, easy installation even in existing structures, use for temporary purpose, usefulness in multidirectional excitation, low running and maintenance cost etc. This makes TLD an economical and viable solution for controlling wind and earthquake vibrations of structures. Slope bottom tank enhances the effectiveness and robustness of TLD as more amount of water take place into the motion. Therefore, a comprehensive study on evaluation of sloped bottom TLD in reducing earthquake response of structures is under consideration. In addition, slope bottom tank can be used in reduction of beating (a process of giving back energy to structure by TLD after cessation of external excitation). Hence, the present study attempts to systematically, explore the effects of various slope bottom TLDs, such as with end, central, dual triangular, combinations of end and central slopes and combination of end and dual triangular slopes for enhancing the reduction in response of structural displacements, considering various earthquake base motion.

CHAPTER 3

CONTROLLING RESPONSE OF STRUCTURE WITH APPLICATION OF CENTRAL SLOPE AND DUAL TRIANGULAR SLOPE TLD

3.1. INTRODUCTION

Use of Tuned Liquid Damper (TLD), for mitigating the response of structures (e.g. buildings) started since by Bauer (1984). As mentioned in the literature review, TLD is a device consisting of tank, partially filled with liquid (usually water) and tank is rigidly attached generally to the roof level of structure. During vibration of structure, sloshing motion of liquid occurs at the free surface of liquid in a tank. Properly tuned TLD imparts force against the motion of structure, due to sloshing of liquid, thereby reducing the dynamic response of structure. TLDs have gained attention due to their simplicity, low installation and maintenance cost and bidirectional properties. TLDs are effectively used in reducing dynamic response of tall buildings subjected to strong winds (e.g. Tamura *et. al.,* 1995 and Wakahara *et. al.* 1992). Sloshing motion of liquid in a tank exhibits highly nonlinear behavior at large response amplitudes (Tait *et. al.* 2004). Most of researchers (Chen *et.al*., 1995, Reed *et.al.* 1998, Sheng and Hua 2001etc.) have investigated performance of TLDs attached to structures subjected to harmonic excitation. These researches provide resemblance to the response of structure with TLD, subjected to wind excitations. Koh *et. al.* (1994) conducted numerical study to investigate use of TLDs for mitigating seismic response of suspension bridge. A reduction in dynamic response of bridge of order 20% to 30% was observed with 1% mass of TLD relative to generalized mass of bridge. Response of TLD subjected to large excitation amplitude was investigated by Reed *et. al.*, (1998). It was observed that, nonlinearity of sloshing motion makes TLD, more effective and robust for control of structural response. A considerable reduction in ductility demand of reinforced

concrete members was observed with use of multiple tuned liquid dampers. A large number of studies have been conducted on use of flat bottom TLDs to mitigate dynamic response of structures, subjected to wind (Chang C. C. and Gu M. 1999) and earthquake excitations (Murudi and Banerji 2012). However very few studies on sloped bottom TLDs have been reported in the literature (Gardarsson 2001, Olson and Reed 2001, Xin 2006, Idir and Ding 2009).

It is observed from literature that flat bottom TLD exhibits a phenomenon of beating, which has adverse effect of giving energy, back to the structure after end of external excitation. Researchers have studied W and V shape slopes of 5º to 30º (Xin 2006) with density variable liquids. Idir and Ding (2009) suggested formula for evaluating sloshing frequency for W and V shape bottom TLD.

Therefore, an attempt to evaluate the performance of slope bottom (**central or W shape or single triangular hereafter will be referred as central slope** and dual triangular slopes) has been made in this study, to investigate the effectiveness of TLD with range of maximum possible slopes at bottom of TLD using finite element analysis.

FE analysis has been performed based on basic code developed by Nanda (2010) but modified suitably for the current work. Finite element formulation is provided in Appendix A. Upon validation of the FE code, parametric investigation of both flat and slope bottom TLDs (attached to at the roof level of a framed structure), when subjected to both harmonic and earthquake excitations, are presented. In this chapter, the influence of various parameters such as tuning ratio (sloshing frequency of liquid / structure's natural frequency), depth ratio (depth of liquid / length of tank) on the performance of TLD in reducing the dynamic response (such as displacement) of structure is investigated. Numerical investigations on flat bottom TLD are presented first, followed by responses of central single and dual triangular slope TLDs. The results of the analysis are then presented in the form of variation of displacement with time.

3.2. FLUID STRUCTURE INTERACTION FORMULATION

The basic finite element (FE) formulation for fluid-structure (in this case frame structure) considered in this study is mentioned below (details provided in Appendix A). A Schematic diagram of a structural frame, attached with TLD at top is shown in Figure 3.1.

$$[M]\{\ddot{X}\} + [C]\{\dot{X}\} + [K]\{X\} = -[M]\{\ddot{X}_g\} + \{F_{TLD}\}$$ (Banerji 2004) (3.1)

where, $[M]$ is global mass matrix of the frame

$[C]$ is global damping matrix of the frame and here it is assumed to be null matrix as inherent damping of structure is neglected

$[K]$ is global stiffness matrix of the frame

$\{X\}$ is global displacement vector for all degrees of freedom

$\{\ddot{X}_g\}$ is ground acceleration vector

$\{F_{TLD}\}$ is resisting force to the structure at respective nodes offered by TLD.

F_{TLD} is given by the expression

$$F_{TLD} = \frac{\rho g b}{2}[(\eta_n + H)^2 - (\eta_0 + H)^2]$$ (Banerji 2004) (3.2)

where ρ is density of liquid, η_n and η_o is wave height right and left wall, and H is the still height of the liquid in the tank (or TLD) (refer Figure 3.2). See formulation (Appendix E). As the current aim of the study is on 2 dimensional (2D) idealization of reinforced concrete frame structure with TLD on the roof level, the above mentioned equation of motion has been translated into a 2D FE formulation, with fluid elements and structural elements modelled using 2D four noded quadrilateral (with two displacement degrees of freedom per node) and 2 noded frame element

(with three degrees of freedom per node: 2 displacements and 1 rotation) respectively. Details of the FE formulation are given in Appendix A.

3.2.1. 2D Structural frame ~ geometry and material properties

An intermediate two-dimensional (2D) representative reinforced concrete frame from a long building (reported in Manish Shrikhande 2006) is being considered for the analysis . The details of the structural 2D frame are listed as under:

- Type of structure: Multi-storey rigid jointed plane frame
- Number of stories: G + 9 (i.e. 10 storey frame)
- Floor height: 3.5 m
- Bay width: 5.0 m
- Live load: 3.5 kN/m^2
- Materials: Concrete (M25), Steel (Fe415)
- Density of reinforced concrete (RCC): 25 kN/m^3
- $E=2.5x10^{10}$ N/m^2 of concrete
- Moment of Inertia of column: $1.9x10^{-3}$ m^4
- Moment of Inertia of beam: $1.33x10^{-3}$ m^4
- Self weight of column per meter: 2.81 kN
- Load on beam per meter (DL + LL): 3245 kN
- Mass of the column per meter: 286.69 kg
- Equivalent mass of beam per meter: 3312 kg

Schemetic diagram of the 2D frame is shown in Figure 3.1(a).

3.3. CONVERGENCE STUDY OF FE MESH

3.3.1. Frame structure

Discretization of 2D frame has been done with plane frame element (i.e. 2 noded element) with three degrees of freedom per node (2 displacements and 1 rotation). Typical discretization of the 2D frame is shown in Figure 3.3(a). In order to assess the effect of mesh refinement, each of the beam / column has been meshed with elements ranging from 1 to 4, thus resulting in 50-200 elements in total. Figure 3.3 (b) and Table 3.1 show variation of the natural frequencies of the first eight modes, with increasing number of elements per member. The mode shapes of initial few modes are also shown in Figure 3.4. It can be seen that for the range of elements considered, there appears to have not much variation in the values of natural frequencies for the lower modes of vibration (e.g. 1^{st} till 7^{th}), however a very mild drop can be seen for the 8^{th} mode of vibration. Hence, for all the subsequent studies, 4 elements have been considered for the frame members, as the main monitoring mode of vibration is the fundamental mode (or 1^{st} mode).

3.3.2. Fluid

The liquid / fluid in the rectangular tank is considered to be bounded by free surface, side walls and bottom. For the mesh convergence study of the liquid, the length and depth of tank are taken as 0.90 m and 0.60 m respectively (following the dimension adopted by Nakayama (1981). Discretization of liquid domain is done by using 2D four noded quadrilateral elements (with two displacement degrees of freedom per node, see Appendix A for the element formulation). Typical FE mesh of the fluid in the rectangular tank is shown in Figure 3.5 (c). In this case, 10 elements have been used along the longer direction (i.e. element length = 0.09 m), while the number of elements along the depth has been varied from 4 to 10 (i.e. element length along the depth = 0.15–0.06 m), resulting in 40 to 100 elements altogether. The tank is then subjected to a horizontal harmonic acceleration of the type

$$\ddot{x} = -x_{0}\omega^{2} \sin \omega t \quad (3.3)$$

where x_0 and ω are amplitude and frequency of forced harmonic excitation respectively, and time, $t \geq 0$, x_0 = 0.002 m and ω = 5.5 rad/s. The results of the analysis are presented in Table 3.2, as free fluid surface elevation at both the right and left walls, at time (t) = 8.34 and 9.0 sec., respectively. It can be seen from Figure 3.6 that, convergence in the values of both the right and left walls elevations can be seen when the number of elements have reached 90, hence, for further analyses, mesh discretization with 10 x 10 elements (i.e. 100 elements in total, with an approximate element size of ~0.09 x 0.06 m) has been considered to be sufficiently fine enough to capture the dynamic response.

3.4. VALIDATIONATION OF FLUID STRUCTURE INTERACTION FE CODE

In order to validate the currently developed FE based fluid-structure, MATLAB code (mentioned above), comparisons have been made of the FE results for both the fluid and structure analyses with those obtained from literature (Nakayama, 1981) and STADD Pro software (STADD Pro, 2019), respectively, are briefly summarized below:

3.4.1. Fluid analysis

A partially filled tank with fluid (water) with length (L) and liquid depth (H) of dimensions 0.90 m and 0.60 m, as mentioned by Nakayama (1981), has been considered, for the dynamic analysis. The tank has been idealized as 2D and subjected to a horizontal (i.e. along the length) harmonic acceleration given by Equation 3.3, with x_0 and ω as 0.002 m and 5.5 rad/sec respectively. Comparison of the present FE results with that of Nakayama (1981) obtained via Boundary Element Method (BEM) is presented in Figure 3.7, in the form of free surface slosh amplitude of liquid at time step t = 0.02 sec. It can be seen from Figure 3.7 that a

close match between the present FE with that obtained by Nakayama (1981) using boundary element method (BEM).

3.4.2. Structural analysis

In order to validate the present code for the linear elastic dynamic analysis of framed structure, a comparison of the free vibration analysis results obtained by the present code and that of the commercial structural analysis software STAAD Pro (V8i), has been presented in Table 3.3. The same 2D reinforced concrete (RC) as mentioned previously (see Figure 3.3 (a); Section 3.2) has been adopted for the comparison. The results from both the analyses are shown in terms of natural frequencies for the first 6 modes of vibration, and are found to be in good agreement, thus validating the developed code, for the RC frame dynamic analysis. An extract of free vibration analysis of the structure by STADD Pro V8i is attached in the Appendix (B).

3.5. EVALUATION OF REDUCTION IN RESPONSE OF STRUCTURE

In order to evaluate the effectiveness of TLD, the reduction in displacement response (*DR*), as a result of dynamic analysis of (RC framed) structure with TLD subjected to base excitation has been computed, using undamped and damped displacements at each time step (data point).

Considering,

Undamped displacement of structure at a time : d_1

Damped displacement of structure with application of TLD at a time: d_2

Absolute difference between undamped and damped displacement at a time: D_1

Absolute undamped displacement: D_2

Sum of all absolute damped displacement differences is then given by

$$DS_1 = \sum_{1}^{n} D_1 \tag{3.4}$$

where n is number of time steps or data points

Similarly, sum of all absolute undamped displacements is also defined as

$$DS_2 = \sum_{1}^{n} D_2 \tag{3.5}$$

Reduction in displacement of structure in percent is then given as

$$DR = \frac{DS_1}{DS_2} 100 \tag{3.6}$$

3.6. SELECTION OF PRILIMINARY DIMENSIONS OF FLAT BOTTOM TLD

Before proceeding into the dynamic analysis of framed structure with sloped bottom TLD, initial approximate dimensions (e.g. depth of liquid, *H*, length of tank, *L*, and width of tank, *B*) of the tank have been arrived at, based on forced vibration analysis (with harmonic loading input of amplitude of 0.01 m and duration of 50 sec). Structure-TLD system is subjected to harmonic loading having frequency close to sloshing frequency (natural sloshing frequency of first antisymmetric mode), for resonance condition. The sloshing frequency of liquid in a tank which is (considered close to structure's natural frequency, to approach resonance for maximum effect) kept constant for TLDs during analysis. It may be noted that the natural frequency of the framed structure has been already evaluated as 2.50 rad/sec, as mentioned in Section 3.4.2. Dimensions of tank, *L* and *H* have been varied in the range 1.72–3.0 m, 0.20–0.67 m respectively, keeping *B* constant at 1.0 m (see Table 3.4). The displacement responses of structure (computed at roof top level) for various dimensions of TLD are plotted in Figures 3.8-3.12. and Table 3.4. It is observed

that at higher depth of liquid ($H \geq 2.08$ m), the beating of damped displacement has been observed. The beating time of damped displacement is also shown in Table 3.4. Here damped displacement response is found to decrease up to a certain time (e.g. 27 sec for H = 3.0 m) from the beginning and thereafter increases after this time due to beating. Based on the dimension sets considered, it can be seen that, beating is found to be absent for L = 1.91 m and H = 0.25 m; and L = 1.72 m and H = 0.20 m. However, the dimensions as L = 1.72 m and H = 0.20 m have been considered for the for further analyses, so as to avoid the phenomenon of beating.

3.7. RESPONSE OF STRUCTURE WITH FLAT TLD TO HARMINIC BASE EXCITATION (INFLUENCE OF TUNING)

The effect of tuning (sloshing frequency of liquid / structure's natural frequency) has been investigated for flat bottom tank, of dimensions L = 1.72 m and B = 1.0 m as mentioned above, by analyzing with an harmonic excitation of frequency 2.5038 Hz and amplitude of 0.01 m. Inherent damping of the structure has been excluded in the analysis, as the study is aimed at assessing the effectiveness of TLD exclusively in mitigating the displacement response of structure. The tuning ratio has been varied by considering by changing liquid dept (H) from 0.16–0.24 m (resulting in 90-110 % tuning respectively or depth ratio (H/L) of 0.09-0.14 respectively) while keeping constant length and width of tank. As before, the sloshing frequency (f_b) has also been kept close to the natural frequency of the structure i.e. 2.5038 rad/sec. The dimensions of TLD, tuning ratio and depth ratio are shown in Table 3.5.

The responses of structure with flat bottom TLD for different tuning ratios from 90-110 % are shown in Figures 3.13-3.20 and Table 3.5. It is observed that the tuning ratio of TLD, greatly affects the response of structure. Some of the important observations made from the dynamic analysis are: a) for 90% tuning of TLD, displacement reduction (DR) of structure is observed to be 10.62 %, b) displacement reduction of structure gradually increases with tuning ratio and

maximum reduction is observed for tuning ratio close to one, c) at 100 % tuning, the reduction in structural displacement is about 41.43 %, d) the reduction in displacement is observed to decrease with increase of tuning above 100 %. The optimum tuning ratio is observed to be very close to one (Figure 3.21). As observed from Figure 3.22 the depth ratio of TLD at optimum tuning is about 0.117.

From the literature (Banerji P. 2004), response reduction of about 30% has been observed for 0.15 depth ratio of TLD, which is close to the *DR* value of about 22.02 % for depth ratio of 0.14, in the present study. (Modi *et. al.*, 1990) stated that energy dissipation rate has been found to have tendency to be maximum for low values of depth ratio, around 1/8 or 0.125. (Sun *et. al.*, 1989) observed that that for shallow depth ratio (< 0.15) the liquid in TLD, developed a strong nonlinearity behavior, leading to more sloshing and improved performance of TLD. Also, Fujii *et. al.*, (1990) used *h/d* ratio of 0.126 and 0.102 for the TLDs installed on two actual tall towers *viz.* Nagasaki airport tower and Yokohama marine tower respectively.

3.8. INVESTIGATION OF TLD WTH CENTRAL SLOPE BOTTOM

Study on performance of flat bottom TLD has been extended to investigate the performance of TLD with central slope at the bottom. Central slope (W shape; see Figure 3.23) TLD has been modelled considering Xin's (2006) approach of equivalent flat bottom TLD, which is based on wetting length of sloping bottom of TLD while keeping maximum water depth remains constant. This approach is found to be applicable to model both central slope and end slope TLDs as well (Xin 2006). Figure 3.23 shows a TLD with central slope (of angle θ) at the bottom. For the dimensions of central slope bottom TLD as *L* (length), *H* (liquid depth) and B (tank width) wetting length of TLD with central slope on one side of center of TLD is define as

$$y = \frac{L/2}{Cos(\theta)} \qquad \text{(Idir and Ding 2009)} \qquad (3.7)$$

Total wetting length of TLD due to central slope

$$L' = 2y \tag{3.8}$$

Considering a constant volume of liquid in the tank (virtual and original), modified width of equivalent flat bottom TLD is given as

$$B' = \frac{V_w}{H'L'} \tag{3.9}$$

where $H' = H$

Where, V_w is the volume of water in TLD. The slope bottom TLD would reduce the natural frequency of the sloshing liquid because of the increased wetting length in the tank, therefore $L' > L$ and $B' < B$.

As the liquid used in the analysis is water (density = 1000 kg/m^3), **percent reduction in volume of liquid is considered as percent reduction in mass**, due to application of slope at TLD bottom.

3.8.1. Selection of dimensions for sloping bottom TLD

A typical investigation of central slope bottom TLD with central slope of 12.5º at bottom , and considering the similar dimensions mentioned above for flat bottom TLD i.e. L = 1.72 m and B = 1.0 m, has been considered, subjected to similar harmonic base excitation (see section above). The effect of tuning ratio has been investigated by varying H from 0.20–0.24 m (see Table 3.6), using the abovementioned equivalent flat bottom approach of Xin (2006). of wetting length to determine sloshing frequency of liquid in slope bottom TLD. Variation of displacement reduction with tuning ratio is also shown in Figure 3.24. It can be seen that for the central angle of 12.5º, maximum displacement reduction (DR) of about 40 % can be seen (corresponding to H of 0.2235 m). The refined dimensions of TLD for further analysis, during application of slope to the bottom of TLD (i. e. L

= 1.72 m, H = 0.2235 m and B = 1.00 m) are used. Based on these derived dimensions of TLD, the tuning ratio calculated is around 1.05 which is in agreement with literature. As reported in literature by Olson and Reed (2001), initial tuning of sloped bottom TLD should be at a value greater than fundamental frequency of structure, to obtain maximum effectiveness.

3.9. RESPONSE OF STRUCTURE WITH TLD DUE TO EARTHQUAKE GROUND MOTION

In the previous sections, results of dynamic analyses of RC frame structure with both flat and single central slope bottom TLDs, subjected to harmonic base excitation have been presented. As a continuation of the investigation, the studies have been extended to observe the effects of earthquake ground motions. Five earthquake time histories viz., El Centro (1940), Loma Prieta (1989), Northridge (1994), San Fernando (1971) (http://strongmotioncenter.org), and Indian Standard (IS) 1893 (Kumar 2004) compatible time history have been used as base excitation inputs, for the analyses (see Figure 3.25 for time histories of above mentioned input motions). As shown in Table 3.7, the chosen time histories have peak Fourier and ground acceleration in the range 0.12-1.09, and 0.34/g-1.80/g respectively. Also, strong motion duration of ground motions are shown in Table 3.7. Minimum and maximum strong motion duration are 5 sec and 17.5 sec for El Centro and IS time history respectively. It may be noted that structure's fundamental frequency (0.39 Hz or 2.5 rad/sec; see Table 3.3) necessarily lies within the range of frequency content of chosen earthquakes (0.1-12 Hz). The dynamic analysis results of both the flat and central triangular slope bottom TLDs have been presented in the following Sub-section 3.9.1 and 3.9.2 respectively. For the slope bottom TLD, two configurations have been investigated, viz., a) central, and b) dual triangular slopes.

3.9.1. Flat bottom TLD

The reduction of response of structure with the application of flat bottom TLD has been evaluated and variation of the displacement response plots for both damped and undamped responses are shown in Figures 3.26 – 3.30, for the aforementioned 5 earthquake time histories. Maximum undamped displacement of structure and time at which this displacement is maximum are shown in Table 3.8. Minimum undamped displacement of 0.05 m and maximum of 0.14 m are observed for El Cento and IS time history respectively. Displacement reduction (*DR*) values corresponding to the earthquake time histories are also provided in Table 3.8. It is observed from the results of dynamic analysis that, the reduction in displacement (i.e. *DR* values) of structure with flat TLD is found to be relatively higher (i.e. > ~ 33%) for lesser Fourier amplitude earthquake motions (say e.g. < 0.41). Maximum reduction in displacement is seen for El Centro earthquake ground motion (*DR* = ~ 40.97 %). Whereas minimum reduction in displacement of about 21.00 % is observed in case of IS compatible time history base motion. Displacement reductions of about 26.90 %, 26.60 % and 33.20 % are observed in case of other earthquake motions like Loma Prieta, Northridge and San Fernando respectively. From author's point of view, the reduction in displacement response may be associated with Fourier amplitude and strong motion duration of an earthquake. More strong motion duration lead to more displacement of structure and less is the reduction in displacement seen.

3.9.2 Central slope bottom TLD

a) Effect of central slope on tuning ratio

Figure 3.31 shows a plot of tuning ratio vs central slope angle and it is seen that the tuning ratio decreases with increase in central slope angle at bottom of TLD. The variation of tuning ratio is seen to be nonlinear. With the increase of central slope, the state of TLD changes from over-tuned to the state of fine-tuned. Maximum

tuning ratio (=~1.05) has been observed at 0º (flat bottom) slope whereas minimum (=~ 1.022) tuning ratio is found to correspond to slope angel of 14º. The increase in reduction of displacement with rise in central slope (as mentioned in the previous section) can be related to the tuning ratio reaching close to 1.00, with rise of central slope value. For sample calculations Appendix B (Section B.2, B.3).

b) Effect of central slope on liquid mass reduction

A plot of liquid mass reduction in TLD vs central slope is shown in Figure 3.32. The liquid mass reduction is seen to increase with increase in central slope value. The variation of liquid mass reduction is seen to be linear. The reduction in liquid mass due to application of slope at bottom of TLD is observed to be ~16.82 %, 25.33 %, 33.92 %, 40.87 % and 47.96 % for the central slopes of 5, 7.5º, 10º, 12.5º and 14º respectively. It can be inferred that the reduction in liquid mass is an additional benefit of using slope at the bottom of TLD, that may lead to economical design.

c) Effect of central slope on reduction of displacement of structure

Dynamic analysis of the structure with TLD having central slope at the bottom (see Figure 3.23 for schematic diagram) has been performed for slope angles of 5º, 7.5º, 10º, 12.5º and 14º (maximum possible angle as the depth of the liquid is limited to 0.22 m). The results of analysis for various earthquake input motions are presented in Table 3.9. Typical plots of time histories of undamped and damped responses of structure subjected to El Centro earthquake ground motion for 5º, 7.5º, 10º and 14º central triangular slopes in Figures 3.33-3.37.

It can be observed that there is an improvement in reduction of displacement of structure with application of central slope at the bottom of TLD. For all the input ground motion considered, for all the bottom slopes of TLD considered, *DR* values in the range 21-53% could be obtained, with minimum (21-26%) and maximum (40-53%) displacement reduction ranges associated with IS compatible time

histories and El Centro, respectively. The displacement reduction (*DR)* is seen to increase with increase of central slope (see Table 3.9 Figure 3.38). The rate of improvement in the reduction of displacement is observed to be marginal for the central slope up to 7.5º. The rate improvement in *DR* values due to application of central slope of 7.5º over flat bottom TLD is observed to be maximum (*DR* = 6.67 %) and minimum (*DR* = 1.10 %) for El Centro and IS compatible time histories, respectively. The rate improvement in DR values for TLD with central slope ≥ 7.5º are observed to be relatively higher than that of central slope values ≤ 7.5º. The rate improvement in reduction of displacement due to central slope of TLD from 7.5º to 14º are observed to be ~8.20 %, 3.90 %, 5.20 %, 9.60 % and 3.90 % for the input motions of El Centro, Loma Prieta, Northridge, San Fernando and IS time histories respectively.

3.9.3. Dual triangular slope bottom TLD

The sloshing characteristics of TLD are governed by the wetting length of TLD as mentioned in Section 3.8, and wetting length can affect the performance of slope bottom TLD. In order to change / increas the wetting length of TLD, dual trianguler slopes provided at the bottom of TLDs are investigated, in this section. Figure 3.39 shows a TLD with dual triangular slopes (with equal slope angles) at the TLD bottom. The dinensins of TLD considered are as stated in Secton 3.8.

Consider, dual triangular slope angle at bottom of TLD: θ_1

Wetting length of TLD on one side of one teiangular slope can be written as,

$$y_1 = \frac{L/4}{Cos(\theta_1)} \tag{3.10}$$

Total wetting length due to dual trianguler slope is then given by,

$$L' = 4y_1 \tag{3.11}$$

Modified equivalent width (B') of TLD is given by Equation (3.9). Using a similar approach as that of central slope bottom, and considering appropriate wetting length (see Equation 3.10, 3.11), dynamic analyses have been carried out, using earthquake times histories as inputs. The results of the analyses are presented in the following sub-sections. Sample calculations are shown in Appendix B (Section B.4).

a) Effect of dual triangular slopes on tuning ratio

Tuning ratio of TLD is observed to decrease with increase of dual triangular slope and the variation of tuning ratio is seen to be nonlinear (see Figure 3.40) . Maximum tuning ratio of 1.05 and minimum of 0.958 have been observed at 0º and 25º dual triangular slopes respectively. It is also seen that the state of tuning of TLD is seen to change from over-timed to under-tuned with rise in dual triangular slopes. At an intermediate state of 100 % tuning which is seen at 20º slope, maximum reduction in displacement has been observed, as discussed in the earlier section. This trend of reduction in displacement has been observed for all the input earthquake motions considered in the analysis.

b) Effect of dual triangular slopes on liquid mass reduction

As observed in the case of central slope TLD, the liquid mass reduction increases with increase in dual triangular slope values (Figure 3.41) . The variation of liquid mass reduction is again seen to be linear. Maximum liquid mass reduction of about 44.70 % is observed at slope angle of 25º. The liquid mass reduction of about 35.01 % is seen for the optimum angle 20º (see Figure 3.41).

c) Effect of dual triangular slopes on reduction of displacement of structure

To assess the effects of angle of slope for the dual triangular slope bottom TLDs, slope angles have been varied up to 25º. Typical time history plots of displacement response of structure with the application of dual triangular slope bottom TLDs are shown in Figures 3.42-3.48, using El Centro time history as input and results of dynamic analyses are given in Table 3.10. The plots of reduction of displacement

(i.e. *DR*) of structure vs slope angle is shown in Figure 3.49. The variation of reduction in displacement is observed to be nonlinear in nature. It is observed that the reduction in displacement of structure increases with slope angle of about 20º and it decreases with rise of slope above 20º, for all the five time histories considered. The rate of increase of displacement reduction is seen to be marginal for slopes up to 5º and it increases for the slopes from 5º to 15º of slope. The rate of increase of displacement reduction become mild for the slopes from 15º to 20º. It can be concluded that 20º slope may be considered as optimum slope for the performance of TLD with dual triangular slopes. At 5º slope, maximum reductions in displacement of about 40.08 % and 21.30 % are seen for the input motions of El Centro earthquake ground motion and IS compatible time history base motion, respectively. For the slope of 15º, maximum reduction in displacement of about 55.60 % and 26.70 % are seen for the input motions of El Centro earthquake ground motion and IS compatible time history base motion respectively. Maximum reduction in displacements of about 59.27 % and 29.00 % are observed for the input motions of El Centro earthquake ground motion and IS compatible time history base motion respectively. The displacement reductions, when the TLDs are subjected to other earthquake ground motions viz. Loma Prieta, Northridge and San Fernando, these are observed to be within the limits mentioned above for El Centro earthquake ground motion and IS compatible time history base motion (see Table 3.10).

From the investigation of central slope TLD and dual triangular slope TLD, it can be seen that dual triangular slope TLD is more effective in mitigating the structural response. The improvement in displacement reduction is seen to be in range of 6.20 -18.30 % (depending on ground motion input) over flat bottom TLD when dual triangular slope is applied at bottom of TLD. This range is 5 % - 12.76 % when central slope is applied. However, reduction in volume of liquid is little higher in case of central slope TLD. Maximum reduction in volume of liquid in case of central slope TLD is observed at 14º slope is 47.96 %. Reduction in volume of

liquid for dual triangular slope TLD at optimum slope of 20^{o} is observed to be 35.01 %.

3.10. CONCLUSIONS

Dynamic fluid-structure interaction analyses of a two-dimensional 2 bay, 10 story reinforced concrete frame, with flat and slope (central and dual triangular) bottom tuned liquid dampers (TLDs) have been analyzed using a finite element based MATLAB code. The analyses have been performed using both harmonic and five earthquake time histories (i.e. El Centro, Northridge, Loma Prieta, San Fernando and IS compatible time history), form the literature. The results of the analyses have been presented and discussed in the form of tuning ratio, mass reduction of liquid and displacement reduction of structure, as a result of the application of TLDs. Summary of the main results are enumerated as follows:

a) Flat bottom TLD

- TLDs can have different sets of dimensions for the same sloshing frequency. However, dimensions of TLD are to be selected properly to avoid beating like phenomenon.
- Tuning ratio of TLD affects the response of structure and at about 100 % tuning, maximum reduction in displacement is observed. An optimum tuning ratio is found to be close to 1.0 and in the present study it is seen to be around 1.007. The reduction in displacement at optimum tuning is found to be ~ 42 %. The depth ratio for shallow, sloshing absorber is normally < 0.15 and in the present study it is 0.11.
- The reduction in displacement of structure with TLD is found to be relatively higher for earthquake motions having lesser Fourier amplitude values and less strong motion duration.

b) Central slope TLD

- Original TLD (before applying slope at the bottom) is required to be tuned to the frequency, slightly greater than structure's natural frequency. In the present study the tuning ratio of original TLD is evaluated as 1.05.

- When central slope is introduced at TLD bottom it is seen that, reduction in displacement of structure increases with increase in central slope angle. Maximum reduction in displacement of structure, of ~ 53.73 % and 26.00 % has been observed at 14º central slope TLD for input motions of El Centro earthquake and IS time history base motion, respectively.

- Tuning ratio of TLD decreases with increase of central slope at the bottom of TLD and variation of tuning ratio is observed to be nonlinear. With the increase of central slope, tuning ratio changes from over-tuned to the value close to 1.

- Liquid mass reduction in TLD is increases with central slope and this may be considered as additional benefit of sloped bottom TLD. The variation of liquid mass is observed to be linear. In the present study liquid mass reduction for central slope of 14º is observed as 47.93 %.

c) Dual triangular slope TLD

- With the application of dual triangular slopes at the bottom of TLD, it is seen that the effectiveness of TLD in reducing displacement of structure, increases with increase of slope of certain value and effectiveness decreases for higher slope values. The rate of increase of effectiveness is relatively smaller at lower slope values than for higher slope values. In the present study an optimum value of dual triangular slopes is observed to be around 20º. In the present study, maximum reduction in displacement of about 59.27 % and 29.00 % is being

observed for the input motions of El Centro earthquake motion and IS time history base motion respectively.

- Tuning ratio of TLD decrease with increase of dual triangular slopes value and the variation is observed to be nonlinear. At smaller slope values TLD is observed to be over-tuned and at higher slopes it is observed to be under-tuned.

- Liquid mass reduction increases with amount of dual triangular slopes and the variation is observed to be linear. Liquid mass reduction of about 35.01 % is observed at optimum slope of 20º.

Table 3.1. Natural frequencies of structure for two bay ten storey frame

Mode Number	Natural Frequencies (rad/sec)			
	50 Elements	100 Eleements	150 Elements	200 Elements
1	2.50	2.50	2.50	2.50
2	7.75	7.74	7.74	7.74
3	13.73	13.71	13.70	13.70
4	20.37	20.31	20.29	20.28
5	27.90	27.77	27.74	27.72
6	34.55	34.34	34.25	34.24
7	36.20	35.98	35.91	35.88
8	44.96	44.64	44.53	44.49

Table 3.2. Mesh convergence study for fluid

Sr. No.	Number of elements	Liquid free surface elevation in TLD (m)	
		Right wall at 8.34 sec	Left wall at 9.00 sec
1	40	0.0351	-0.0252
2	50	0.0371	-0.0299
3	60	0.0379	-0.0325
4	70	0.0384	-0.0339
5	80	0.0387	-0.0347
6	90	0.0389	-0.0352
7	100	0.0390	-0.0356

Table 3.3. Natural frequency of 2D structural frame

Sr. No.	Mode Number	Natural Frequency (Hz)	
		Present code (rad/sec)	STADD Pro (rad/sec)
1	1	2.50	2.40
2	2	7.74	7.41
3	3	13.71	13.12
4	4	20.31	20.26
5	5	27.77	26.55
6	6	34.34	32.81

Table 3.4. Dimensions of tank (or TLD) for resonance condition

Sr. No.	*L* (m)	*H* (m)	*B* (m)	Frequency (*fs*) (rad/sec)	Time of Beating (sec)
1	3.00	0.67	1.00	2.50	27
2	2.38	0.40	1.00	2.50	37
3	2.08	0.30	1.00	2.50	47
4	1.91	0.25	1.00	2.50	-
5	1.72	0.20	1.00	2.50	-

Table 3.5. Dimensions of TLD for different percentage of tuning ratio

Sr. No.	% Tuning	f_w (rad/s)	f_s (rad/s)	*L* (m)	*B* (m)	*H* (m)	*H/L* Ratio	Displacement reduction (*DR*) (%)
1	90	2.56	2.50	1.72	1.00	0.16	0.09	10.62
2	95	2.37	2.50	1.72	1.00	0.17	0.10	23.85
3	97	2.42	2.50	1.72	1.00	0.18	0.10	32.47
4	100	2.50	2.50	1.72	1.00	0.20	0.11	41.43
5	103	2.57	2.50	1.72	1.00	0.21	0.12	38.23
6	105	2.63	2.50	1.72	1.00	0.22	0.12	31.17
7	107	2.67	2.50	1.72	1.00	0.23	0.13	26.24
8	110	2.75	2.50	1.72	1.00	0.24	0.14	22.02

Table 3.6. Influence of tuning ratio on response (12.5º Central slope TLD Xin approach)

Sr. No.	*H* (m)	*L* (m)	*L´* (m)	*B* (m)	*B´* (m)	Sloshing frequency for		TR for *L*=1.72 m	*TR* for *L*=*L'*	*DR* (%)
						L=1.72m	*L*=*L'* m			
1	0.20	1.72	1.76	1.00	0.97	2.50	2.44	1.00	0.97	36.96
2	0.22	1.72	1.76	1.00	0.97	2.63	2.57	1.05	1.01	40.09
3	0.23	1.72	1.76	1.00	0.97	2.67	2.61	1.06	1.04	33.83
4	0.24	1.72	1.76	1.00	0.97	2.75	2.69	1.09	1.07	26.30

Table 3.7. Characteristics of earthquake ground motions and IS compatible time history

Sr. No.	Ground motion	Date	Magnitude	Peak Fourier amplitude	*PGA/g*	Strong motion duration (sec)
1	El Centro	May 1940	6.90	0.12	0.34	5
2	Loma Prieta	Oct 1989	6.90	0.64	0.60	7
3	Northridge	Jan 1994	6.07	0.47	1.80	8
4	San Fernando	Feb 1971	6.05	0.41	1.25	8
5	IS Time History	-	-	1.09	1.00	17.5

Table 3.8. Response of structure with flat bottom TLD to different earthquake

Sr. No.	Earthquake Input	Dimensions of TLD			Max. m undamped displacement (m)	Time at max. displacement (sec)	DR (%)
		L (m)	B (m)	*H* (m)			
1	El Centro	1.72	1.00	0.22	0.05	6.92	40.97
2	Loma Prieta	1.72	1.00	0.22	0.07	19.63	26.90
3	Northridge	1.72	1.00	0.22	0.06	22.86	26.60
4	San Fernando	1.72	1.00	0.22	0.08	39.25	33.20
5	IS Time History	1.72	1.00	0.22	0.14	27.78	21.00

Table 3.9. Response reduction of structure with central slope TLD to various base motions

Sr. No.	θ^o	Dimensions (m)		*TR*	Displacement reduction (%)					*MR* (%)
		L	*B*		El Centro	Loma Prieta	North ridge	San Fernando	IS History (%)	
1	0	1.72	1.00	1.05	40.97	26.90	26.60	33.20	21.00	-
2	5	1.72	0.99	1.04	40.71	27.60	27.70	34.70	21.50	16.82
3	7.5	1.73	0.99	1.04	45.53	28.30	28.70	36.20	22.10	25.33
4	10	1.74	0.98	1.03	47.01	30.00	31.00	40.00	23.50	33.92
5	12.5	1.76	0.97	1.02	51.04	31.40	32.80	43.50	25.00	40.87
6	14.0	1.77	0.97	1.02	53.73	32.20	33.90	45.80	26.00	47.96

Table 3.10. Response reduction of structure with dual triangular slope TLD to various base motions

Sr. No.	θ_1^o	Dimensions (m)		*TR*	Displacement reduction (%)					*MR* (%)
		L	*B*		El Centro	Loma Prieta	North ridge	San Fernando	IS History (%)	
1	0	1.72	1.00	1.05	40.97	26.90	26.60	33.20	21.00	-
2	5	1.72	0.99	1.04	40.08	27.40	27.30	34.20	21.30	8.42
3	7.5	1.73	0.99	1.04	43.46	28.70	29.20	37.00	22.40	12.66
4	10	1.74	0.98	1.03	46.87	30.00	30.90	39.90	23.50	16.95
5	15	1.78	0.96	1.01	55.60	32.70	34.60	47.40	26.70	25.77
6	20	1.83	0.93	0.99	59.27	33.10	35.10	51.30	29.00	35.01
7	22.5	1.86	0.92	0.95	55.18	31.50	33.00	48.80	28.40	39.84
8	25	1.89	0.90	0.97	46.56	28.10	28.90	41.60	26.10	44.70

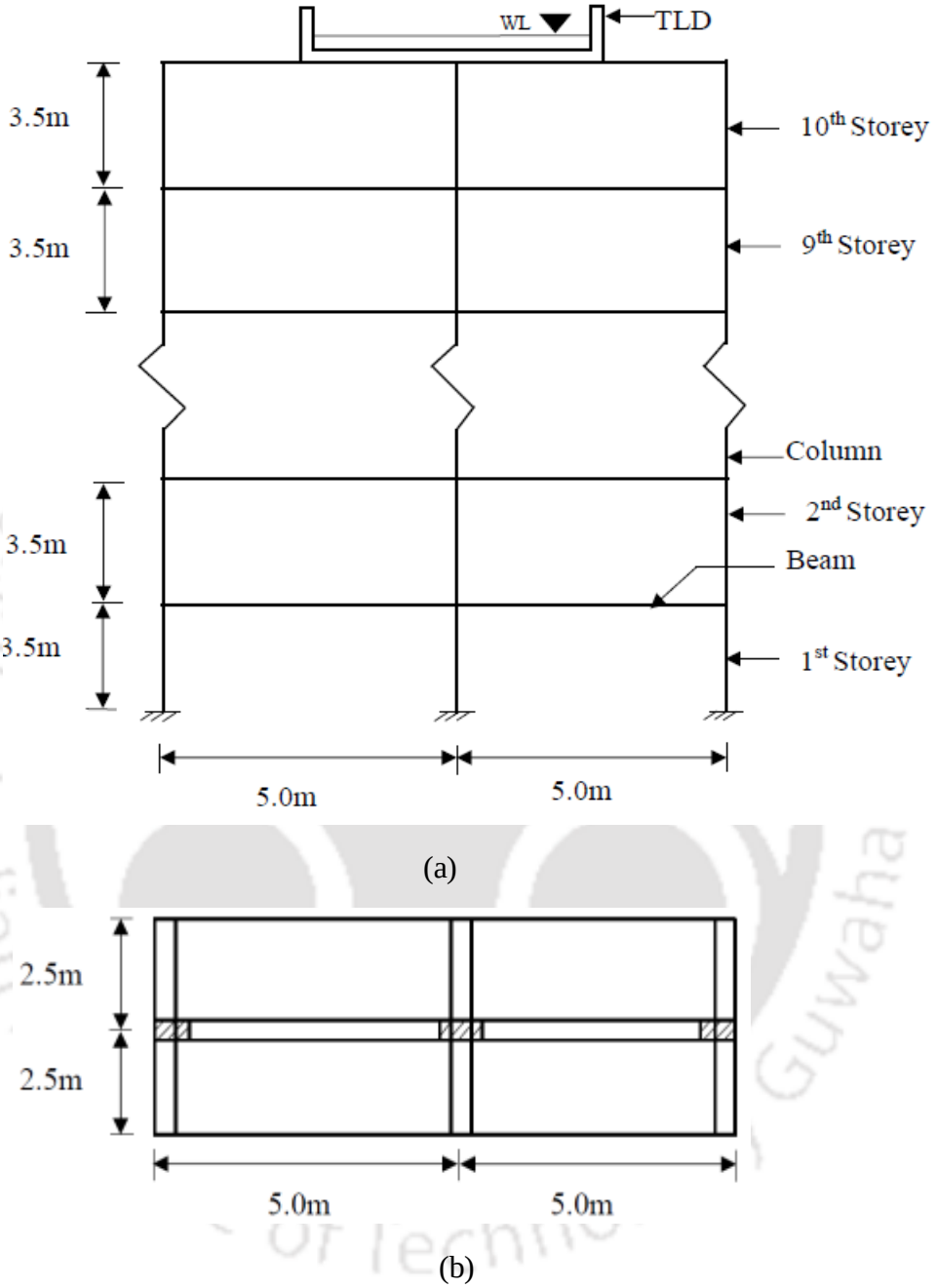

Figure 3.1. Structural model of a 2D representative frame (a) Elevation, (b)Plan

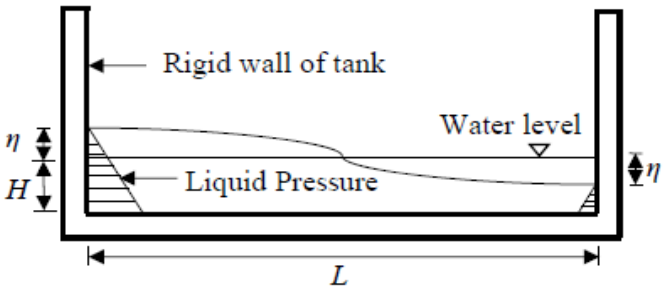

Figure 3.2. Dynamic liquid pressure on wall of TLD

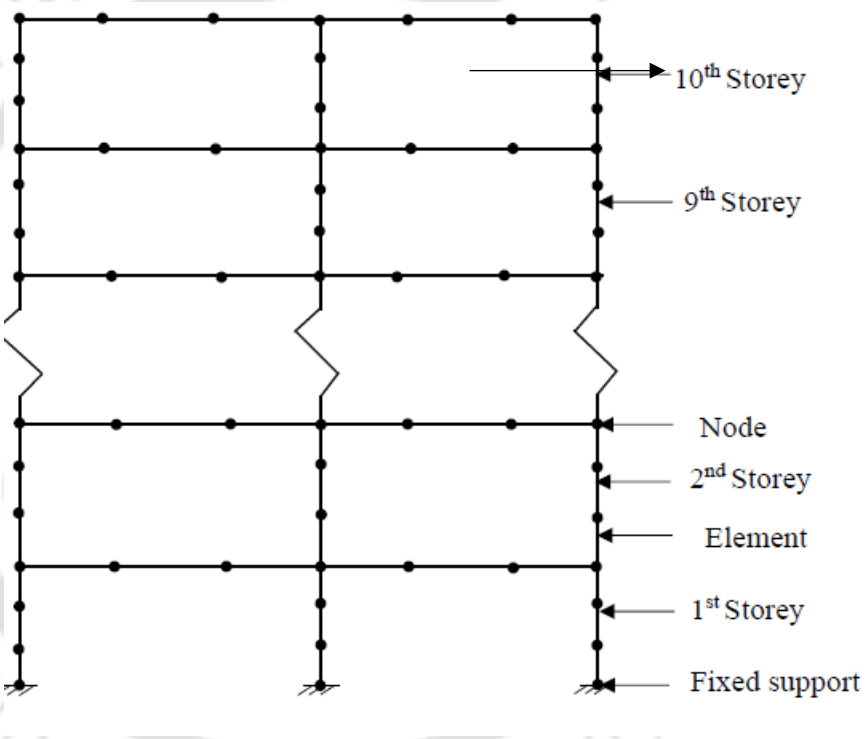

(a)

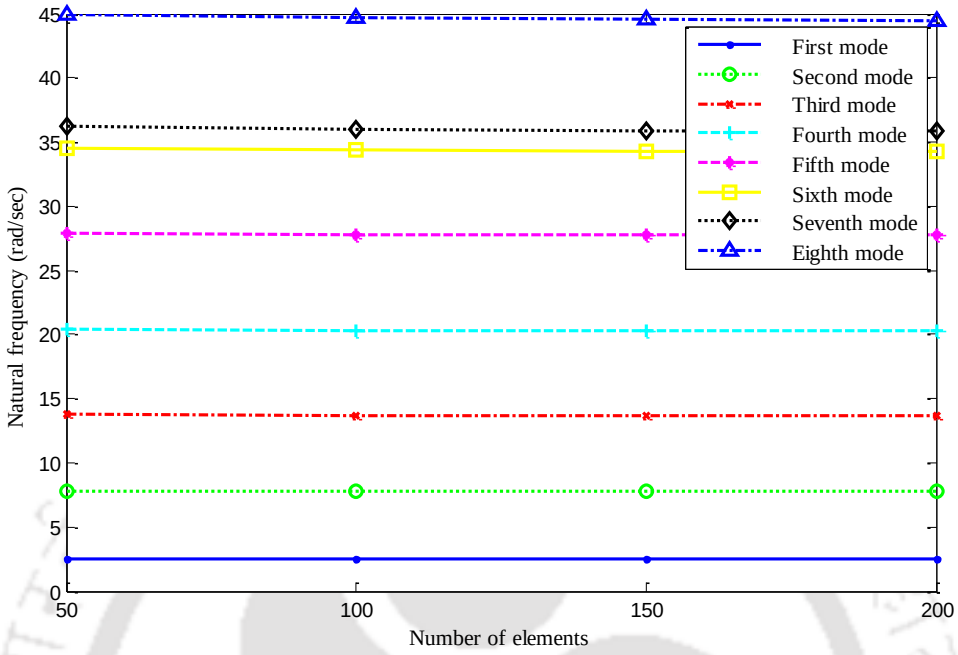

(b)

Figure 3.3. (a) Discretization of 2D freme and mesh generation, (b) Mesh convergence of natural frequencies of initial eight modes of vibration of frame

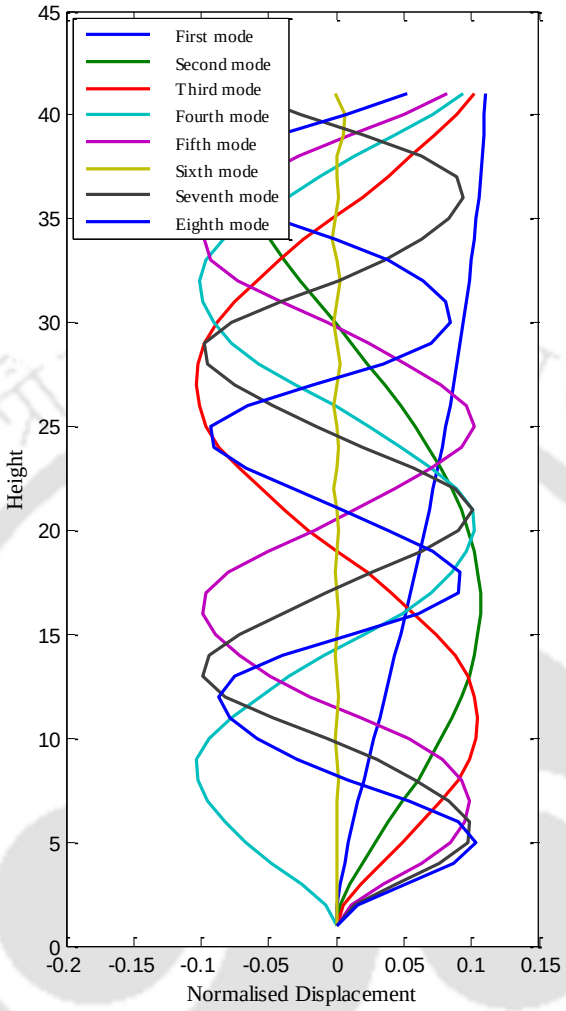

Figure 3.4. Mode shapes of initial eight modes of vibration of structure

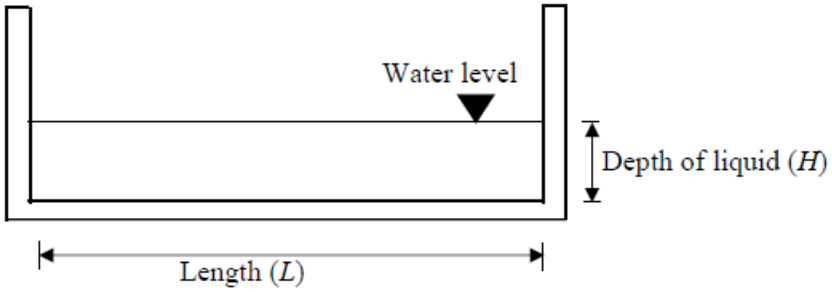

Elevation

(a)

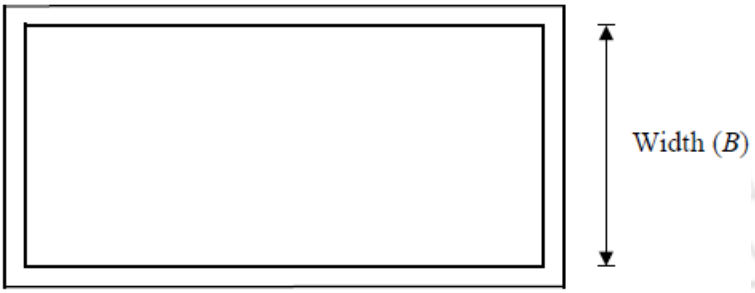

Plan

(b)

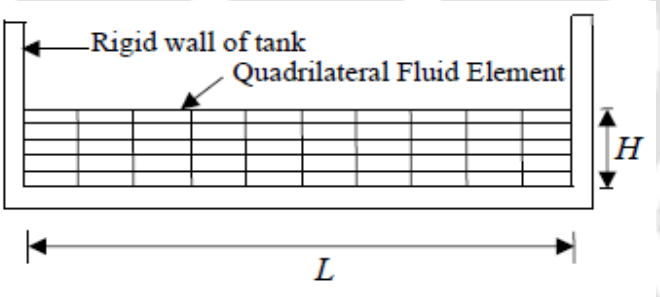

(c)

Figure 3.5. Flat bottom tuned liquid damper (a) Elevation, (b) Plan, (c) Discretization of fluid element and mesh generation in TLD

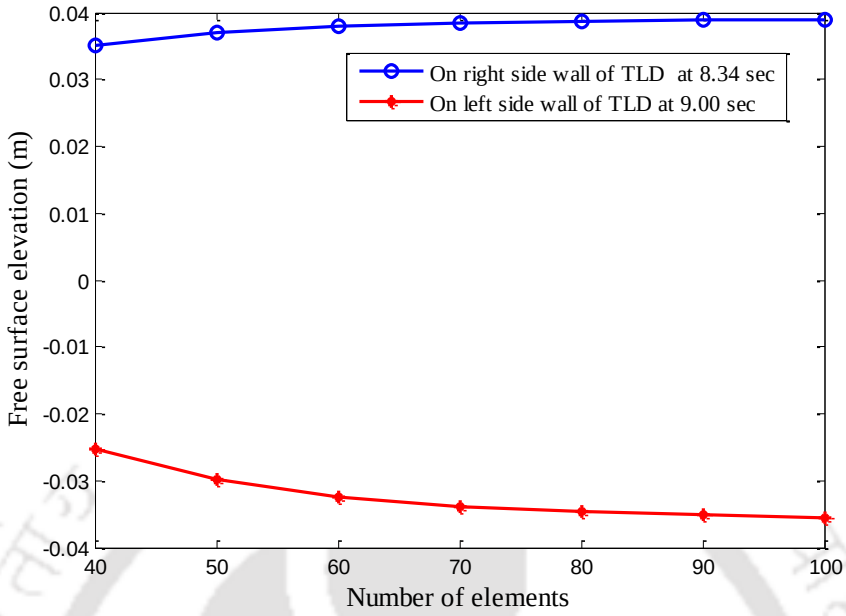

Figure 3.6. Mesh convergence of free surface elevation in rectangular flat bottom TLD

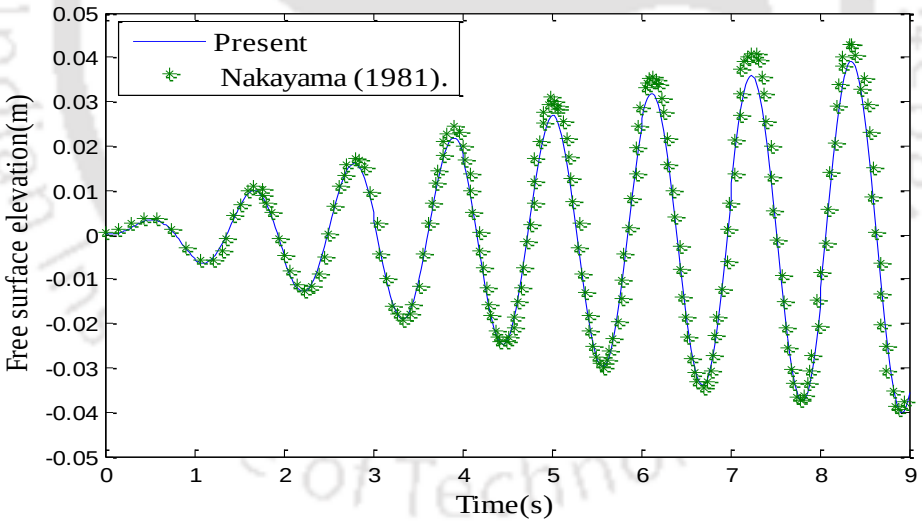

Figure 3.7. Free surface elevation near wall of tank/TLD (H = 0.60m, B = 0.90m) under harmonic excitation $\ddot{x} = -x_{00}\omega^2 \sin \omega t$ (x_0 = 0.002 m and ω = 5.50 rad/sec).

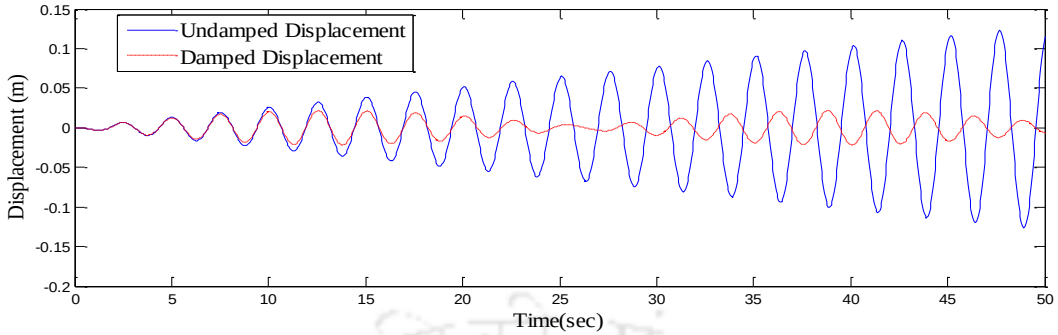

Figure 3.8. Response of structure with TLD: dimensions L = 3.00 m and H = 0.677 m

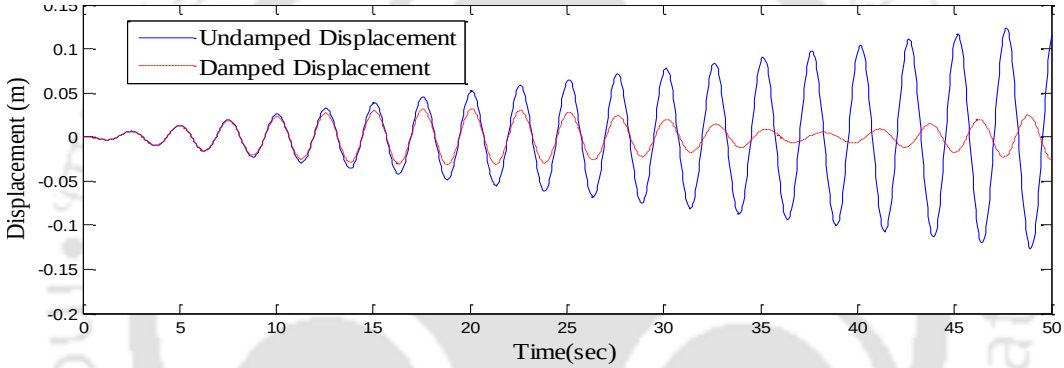

Figure 3.9. Response of structure with TLD: dimensions L = 2.38 m and H = 0.40 m

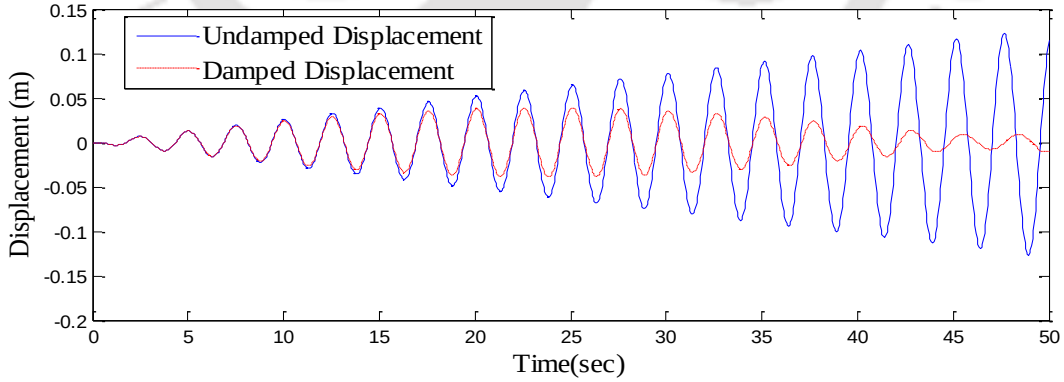

Figure 3.10. Response of structure with TLD: dimensions L = 2.08 m and H= 0.30 m

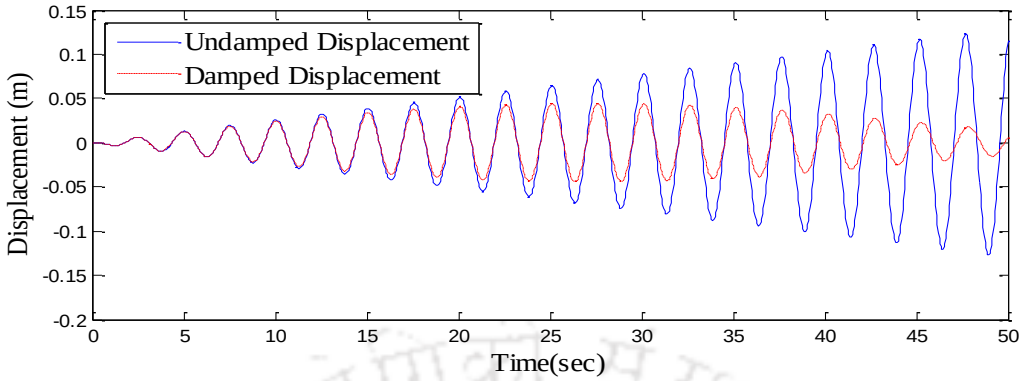

Figure 3.11. Response of structure with TLD: dimensions L = 1.91 m and H = 0.25 m

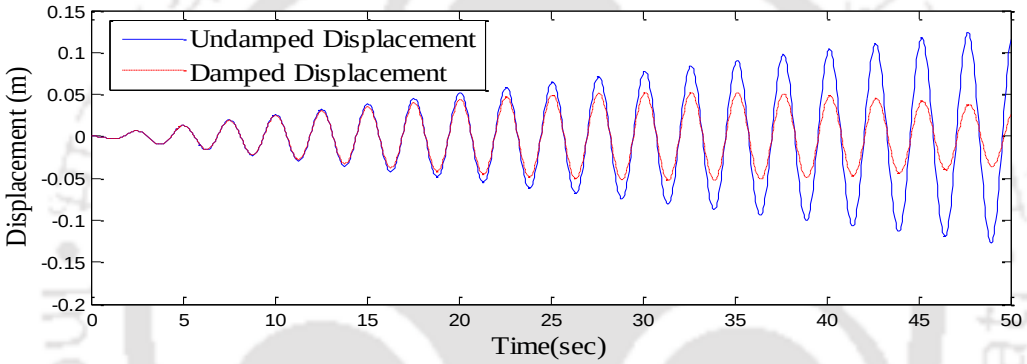

Figure 3.12. Response of structure with TLD: dimensions L = 1.72 m and H = 0.20 m

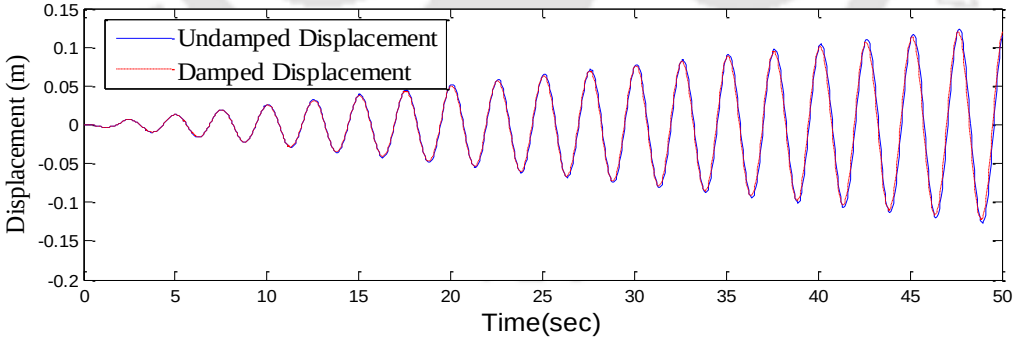

Figure 3.13. Response of structure with TLD for 90 % tuning

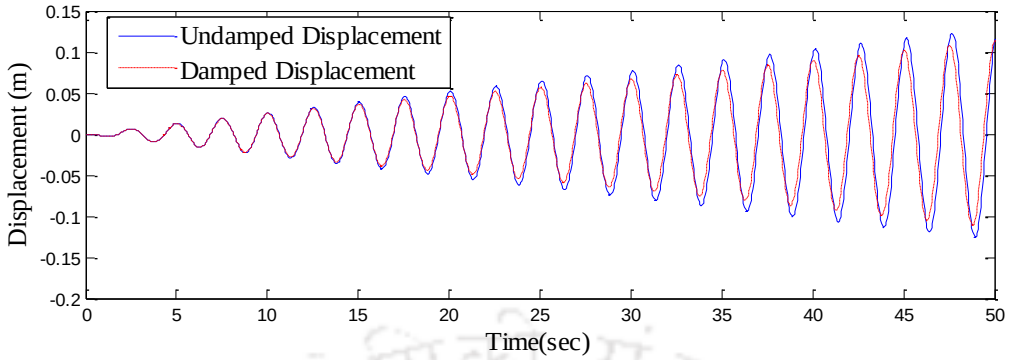

Figure 3.14. Response of structure with TLD for 95 % tuning

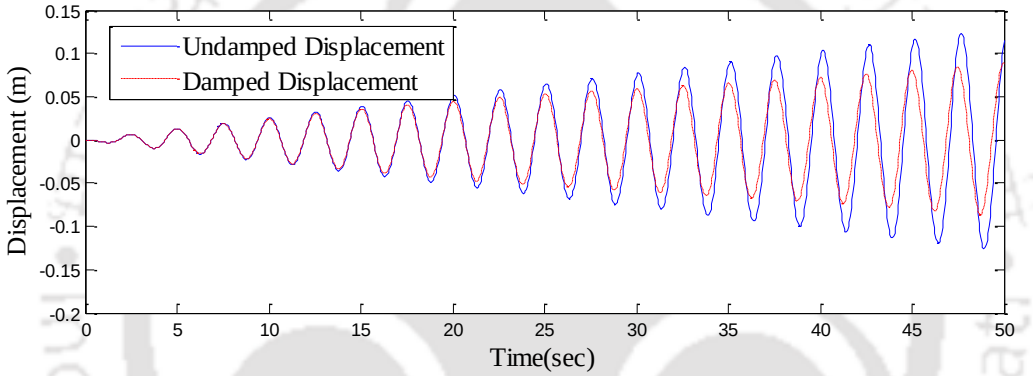

Figure 3.15. Response of structure with TLD for 97 % tuning

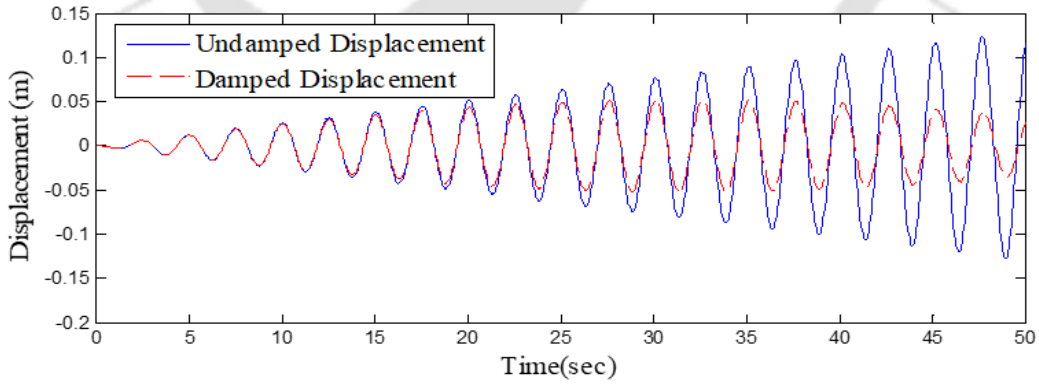

Figure 3.16. Response of structure with TLD for 100 % tuning

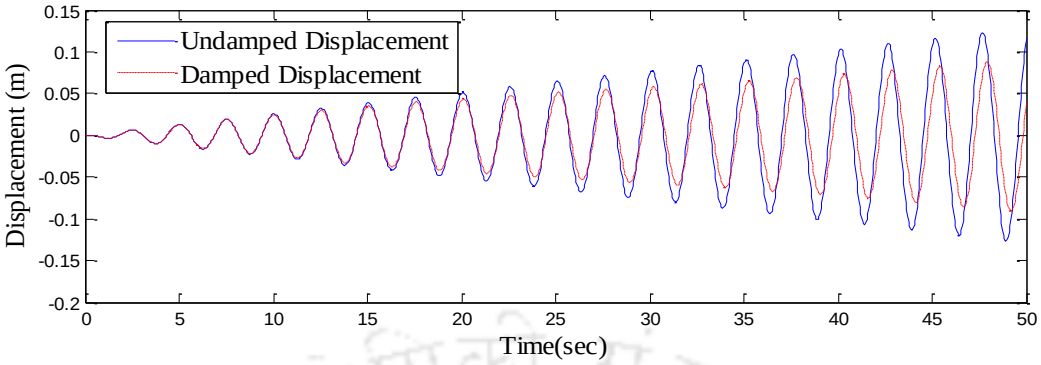

Figure 3.17. Response of structure with TLD for 103 % tuning

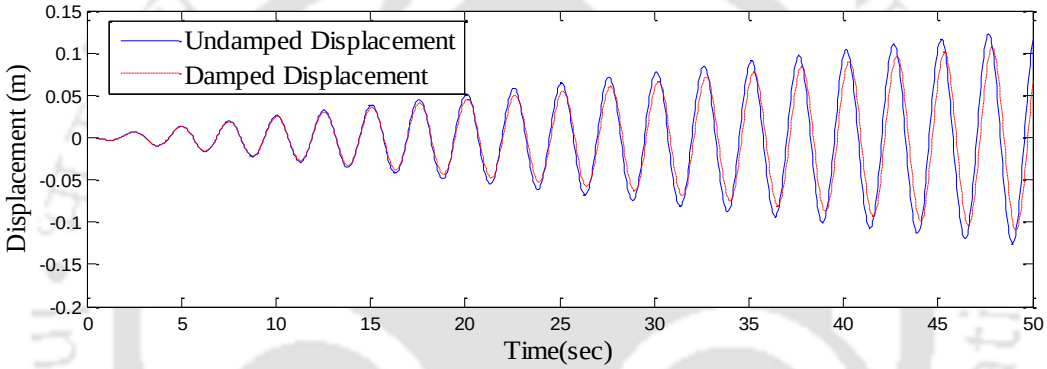

Figure 3.18. Response of structure with TLD for 105 % tuning

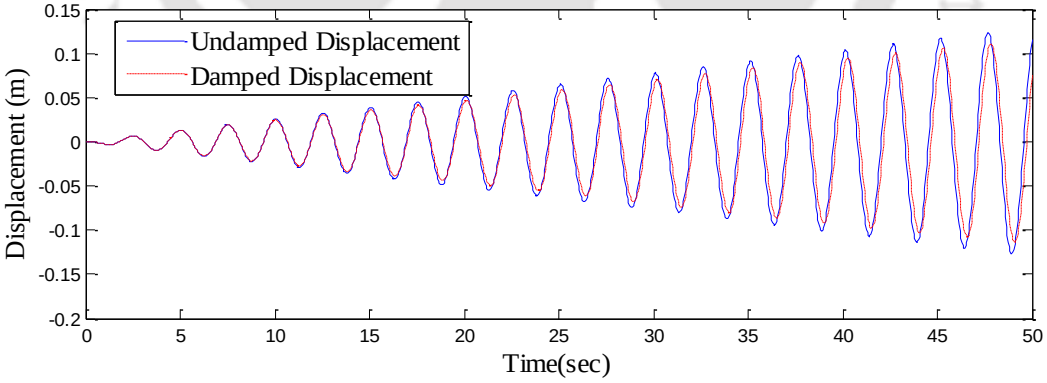

Figure 3.19. Response of structure with TLD for 107 % tuning

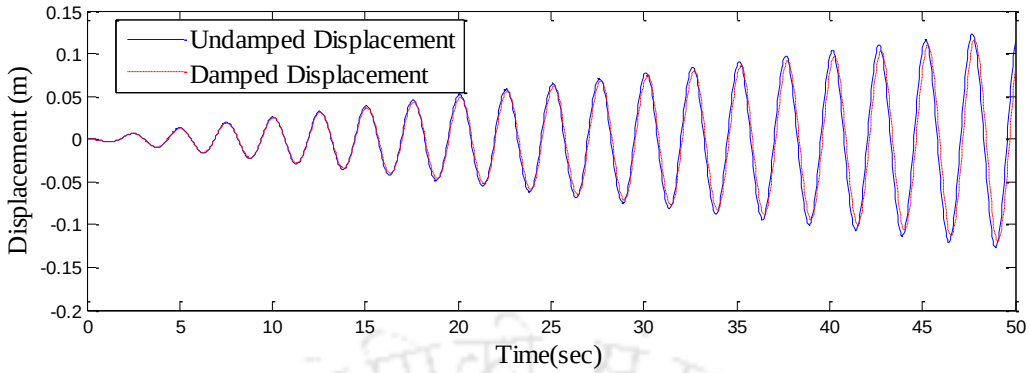

Figure 3.20. Response of structure with TLD for 110 % tuning

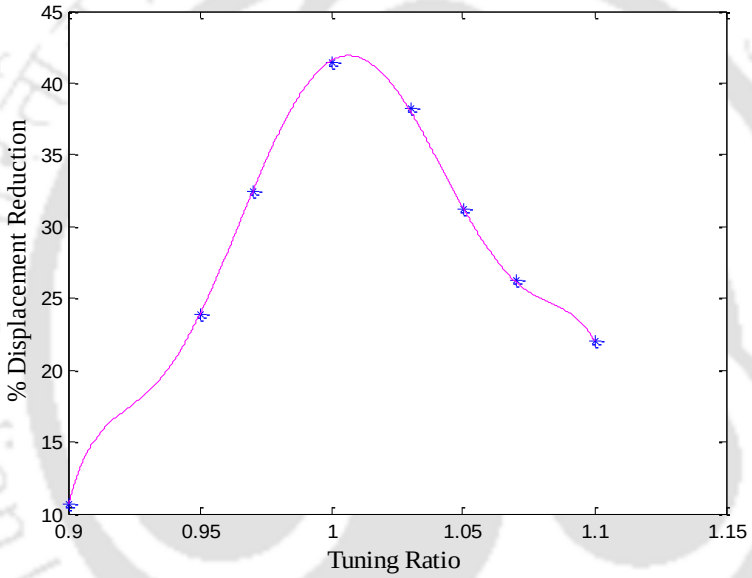

Figure 3.21. Variation of reduction in displacement of structure with tuning ratio of TLD

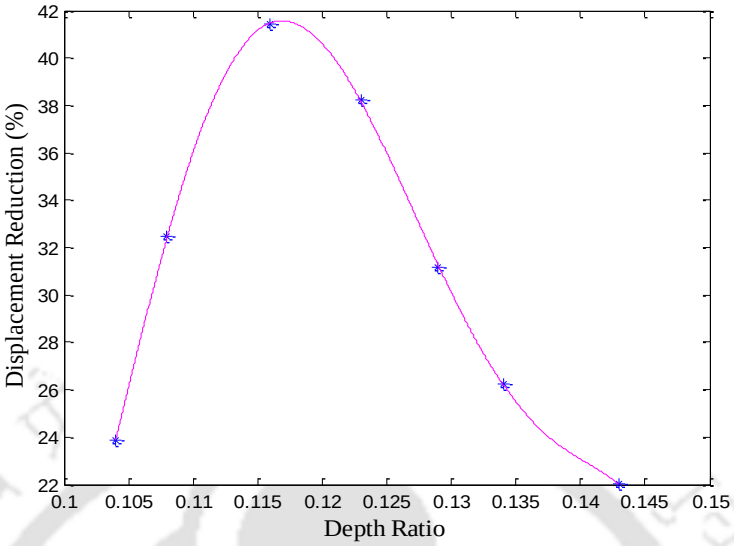

Figure 3.22. Variation of reduction in displacement of structure with depth ratio (*H/L*) of TLD

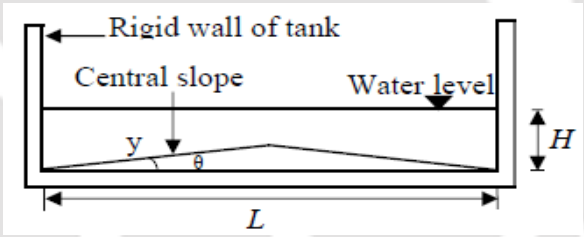

(a)

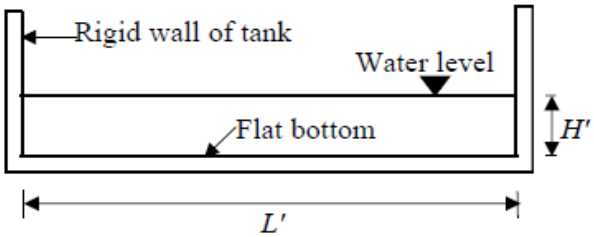

(b)

Figure 3.23. Sloped bottom TLD (a) Central slope TLD, (b) Equivalent flat bottom

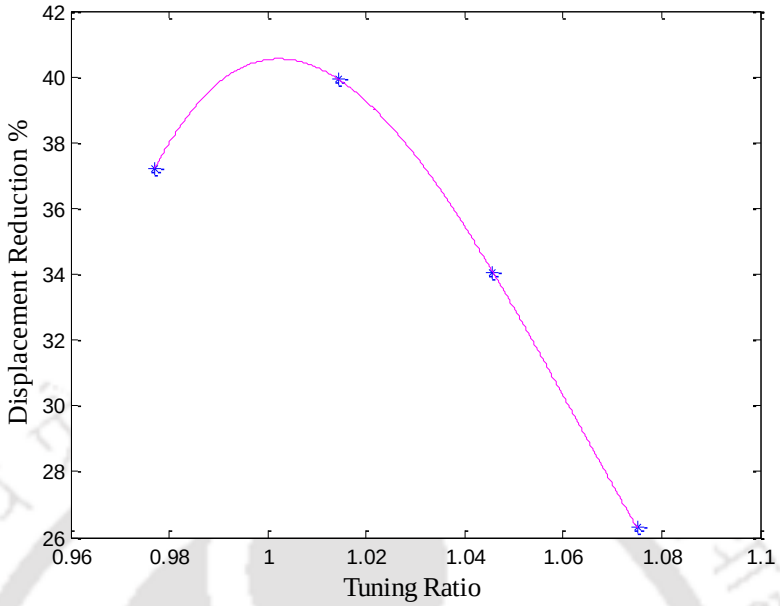

Figure 3.24. Optimum tuning with TLD length $L = L'$ and varying depth of liquid for 12.5º central slope (Xin's approach)

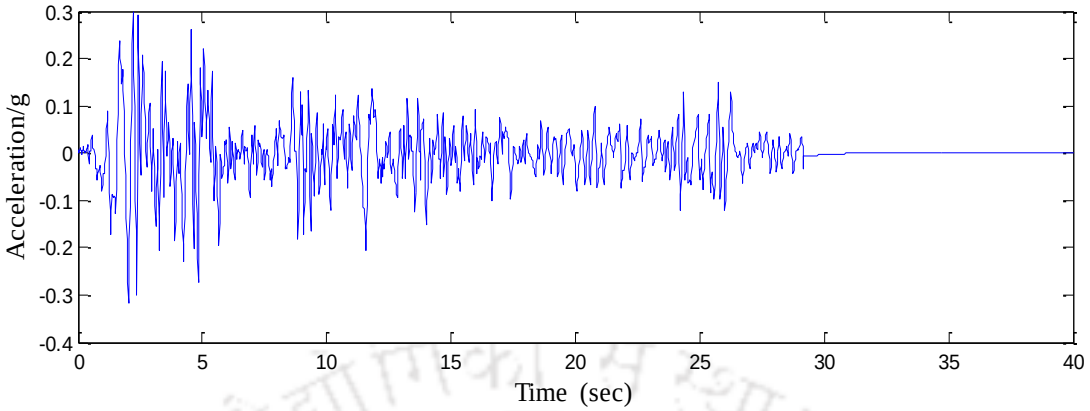

(a)

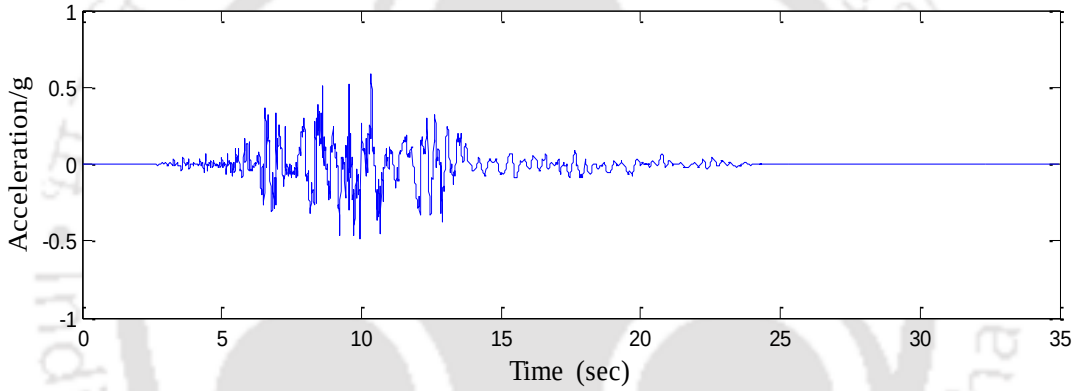

(b)

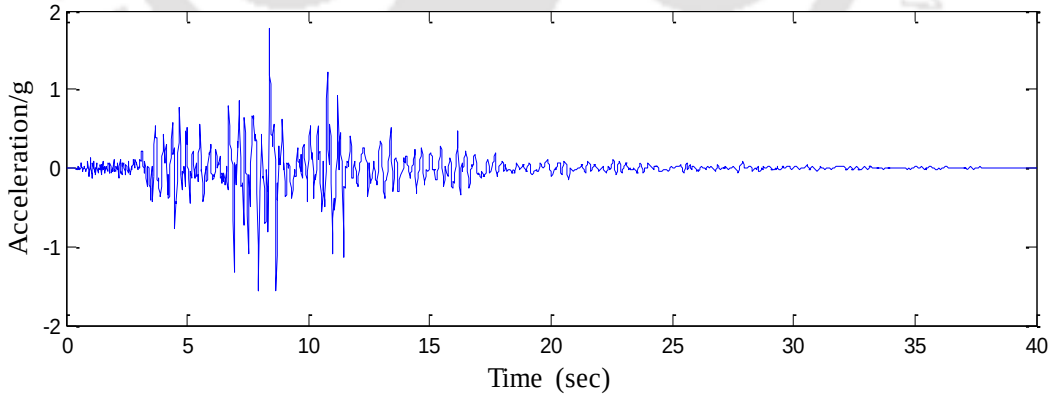

(c)

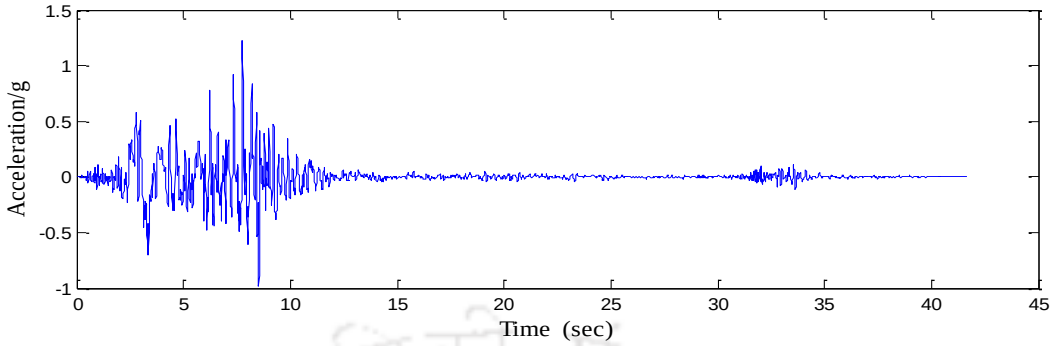

(d)

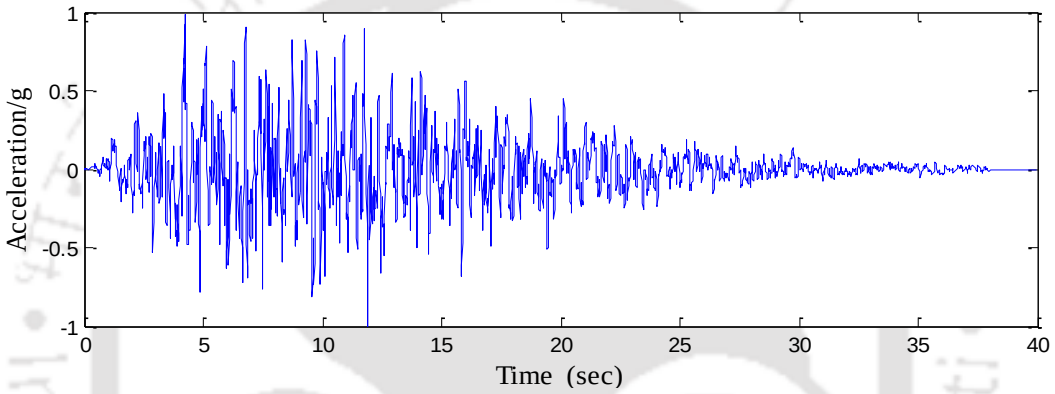

(e)

Figure 3.25. Time history of earthquake ground motions: (a) El Centro, (b) Loma Prieta, (c) Northridge, (d) San Fernando and (e) IS (1893) compatible time history

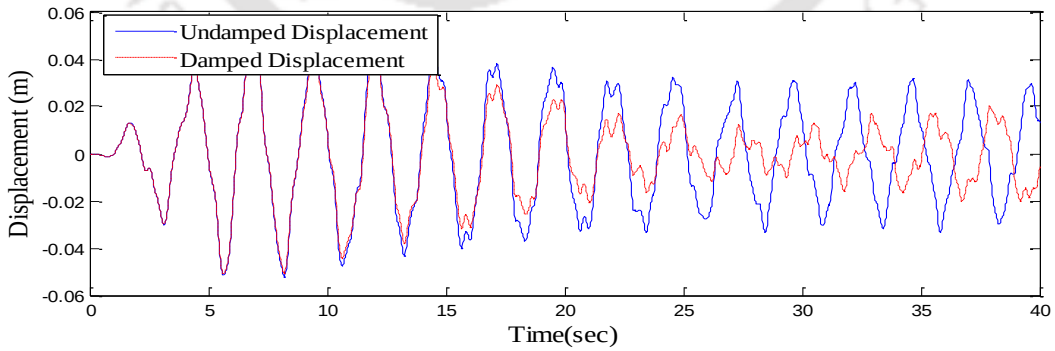

Figure 3.26. Response of structure with flat bottom TLD to El Centro earthquake

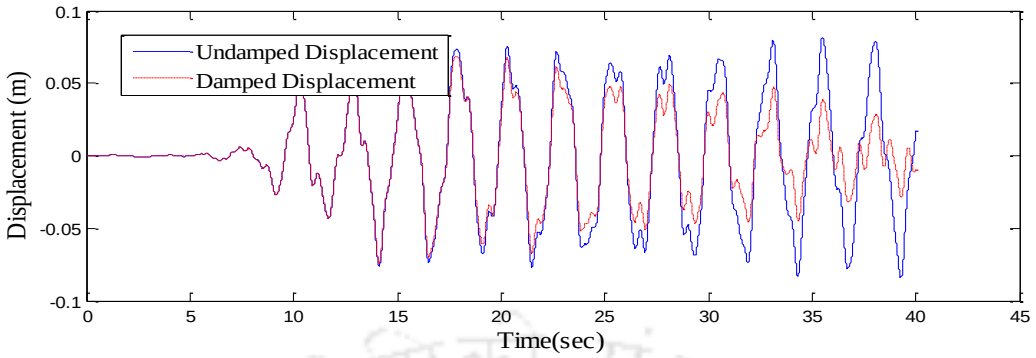

Figure 3.27. Response of structure with flat bottom TLD to Loma Prieta earthquake

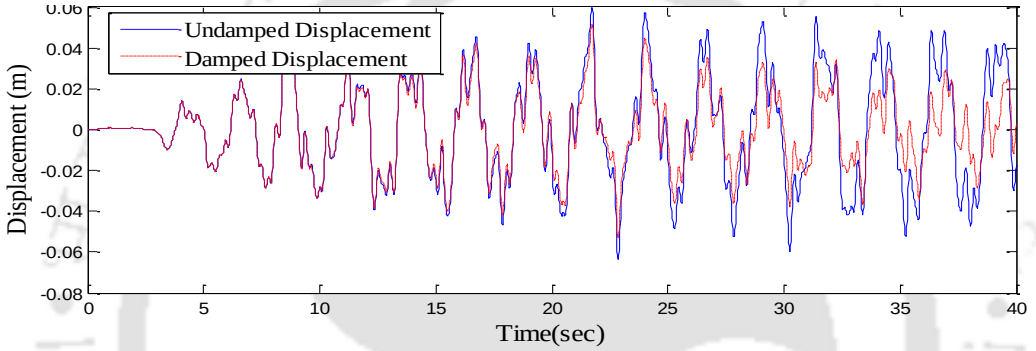

Figure 3.28. Response of structure with flat bottom TLD to Northridge earthquake

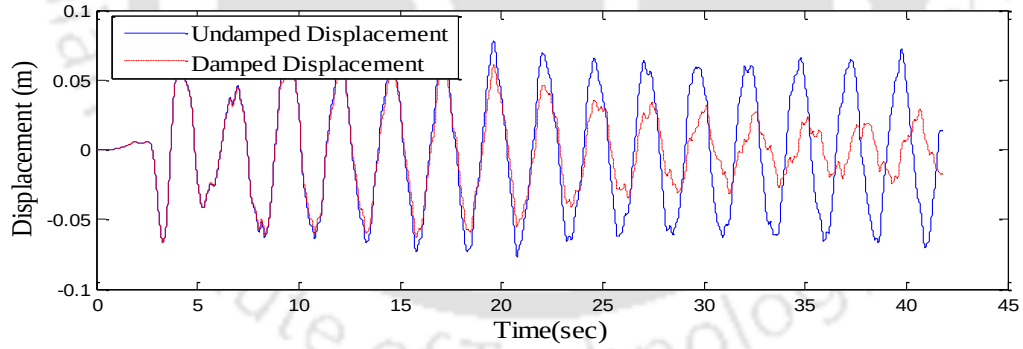

Figure 3.29. Response of structure with flat bottom TLD to San Fernando earthquake

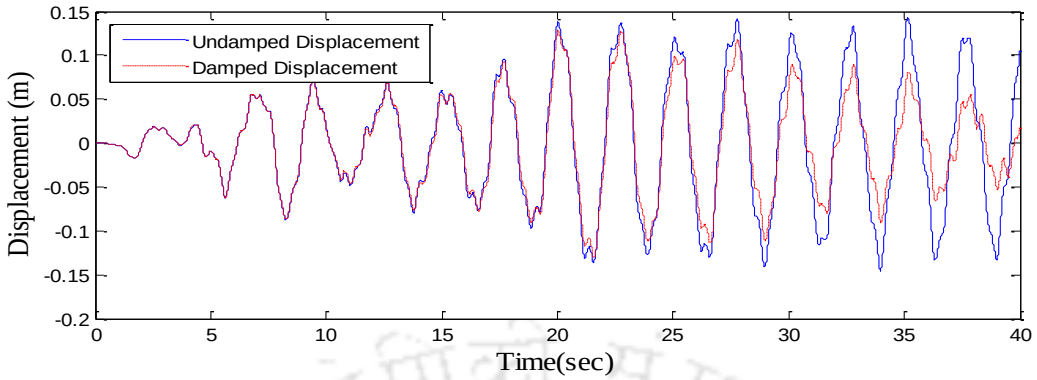

Figure 3.30. Response of structure with flat bottom TLD to IS compatible time history

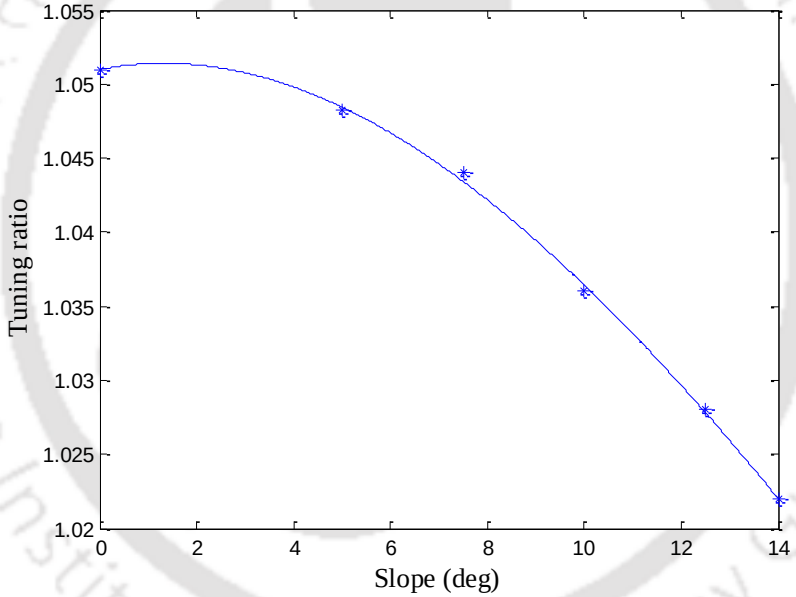

Figure 3.31. Variation of tuning ratio with central slope of TLD

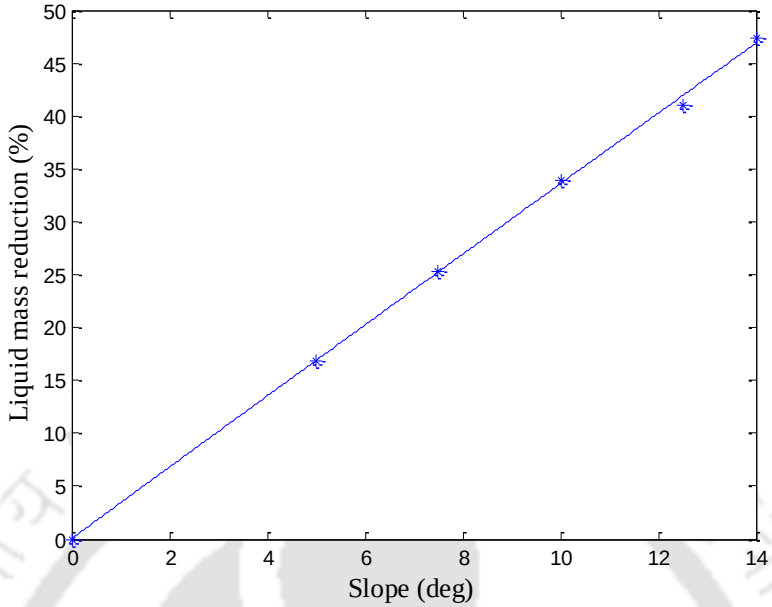

Figure 3.32.Variation liquid mass reduction with central slope of TLD

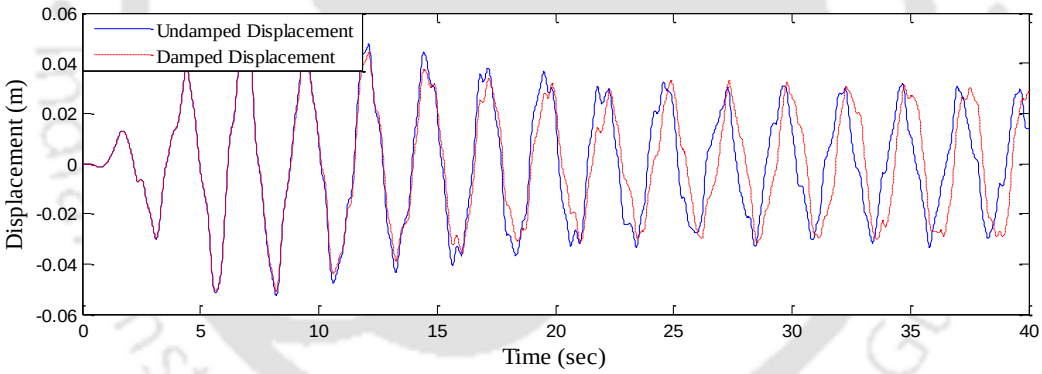

Figure 3.33. Response of structure with 5º central sloped TLD to El Centro earthquake

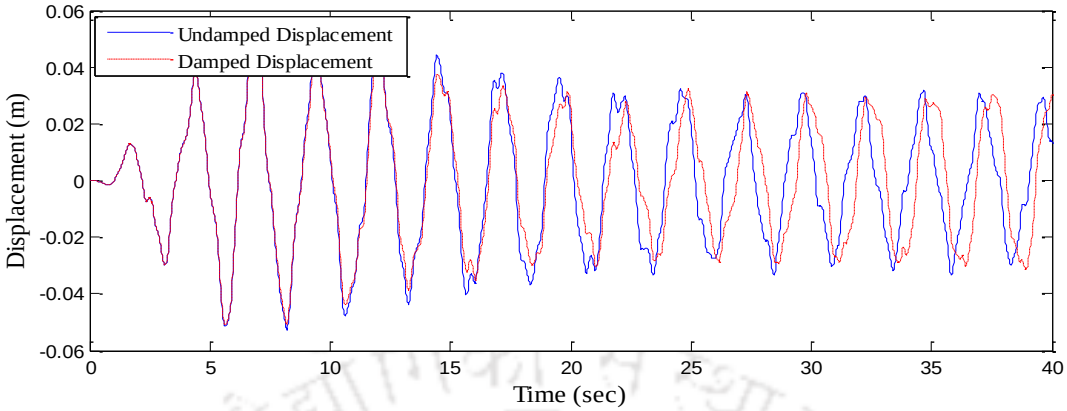

Figure 3.34. Response of structure with 7.5º central sloped TLD to El Centro earthquake

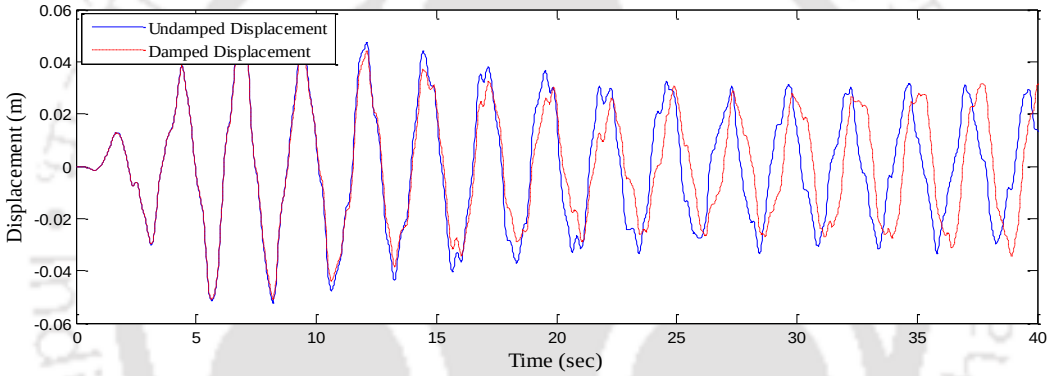

Figure 3.35. Response of structure with 10º central sloped TLD to El Centro earthquake

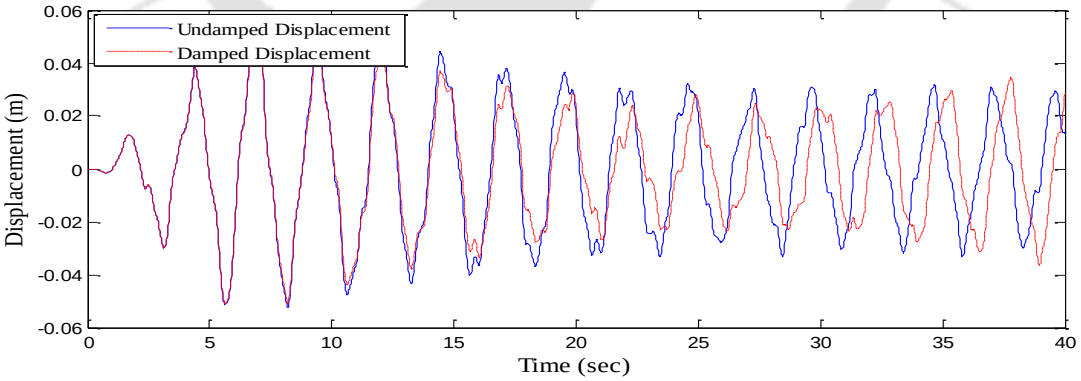

Figure 3.36. Response of structure with 12.5º central sloped TLD to El Centro earthquake

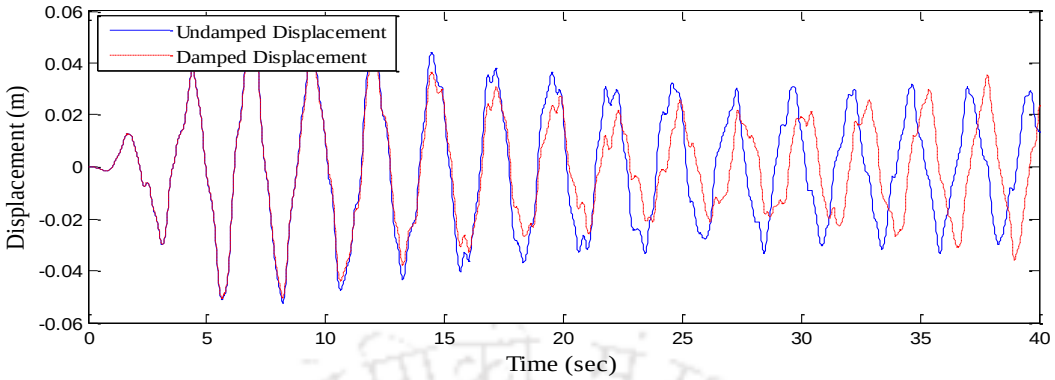

Figure 3.37. Response of structure with 14º central sloped TLD to El Centro earthquake

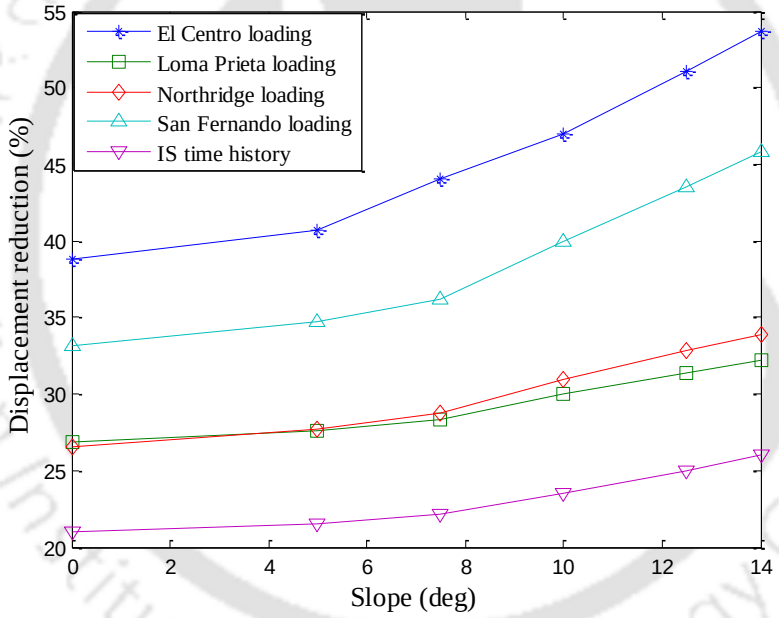

Figure 3.38. Variation of reduction in displacement of structure with central slope of TLD subjected to earthquakes and IS time history

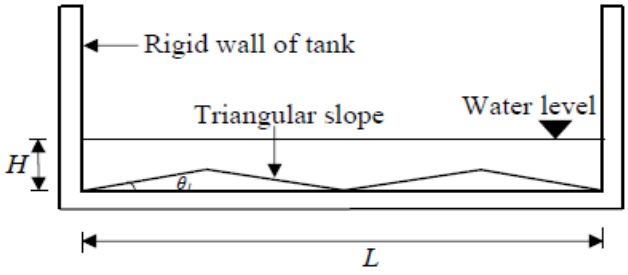

(a)

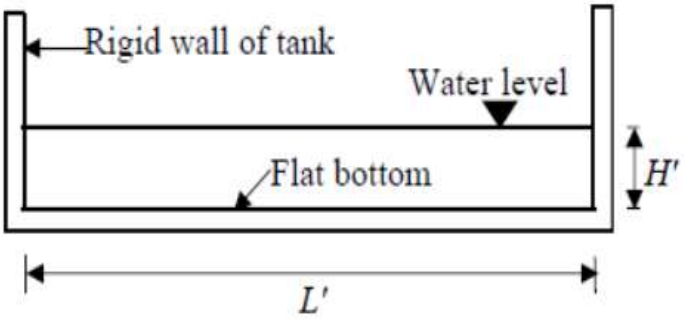

(b)

Figure 3.39. Sloped bottom TLD (a) Dual triangular slope TLD, (b) equivalent flat bottom TLD

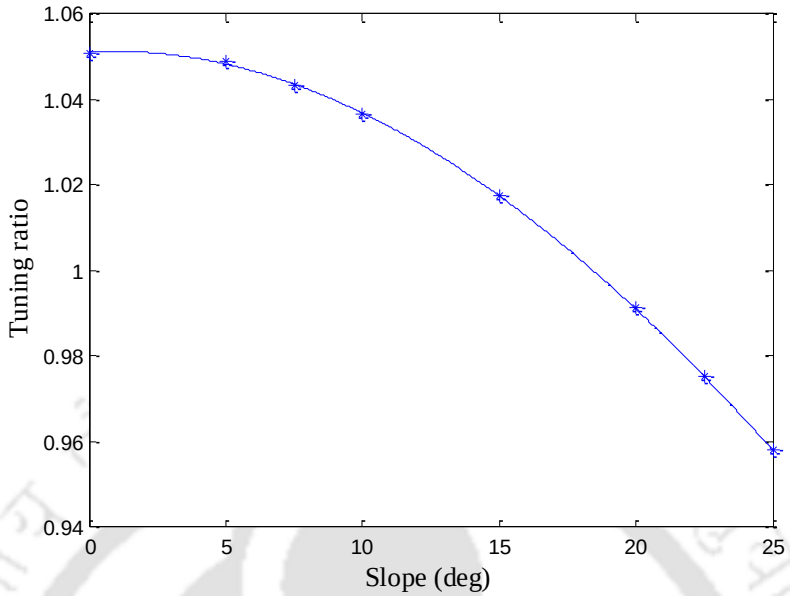

Figure 3.40. Variation of tuning ratio with dual triangular slope of TLD

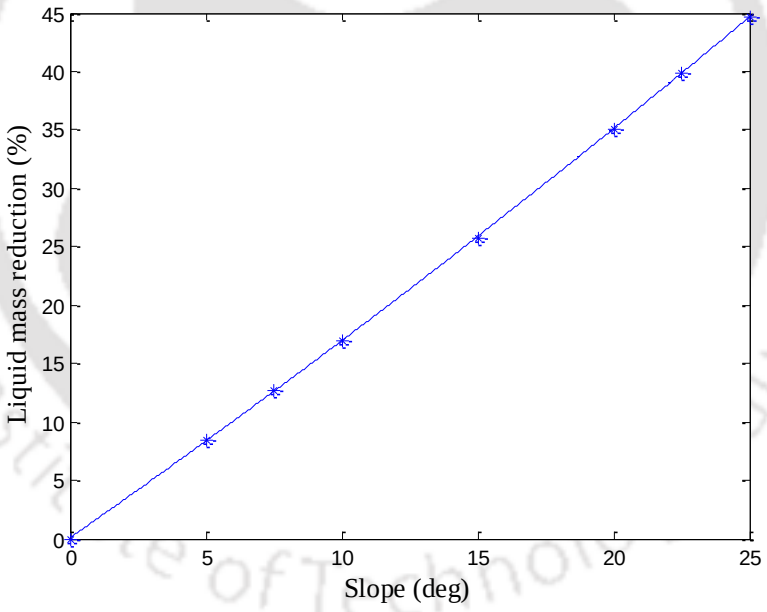

Figure 3.41. Variation of liquid mass reduction with dual triangular slope of TLD

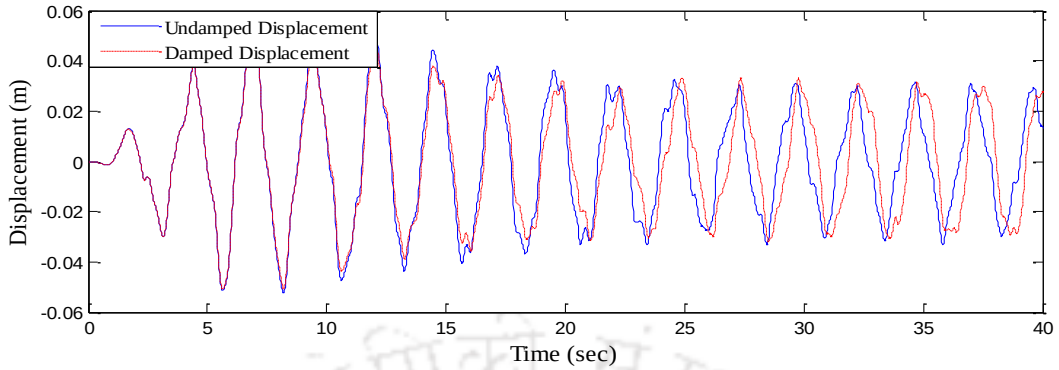

Figure 3.42. Response of structure with 5º dual triangular sloped TLD to El Centro earthquake

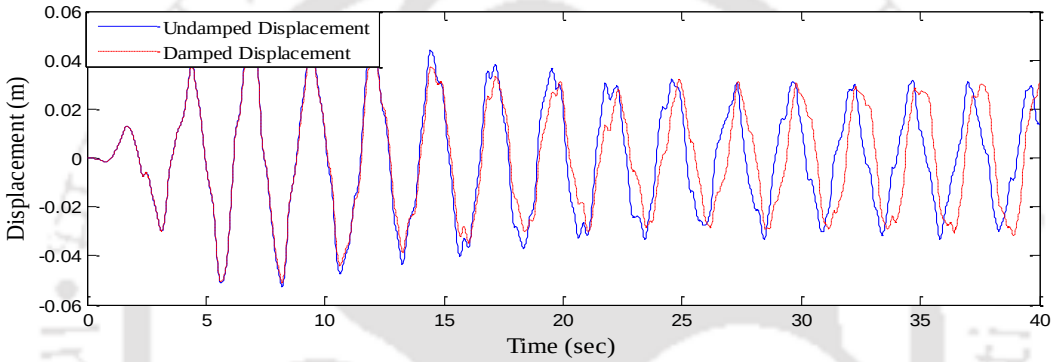

Figure 3.43. Response of structure with 7.5º dual triangular sloped TLD to El Centro earthquake

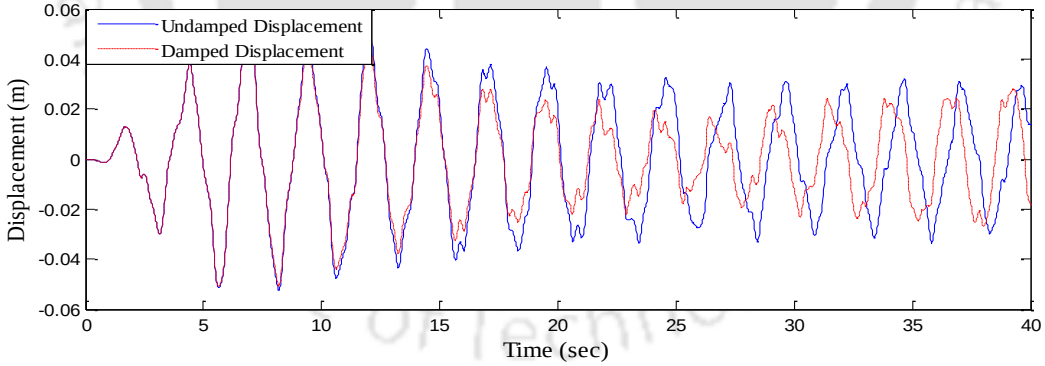

Figure 3.44. Response of structure with 10º dual triangular sloped TLD to El Centro earthquake

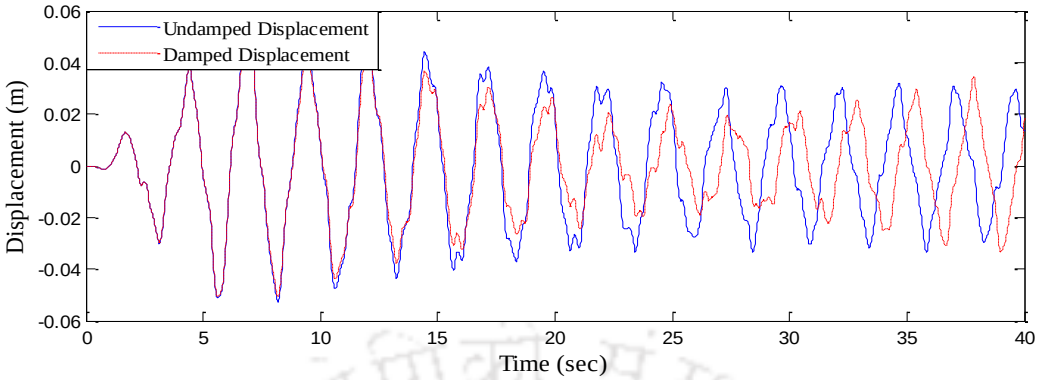

Figure 3.45. Response of structure with 15º dual triangular sloped TLD to El Centro earthquake

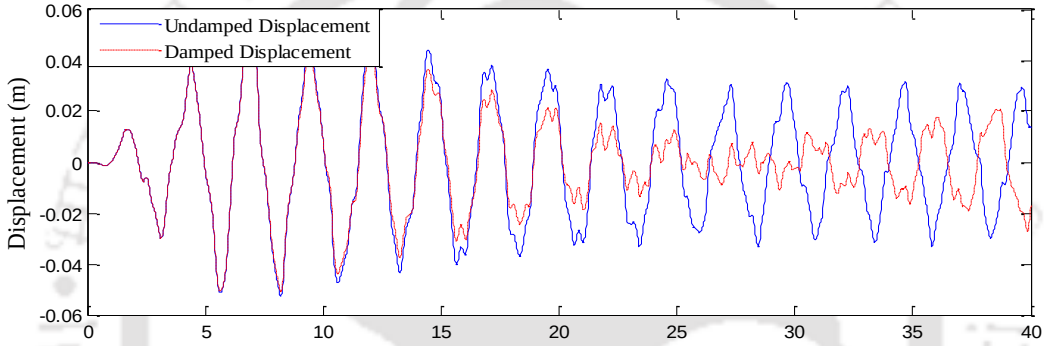

Figure 3.46. Response of structure with 20º dual triangular sloped TLD to El Centro earthquake

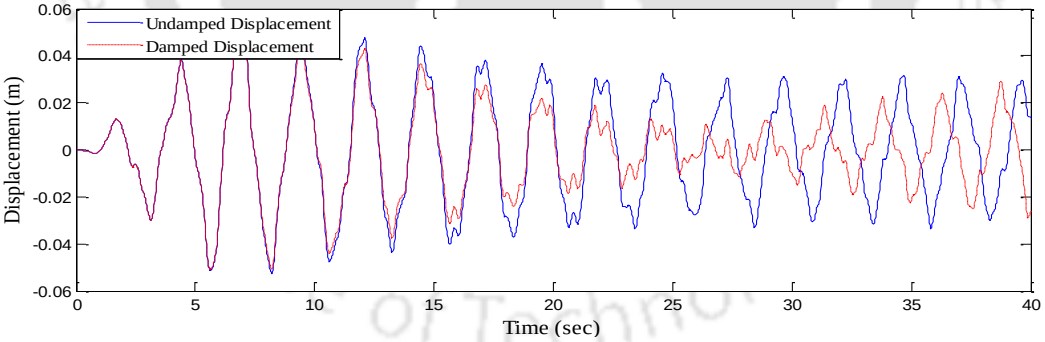

Figure 3.47. Response of structure with 22.5º dual triangular sloped TLD to El Centro earthquake

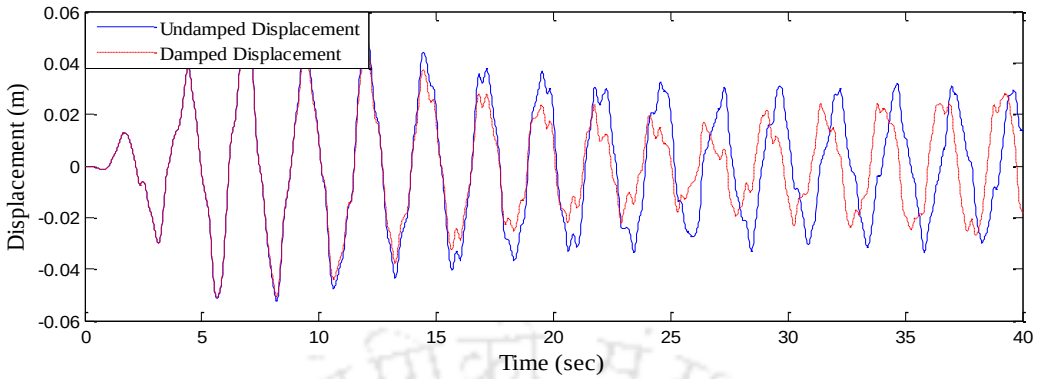

Figure 3.48. Response of structure with 25º dual triangular sloped TLD to El Centro earthquake

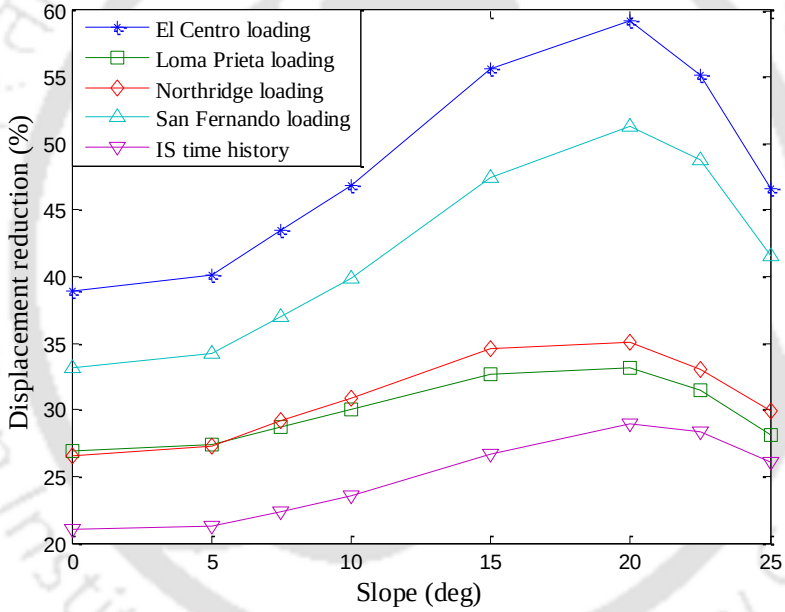

Figure 3.49. Variation of reduction in displacement of structure with dual triangular slope of TLD subjected to earthquakes and IS time history

CHAPTER 4

CONTROLLING RESPONSE OF STRUCTURE WITH APPLICATION OF END SLOPE BOTTOM TLD

4.1. INTRODUCTION

During forced excitation, liquid wave motion in a TLD may associate with initial few sloshing periods. However, the ensuing wave motion does not stop immediately after cessation of the excitation and leading to time lag for liquid motion to stop. This phenomenon of giving energy back to the attached structure (from the liquid in the TLD), is called beating and is known to have adverse effect on the performance of TLD. Such beating phenomenon may be minimised / avoided, if end slope TLD (see Figure 4.1) is used instead of the flat bottom TLD, as in the case of sloping beach where energy dissipation of water wave takes place. Further, as the runup-height amplification of wave is greater for sloping bottom than the vertical wall, greater horizontal force may be created with less water mass (Gardarsson *et. al.* 2001). The major benefit derived from the sloped bottom tank is more efficient use of liquid sloshing. (Olson and Reed 2001) reported and mentioned earlier in Section 2.3, initial tuning of slope bottom TLD should be at value, slightly greater than fundamental frequency of structure, for maximum effectiveness. As mentioned in the literature, Gararssson (2001) conducted limited experimental and numerical studies on isolated end slope TLDs. Hence, a detailed systematic study is being attempted on the dynamic response behaviour of end slope TLD attached on top of a 10-story reinforced concrete frame, as an alternative approach to central slope TLDs presented in the previous chapter (i.e. Chapter 3). More specifically, effect of end slope angles on the displacement reduction have

been computed using fluid-structure interaction finite element analyses, with both harmonic and earthquake time histories as base excitation inputs.

4.2. MODELLING OF END SLOPE TLD

For modelling the end slope TLD (Figure 4.1), two approached reported in the literature have been considered, *viz.*, Gardarsson's approach (Gardersson 2001) and 2) Xin's approach (Xin 2006). These two approaches, convert an end slope TLD into a virtual / equivalent flat bottom TLD, and thus enables the finite element formulation for flat bottom TLD to be used for the dynamic analysis. The two approaches are briefly described in the following sub-sections:

4.2.1. Gardarsson's approach

Gardarsson (2001) suggested that, for small *H/L* ratio (say (< 0.15 i.e. for shallow depth TLD) fundamental frequency of sloshing of liquid for a flat bottom TLD can be given by an approximate relation

$$fb = \sqrt{\frac{gH}{2L}} \tag{4.1}$$

$$\text{Or, } f_b = \sqrt{\frac{\pi g}{L}} \tanh \frac{\pi H}{L} \tag{4.2}$$

where L is length of tank in flat bottom or box shaped TLD, and it is the length of still water surface in sloped bottom TLD. The geometric parameter suggested by Garsersson (2001) '***s***' (see Figure 4.2), is the ratio of horizontal distance *'x + x'* (see Figure 4.1 (a)) over sloped surface to water surface length *L*. Thus, the geometric parameter is given by:

$$s = \frac{x + x}{L} \tag{4.3}$$

For triangular shaped TLD; *s* = 1 and for box (flat bottom) shaped TLD; *s* = 0 (Figure 4.2).

The sloshing frequency of liquid in sloped bottom tank (f) is then, determined from the geometric curve (plot of f_s/f_b vs. s), primarily developed from 30º slope bottom TLD. After determining the natural frequency of liquid (f) in the slope bottom TLD and considering the depth of liquid to be equal to the deepest liquid depth of the original sloping bottom tank (i.e. $H' = H$), the corresponding length (L') of the virtual flat bottom can be calculated using the relation:

$$f = \sqrt{\frac{\pi g}{L'}} \tanh \frac{\pi H}{L'} \tag{4.4}$$

Again, considering a constant total mass of liquid in the tanks (virtual and original tanks), the width of the virtual flat bottom tank can be determined by Equation 3.9 as

$$B' = \frac{V_w}{H'L'}$$

As stated earlier in Section 3.8, $L' > L$ and $B' < B$. However, it may be noted that Gardarsson's approach has limitations to implement for slopes other than end slope. For sample calculations see Appendix B (Section B.5, B.6).

4.2.2 Xin's approach

TLD with end slopes at the bottom can be modified to an equivalent flat bottom TLD using Xin's approach (detailed in Chapter 3). As discussed earlier, Xin's approach is based on wetting length, and thus this approach can be used to convert various slope TLDs such as central slope TLD, dual triangular slope TLD and end slope TLD in to equivalent flat bottom TLD.

Thus, for ends slope angle, α, wetting length of TLD with end slope at one end is given by

$$y' = \frac{H}{Sin(\alpha)} \tag{4.5}$$

Therefore, the total wetting length of the TLD with two ends slopes are given by

$$L' = L_1 + 2y' \quad \text{(Olson and Reed2001)} \tag{4.6}$$

where L_1 is the horizontal distance of TLD at bottom (Figure 4.1).

Width of tank is determined by using the principle of equal volume and same depth of liquid in slope bottom and equivalent flat bottom tank.

4.3. DYNAMIC ANALYSIS OF STRUCTURE WITH END SLOPE BOTTOM TLD

For the dynamic analyses of the structure with end slope bottom TLD, the depth of the liquid has been adopted as 0.2235 m, to make the analyses consistent with the earlier study with central slope TLD (presented in Chapter 3). For the finite element analyses, the end slope TLDs are converted to equivalent / virtual flat bottom TLDs, using the approach proposed by Gardarsson (2001) or Xin (2006). To assess the effect of end slope, the angle of end slope has been varied from 15º to 50º. This range of end slope angles has been arrived at based on trial runs, so as to have improved performance as compared to comparable flat bottom TLD. Effect of both harmonic and earthquake time histories have also been evaluated. Again, in order to evaluate the effectiveness of TLD alone, inherent damping of structure is not taken into account in the analysis, as before. Horizontal force offered by TLD is applied at the roof level of frame structure, i.e. at the base level of the TLD. Similar discretisation of both the liquid domain and frame members have been adopted, as used in the earlier study (see Chapter 3). The results of the analyses have been presented in the form of variation of roof level displacements with time. The results obtained through the finite element analyses have been grouped based on the approached adopted (Gardersson's and Xin's approaches), as follows.

4.3.1. Dynamic analysis with slope bottom TLD (Gardarsson's approach)

Gardarsson's approach provides a relationship between the sloshing frequency of liquid in the TLD to the geometric shape parameter of the end slope bottom TLD, as described in Section 4.2.1. A plot of the variation of f/f_b (frequency of sloshing in sloped bottom TLD/frequency of sloshing in box shaped TLD) vs shape or geometric parameter (s) is shown in Figure 4.2. Using initial dimensions of the TLD as L = 1.72 m, H = 0.2235 and B = 1.0 m, as arrived based on harmonic analysis of flat bottom TLD, and presented in Chapter 3, have been used, to compute equivalent flat bottom TLD dimensions, for end slope bottom TLD dimensions, using the curve plotted in Figure 4.2. The details of the equivalent flat bottom TLDs, for end slope angles ranging from 15-50º are given in Table 4.1. The length and width of the equivalent flat bottom tank, ranges from 2.2-1.73 m and 0.40-0.88 m, respectively. As stated earlier, the depth of liquid remains constant in sloped bottom TLD and equivalent flat bottom TLD. Using these various equivalent flat bottom TLD dimensions, FE analyses have been performed for both harmonic and earthquake time history base excitations (mentioned in Chapter 3), and are presented in the form of variation displacement with time.

4.3.1.1. Response of structure with TLD subjected to harmonic motion

Results of the FE analyses of the reinforced concrete frame with end slope bottom TLDs, subjected to harmonic base excitations, have been shown in Appendix D (see Figures D.1–D.3 for 15º, 30º and 45º end slopes). From the analyses it has been found that the optimum end slope angle for maximum displacement response reduction is around 30.5º (see Figure D.4). The displacement response reduction observed at optimum slope is around 37.72 %. Ratio, (Mass of liquid in flat TLD / Mass liquid in slope TLD) at optimum slope is observed to be around **1.282.** Gardarsson (2001) also found this ratio as **1.28.**

a) Influence of slope on tuning ratio of TLD

Tuning ratios for TLD with end slopes are presented in Table 4.1. A plot of tuning ratio vs slope at the TLD bottom is shown in Figure 4.3. It is seen that the tuning ratio of TLD increases with increase in end slope angle and the variation is found to be nonlinear. At lower angles of slope, the rate of increase of tuning ratio is relatively higher and at higher angles of end slope, the rate of increase is marginal and flattens out. Minimum tuning ratio of 0.828 and maximum of 1.043 have been observed at slope angle of 15º and 50º respectively. A tuning ratio of 1.0 can be seen at end slope angle of 30.5º. Optimum tuning ratio (where displacement response reduction maximum) is observed to be around 1. At higher angles of end slope of TLD (> 45º), the variation in tuning ratio is seen to be negligible.

b) Influence of slope on liquid mass reduction

Liquid mass reduction with the application end slopes at the bottom of TLD are sown in Table 4.1. It is observed that the liquid mass reduction in TLD decreases with increase of end slope at the TLD bottom and variation of liquid mass reduction is observed to be nonlinear (see Figure 4.4). Maximum liquid mass reduction of about 48.46 % and minimum liquid mass reduction of about 10.90 % have been observed for 15º and 50º end slopes, respectively. The liquid mass reduction of about 22 % is observed for the optimum angle of 30.5º (for maximum value of displacement response reduction).

4.3.1.2. Response of structure with TLD subjected to earthquake ground motion

Five earthquake time histories viz., El Centro (1940), Loma Prieta (1989), Northridge (19940 and San Fernando (1971) earthquake ground motions and IS compatible time histories (see Figures 3.25 of Chapter 3) have again been considered as input motions at the base of the RC frame structure with end slope

bottom TLD, and analyse has been performed using the developed FE code. The displacement responses of the structure with TLD are monitored and results are presented in the following sub-sections for each of the time histories.

a) Response to El Centro earthquake ground motion

FE analysis of structure with TLD subjected to El Centro earthquake ground motion has been performed. Representative displacement response time histories of undamped and damped displacements of structure for TLDs with slopes of 15º, 20º, 25º, 30º, 35º, 40º, 45º and 50º are shown in Figures 4.5-4.12. Results of the dynamic analyses are shown in the Table 4.2. The reduction in displacement of structure with flat bottom TLD as evaluated in Chapter 3 is 40.97 %. From the results it is seen that the reduction in displacement of the structure increases with increase in end slope angle of the TLD. Reduction in displacement of structure with application of TLDs having end slope 15º, 20º, 25º, and 30º increases and are found to be ~3.30%, 21.22 %, 43.81 % and 47.51 % respectively. Whereas reduction in displacement with TLDs having end slopes 35º, 40º, 45º, and 50º decreases and are observed to be ~43.68 %, 42.63 % and 40.53% and 39.36% respectively. As observed from Figure 4.13, there is relatively a sharp rise in displacement reduction of structure with TLDs having slope 15–25º. The rate of reduction in displacement is relatively mild for the TLDs with slope 25º - 30º and it decreases for end slope of 30º and above. Also, it is observed that the reduction in displacement with TLD having 45º slope is approximately similar to that of flat TLD, suggesting that TLDs having end slope ≥ ~ 45º, there is no benefit of the TLD with end slope over flat bottom TLD (for 45º end slope TLD DR = 40.53 % and for flat TLD DR = 40.97 %).

b) Response to Loma Prieta earthquake ground motion

Displacement response of structure with slope bottom TLD to Loma Prieta earthquake are shown in Table 4.2. From the analysis it is observed that the

reduction in displacement is increasing with slope of TLD up to 30º and marginally reducing for higher end slope angle. The displacement reduction of the structure with TLDs having slope of 15º, 20º, 25º and 30º are observed to be ~3.30 %, 14.00 %, 24.10 % and 26.50 % respectively. The displacement reduction of structure with application of TLDs having end slopes of 35º, 40º, 45º and 50º are observed to be ~26.40 %, 26.40 %, 26.10 % and 25.00 % respectively. The rate of increase in damping (reduction in displacement) is observed to be relatively faster for smaller end slope angles (e.g. 15–25º) at bottom of TLD (Figure 4.13). The rate of increase in damping is relatively small for the TLDs with slopes 25-30º. The rate of decrease of damping of structure is almost nil for TLDs having end slope above 30º. Again, for the case of TLD with end slope of 45º

, reduction in displacement is nearly the same as that of flat bottom TLD (for 45º end slope TLD DT = 26.10 % and for flat TLD *DR* = 26 %).

c) Response to Northridge earthquake ground motion

The results of dynamic analysis for the input of Northridge earthquake ground motion are provided in Table 4.2. As seen from Figure 4.13, the rate of reduction of displacement of structure is found to be relatively higher (~2.23 % values) for the TLDs with end slopes 15–25º and it becomes moderate (~ 0.56 % values) for angles of TLD 25-30º. It is observed that the reduction in displacement of the structure increases with increase in end slope angle up to 30º. However, the reduction in displacement for end slopes of 15º, 20º, 25º, 30º are observed to be ~3.30 %, 14.00 %, 25.60 %' and 28.40 % respectively. Further, it is seen that TLD becomes less effective in mitigating the displacement of structure for end slopes of above 30º. The reduction in displacement for TLDs with end slopes of 35 º, 40 º, 45º and 50 º are observed to be 27.40 %, 27.70 %, 26.90 % and 26.40 % respectively.

d) Response to San Fernando earthquake ground motion

Response of structure with sloped bottom TLD to San Fernando earthquake ground are shown in Table 4.2. It is seen from the dynamic analysis that the reduction in displacement increases with increase in end slope angle of TLD. Maximum reduction in displacement is observed at the slope angle of 30º. The reduction in displacements are observed to be ~4.20 %, 19.10 %' 38.40 %' and 40.60 % for end slopes of 15º, 20º, 25º and 30º, respectively. Above 30º of end slope angle the reduction in displacement is found to gradually reduced. The reduction in displacement of 37.20 %, 36.30 %, 34.40 %, and 33.50 % is seen for the TLDs with slope of 35º, 40º, 45º and 50º respectively. As observed in case of other input earthquake motions mentioned above, the rate of reduction of response is relatively faster (~3.42 % value) for TLDs with end slopes of 15-25º, and it is relatively moderate(~0.44 % value) for slope of 25–30º (see Figure 4.13). Rate of decrease in damping of structure for TLDs having slope above 30 is found to be relatively more for San Fernando earthquake ground motion, as compared to other earthquake ground motions mentioned above.

e) Response to IS compatible time history base motion

Displacement of the structure with end slope bottom TLD to IS time history is presented in Table 4.2. It is observed that the displacement reduction of structure increases with increasing in slope angle of TLD. Maximum reduction in displacement is seen at an angle of 30º of TLD. Reduction in displacement of with TLD having slope of 15º, 20º, 25º and 30º is observed to be ~3.10 %, 13.60 %, 21.50 % and 22.30 % respectively. The displacement reduction of structure is marginally reduced for end slope > 30º. Reduction in displacement for end slopes of 35º, 40º, 45º and 50º are observed to be ~20.70 %, 20.70 %, 20.20 % and 20.00 % respectively. Displacement reduction rate up to 25º end slope is around 1.84 % and it is 0.16 % for end slope of 25-30º.

In general, it also can be concluded that the rate of increase in response reduction is relatively higher at lower end slope angles of TLD. The displacement reduction of structure for end slopes above 30º decreases very slowly. Maximum reduction in displacement has been observed in the case of El Centro earthquake ground motion input and minimum reduction in displacement in case of IS compatible time history base motion. This is due to the reasons as mentioned in the Chapter 3, *viz.* Fourier amplitude values and duration of string motion of earthquake.

4.3.2. Dynamic analysis with slope bottom TLD (Xin's approach)

Sloshing frequency of liquid in a sloped bottom TLD is determined based on wetting length of TLD. As mentioned in Section 4.2.2, sloped bottom TLD may be converted in to equivalent flat bottom TLD based on equal volume of liquid and same depth of liquid (Xin 2006). The dimensions of sloped TLD *viz.* L = 1.72 m, H = 0.2235 m and B = 1.00 m which have been evaluated earlier are modified according to Xin's modelling approach. For example, the lengths of equivalent flat bottom TLD are evaluated to be 1.78 m and 1.92 m for end slopes of 15º and 50º respectively. The widths of equivalent flat bottom TLD evaluated are 0.51 m and 0.79 m for the end slopes of 15º and 50º respectively (see Table 4.3, for other end slope angles). Again, using the dimensions of the equivalent flat bottom TLDS (corresponding to end slope bottom TLDs), FE analyses have been carried out, using both harmonic and earthquake ground time histories as input base excitations. The results are then presented in the following sub-sections.

4.3.2.1. Response to harmonic excitation

Dynamic analysis of the RC framed structure with end sloped bottom TLD subjected to harmonic motion has been performed using the FE code developed, and are detailed Appendix D. The key result of the FE analyses are presented in Table D.2 and time history plots for 15º, 30º and 45º end slopes

\are shown in Figure D.5–D.7. A plot of the displacement reduction vs end slope angle is shown in Figure D.8. As seen from Figure D.8, the optimum end slope angle has observed to be around 29.5º, for maximum reduction in displacement of value 35.65 %.

a) Influence of end slope on tuning ratio of TLD

Unlike the variation of tuning ration as in the case of Gardarsson's approach (see Section 4.2.1 and Figure 4.3), tuning ratio in the case of Xin's approach, decreases with increase of end slope angle of TLD. At lower angles e.g. 15º to 25º of end slope, the variation of tuning ratio is found to be to be nonlinear. For higher angles e.g. > 25º the variation appears to be linear (Figure 4.14). Maximum tuning ratio of 1.051 and minimum of 0.943 have been observed at end slope angles of 15º and 50º , respectively. Tuning ratio of about 0.99 has been observed at an optimum angle of 29.5º (i.e. corresponding to maximum displacement reduction, see Table 4.3).

b) Influence of slope on liquid mass reduction

As both the Gardarsson's and Xin's approaches, similar dimensions of the TLD are used for determining sloshing frequency in sloped bottom TLD, the liquid mass reduction for end slope bottom TLDs will be same in as per both the approaches, this has been discussed in Section 4.3.1.1(b) (see also Figure 4.4, and Table 4.1). The liquid mass reduction at an optimum slope of 29.5º is observed to be around 23%.

4.3.2.2. Response to earthquake ground motion

Performance of end sloped bottom TLD in mitigating structural response, subjected to the earthquake ground motions mentioned above *viz.,* El Cento, Loma Prieta, Northridge, San Fernando and IS time history, as stated earlier are evaluated in the following sub-sections.

a) Response to El Centro earthquake ground motion

Plots of time history displacement response of the RC frame structure with TLD having end slopes of 15º, 20º, 25º, 30º, 35º, 40º, 45 º and 50º are shown in Figures 4.15-4.22. Results of the dynamic analysis are shown in Table 4.4. From the analysis, it is observed that the reduction in displacement of structure increases with increase in end slopes; and maximum reduction of 47.47 % is seen for 30º end slope (see Figure 4.23). Displacement reductions are observed to be ~32.88 %, 40.39 %, 44.00 % and 47.47 % with end slope angle of 15º, 20º, 25º and 30º respectively. Damping (reduction in displacement) decreases with end slope angle ≥ 30º . Reductions in displacement are observed to be ~46.77 %, 43.99 %, 39.56 % and 34.91 % for end slope angle of 35º, 40º, 45º and 50º respectively. It may be seen that for end slope angle ≥ 45º there is no improvement in displacement reduction as compared to flat bottom TLD (displacement reduction of structure with flat bottom TLD is 40.97 %.; see Chapter 3)

b) Response to Loma Prieta earthquake ground motion

Displacement response of structure with end the sloped bottom TLD to Loma Prieta earthquake is evaluated and results of dynamic analysis are shown in Table 4.4 and Figure 4.23. From Figure 4.23, it is seen that reduction in structural displacement gradually increases with increase in end slope angle and maximum reduction of 26.30 % has been observed for 35º end slope. Reductions in displacement are found to be 18.50 %, 22.40 %, 24.00 %, 26.10 % and 26.30 % for end slope angle of 15º, 20º, 25º, 30º and 35º respectively (see Table 4.4 and Figure 4.23). However, for end slope angle > 35º, reduction in displacement decreases i.e. < 26.60 %. It is found that there is no improvement in performance of TLD if the end slope is approximately above 40º as compared to reduction in displacement by use of flat bottom TLD (*DR* = 26 % for flat bottom TLD).

c) Response to Northridge earthquake ground motion

Results of dynamic analysis of the RC framed structure with end slope TLD, subjected to Northridge earthquake ground motion are shown in Table 4.4. Displacement reduction of structure with TLD is observed to increase with increase in end slope up to 30º. Reductions in displacement are observed to be 20.00 %, 24.10 %, 25.80 % and 27.80 % for end slopes of 15º, 20º, 25º and 30º respectively (Figure 4.23). Reduction in displacement of structure is then seen to decrease for the TLD having end slope above 30º: displacement reductions are in the order 27.70 %, 26.60 %, 24.60 % and 22.40 % for end slopes of 35º, 40º, 45º and 50º respectively. No improvement in reduction of displacement is observed for TLD with end slope above 40º (flat bottom TLD *DR* = 26.60 %).

d) Response to San Fernando earthquake ground motion

The results of dynamic analysis of the RC frame structure with end slope bottom TLD are shown in Table 4.4, for San Fernando earthquake excitation It is seen that displacement reduction of structure increases with end slope angle of TLD and maximum reduction is observed to be 41.30 % at 30º angle of end slope. Reductions in displacement observed are found to be ~28.20 %, 34.50 %, 38.80 %, and 41.30 % for the TLDs having end slopes of 15º, 20º, 25º and 30º respectively (Figure 4.23). However, for end slope greater than 30º the displacement reduction values are found to decrease, i.e. DR = 41.30 %, 39.20 %, 35.40 % and 31.30 % for end slope values of 35º, 40º, 45º and 50º respectively. Further, for TLDs with end slope above 45º, no significant benefit has been observed with end slopes, as compared to flat bottom TLDs (flat bottom TLD *DR* = 33.20 %).

e) Response to IS time history base motion

The dynamic results of the end slope bottom TLDs subjected to IS time history are shown in Table 4.4 and Figure 4.23. From Figure 4.23, it is observed that the reduction in displacement (of the framed RC structure) increases with increasing slope angle up to 35º, with the reduction in displacement being 15.20 %, 18.80 %, 20.80%, 23.10% and 23.70% for end slopes of 15º, 20º, 25º, 30º and 35º respectively. Thereafter, for end above 35º, the reduction in displacements decreases with increasing end slopes. Reductions in displacement are seen to ~~to~~ be 23.50 %, 22.50 % and 21.10 % for the TLDs correspond to end slopes of 40º, 45º and 50º respectively. No significant improvement in mitigating/reducing the displacement has been observed for the TLDs with end slopes > 45º (*DR* = 21 % for flat bottom TLD).

Thus, it is seen that the reduction in displacement of the RC framed structure with end slope TLDs increases with increasing with slope angle of TLD of around 30º - 35º. i.e. maximum reduction in displacement could be seen for end slope of 30-35º, for all the five earthquake time histories considered. Thereafter, the displacement reduction decreased for higher (>35º) end slope angles. The end slope angle values of ~30–35º appears to give maximum reduction in displacement. Moreover, in most of the cases of input earthquake ground motions, no significant improvement in mitigating the displacement can be observed with TLDs having end slope ≥ ~40-45º.

4.4. CONCLUSIONS

In this chapter, finite element analyses of an RC frame 10 storey structure with end slope bottom TLD has been investigated, considering the fluid-structure effect. Effects of both harmonic and earthquake time histories (as base excitations) on the displacement reductions of the frame structure have been studied. End slope angles

varying from 15º to 50º have be considered for the parametric assessment. The summary of results of the investigation are presented below, using both Gardarsson's and Xin's modelling approaches.

- Results of dynamic analysis of structure with TLD having end slope by two approaches are found nearly similar. Results of harmonic input show that an optimum slope angle of 30.5º with *DR* = 37.72 % and 29.5º with *DR* = 35.65 % by Gardarsson's and Xin's approach respectively.

- Gardarsson's approach gives maximum reduction in displacement response for the end slope of around 30º for all input excitations. However, Xin's approach gives maximum reduction for the end slope angle range of 30-35º.

- With respect to Gardarsson's approach, there seems to be no improvement in displacement reduction for TLD with end slope angle of > 45º. In case of Xin's approach this slope, angle has a range of 40-45º.

- In case of Gardarsson's approach the end slope angle of around 25º and above, results in improvement in response reduction in comparison to flat TLD. Form the Xin's approach this angle of end slope is 25-30º.

- Liquid mass reduction at an optimum slope angle is observed to be 22 % and 23 % when Gardarsson's and Xin's approach of modelling is used respectively.

Table 4.1. Dimensions of sloped bottom TLD and equivalent flat bottom tank (Gardarsson's (2001) modelling approach)

Sr. No.	Slope (°)	Depth of liquid *H* (m)	Equivalent flat bottom tank dimensions (conversion of sloped TLD)		Sloshing frequency (rad/sec)	Frequency ratio	Liquid volume reduction (*MR*) (%)
			Length (m)	Width (m)			
1	15	0.22	2.20	0.40	2.07	0.82	48.49
2	20	0.22	1.94	0.55	2.33	0.93	35.69
3	25	0.22	1.84	0.67	2.45	0.98	27.86
4	30	0.22	1.80	0.74	2.52	1.00	22.50
5	35	0.22	1.77	0.76	2.56	1.02	18.55
6	40	0.22	1.75	0.82	2.58	1.03	15.47
7	45	0.22	1.74	0.85	2.60	1.03	12.98
8	50	0.22	1.73	0.88	2.51	1.04	10.90

Table 4.2. Displacement response reduction of structure with end slope TLD to various base motions using Gardearsson (2001) approach

Sr. No.	α^o	Displacement reduction (%)									
		El Centro		Loma Prieta		Northridge		San Fernando		IS History	
		Flat TLD	Slope TLD	Flat TLD	Slope TLD	Flat TLD	Slope TLD	Flat TLD	Slope TLD	Flat TLD	Slope TLD
1	15	40.97	5.84	26.00	3.30	26.60	3.30	33.20	4.20	21.00	3.10
2	20	40.97	21.22	26.00	14.00	26.60	14.00	33.20	19.10	21.00	13.60
3	25	40.97	43.81	26.00	24.10	26.60	25.60	33.20	38.40	21.00	21.50
4	30	40.97	47.51	26.00	26.50	26.60	28.40	33.20	40.60	21.00	22.30
5	35	40.97	43.68	26.00	25.80	26.60	27.40	33.20	37.20	21.00	20.70
6	40	40.97	42.63	26.00	26.40	26.60	27.70	33.20	36.30	21.00	20.70
7	45	40.97	40.53	26.00	26.10	26.60	26.90	33.20	34.40	21.00	20.20
8	50	40.97	39.36	26.00	25.00	26.60	26.40	33.20	33.50	21.00	20.00

Table 4.3. Dimensions of sloped bottom TLD and equivalent flat bottom TLD (Xin's (2006) modelling approach)

Sr. No.	α^o	H (m)	Equivalent flat bottom TLD		f_w (rad/sec)	TR	MR (%)
			L (m)	B (m)			
1	15	0.22	1.78	0.51	2.63	1.05	48.49
2	20	0.22	1.79	0.61	2.52	1.00	35.69
3	25	0.22	1.81	0.65	2.49	0.99	27.86
4	30	0.22	1.83	0.72	2.47	0.98	22.50
5	35	0.22	1.86	0.75	2.44	0.97	18.55
6	40	0.22	1.88	0.77	2.41	0.96	15.47
7	45	0.22	1.90	0.78	2.38	0.95	12.98
8	50	0.22	1.92	0.79	2.36	0.94	10.90

Table 4.4. Displacement response reduction of structure with end slope TLD to various base motions using Xin (2001) approach

Sr. No.	α^o	Displacement reduction (%)									
		El Centro		Loma Prieta		Northridge		San Fernando		IS History	
		Flat TLD	Slope TLD	Flat TLD	Slope TLD	Flat TLD	Slope TLD	Flat TLD	Slope TLD	Flat TLD	Slope TLD
1	15	40.97	32.88	26.00	18.50	26.60	20.00	33.20	28.00	21.00	15.20
2	20	40.97	40.39	26.00	22.40	26.60	24.10	33.20	34.50	21.00	18.80
3	25	40.97	44.00	26.00	24.00	26.60	25.80	33.20	37.80	21.00	20.80
4	30	40.97	47.47	26.00	26.10	26.60	27.80	33.20	41.30	21.00	23.10
5	35	40.97	46.77	26.00	26.30	26.60	27.70	33.20	41.30	21.00	23.70
6	40	40.97	43.99	26.00	25.60	26.60	26.60	33.20	39.20	21.00	23.50
7	45	40.97	39.56	26.00	24.10	26.60	24.60	33.20	35.40	21.00	22.50
8	50	40.97	34.91	26.00	22.10	26.60	22.40	33.20	31.30	21.00	21.10

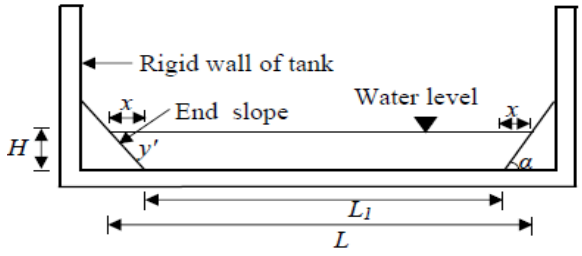

(a)

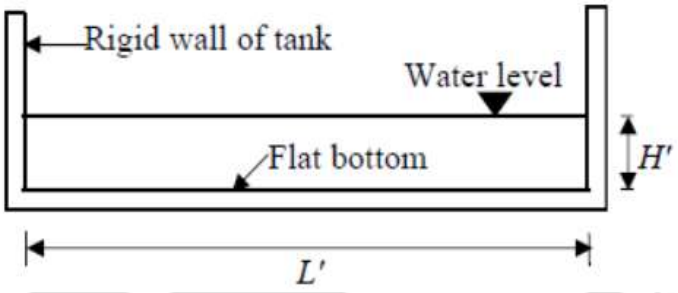

(b)

Figure 4.1. (a) Sloped bottom TLD, (b) Equivalent flat bottom TLD

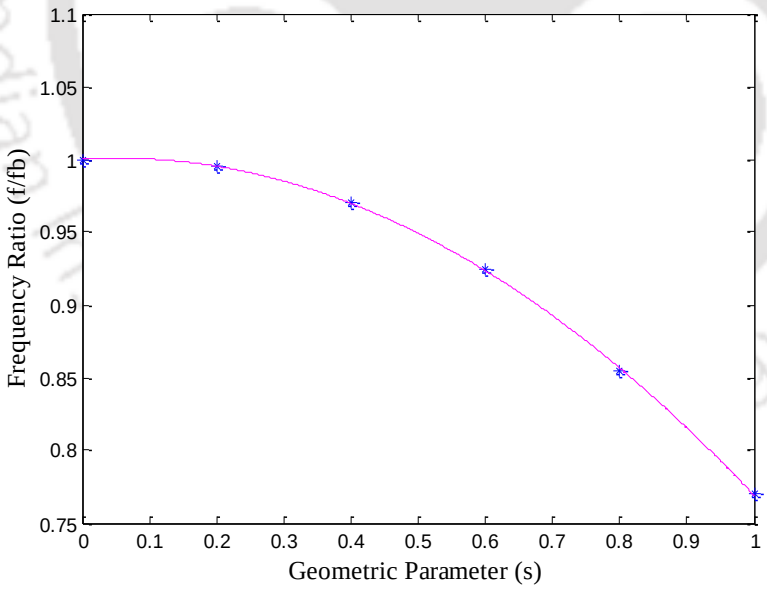

Figure 4.2. Graph of *f/fb* (frequency of sloshing in sloped bottom TLD/ frequency of sloshing in box shaped TLD) vs shape or geometric parameter (*s*) (Gardarsson 2001)

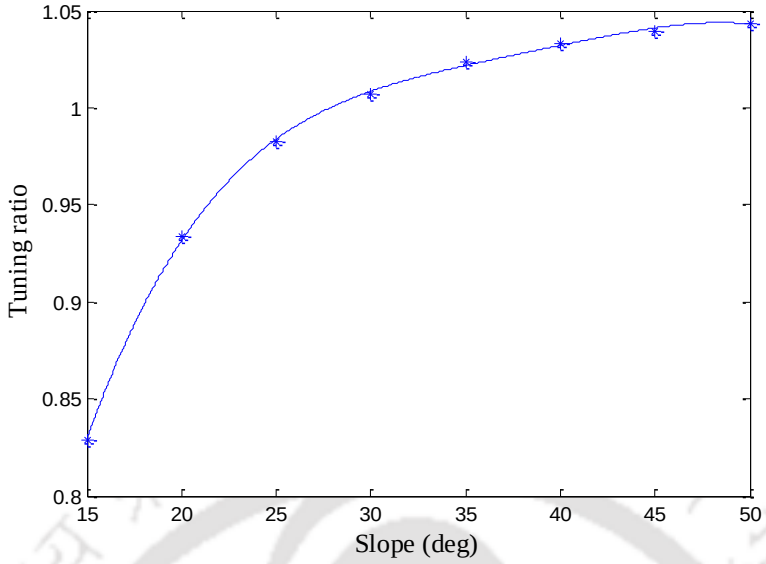

Figure 4.3. Variation of tuning ratio with slope of TLD (Gardarsson's approach)

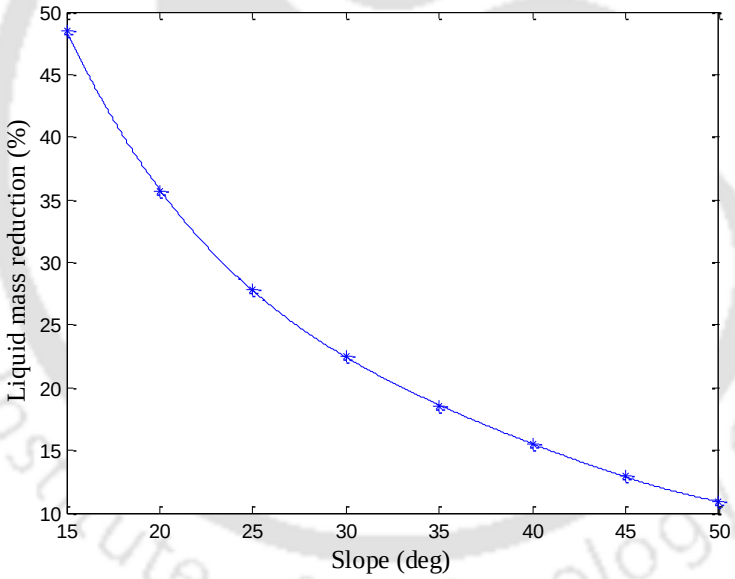

Figure 4.4. Variation of liquid mass reduction with slope of TLD

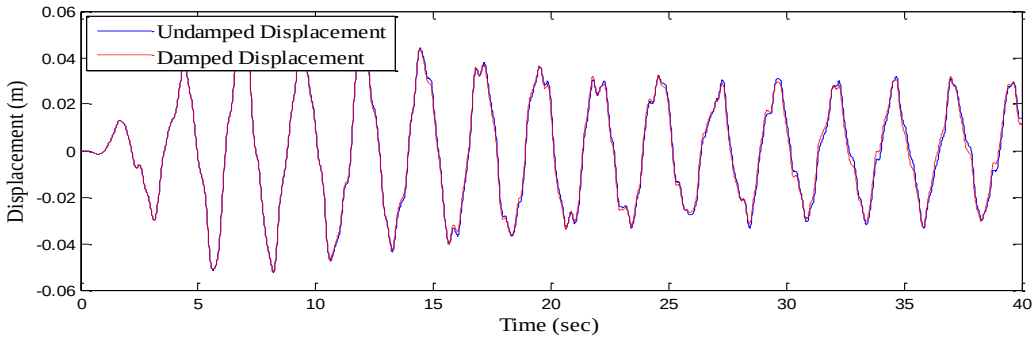

Figure 4.5. Response of structure with 15º slope TLD subjected to El Centro earthquake

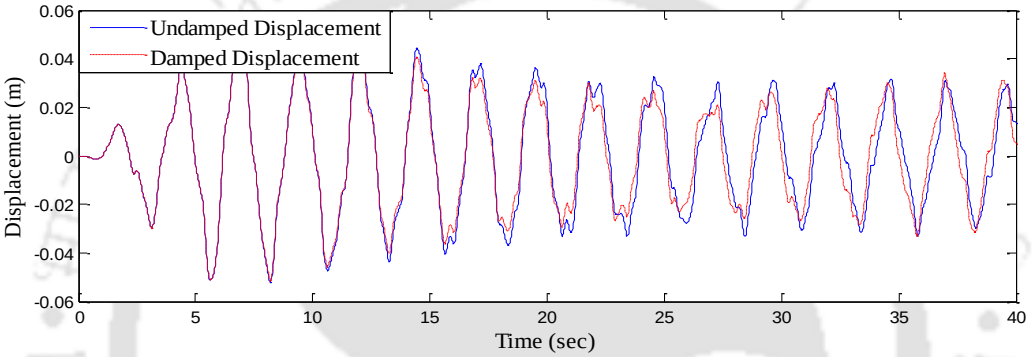

Figure 4.6. Response of structure with 20º slope TLD subjected to El Centro earthquake

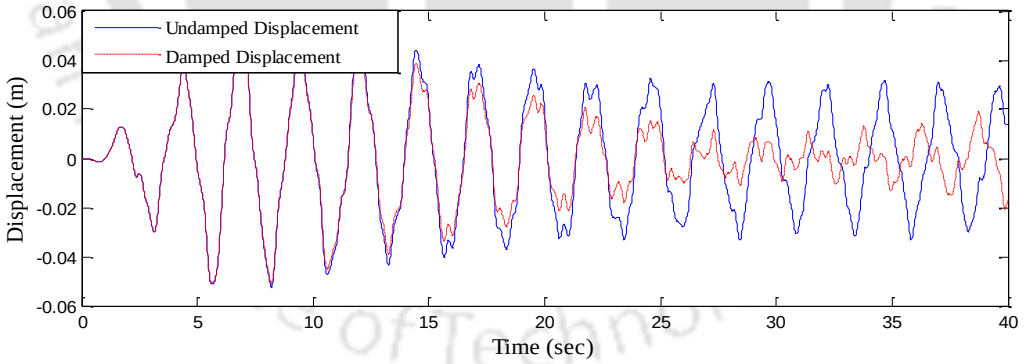

Figure 4.7. Response of structure with 25º slope TLD subjected to El Centro earthquake

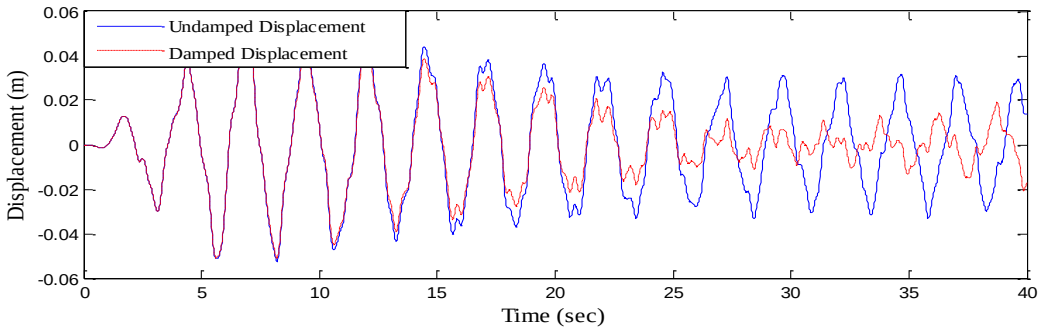

Figure 4.8. Response of structure with 30° sloped TLD subjected to El Centro earthquake

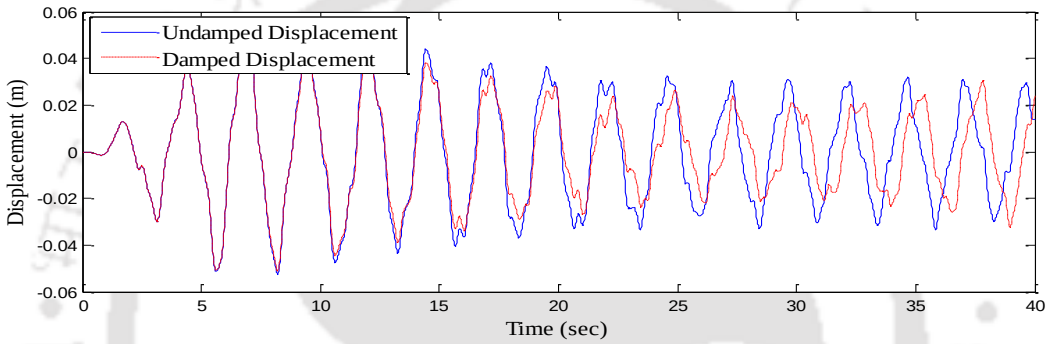

Figure 4.9. Response of structure with 35° slope TLD subjected to El Centro earthquake

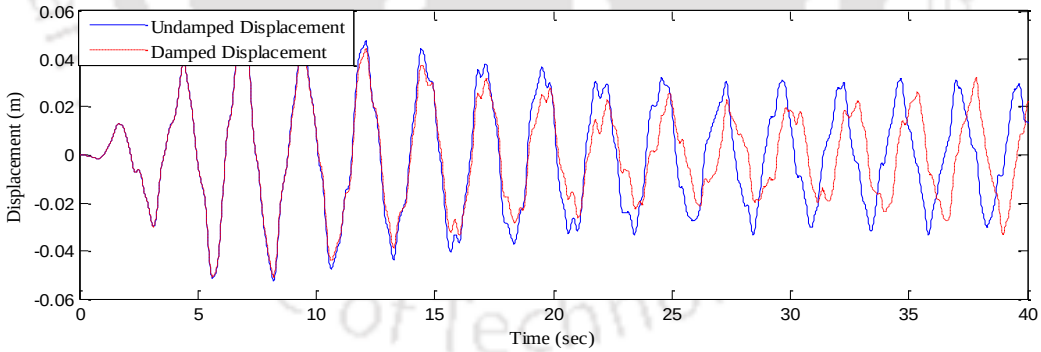

Figure 4.10. Response of structure with 40° slope TLD subjected to El Centro earthquake

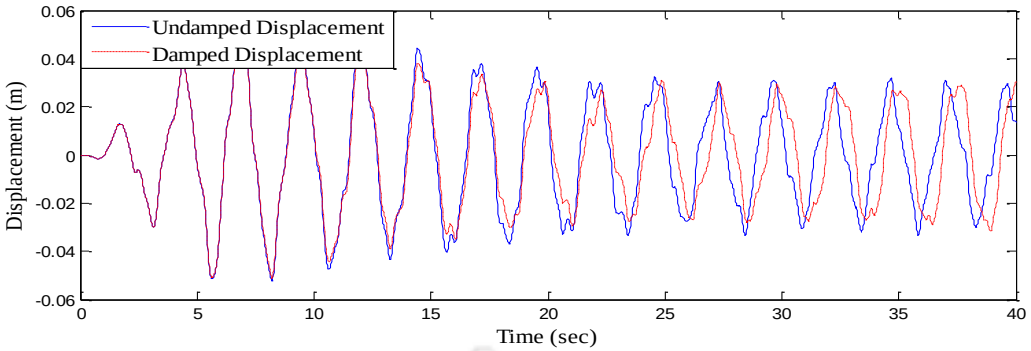

Figure 4.11. Response of structure with 45° slope TLD subjected to El Centro earthquake

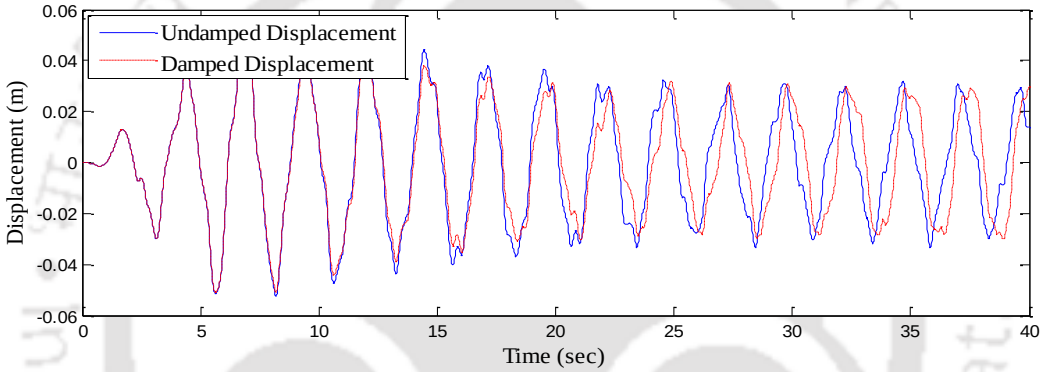

Figure 4.12. Response of structure with 50° slope TLD subjected to El Centro earthquake

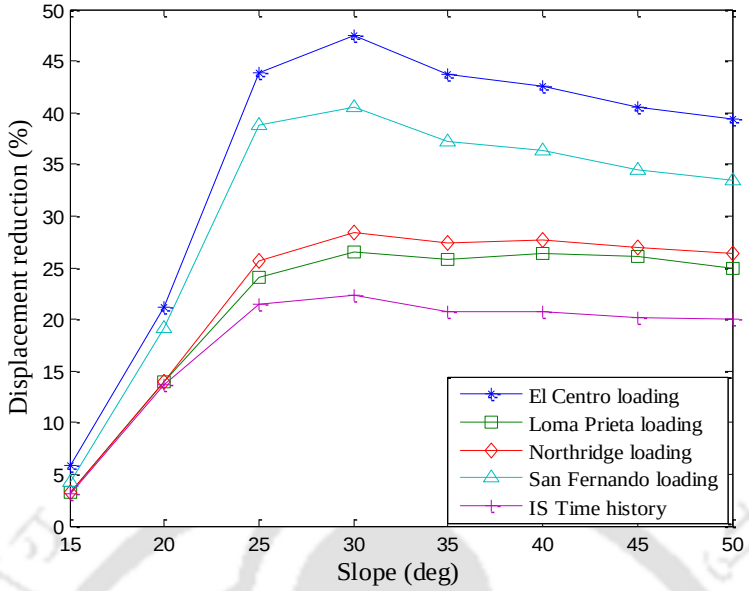

Figure 4.13. Variation of reduction in displacement of structure with slope of TLD subjected to earthquakes and IS time history (Gardarsson's approach)

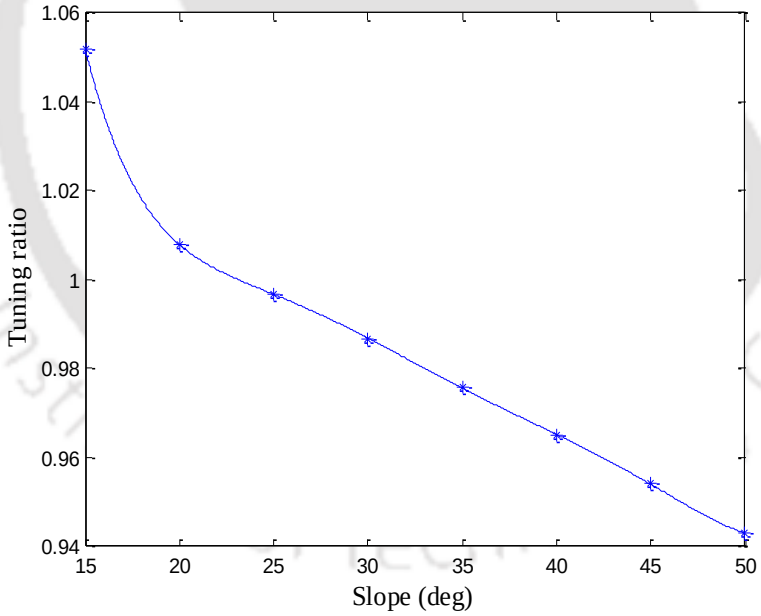

Figure 4.14. Variation of tuning ratio with slope of TLD (Xin's approach)

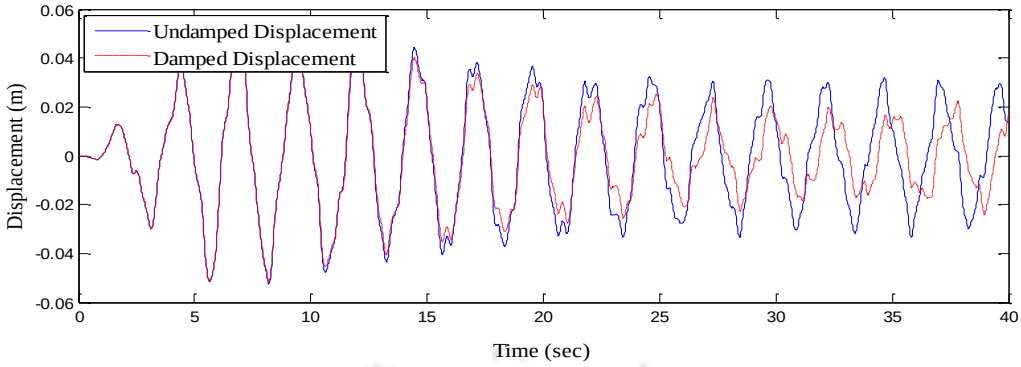

Figure 4.15. Response of structure with 15º slope TLD subjected to El Centro earthquake

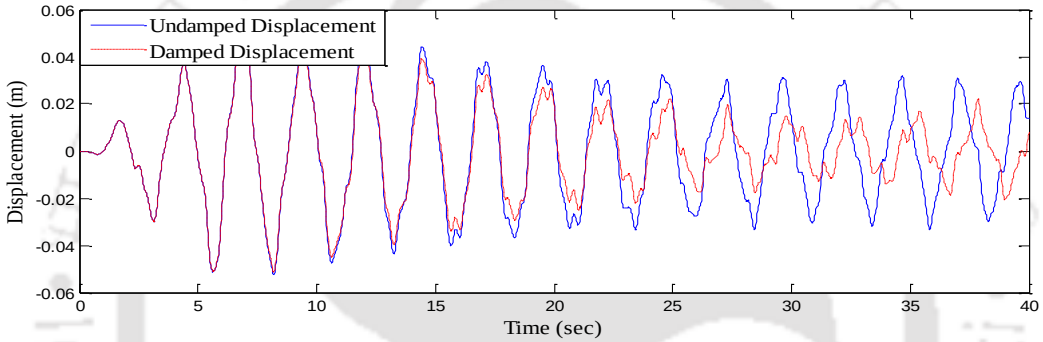

Figure 4.16. Response of structure with 20º slope TLD subjected to El Centro earthquake

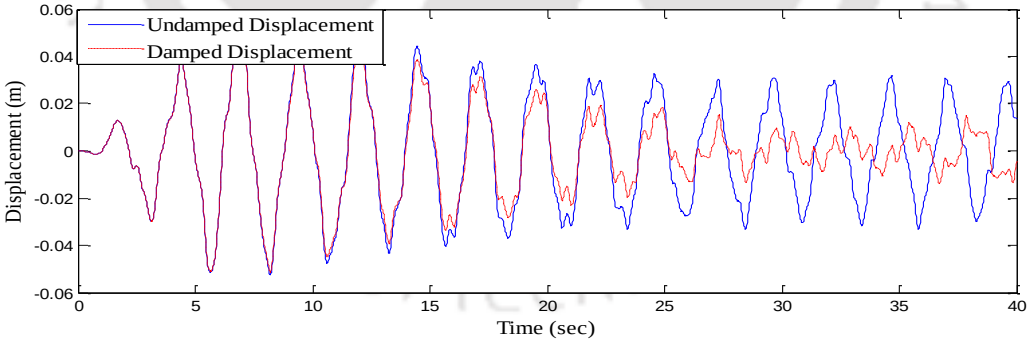

Figure 4.17. Response of structure with 25º slope TLD subjected to El Centro earthquake

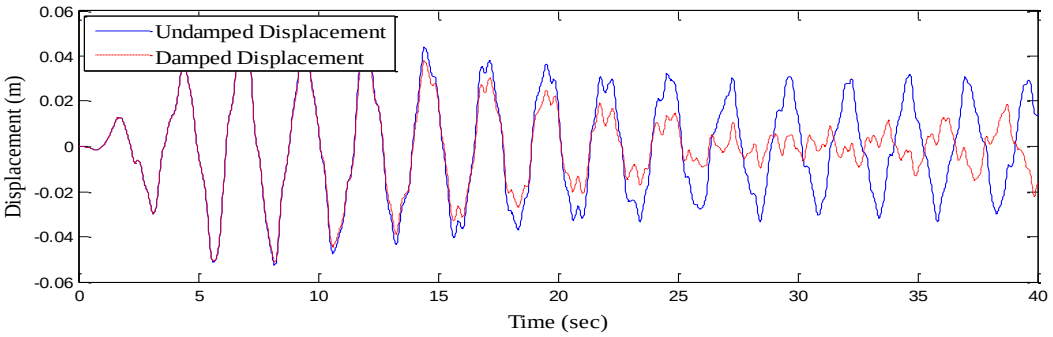

Figure 4.18. Response of structure with 30° slope TLD subjected to El Centro earthquake

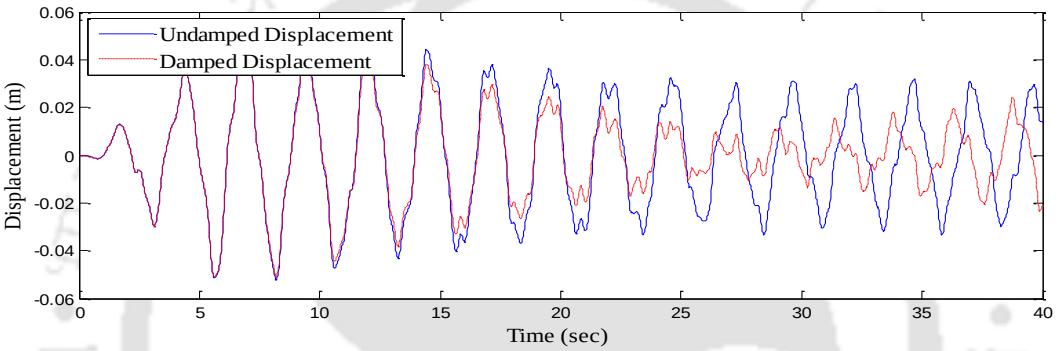

Figure 4.19. Response of structure with 35° slope TLD subjected to El Centro earthquake

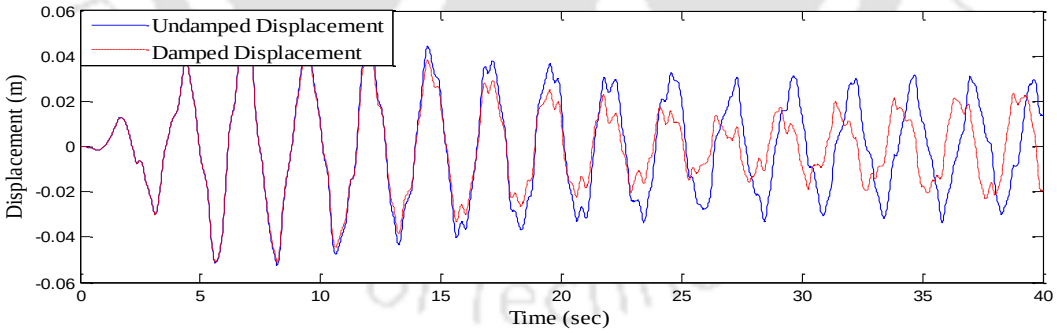

Figure 4.20. Response of structure with 40° slope TLD subjected to El Centro earthquake

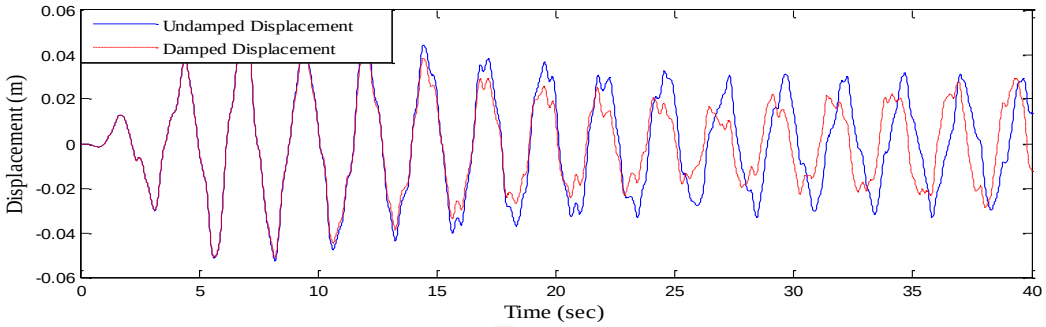

Figure 4.21. Response of structure with 45º slope TLD subjected to El Centro earthquake

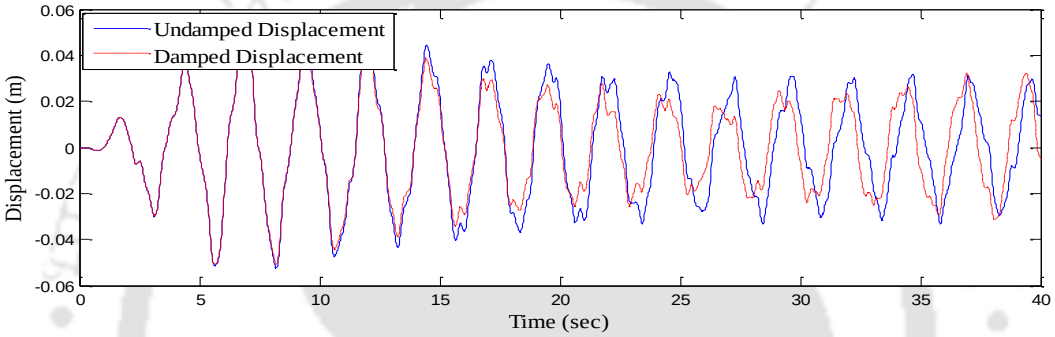

Figure 4.22. Response of structure with 50º slope TLD subjected to El Centro earthquake

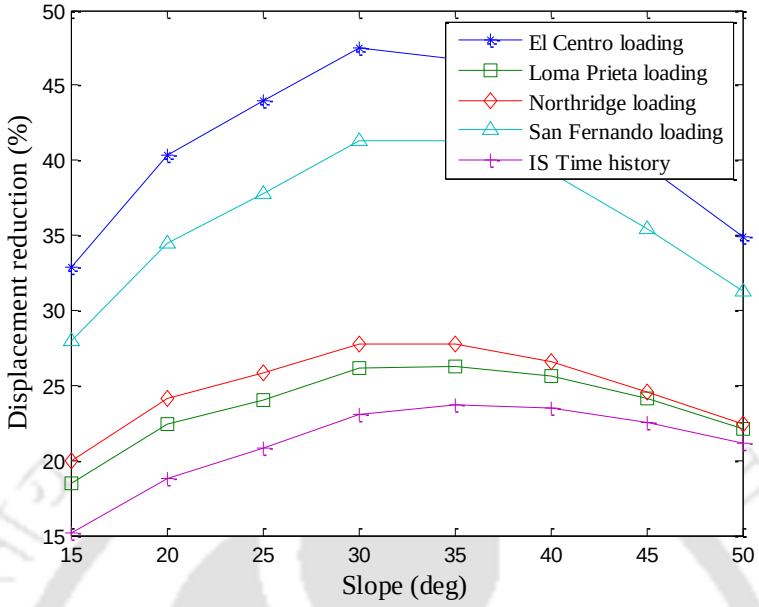

Figure 4.23. Variation of reduction in displacement of structure with slope of TLD subjected to earthquakes and IS time history (Xin's approach)

CHAPTER 5

CONTROLLING RESPONSE OF STRUCTURE WITH APPLICATION OF TLD HAVING COMBINATION OF SLOPES AT BOTTOM

5.1. INTRODUCTION

Study on the performance (i.e. displacement reduction, tuning ratio, liquid mass reduction) of TLD with central slope and dual triangular slopes at the bottom has been presented in Chapter 3. And, study on the effects of end slopes on the performance of TLDs have been presented in Chapter 4. As mentioned in Chapter 2, limited studies have been reported on TLDs with end slopes (Gardarsson *et al.* (2001), Olson *et al.* (2001)) and central slopes (Xin 2006). However, to the best of author's knowledge, no study has been reported on the investigation of TLD with combination of end slope with central slopes at bottom. Hence, in this chapter an attempt has been made to extend the previous studies (Chapters 3 and 4) to evaluate the performance of TLD with combination of end slope with central slope; and end slope with dual triangular slopes at the bottom of TLD. The RC frame with combined end and central slope / dual triangular slope TLDs have been analysed, using the fluid-structure interaction, for earthquake base excitations. These results are presented in the form of displacement reductions, Further, the displacement response reduction results are also compared with those of central slope, dual triangular slopes and end slope bottom TLDs, discussed in earlier chapters (Chapters 3 and 4).

5.2. MODELLING OF TLD WITH COMBINED END SLOPE AND CENTRAL SLOPE

Xin's (2006) modelling approach (described previously in Chapter 3) which is based on wetting length for determining sloshing frequency in slope bottom TLD, has been used to model TLDs with combination of end slope with central single slope at the bottom of TLD, by converting into equivalent flat bottom TLDs. Consider a TLD with end slope and central slope at the bottom as shown in Figure 5.1.

If θ and α are the central and end slope angles, the wetting length of TLD with end slope at one side is given by Equation 4.5 as

$$y' = \frac{H}{Sin(\alpha)}$$

Wetting length of TLD with central slope on one side is given by Equation 3.7 as

$$y = \frac{L_1 / 2}{Cos(\theta)}$$

where L_1 is the distance between end slope points at the bottom of TLD

Wetting length due end slope and central triangular slope can be expressed as

$$L' = 2y + 2y' \tag{5.1}$$

where 2y is the net wetting length for central triangular slope, and 2y' is the net wetting length for end slope.

The modified width of TLD is derived from the Equation 3.9 (equating volumes of liquid in both the original i.e. combined end and central slope TLD, and equivalent flat bottom TLD).

$$B' = \frac{V_w}{H' L'}$$

where V_w is the total volume of water in the sloping bottom tank with $H' = H$ Thus making, the length of equivalent flat bottom TLD $L' > L$ and width of TLD $B' < B$.

5.2.1. Performance of TLD with end and central slopes

As mentioned in the previous section, and as the equivalent flat bottom TLD has been derived in, based on the equivalent liquid volume (between slope bottom and equivalent flat bottom TLD) concept as one of the criteria, the maximum central slope that can be introduced at the bottom of TLD can be limited, based on the dimensions of TLD *viz.* length and depth of liquid and amount of end slope. For instance, for a TLD with end slope of 15º, there is no sufficient space available for the central slope portion. Hence, the end slopes considered at the bottom of TLD have been varied from 20º to 50º. Thus, for TLDs with end slope values ranging from 20º-30º, 35º and 40º, and 45º and 50º, central slopes of up to 25º, 20º, and 15º have been, respectively, introduced.

Dynamic analyses of the RC framedstructure with TLD having combined end slope and central slope have been conducted using input earthquake time histories *viz.* El Centro (1940), Loma Prieta (1989), Northridge (1994), San Fernando (1971) and IS 1893 compatible time histories. Typical time history plots of undamped and damped displacements of structure subjected to El Centro earthquake base excitation are shown in Figures 5.5-5.11. It can be observed that the displacement response reduction of structure is found to be relatively more for the input of earthquake ground motion having lesser Fourier amplitude values and lesser strong motion duration. Also, as seen from the time histories of earthquake ground motion (Chapter 3, Table 3.7) the duration of strong motion is least for El Centro earthquake and maximum for IS time history. It can also be concluded that if less is the duration of strong motion of earthquake less is the response and more would be the reduction in response due to application of TLD.

Due to the large parametric data arising to the consideration of both central and end slope bottom TLDs, for the convenience of discussion, depending on the rate of relative displacement reduction of response per degree central slope, the entire results have been classified into three folds, based on the end slope angles: 1) small (20–30º) end slope (large rate of displacement reduction of response), medium (35-40º) end slope (small rate of displacement reduction) and large (45-50º) end slope TLD (constant/stable / very low rate of displacement reduction) TLDs and are shown Table 5.1. Sample calculations are shown in Appendix B (Section B.8)

5.2.2. Effect of central slope on tuning ratio

The tuning ratio of TLD decreases with increase of central slope angle of TLD (Figure 5.2) and the variation is seen to be nonlinear. In the case of TLD with 20º end slope, when central slope angles vary from 0º to 25º, tuning of the TLD is found to change from little over-tuned (tuning ratio: 1.01) to under-tuned (tuning ratio: 0.98) state. The variation of tuning ratio for the low end slope TLDs (end slope 20-30º) are seen to be in the range 1.01–0.92. In case of medium end slope TLDs (end slope 35º and 40º), the tuning ratio varies from 0.97–0.92. For the large end slope TLDs, the variation of tuning ratio is observed to be in the range of 0.95–0.92. The decrease in tuning ratio is associated with increase of wetting length of TLD with increase in central slope value. Increase in wetting length decreases the sloshing frequency of liquid in TLD as more time is required for the liquid to move on the TLD surface. Decrease in value of tuning ratio is relatively lesser for the range of 0-5º (Figure 5.2) central slopes.

5.2.3. Effect of central slope on liquid mass reduction

The liquid mass in TLD decreases with increase in central slope angle of TLD. The reduction of liquid mass is found to have a linear relation with central slope of TLD. Also, it is seen that the rate of reduction in liquid mass increases with increase

in end slope angle of TLD (Figure 5.3). The rate of reduction of liquid mass for small end slope TLDs increases from 0.3-1.07 % per degree increase in central slope (Figure 5.4). Reduction in mass of liquid due to central slope of 2.5º is observed to be of order of 0.68 %, 1.63 % and 2.38 % for end slopes of 20º, 25º and 30º respectively. In case of medium end slope TLDs, the rate of reduction increases from 1.39 % to 1.66 % per degree increase in central slope. Liquid mass reduction due to central slope of 2.5º is seen as 3.31 % and 4.01 % for the end slopes of 35º and 40º, respectively. For the large end slope TLDs, the rate of liquid mass reduction is observed to increase from 1.82 % to 2.1 % per degree increase in central slope (Figure 5.4 and Table 5.10). Mass reduction due to application 2.5º central slope are found to be ~4.56-5.30 % for end slopes of 45º and 50º TLDs respectively. Maximum liquid mass reduction of around 49.47 % is seen for the TLD with end slope of 30º and central slope of 25º. Minimum liquid mass reduction of 10.90 % is seen for the case of TLD with 50º end slope and no (0º) central slope. It has been also seen from the Figure 5.3 that various combinations of end slope and central slope, nearly same volume reduction of liquid e. g. 20º end slope and 15º central slope and 45º end slope and 15º central slope the liquid volume reductions are 39.87 % and 40.35 % respectively.

5.2.4. Effect of central slope on displacement reduction of structure

From the analysis it is observed that the displacement response reduction decreases with increase in central slope, for a constant end slope (see Figures 5.12-5.18). The variation of displacement reduction is found to be nonlinear with increase in central slope angle. Similar trend has been seen for all input earthquake base excitations (see Figures 5.12-5.18). Maximum reduction in response has been observed for El Centro earthquake input ground motion, while minimum displacement response reduction is seen in the case of IS compatible time history base motion.

In the case of small end slope TLDs, maximum reduction in displacement response (i.e. damping) of 47.47 % and 23.10 % are found for El Centro earthquake and IS compatible time history base motions, respectively. For rest of the input motions (e.g. Loma Prieta, Northridge and San Fernando earthquake time histories), the reductions in displacement response are in the range of 47.47-23.10 %. Thus, it is seen that for a TLD with 25º end slope and 2.5º central slope, a marginal improvement (0.2-0.5 %) in performance can be seen over the performance of TLD with only end slope (Figure 5.13). Damping or reductions in displacement response, is found to decrease at a rate of decrease 1.15% and 0.46 % per degree increase of central slope, for El Centro and IS compatible time history inputs respectively.

Study on medium slope TLDs shows that maximum displacement response reduction of structure (damping) is seen to be ~46.77 % and 23.70 % for the input motion of El Centro earthquake ground motion and IS compatible time history base motions respectively. In the case of input motions of Loma Prieta, Northridge and San Fernando earthquakes the reductions in displacement response are in the range 46.77-23.70 %. The rate of decrease in damping is seen up to be 1.39 % and 0.64 % per degree increase in central slope for El Centro ground motion IS time history inputs respectively.

For large end slope TLDs, reductions in displacement response up to 39.56 % and 22.5 % are observed when subjected to El Centro and IS time history ground motions respectively. For the rest of the input of earthquake ground motions as mentioned earlier, the displacement reductions are in the range 39.56-22.50 %. Decrease in damping per degree increase in central slope angle are observed to be 1.30% and 0.70% for El Centro earthquake and IS time history base motions respectively. Also, the rate of decrease of damping for other earthquake ground motions are found of be in the range 1.30-0.7 %.

TLDs with small end slope angle are likely to perform better in mitigating response of structure, as compared to medium and large end slope TLDs. More particularly, the TLD with 25º end slope and 2.5º central slope would perform better. However, it is seen that there is no improvement in performance with introduction of central slope at TLD bottom. The benefit of introducing central slope would be reduction in liquid volume.

5.2.5. Response reduction per degree rise of central slope

Variation of rate of displacement reduction of structure is shown in Figure 5.19. It is observed that the rate of displacement reduction of structure per degree rise of central slope increases rapidly (e. g. 0.18–1.15 for El Centro earthquake and 0.05 – 0.48 for IS time history) with the amount of end slope of TLD from 20º to 30º. This rate of increase of reduction of displacement of structure increases moderately (e. g. 1.22–1.39 for El Centro earthquake and 0.51–0.64 for IS time history) for end slopes of TLD between 30º and 40º. Above mentioned trend of rate of increase of displacement has been observed in all input motions of earthquakes. The rate of displacement reduction for higher end slopes almost remains constant / stable. However, for the input earthquake motions of El Centro and San Fernando the rate of displacement reduction decreases marginally for higher end slopes. Indecently, it has been seen that the response reduction for these earthquake ground motions are more compared to other input motions of earthquake.

5.3. MODELLING OF TLD WITH COMBINED END SLOPE AND DUAL TRIANGULAR SLOPES

Figure 5.20 shows a schematic diagram of a TLD with combined end slope and dual triangular slopes at the bottom. The amount of dual triangular slopes on either side of midsection is kept constant. Sloshing frequency of liquid is governed by net wetting length of tank at the bottom which consists of wetting length due to end

slope and wetting length due to dual triangular slopes, as also mentioned above. The wetting length of TLD is due to end slope is given by Equation 4.5.

Wetting length of TLD due to dual triangular slopes is given by Equation 3.10 as

$$y = \frac{L_1 / 4}{Cos(\theta_1)}$$

Wetting length due end slope and dual triangular slopes is then given by

$$L' = 4y + 2y' \tag{5.2}$$

where L_1 is the distance between end slope points at the bottom of TLD

Equivalent width of TLD is derived from the Equation 3.9 as

$$B' = \frac{V_w}{H' L'}$$

5.3.1. Performance of TLD with end slope and dual triangular slopes

In this section an attempt has been made to investigate the performance of TLD with combined of end slope and dual triangular slopes at the bottom of TLD. Similar range of end slopes (20-50º) as provided Section 5.2.1, has been considered. The range of dual triangular slopes provided has been varied from 0-25º for all the end slope angles adopted in this study. Dimensions of slope bottom TLD and dimensions of equivalent flat bottom TLD, tuning ratio and liquid mass reduction are shown in Table 5.12-5.18. Based on reductions of displacement per degree of the dual triangular slopes the TLDs with combined of end slope and dual triangular slopes have been divided in to three groups (Table 5.11) e.g. small end slope (20-35º) TLDs (corresponding to large variation in rate of reduction in displacement), medium end slope (40-45º) TLDs (corresponding to small variation in rate of reduction of displacement) and large end slope (50º) TLD (corresponding to near constant / stable rate or marginally declining rate of reduction in displacement) (see Table 5.11) (to discuss in subsequent sub sections). Dynamic analysis of the RC

frame structure with TLD having combined end slope and dual triangular slops have been carried out for the input earthquake ground excitations mentioned earlier. Typical time history plots of undamped damped displacements subjected to El Centro earthquake ground motion are shown in Figures 5.24-5.30. Effects of the angles of dual slopes on the reduction of displacements, tuning ratio, liquid mass ratio etc. are presented below. For sample calculations see Appendix B (B.9)

5.3.2. Effect of dual triangular slopes on tuning ratio

It is observed that the TLD tuning ratio decreases with increasing amount of dual triangular slopes, at the bottom of TLD (Figure 5.21). The decrease in tuning ratio is associated with the increase of wetting length of TLD. Variation of tuning ratio with dual triangular slopes is observed to be nonlinear. The range of variation of tuning ratio in the small end slope (20-35º) medium end slope (40-45º), and large end slope (> 50º) TLDs are found to be 1.01–0.92 (Table 5.12-5.15); 0.96-0.89 (Table 5.16-5.17) and e.g. 0.94–0.88 (Table 5.18), respectively.

5.3.3. Effect of dual triangular slopes on liquid mass reduction

The liquid mass in TLD decreases with increase of dual triangular slopes and its variation with increasing slope is found to be linear. As seen previously, similar to the case of TLD with central slope, the rate of reduction of liquid mass increases with increasing amount of end slope (Figure 5.22). Liquid mass reduction per degree increase in dual triangular slope increases from 0.11 to 0.57 ; 0.69 to 0.79 (Figure 5.23); and ~0.89; for small, medium and large end slope angles, respectively. Maximum liquid mass reduction of around 39.81 %, due to application of dual triangular slope is found for the TLD with 20º end slope and 25º dual triangular slopes. Liquid mass reduction per degree dual triangular slope is shown in Figure 5.23.

5.3.4. Effect of dual triangular slopes on displacement reduction of structure

Reductions in displacement of the RC framed structure decreases with increase in the value of dual triangular slop angle, for a fixed end slope (Figures 5.31-5.37), for all input earthquake motions. As in the case of TLD with combination of central slope and end slope (presented in Section 5.2.4) the maximum and minimum reduction in displacement is observed in the case of El Centro and IS compatible base motions respectively.

It has been seen that, for small end slope angle (30º end slope and 5º dual triangular slope) TLDs, maximum reductions in displacement of structure of about 45.75 % and 22.40 % is seen for El Centro earthquake motion IS compatible time history base motions, respectively. In case of TLD with end slope of 25º and dual triangular slope angle of 5º the performance of TLD is marginally improved and it is of the order of 0.30-0.58 % (Figure 5.32), for all the time histories considered. It is seen that damping decreases with the amount of dual triangular slopes. The decrease of damping per degree rise of dual triangular slope is seen to be ~1.05 % and 0.41 % for El Centro earthquake and IS time history base motions respectively

For the TLDs with medium end slope (40º end slope and 5º dual triangular slopes), maximum reductions in displacement of 40.98 % and 22.20 % are seen for El Centro earthquake motion and IS compatible base input motions, respectively. Reduction on displacement for the input motions of rest of the earthquakes are observed in the above-mentioned range (22.20–40.98 %). Peak decrease in damping per degree rise of dual triangular slope is observed to be ~1.10 % and 0.54 % for El Centro earthquake motion and IS compatible base input motions respectively

In the case of large end slope TLDs, maximum reductions in displacement of about 31.78 % and 19.50 % are seen for the input motions of El Centro earthquake and IS compatible time histories respectively. For the other considered input earthquake motions, the reductions in displacement are in the range of 31.78-19.50 %. The decrease in damping per degree rise dual central slopes is seen to be 0.88 % and 0.52 % for input earthquake motions of El Centro earthquake and IS time histories respectively.

As in case of combination of end slope and central slope TLDs, similar trends of displacement reductions are seen in the combination of end slope and dual triangular slope TLDs. Small end slope (particularly 25º) and dual triangular slope of 2.5º performed better in mitigating the response of structure. For medium end slope and large end slope TLDs, no improvement in performance is seen by application of dual triangular slopes. Also, it is seen that there is less benefit with respect to liquid volume reduction in comparison to end slope and central slope combination TLDs.

5.3.5. Response reduction per degree rise of dual triangular slopes

Displacement reductions for the RC framed structure per degree rise of dual triangular slopes are shown in Figure 5.38. The rate of displacement reduction of structure per degree rise of dual triangular slopes increases relatively faster with increase in the amount of end slope of TLD, from 20º to 35º. This rate of increase of reduction of displacement of structure increases moderately for end slopes of TLD between 35º and 40º. The rate of displacement reduction nearly remains constant for end slopes between 40-45º (i.e. for medium end slopes). Similar trend for the rate of displacement reduction has been observed for all input motions of earthquakes. The rate of displacement reduction for higher end slopes drops (i.e. 1.09 for El Centro earthquake see Table 5.19) for end slope of 45º and above.

5.4. CONCLUSIONS

In this chapter, dynamic analyses of a RC frame structure with combined end and single / dual slope TLDs, subjected to earthquake time histories have been presented, using the fluid-structure FE code developed. The effects of angle of end and central, dual slopes have been assessed on the performance (i.e. displacement reduction) of the RC frame with TLDs. Further, studies have also been conducted to investigate the effects of the slope angles on the tuning and mass reduction ratios. The results of the analyses have been summarised below.

a) On performance of TLD with end slope and central slope

- Damping decreases with increasing amount of central slope angle for a fixed end slope. Marginal improvement (0.2-0.5 %) in performance (i.e. displacement reduction re) is seen for TLD with 25º end slope and 2.5º central slope.

- The tuning ratio of TLD decreases with increase in central slope angle at the bottom of TLD, for a constant end slope. Maximum tuning ratio has been observed to be 1.01 end slope of 20º and central slope of 2.5º. Whilst, minimum tuning ratio has been seen to be 0.92 for the TLD with 50º end slope and 15º central slope.

- The liquid mass in TLD decreases with increase in central slope angle of TLD and that the rate of reduction in liquid mass increases with increase in end slope value of TLD. Maximum liquid mass reduction of around 49.47 % is seen for the TLD with end slope of 30º and central slope of 25º. Minimum liquid mass reduction of 10.90 % is seen for the case of TLD with 50º end slope and no (0º) central slope.

- Rate of displacement reduction of structure per degree rise of central slope increases rapidly with the amount of end slope of TLD from 20º to 30º. This rate of increase of reduction of displacement of structure increases moderately for end slopes of TLD between 30º and 40º. The rate of displacement reduction for higher end slopes almost remains constant.

b) On performance of TLD with end slope and dual triangular slopes

- Reduction in displacement of structure decreases with increase in value of dual triangular slope while end slope is constant. In case of TLD with end slope of 25º and dual triangular slope of 5º the performance of TLD is marginally improved. TLDs with 30º end slope and 5º dual triangular slopes, maximum reduction in displacement of structure of about 45.75 % and 22.40 % is seen for El Centro earthquake motion IS compatible time history base motion respectively.

- Tuning ratio of TLD decreases with the amount of dual triangular slope at the bottom of TLD and variation of tuning ratio with dual triangular slopes is observed to be nonlinear. The range of variation of tuning ratio is seen from 1.01– 0.88.

- The liquid mass in TLD decreases with increase of dual triangular slopes and its variation with slope is found to be linear. The rate of reduction of liquid mass increases with amount of end slope of TLD. Maximum liquid mass reduction due to application of dual triangular slope is found for the TLD with 20 end slope and 25 dual triangular slopes.

- The rate of displacement reduction of structure per degree rise of dual triangular slopes increases relatively faster with the amount of end slope up to 30º. The rate of increase of reduction of displacement of structure increases moderately for end slopes of TLD between 30º and 40º. The rate of displacement reduction nearly remains constant for end slopes between 40º-45º. Same trends of rete of displacements are observed in all input motions of earthquakes. The rate of displacement reduction for higher end slopes drops for end slope of 45º and above.

Table 5.1. Classification of TLD with combination of End slope and central slope

Sr. No.	End slope at TLD bottom (º)	Central slope provided at TLD bottom (º)	Group of TLD
1	20, 25 and 30	2.5, 5, 10, 15, 20 and 25	Small end slope TLD
3	35 and 40	2.5, 5, 10, 15 and 20	Medium end slope TLD
3	45 and 50	2.5, 5, 10 and 15	Large end slope TLD

Table 5.2. Response reduction of structure with end slope and central slope TLD to various base motions (end slope: 20º)

Sr. No.	θ◦	Dimensions (m)		*TR*	Displacement reduction (%)					*MR* (%)
		L	*B*		El Centro	Loma Prieta	North ridge	San Fernando	IS History	
1	0	1.79	0.61	1.01	40.39	22.40	24.10	34.50	18.80	35.69
2	2.5	1.79	0.60	1.012	39.79	22.10	23.80	34.00	18.50	36.37
3	5	1.79	0.60	1.012	39.44	21.80	23.50	33.70	18.30	37.06
4	10	1.80	0.57	1.007	38.81	21.20	22.80	33.00	18.00	38.44
5	15	1.81	0.57	1.001	38.75	21.10	22.70	33.00	18.10	39.87
6	20	1.82	0.55	0.990	37.61	20.40	22.00	32.60	17.80	41.37
7	25	1.84	0.53	0.980	35.83	19.50	20.80	31.30	17.40	42.97

Table 5.3. Response reduction of structure with end slope and central slope TLD to various base motions (end slope: 25º)

Sr. No.	θ◦	Dimensions (m)		*TR*	Displacement reduction (%)					*MR* (%)
		L	*B*		El Cento	Loma Prieta	Northridge	San Fernando	IS History	
1	0	1.81	0.66	1.001	44.00	24.00	25.80	37.80	20.80	27.86
2	2.5	1.81	0.66	0.997	44.58	24.40	26.20	38.30	21.00	29.49
3	5	1.82	0.65	0.995	43.65	23.80	25.60	37.50	20.60	31.14
4	10	1.83	0.61	0.980	41.65	22.60	24.30	36.00	19.80	34.48
5	15	1.84	0.57	0.970	38.78	21.10	22.60	33.90	18.80	37.92
6	20	1.86	0.54	0.958	34.46	19.20	20.30	30.50	17.40	41.53
7	25	1.89	0.49	0.940	27.87	16.20	16.90	24.90	15.20	45.36

Table 5.4. Response reduction of structure with end slope and central slope TLD to various base motions (end slope: 30º)

Sr. No.	θ◦	Dimensions (m)		*TR*	Displacement reduction (%)					*MR* (%)
		L	*B*		El Cento	Loma Prieta	Northridge	San Fernando	IS History	
1	0	1.83	0.72	0.991	47.47	26.10	27.80	41.30	23.10	22.50
2	2.5	1.84	0.70	0.980	46.30	25.40	27.10	40.30	22.50	24.88
3	5	1.84	0.67	0.980	44.58	24.50	26.10	38.90	21.70	27.43
4	10	1.85	0.61	0.970	40.25	22.20	23.60	35.40	19.90	32.60
5	15	1.87	0.56	0.970	35.30	19.90	20.90	31.30	18.10	37.93
6	20	1.89	0.51	0.950	28.06	16.60	17.70	25.10	15.40	43.52
7	25	1.93	0.42	0.940	18.62	11.80	11.90	16.70	11.40	49.47

Table 5.5. Response reduction of structure with end slope and central slope TLD to various base motions (end slope: 35º)

Sr. No.	θ◦	Dimensions (m)		*TR*	Displacement reduction (%)					*MR* (%)
		L	*B*		El Cento	Loma Prieta	Northridge	San Fernando	IS History	
1	0	1.86	0.75	0.976	46.77	26.30	27.70	41.30	23.70	21.56
2	2.5	1.86	0.72	0.975	44.98	25.30	26.60	39.70	22.80	21.86
3	5	1.86	0.69	0.974	42.97	24.20	25.40	38.00	21.90	25.19
4	10	1.87	0.62	0.967	37.57	21.40	22.40	33.40	19.60	31.91
5	15	1.89	0.55	0.957	30.43	17.90	18.50	27.20	16.70	38.89
6	20	1.92	0.49	0.942	22.27	13.90	14.10	20.00	13.40	46.37

Table 5.6. Response reduction of structure with end slope and central slope TLD to various base motions (end slope: 40º)

Sr. No.	θ◦	Dimensions (m)		*TR*	Displacement reduction (%)					*MR* (%)
		L	*B*		El Cento	Loma Prieta	Northridge	San Fernando	IS History	
1	0	1.88	0.77	0.966	43.99	25.60	26.60	39.20	23.50	15.47
2	2.5	1.88	0.73	0.964	41.88	24.30	25.30	37.30	22.40	19.48
3	5	1.88	0.69	0.962	39.43	23.00	23.90	35.20	21.20	23.49
4	10	1.90	0.61	0.956	32.98	19.60	20.20	29.50	18.30	31.63
5	15	1.92	0.53	0.940	24.97	15.50	15.70	22.40	14.80	40.03
6	20	1.95	0.44	0.920	16.18	10.80	10.80	14.60	10.60	48.83

Table 5.7. Response reduction of structure with end slope and central slope TLD to various base motions (end slope: 45º)

Sr. No.	θ◦	Dimensions (m)		*TR*	Displacement reduction (%)					*MR* (%)
		L	*B*		El Cento	Loma Prieta	North ridge	San Fernando	IS History	
1	0	1.90	0.78	0.956	39.56	24.10	24.60	35.40	22.50	12.98
2	2.5	1.90	0.74	0.953	37.47	22.70	23.30	33.60	21.30	17.54
3	5	1.90	0.70	0.951	34.78	21.20	21.70	31.20	20.00	22.18
4	10	1.92	0.61	0.944	28.00	17.50	17.70	25.10	16.70	31.55
5	15	1.94	0.51	0.933	20.00	13.10	13.10	18.00	12.80	40.35

Table 5.8. Response of structure with end slope and central slope TLD to various base motions (end slope: 50º)

Sr. No.	θ◦	Dimensions (m)		*TR*	Displacement reduction (%)					*MR* (%)
		L	*B*		El Cento	Loma Prieta	North ridge	San Fernando	IS History	
1	0	1.92	0.79	0.947	34.91	22.10	22.40	31.30	21.10	10.90
2	2.5	1.92	0.74	0.942	32.12	20.50	20.70	28.80	19.60	16.20
3	5	1.93	0.70	0.940	29.53	18.90	19.10	26.50	18.20	21.18
4	10	1.94	0.60	0.930	22.88	15.10	15.10	20.60	14.70	31.63
5	15	1.97	0.50	0.920	15.43	10.80	10.70	14.00	10.60	42.40

Table 5.9. Rate of reduction of displacement response per degree rise of central slope

Sr. No.	End slope (º)	Input motion				
		El Centro	Loma Prieta	Northridge	San Fernando	IS time history
1	20	0.18	0.11	0.13	0.12	0.05
2	25	0.64	0.31	0.35	0.51	0.22
3	30	1.15	0.57	0.63	0.98	0.46
4	35	1.22	0.62	0.68	1.06	0.51
5	40	1.39	0.74	0.79	1.23	0.64
6	45	1.30	0.73	0.76	1.16	0.64
7	50	1.29	0.74	0.78	1.15	0.67

Table 5.10. Rate of liquid mass reduction per degree Central slope

	End slope (º)						
	20	25	30	35	40	45	50
Liquid mass reduction rate	0.29	0.70	10.7	1.39	1.66	1.82	2.10

Table 5.11. Classification of TLD with combination of End slope and dual triangular slope

Sr. No.	End slope at TLD bottom (º)	Central dual slope provided at TLD bottom (º)	Group of TLD
1	20, 25,30 and 35	5, 10, 15, 20 and 25	Small end slope TLD
3	40 and 45	5, 10, 15, 20 and 25	Medium end slope TLD
3	50	5, 10, 15, 20 and 25	Large end slope TLD

Table 5.12. Response reduction of structure with end slope and dual triangular slope TLD to various base motions (end slope: 20º)

Sr. No.	θ_1°	Dimensions (m)		*TR*	Displacement reduction (%)					*MR* (%)
		L	*B*		El Cento	Loma Prieta	North ridge	San Fernando	IS History	
1	0	1.79	0.61	1.012	40.39	22.40	24.10	34.50	18.80	35.69
2	5	1.80	0.60	1.007	40.14	22.10	23.90	34.30	18.70	36.39
3	10	1.80	0.59	1.003	40.17	21.60	23.70	34.30	18.70	37.09
4	15	1.81	0.58	0.998	39.61	21.50	23.20	34.00	18.50	37.79
5	20	1.83	0.57	0.991	39.31	21.30	22.90	34.00	18.50	38.55
6	25	1.84	0.56	0.981	37.56	20.30	21.90	32.90	18.40	39.38

Table 5.13. Response reduction of structure with dual triangular slope TLD to various base motions (end slope: 25º)

Sr. No.	θ_1°	Dimensions (m)		*TR*	Displacement reduction (%)					*MR*(%)
		L	B		El Cento	Loma Prieta	North ridge	San Fernando	IS History	
1	0	1.81	0.66	1.001	44.00	24.00	25.80	37.80	20.80	27.86
2	5	1.82	0.66	0.996	44.58	24.30	26.01	38.30	21.10	29.42
3	10	1.82	0.64	0.992	43.45	23.70	25.40	37.50	20.70	31.21
4	15	1.84	0.62	0.984	41.54	22.70	24.20	36.30	20.20	32.88
5	20	1.86	0.60	0.973	37.93	21.20	22.40	33.60	19.20	34.67
6	25	1.89	0.57	0.957	31.26	18.40	19.10	28.00	17.20	36.55

Table 5.14. Response reduction of structure with dual triangular slope TLD to various base motions (end slope: 30º)

Sr. No.	θ_1°	Dimensions (m)		*TR*	Displacement reduction (%)					*MR* (%)
		L	*B*		El Cento	Loma Prieta	North ridge	San Fernando	IS History	
1	0	1.83	0.72	0.991	47.47	26.10	27.80	41.30	23.10	22.50
2	5	1.84	0.69	0.984	45.75	25.20	26.80	39.90	22.40	25.02
3	10	1.85	0.67	0.979	43.22	24.00	25.40	38.00	21.50	27.60
4	15	1.87	0.64	0.969	39.20	22.10	23.20	34.70	20.20	30.25
5	20	1.90	0.60	0.956	32.53	19.30	18.90	29.10	18.00	33.03
6	25	1.93	0.56	0.939	23.87	15.30	15.40	21.40	17.80	36.03

Table 5.15. Response reduction of structure with dual triangular slope TLD to various base motions (end slope: 35º)

Sr. No.	θ_1°	Dimensions (m)		*TR*	Displacement reduction (%)					*MR* (%)
		L	*B*		El Cento	Loma Prieta	North ridge	San Fernando	IS History	
1	0	1.86	0.75	0.976	46.77	26.30	27.70	41.30	23.70	21.56
2	5	1.86	0.71	0.974	44.50	25.10	26.30	39.30	22.60	22.32
3	10	1.87	0.68	0.968	40.67	22.30	24.30	36.20	21.20	25.70
4	15	1.89	0.64	0.957	34.80	20.60	21.30	31.10	19.20	29.16
5	20	1.92	0.60	0.943	26.76	16.80	17.00	24.00	16.20	32.80
6	25	1.96	0.55	0.925	18.21	12.60	12.40	16.40	12.30	36.68

Table 5.16. Response reduction of structure with dual triangular slope TLD to various base motions (end slope: 40º)

Sr. No.	θ_1°	Dimensions (m)		*TR*	Displacement reduction (%)					*MR* (%)
		L	*B*		El Cento	Loma Prieta	North ridge	San Fernando	IS History	
1	0	1.88	0.77	0.966	43.99	25.60	26.60	39.20	23.50	15.47
2	5	1.88	0.73	0.962	40.98	24.00	24.90	36.60	22.20	19.45
3	10	1.90	0.69	0.955	36.26	21.70	22.30	32.40	20.30	23.51
4	15	1.92	0.64	0.944	29.29	18.30	18.60	26.30	17.50	27.65
5	20	1.95	0.59	0.928	20.82	14.10	14.00	18.70	13.80	32.12
6	25	2.00	0.54	0.908	13.30	9.70	9.50	12.10	9.40	36.83

Table 5.17. Response reduction of structure with dual triangular slope TLD to various base motions (end slope: 45º)

Sr. No.	θ_1°	Dimensions (m)		*TR*	Displacement reduction (%)					*MR* (%)
		L	*B*		El Cento	Loma Prieta	North ridge	San Fernando	IS History	
1	0	1.90	0.78	0.956	39.56	24.10	24.60	35.40	22.50	12.98
2	5	1.90	0.74	0.953	38.37	23.00	23.70	34.30	21.60	17.60
3	10	1.92	0.69	0.945	31.50	19.70	20.00	28.20	18.80	22.11
4	15	1.94	0.64	0.933	24.26	16.10	16.10	21.80	15.60	27.08
5	20	1.98	0.58	0.916	16.47	11.80	11.60	14.90	11.50	32.12
6	25	2.03	0.52	0.895	10.98	7.80	7.80	10.00	7.50	37.51

Table 5.18. Response reduction of structure with dual triangular slope TLD to various base motions (end slope: 50º)

Sr. No.	θ_1°	Dimensions (m)		*TR*	Displacement reduction (%)					*MR* (%)
		L	*B*		El Cento	Loma Prieta	North ridge	San Fernando	IS History	
1	0	1.92	0.79	0.947	34.91	22.10	22.40	31.30	21.10	10.90
2	5	1.93	0.74	0.941	31.78	20.30	20.50	28.50	19.50	15.99
3	10	1.94	0.69	0.934	26.42	17.50	17.50	23.80	17.00	21.22
4	15	1.97	0.63	0.922	19.49	13.70	13.50	17.60	13.40	27.00
5	20	2.01	0.57	0.905	13.51	9.80	9.70	12.30	9.50	32.25
6	25	2.06	0.51	0.883	9.60	6.60	6.60	8.70	6.30	38.26

Table 5.19. Rate of reduction of response per degree rise of dual triangular slope

Sr. No.	End slope (º)	Input motion				
		El Centro	Loma Prieta	Northridge	San Fernando	IS time history
1	20	0.10	0.06	0.08	0.05	0.01
2	25	0.53	0.23	0.28	0.41	0.15
3	30	0.87	0.39	0.45	0.74	0.30
4	35	1.05	0.52	0.55	0.91	0.41
5	40	1.10	0.57	0.61	0.98	0.51
6	45	1.09	0.60	0.63	0.97	0.54
7	50	0.88	0.54	0.55	0.79	0.52

Table 5.20. Rate of liquid mass reduction per degree dual triangular slope

	End slope (º)						
	20	25	30	35	40	45	50
Liquid mass reduction rate	0.11	0.28	0.43	0.57	0.69	0.79	0.89

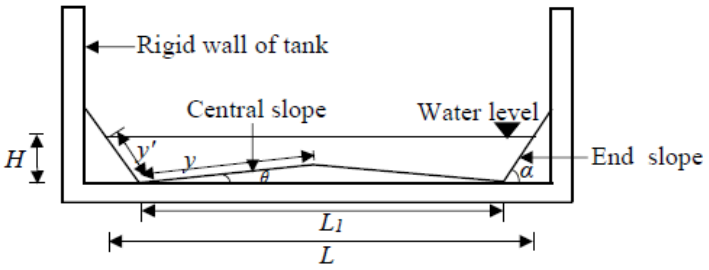

(a)

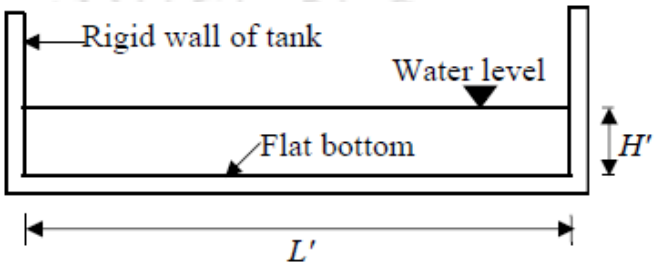

(b)

Figure 5.1. Sloped bottom TLD (a) Combined end slope and central slope TLD, (b) Equivalent flat bottom TLD

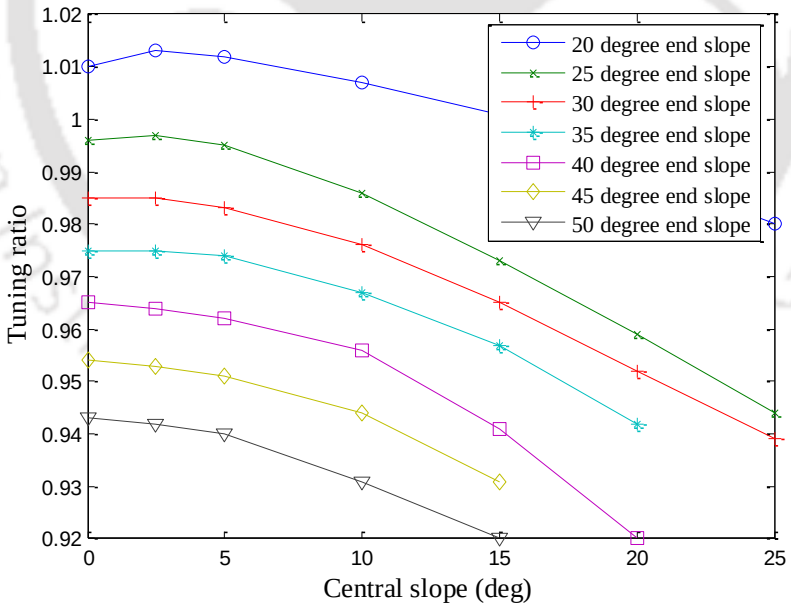

Figure 5.2. Variation of tuning ratio with central slope of TLD

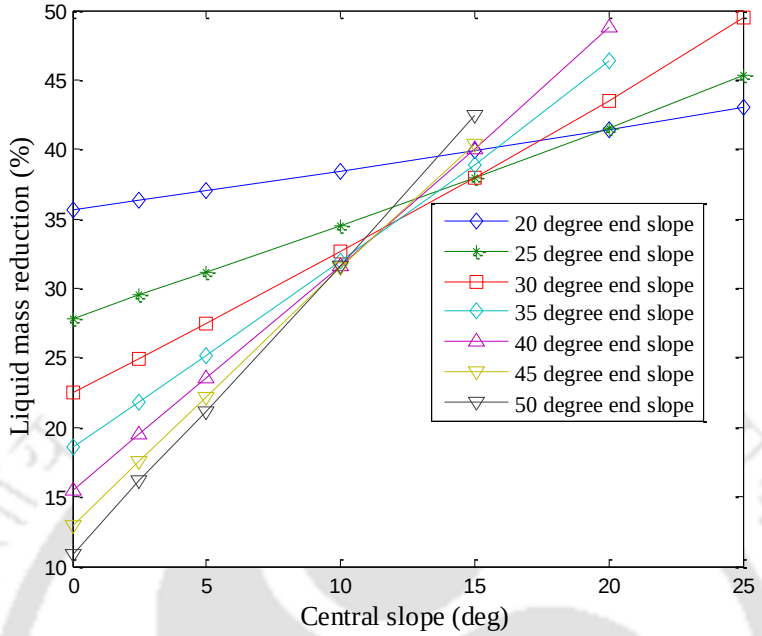

Figure 5.3.Variation of liquid mass reduction with central slope of TLD

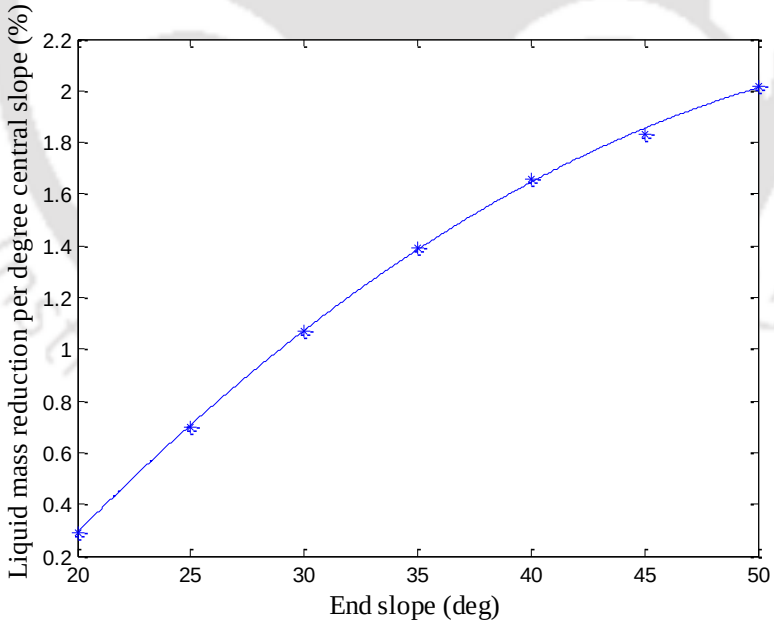

Figure 5.4. Variation of rate of liquid mass reduction per degree central slope with end slope angle of TLD

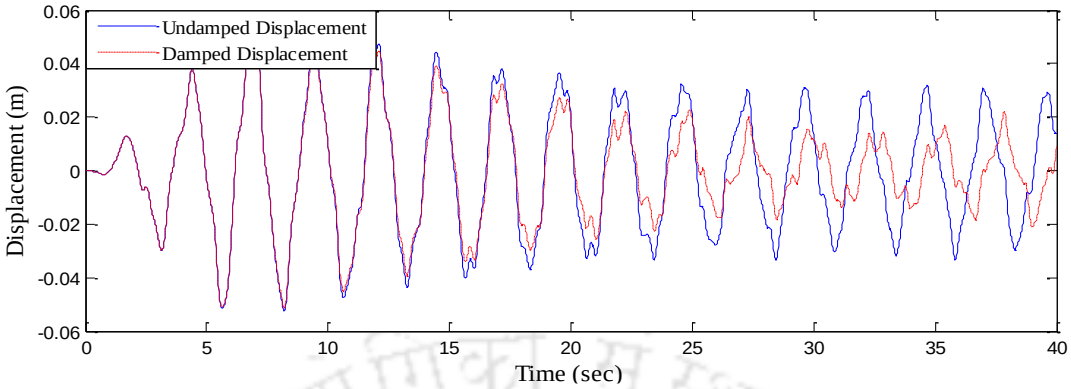

Figure 5.5. Response of structure with 20º end slope and 5º central slope TLD subjected to El Centro earthquake

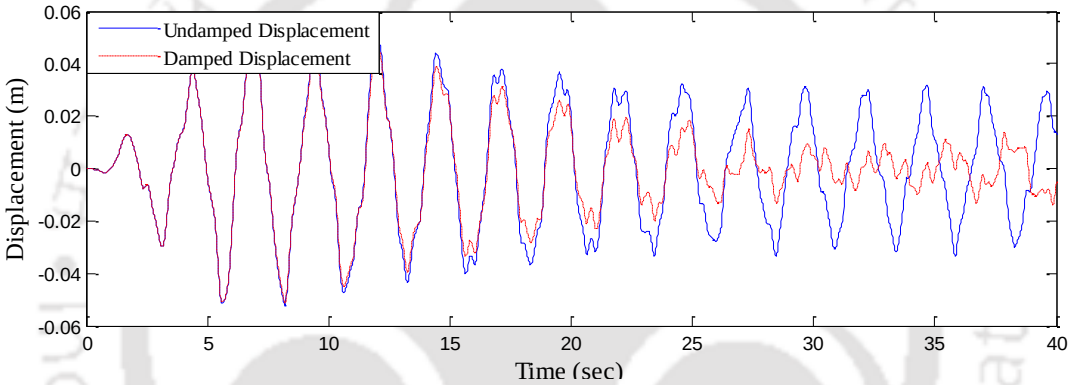

Figure 5.6. Response of structure with 25º end slope and 5º central slope TLD subjected to El Centro earthquake

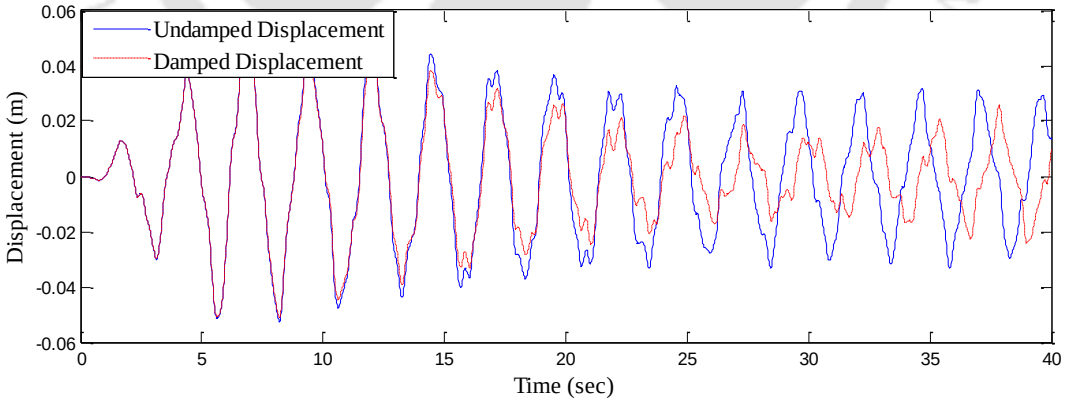

Figure 5.7. Response of structure with 30º end slope and 5º central slope TLD subjected to El Centro earthquake

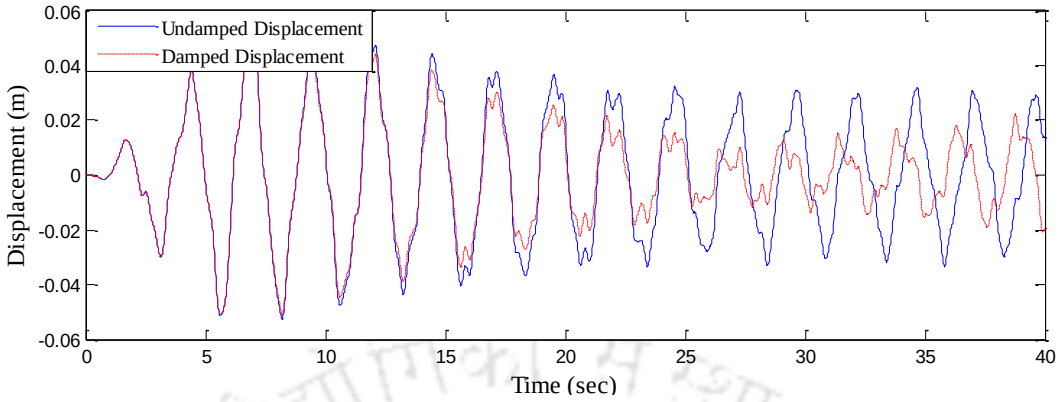

Figure 5.8. Response of structure with 35º end slope and 5º central slope TLD subjected to El Centro earthquake

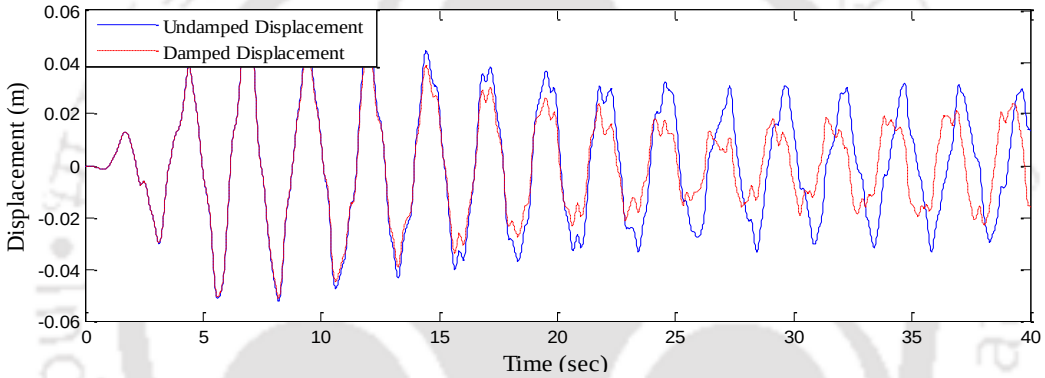

Figure 5.9. Response of structure with 40º end slope and 5º central slope TLD subjected to El Centro earthquake

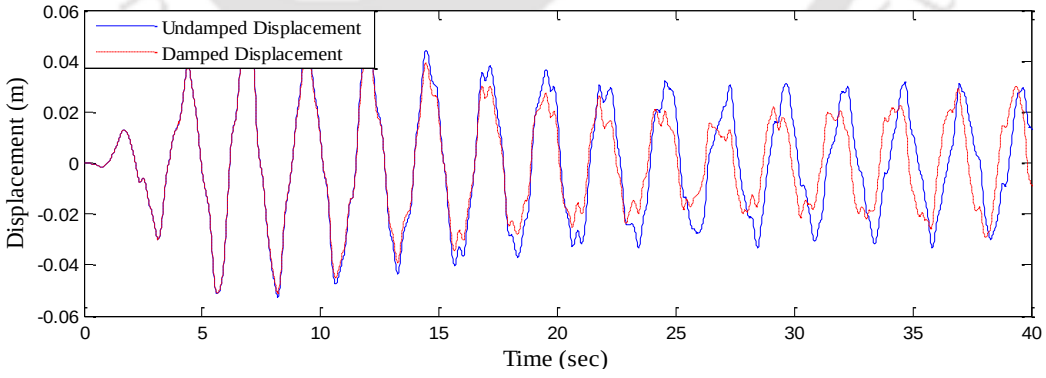

Figure 5.10. Response of structure with 45º end slope and 5º central slope TLD subjected to El Centro earthquake

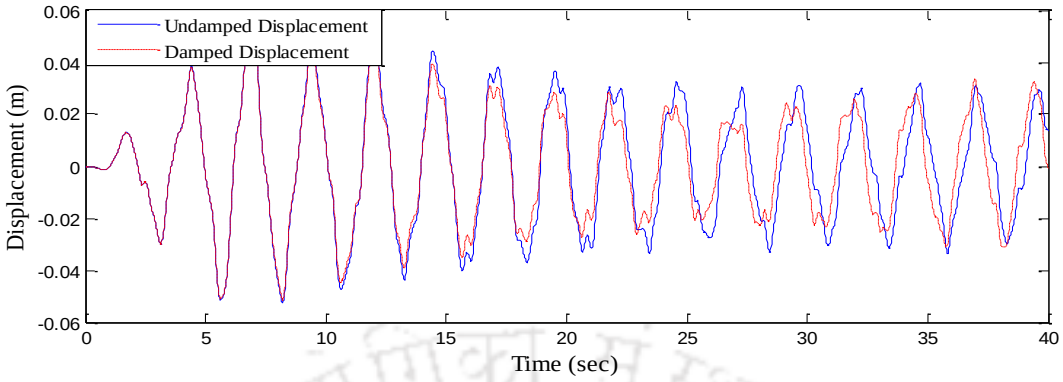

Figure 5.11. Response of structure with 50º end slope and 5º central slope TLD subjected to El Centro earthquake

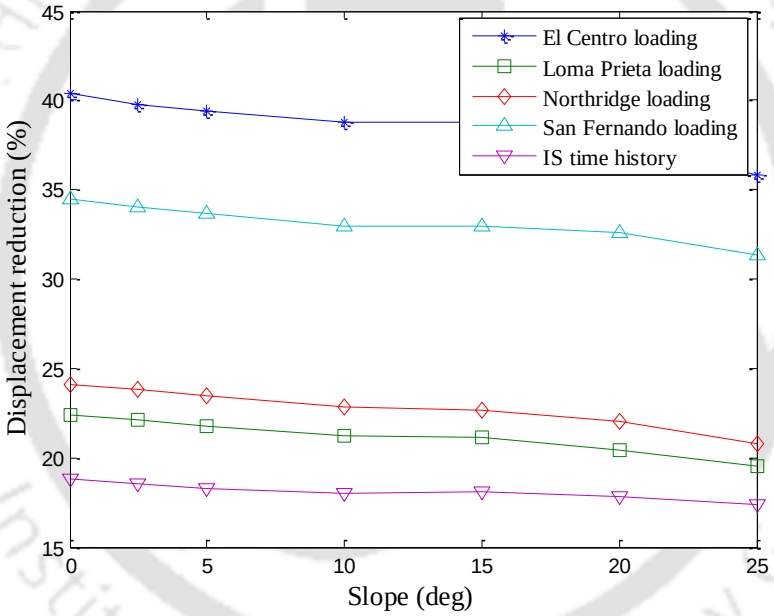

Figure 5.12. Variation of displacement reduction (DR) with central bottom slope (end slope = 20º)

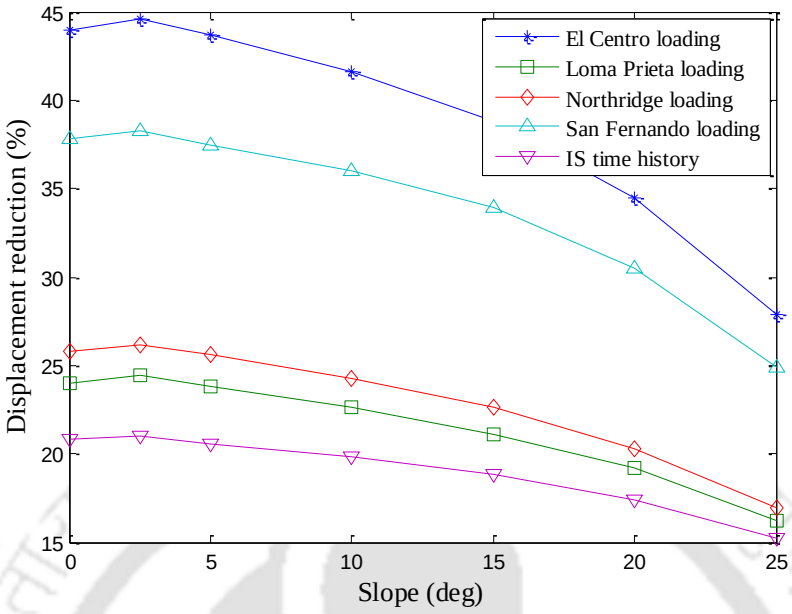

Figure 5.13. Variation of displacement reduction (DR) with central bottom slope (end slope = 25º)

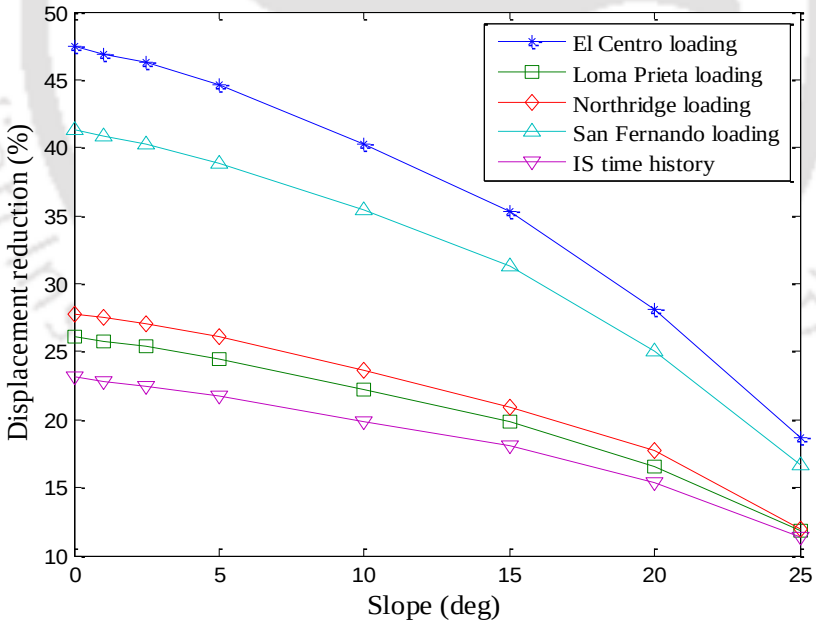

Figure 5.14. Variation of displacement reduction (DR) with central bottom slope (end slope = 30º)

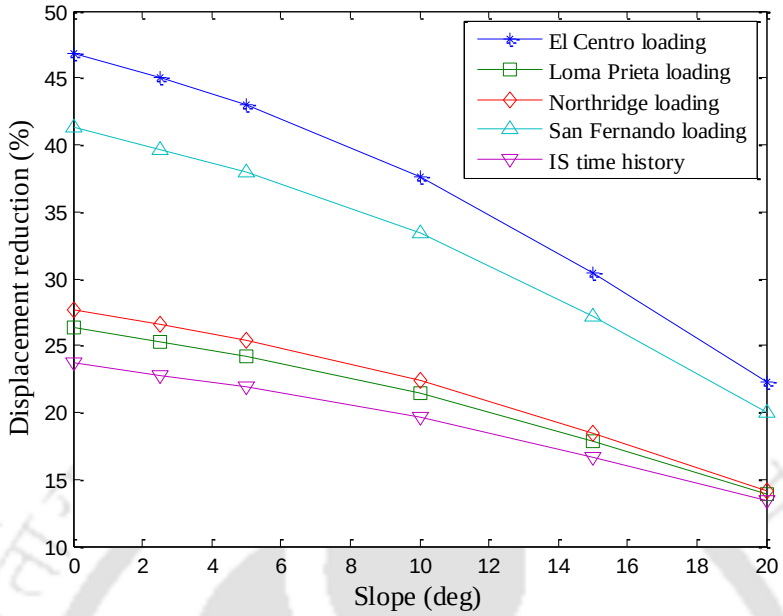

Figure 5.15. Variation of displacement reduction (DR) with central bottom slope (end slope = 35º)

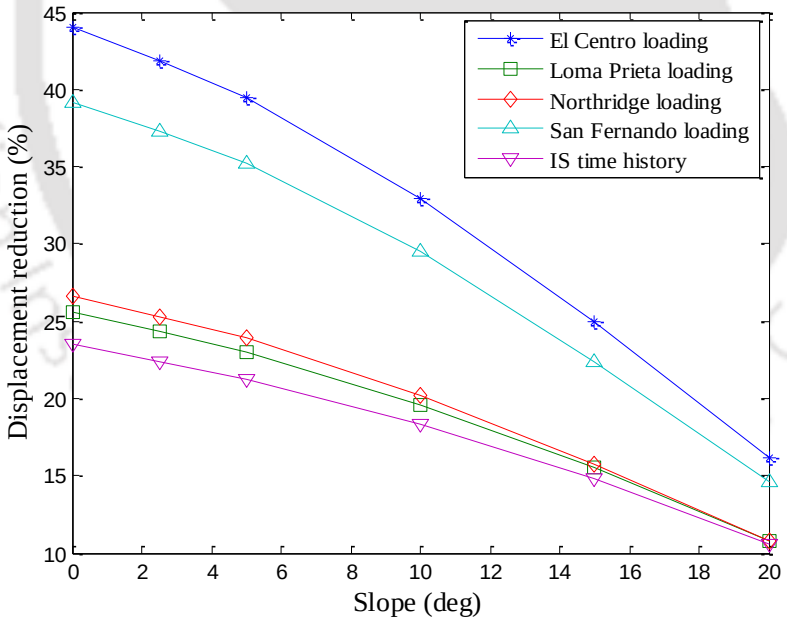

Figure 5.16. Variation of displacement reduction (DR) with central bottom slope (end slope = 40º)

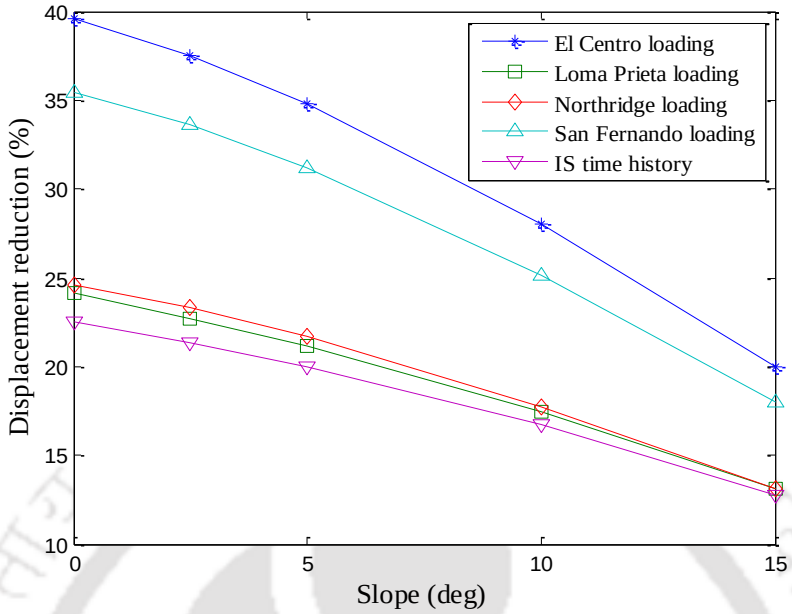

Figure 5.17. Variation of displacement reduction (DR) with central bottom slope (end slope = 45º)

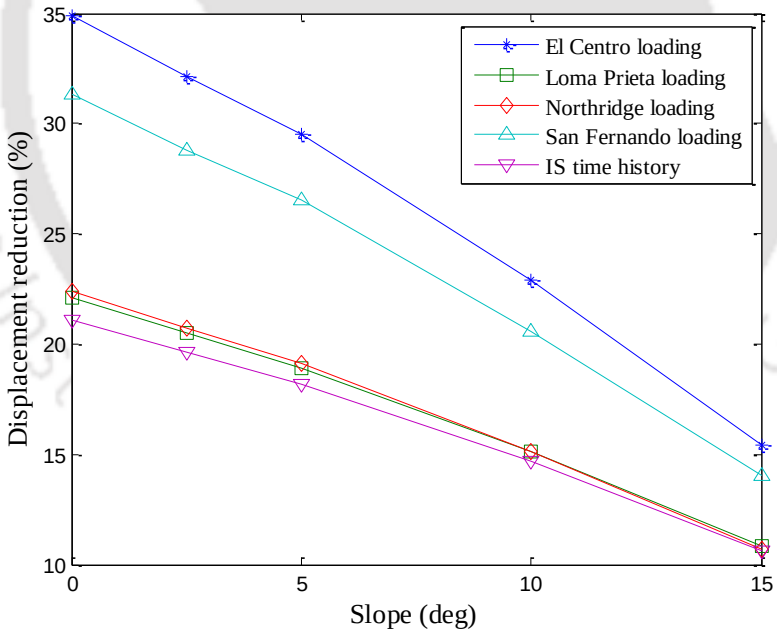

Figure 5.18. Variation of displacement reduction (DR) with central bottom slope (end slope = 50º)

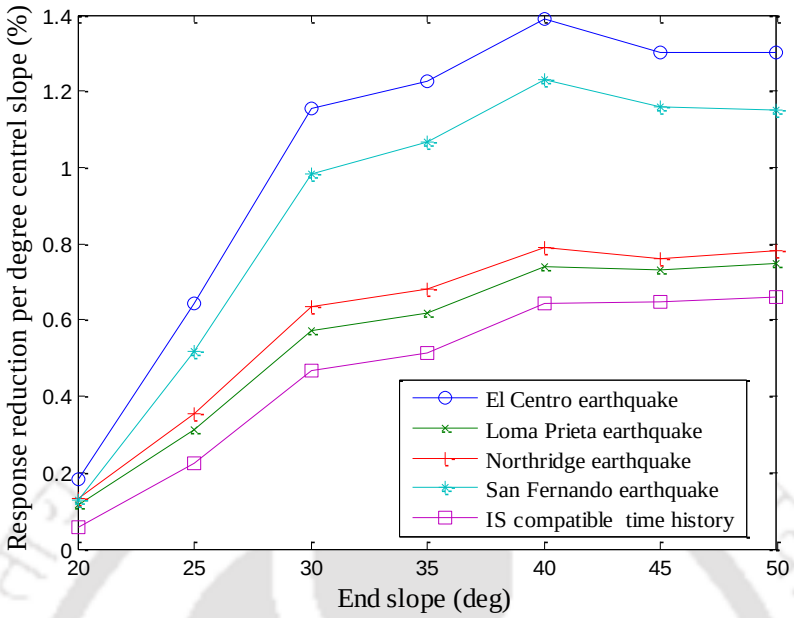

Figure 5.19. Variation of rate of response reduction of structure per degree central slope with end slope angle of TLD

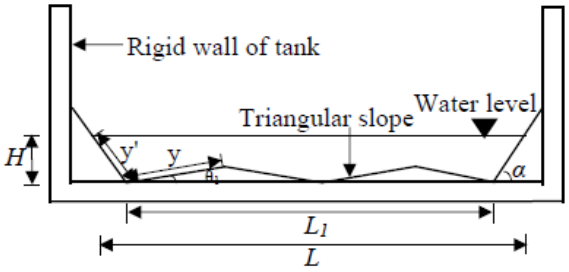

(a)

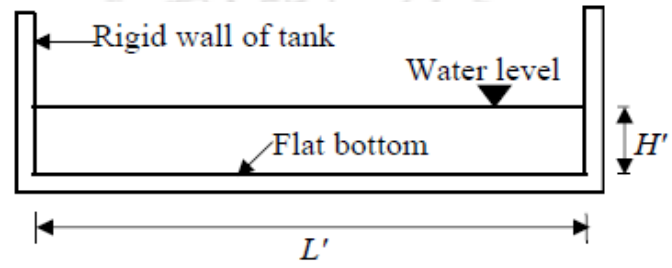

(b)

Figure 5.20. Sloped bottom TLD (a) Combined end slope and dual triangular slope TLD, (b) Equivalent flat bottom TLD

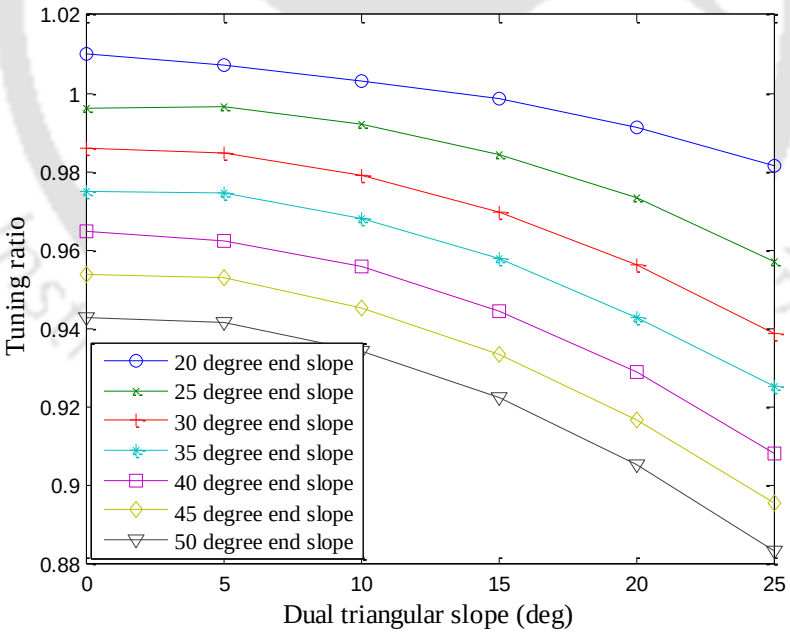

Figure 5.21. Variation of tuning ratio with dual triangular slope of TLD

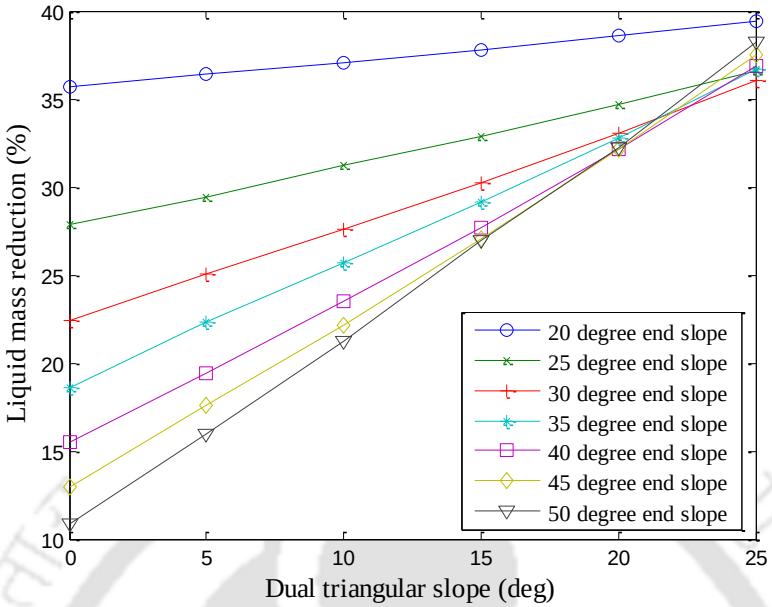

Figure 5.22. Variation of liquid mass reduction with dual triangular slope of TLD

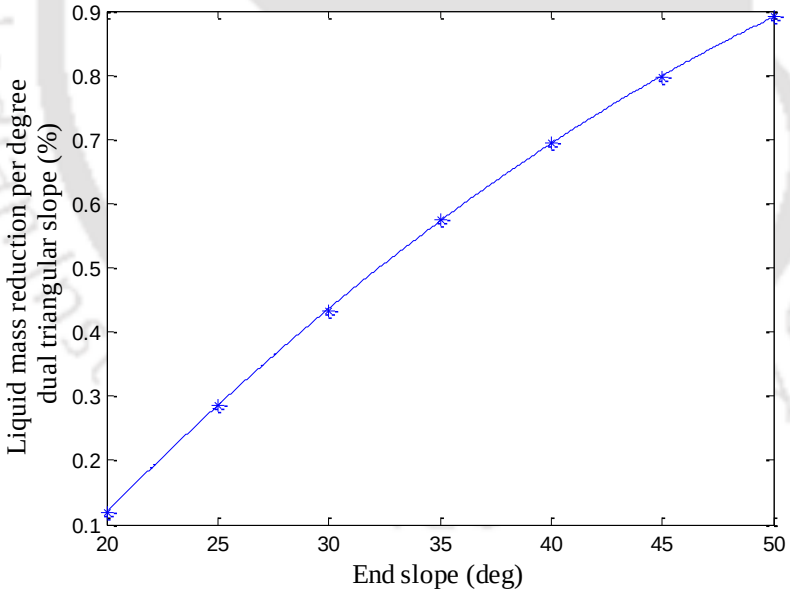

Figure 5.23. Variation of rate of liquid mass reduction per degree dual triangular slope with end slope angle of TLD

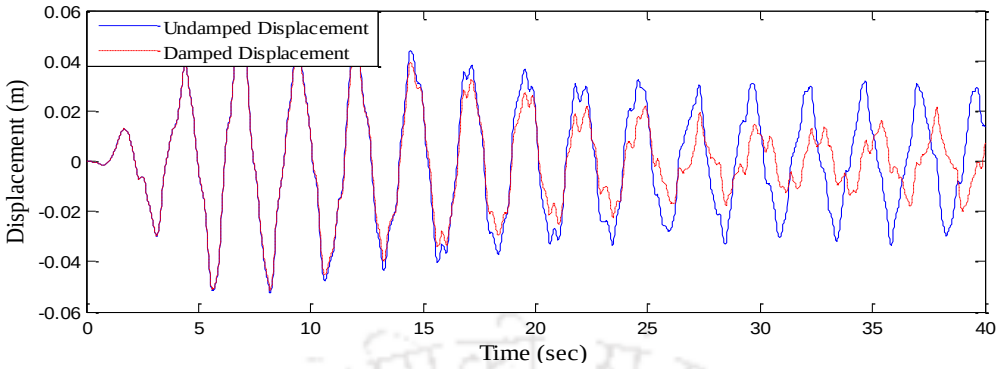

Figure 5.24. Response of structure with 20º end slope and 5º dual triangular slope TLD subjected to El Centro earthquake

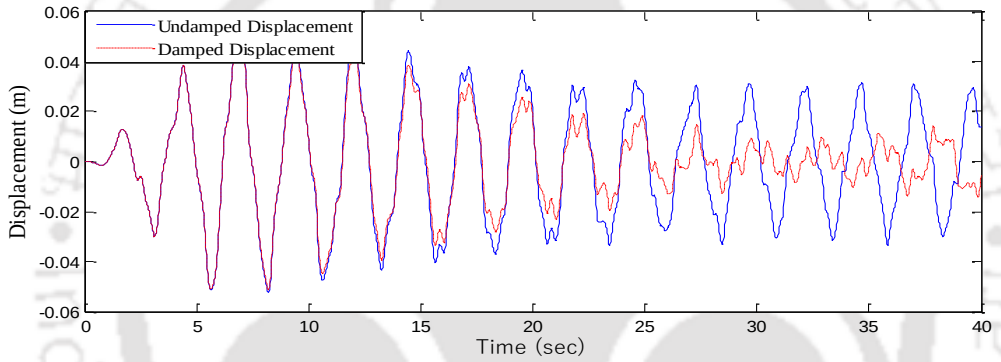

Figure 5.25. Response of structure with 25º end slope and 5º dual triangular slope TLD subjected to El Centro earthquake

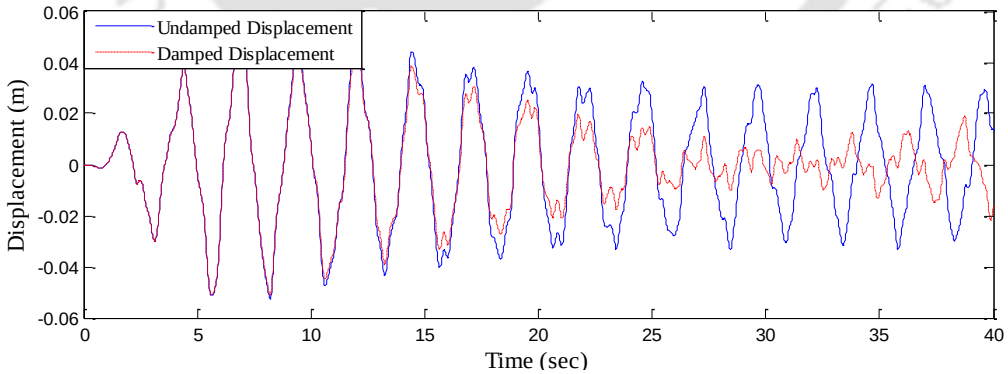

Figure 5.26. Response of structure with 30º end slope and 5º dual triangular slope TLD subjected to El Centro earthquake

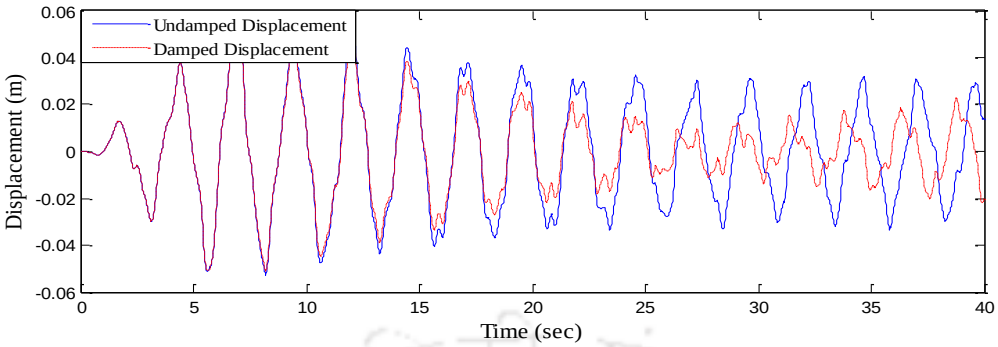

Figure 5.27. Response of structure with 35º end slope and 5º dual triangular slope TLD subjected to El Centro earthquake

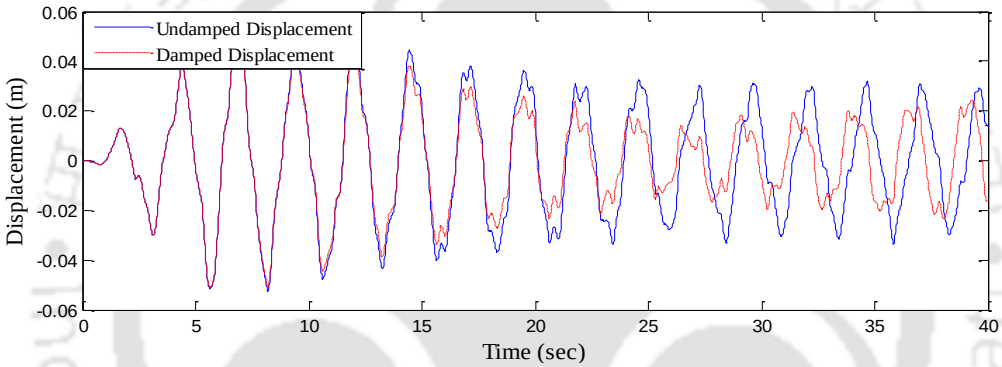

Figure 5.28. Response of structure with 40º end slope and 5º dual triangular slope TLD subjected to El Centro earthquake

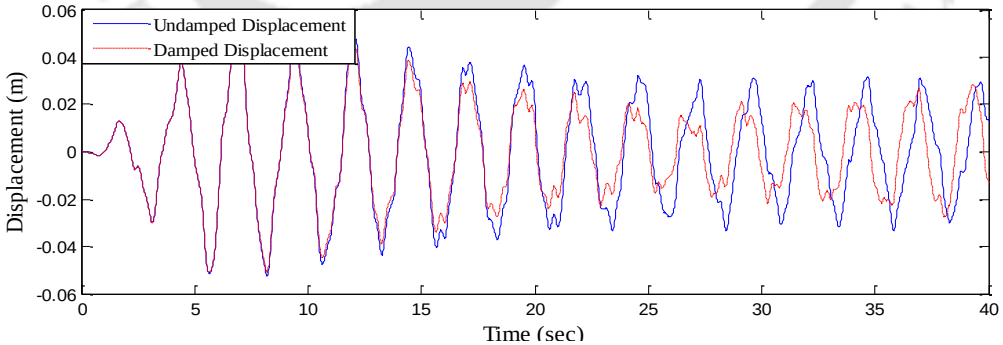

Figure 5.29. Response of structure with 45º end slope and 5º dual triangular slope TLD subjected to El Centro earthquake

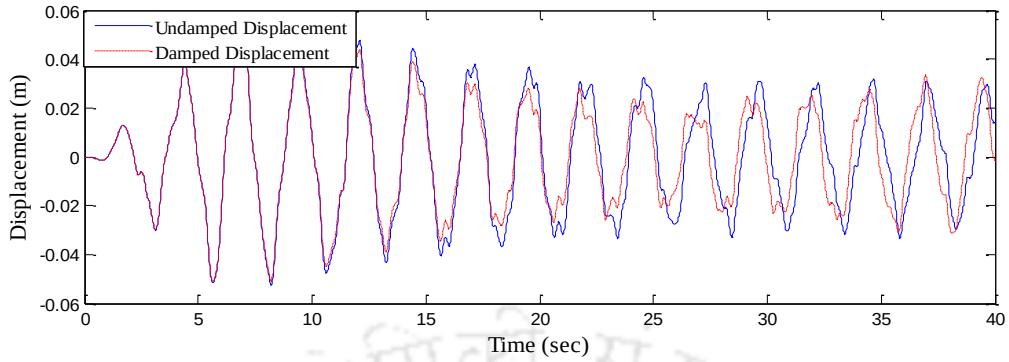

Figure 5.30. Response of structure with 50º end slope and 5º dual triangular slope TLD subjected to El Centro earthquake

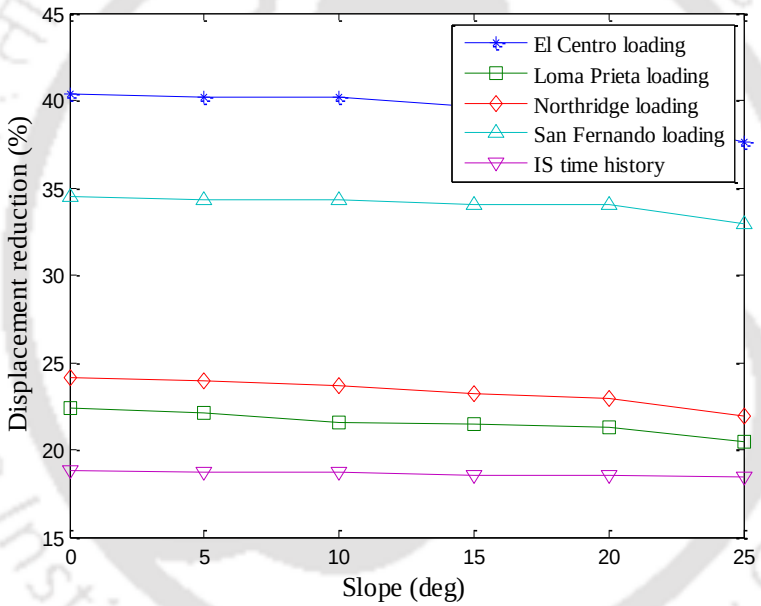

Figure 5.31. Variation of displacement reduction (*DR*) with dual triangular bottom slopes (end slope = 20º)

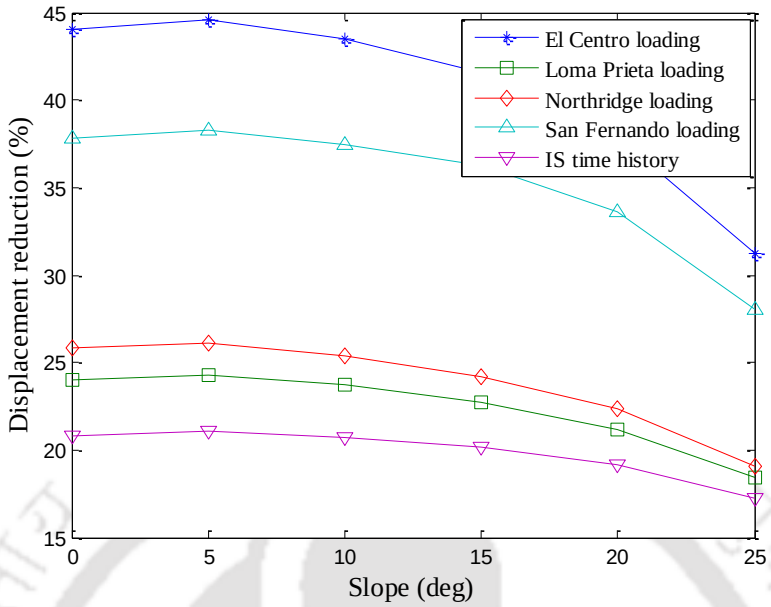

Figure 5.32. Variation of displacement reduction (*DR)* with dual triangular bottom slopes (end slope = 25º)

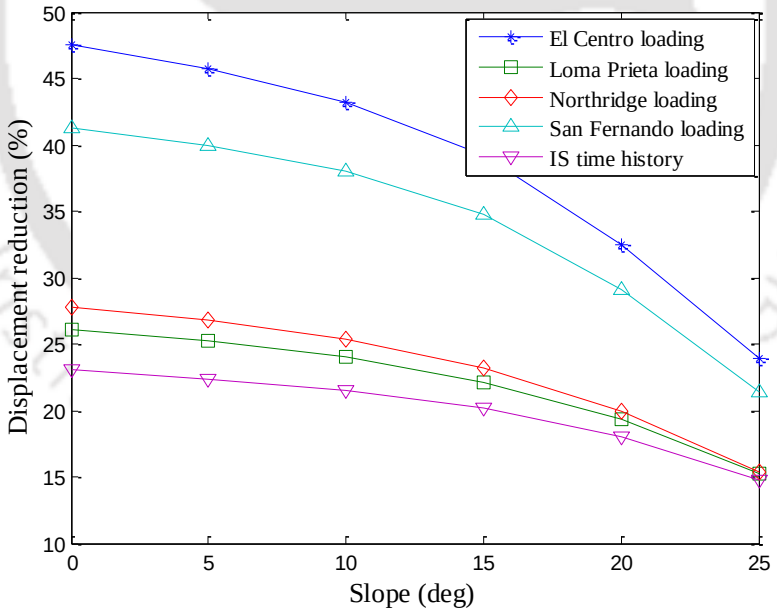

Figure 5.33. Variation of displacement reduction (*DR*) with dual triangular bottom slopes (end slope = 30º)

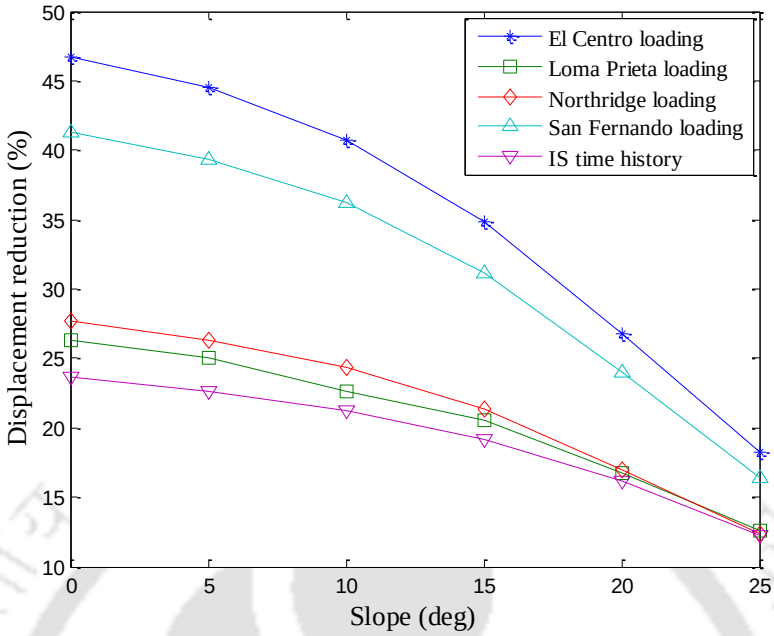

Figure 5.34. Variation of displacement reduction (*DR*) with dual triangular bottom slopes (end slope = 35º)

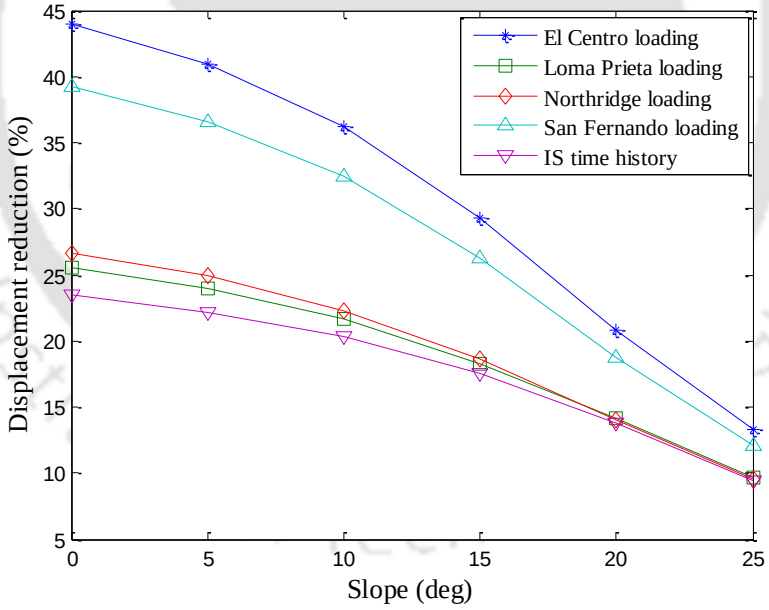

Figure 5.35. Variation of displacement reduction (*DR*) with dual triangular bottom slopes (end slope = 40º)

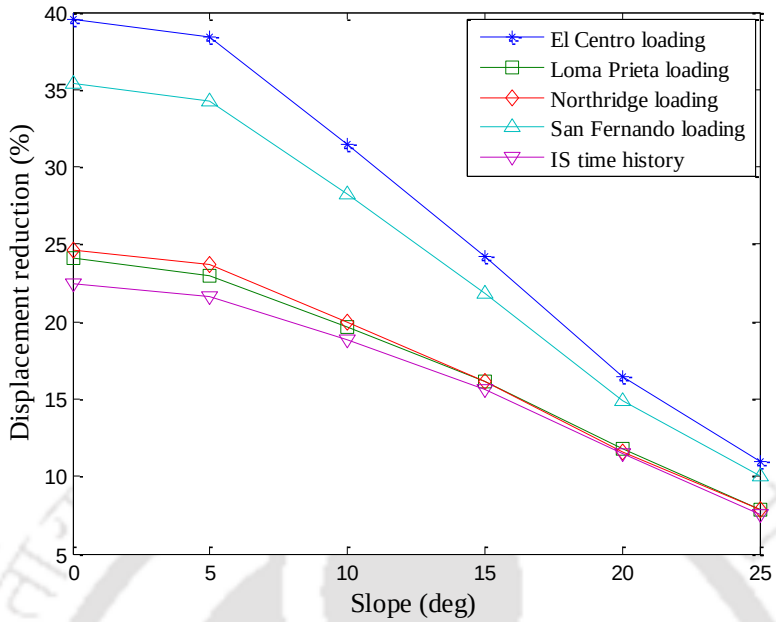

Figure 5.36. Variation of displacement reduction (*DR*) with dual triangular bottom slopes (end slope = 45º)

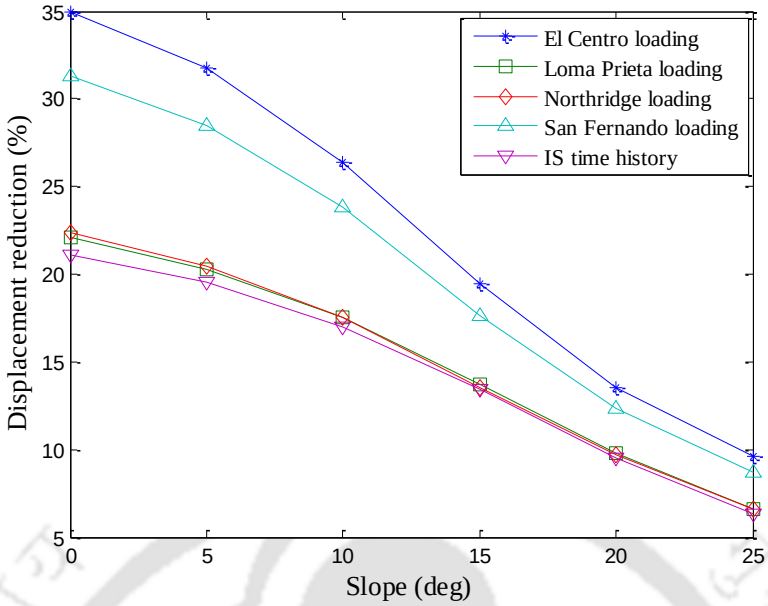

Figure 5.37. Variation of displacement reduction (*DR*) with dual triangular bottom slopes (end slope = 50º)

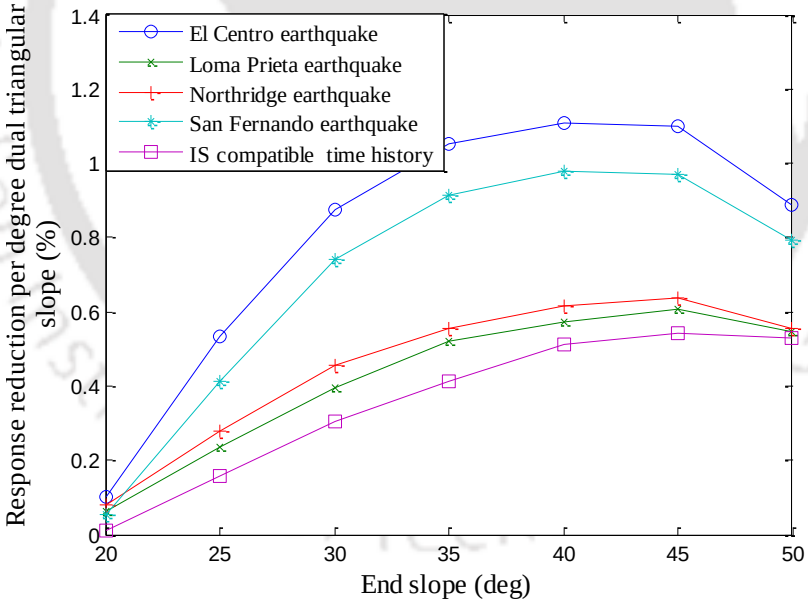

Figure 5.38. Variation of rate of response reduction of structure per degree dual triangular slope with end slope angle of TLD

CHAPTER 6

CONCLUSIONS AND SUGGESTIONS FOR FUTURE WORK

6.1. CONCLUSIONS

In this thesis, dynamic (time history) analyses of a reinforced concrete framed structure with rectangular tuned liquid dampers (TLDs) at the roof level, subjected to both harmonic and earthquake excitations have been conducted, using finite element analysis. The study focused on assessing the effects of tuning ratio, liquid mass reduction and displacement response reduction of the structure, due to the use of rectangular TLDs of various bottom cross-sections viz., i) central slope and dual triangular slopes, ii) end slope and iii) combined end and central slope and combined end and dual triangular slopes. Based on the FE study, the following main conclusions have been summarized.

A) Flat bottom TLD

- TLDs can have different sets of dimensions for same sloshing frequency. However, dimensions of TLD are to be selected properly to avoid beating phenomenon.

- Tuning ratio of TLD has been seen to affect the response of structure and at about 100 % tuning, maximum reduction in displacement is observed. An optimum tuning ratio is close to 1.0 (~1.007) has been seen this the present study. The reduction in displacement at optimum tuning (~1.007) is observed to be ~42 %. The depth ratio for shallow, sloshing absorber is normally < 0.15 and in the present study it is 0.117.

B) TLD with central triangular slope

- When central slope is introduced at TLD bottom it is seen that, reduction in displacement of structure is found to increase with increasing slope. Maximum reduction in displacement of structure, of about 53.73 % and 26.00 % have been observed at 14º central triangular slope TLD, for input motions of El Centro earthquake and IS time history base motions respectively.

- Tuning ratio of TLD decreases with increase of slope at the bottom of TLD and variation is of tuning ratio with angle (0-14º) is found to be nonlinear. With increase of slope, tuning ratio is seen to change from over-tuned (tuning ratio > 1.0) to a value close to 1.

- Liquid mass reduction in TLD is observed to increase with increasing slope, leading to an additional benefit of sloped bottom TLD. The variation of liquid mass reduction with slope has been observed to be linear. In the present study, liquid mass reduction for slope of 14º is observed to be 47.93 %.

C) TLD with dual triangular slopes at bottom

- With the application of dual triangular slopes at the bottom of TLD, it is seen that the effectiveness of TLD in reducing displacement of structure, increases with increase of slope up to an optimal slope angle. The rate of increase of effectiveness (in displacement reduction) is found to be relatively smaller at lower slope values. In the present study, an optimum value of dual triangular slopes is observed to be around 20º. Maximum reduction in displacement of about 59.27 % and 29.00 % have been observed for the input motions of El Centro earthquake motion and IS time history base motion respectively.

- Tuning ratio of TLD decreases with increase of slope value (e.g. 0-25º) and the variation has been observed to be nonlinear.

- Liquid mass reduction increases with increasing amount of slope and the variation is observed to be linear. Liquid mass reduction of about 35.01 % has been observed at optimum slope of 20º.

D) TLD with end slope

- Results of dynamic analysis of structure with TLD having end slope by two approaches are found nearly similar. Results of harmonic input show that an optimum slope angle of 30.5º with *DR* = 37.72 % and 29.5º with *DR* = 35.65 % by Gardarsson's and Xin's approach respectively.

- Gardarsson's approach gives maximum reduction in displacement response for the end slope of around 30º for all input excitations. However, Xin's approach gives maximum reduction for the end slope angle range of 30-35º.

- With respect to Gardarsson's approach, there seems to be no improvement in displacement reduction for TLD with end slope angle of > 45º. In case of Xin's approach this slope, angle has a range of 40-45º.

- In case of Gardarsson's approach the end slope angle of around 25º and above, results in improvement in response reduction in comparison to flat TLD. Form the Xin's approach this angle of end slope is 25-30º.

- Liquid mass reduction at an optimum slope angle is observed to be 22 % and 23 % when Gardarsson's and Xin's approach of modelling is used respectively.

E) TLD with end slope and central slope

- Damping decreases with amount of central slope while end slope of TLD is constant. Marginal improvement (0.2-0.5 %) in performance (displacement reduction of structure) is seen for TLD with 25º end slope and 2.5º central triangular slope.

- The tuning ratio of TLD decreases with increase of central slope at the bottom of TLD while end slope is constant. Maximum tuning ratio observed is 1.01 for the TLD with end slope of 20º and central slope of 2.5º. Minimum tuning ratio observed is 0.92 for the TLD with 50º end slope and 15º central triangular slope.

- The liquid mass in TLD decreases with increase of central slope of TLD and that the rate of reduction in liquid mass increases with end slope value of TLD. Maximum liquid mass reduction of around 49.47 % is seen for the TLD with end slope of 30º and central slope of 25º. Minimum liquid mass reduction of 10.90 % is seen for the case of TLD with 50º end slope and no (0º) central triangular slope.

- Rate of displacement reduction of structure per degree rise of central slope increases rapidly with the amount of end slope of TLD from 20º to 30º. This rate of increase of reduction of displacement of structure increases moderately for end slopes of TLD between 30º and 40º. The rate of displacement reduction for higher end slopes almost remains constant.

F) TLD with end slope and dual triangular slopes

- Reduction in displacement of structure decreases with increase in value of dual triangular slope while end slope is constant. In case of TLD with end slope of 25º and dual triangular slope of 5º the performance of TLD is

marginally improved. TLDs with 30º end slope and 5º dual triangular slopes, maximum reduction in displacement of structure of about 45.75 % and 22.40 % is seen for El Centro earthquake motion IS compatible time history base motion respectively.

- Tuning ratio of TLD decreases with the amount of dual triangular slope at the bottom of TLD and variation of tuning ratio with dual triangular slopes is observed to be nonlinear. The range of variation of tuning ratio is seen from 1.01–0.88.

- The liquid mass in TLD decreases with increase of dual triangular slopes and its variation with slope is found to be linear. The rate of reduction of liquid mass increases with amount of end slope of TLD. Maximum liquid mass reduction due to application of dual triangular slope is found for the TLD with 20º end slope and 25º dual triangular slopes.

- The rate of displacement reduction of structure per degree rise of dual triangular slopes increases relatively faster with the amount of end slope up to 30º. The rate of increase of reduction of displacement of structure increases moderately for end slopes of TLD between 30º and 40º. The rate of displacement reduction nearly remains constant for end slopes between 40-45º. Same trends of rete of displacements are observed in all input motions of earthquakes. The rate of displacement reduction for higher end slopes drops for end slope of 45º and above.

6.2. SUGGESTIONS FOR FURTHER WORK

Following are some of the suggestions about the extension present study.

1. Investigation of performance of sloped bottom TLD with variable density and variable viscosity of liquid.

2. Develop design curves for structures, covering range of natural frequencies and optimum depth ratio (depth of liquid/ length of TLD) of TLD.

3. Investigate performance of TLD while structure is subjected to components of earthquake ground motion in two mutually perpendicular direction.

4. Investigate performance of TLD with curved edges of varying radii at bottom.

REFERENCES

Abramson, H. N. (1966). The dynamic behaviour of liquids in moving containers, *NASA SP*-106.

Ahmad, M. J., et. al. (2016) Use of water tank as tuned liquid damper (TLD) for reinforced concrete structures. *Arab J Sci Engineering*, 41, 4953 – 4965.

Ali, A. S., James, K. and Oya, M. (2014). Investigation of the use of multiple tuned liquid dampers in vibration control. *Structures Congress 2014@ ASCE*.

Ali, A. S., Hadi, M. and Ghaemmaghami, A. (2016). Experimental investigation of tuned liquid damper-structure interaction in resonance considering multiple parameters. *Journal of Sound and Vibration*, 388, 141-153.

Banerji, P. (2004). Tuned liquid dampers for controlling earthquake response. *13th World Conference on Earthquake Engineering,* Vancouver, B C Canada, Paper No. 1666.

Banerji, P., Murudi, M., Shah, A. H. and Poppliwell, N. (2000). Tuned liquid dampers for controlling earthquake response of structures. *Earthquake Engineering and Structural Dynamics*, 29, 587 - 602.

Bang-Fuh, C. and Shih-Ming, H. A, (2015). Numerical study of liquid tank and structure interaction. *Journal of Marine Science and Technology*, 23, 781 - 791.

Bathe, K. J. (2004). Finite element procedures, *Prentice Hall of India*, Edition, 2004.

Bauer, H. F. (1984). Oscillations of immiscible liquids in a rectangular container: a new damper for excited structures. *Journal of Sound and Vibration*, 93(1), 117 - 133.

Bhattacharjee, E., Halder, L. and Sharma, R. P. (2013). An experimental study on tuned liquid damper for mitigation of structural response. *International Journal of Advanced Structural Engineering*, Feb, 3-8.

Bhattacharyya, S. and Ghosh, A. (2012). Seismic vibration control of elevated water tank by multiple tuned liquid dampers. *ISEI Golden Jubilee Symposium*, IIT Roorkee, October 20 – 21 2012.

Biswal, K. C., Bhattacharya, S. K. and Sinha, P. K. (2003). Dynamic characteristics of liquid filled rectangular tank with baffles. *The Institution of Engineers*, India, 84, 145 - 148.

Chang, C. C. and Gu, M. (1999). Suppression of Vortex-excited vibration of tall buildings using tuned liquid dampers. *Journal of Wind Engineering and Industrial Aerodynamic*, 83, 225 - 237.

Chang, Y. (2015). Analytical and experimental investigations of modified tuned liquid dampers (MTLDs). *Master of Applied Science Thesis,* University of Toronto.

Chen, Y. H., Hwang, W. S., Chiu, L. T. and Sheu, S. M. (1995). Flexibility of TLD to high rise buildings by simple experiment and comparison. *Computer Journal of Wind Engineering and Industrial Aerodynamics*, 57, 855 - 861.

Chopra, A. K. (2003). Structural dynamics, theory and application to earthquake engineering. *Prentice Hall of India Private Limited*, New Delhi.

Corbi, O. (2006). Experimental investigation on sloshing water dampers attached to rigid blocks. *Proceedings of the Fifth WSEAS International Conference on Applied Computer Science*, Hangzhou, China 2006 April, 682 - 687.

El Damatty, A. A. (2002). Studies on application of tuned liquid dampers (tld) to up-grade the seismic resistance of structures. *Institute of Catastrophic Loss Reduction*, paper series – No. 17.

Eswaran, M. (2011). Numerical and experimental investigations on free surface characteristics of sloshing waves in externally induced tanks. study on liquid sloshing in rectangular tanks. *PhD Thesis, Departmental of Mechanical Engineering*, IIT Guwahati.

Eswaran, M., Saha, U. K. and Maity, D. (2009). Effect of baffles on a partially filled cubic tank: numerical simulation and experimental validation. *Computers and Structures*, 87, 198 - 205.

Falcao, S. and Campos, C. (2008). Experimental studies on the characteristics of tuned liquid dampers for reducing vibration in structures. *The 14th World Conference on Earthquake Engineering*, Beijing, China 2008 Oct 12-17.

Faltinsen, O. M., Firoozkoohi, R. and Timokha, A. N. (2011). Steady-state liquid sloshing in a rectangular tank with a slat-type screen in a middle: quasilinear model analysis and experiments. *Physics of Fluids*, 23, 2 - 18.

Frandsen, J. B. (2005). Numerical predictions of tuned liquid tank structural systems. *Journal of Fluids and Structures*, 20, 309 - 329.

Fujii, K., Tamura, Y., Sato, T. and Wakahara, T. (1990). Wind induced vibration of tower and practical applications of tuned sloshing damper. *Journal of Wind Engineering and Industrial Aerodynamics*, 33**,** 263 - 272.

Fujino, Y., Sun, L., Pacheco, B. M. and Chaiseri, P. (1992). Tuned liquid damper (TLD) for suppressing horizontal motion of structures. *Journal of Engineering Mechanics*, 118(10), 2017 – 20130.

Fujino, Y., Pacheco, B. M., Chaiseri, P. and Sun, L. M. (1988). Parametric studies on tuned liquid damper (tld) using circular containers by free oscillation experiments. *Structural Engineering / Earthquake Engineering*, 5, 381s - 391s.

Gabriele, B., Souto, A. I., Louis, D. and Boita, E. V. (2010). Smoothened particle hydrodynamics (SPH) simulation of tuned liquid damper (TLD) with angular motion. *Journal of Hydraulic Research*, 48, 28 - 39.

Gardarsson, S. and Yeh, H. (2007). Hysteresis in shallow water sloshing. *Journal of Engineering Mechanics*, 133, 1093 - 1100.

Gardarsson, S., Yeh, H. and Reed, D. (2001). Behaviour of sloped-bottom tuned liquid dampers. *Journal of Engineering Mechanics*, 127, 266 - 271.

Griffiths, D. V. Programming the finite element method. *John Wiley and Sons*, Second Edition

Hossein, S., Adnan, A. B., Behbahani, H. P. (2013). Performance evaluation of tuned liquid dampers on resonance of SDOF system under earthquake excitation and harmonic load. *Research Journal of Applied Science, Engineering and Technology*, 6(16), 3018 – 3021.

Ibrahim, R. A. (2005). Liquid Sloshing Dynamics Theory and Applications. *Cambridge University Press*, 2005.

Ikeda, T. (2003). Nonlinear parametric vibration of an elastic structure with a rectangular liquid tank. *Nonlinear Dynamics*, 33, 43 - 70.

Idir M. and Ding X. (2009). Fundamental frequency of water sloshing waves in sloped bottom tank as tuned liquid damper. *Structures*, ASCE.

Jin, Q., Li, X., Sun, N., Zhou, J. and Gaun, J. (2007). Experimental and numerical study on tuned liquid dampers for controlling earthquake response of jacket offshore platform. *Marine Structures*, 20, 238 - 254.

Kaneko, S., and Ishikawa, S. (1999). Modelling of tuned liquid damper with submerged nets. *Journal of Pressure Vessels Technology*, 121(3), 334 - 342.

Kaneko, S. and Mizota, Y. (2000). Dynamical modelling of deep water-type cylindrical tuned liquid damper with a submerged net. *Journal of Pressure Vessels Technology*, 122, 96-104.

Kattan, P. I. (2008). MATLAB guide to finite elements an, interactive approach. *Springer*.

Koh, C. G., Mahatma, S. and Wang, C. M. (199) Reduction of structural vibrations by multiple mode liquid damper. *Engineering Structures*, 17 2, 122-128.

Kumar A. (2004). Software for generation of spectrum compatible time history. *13th World Conference on Earthquake Engineering*, Vancouver, Canada, Paper No. 2096.

Kwon, Y. W. and Bang, H. (1997). The finite element method using MATLAB. *CRC Press.*

Love, J. S. and Tait, M. J. (2011). Nonlinear multimodal model for tuned liquid dampers of arbitrary tank geometry. *International Journal of Nonlinear Mechanics* 2011 accepted.

Love, J. S. and Tait, M. J. (2010). Nonlinear simulation of tuned liquid damper with damping screens using modal expansion technique. *Journal of Fluids and Structures,* 26, 1058 - 1077.

Love, J. S., Tait, M. J. and Toopchi, H. (2010). A hybrid structural control system using a tuned liquid damper to reduce the wind induced motion of a base isolated structure. *Engineering Structures* 2010; **33**:738-746.

Marivani, M. and Hamid, M. S. (2009). Numerical simulation of structure response outfitted with a tuned liquid damper. *Computers and Structures,* 87, 1154 - 1165.

Marsh, A. P., Prakash, M., Semercigil, S. E. and Tarun, O. F. (2010). A Shallow-Depth Sloshing Absorber for Structural Control. *Journal of Fluids and Structures,* 36, 780 - 792.

Marsh, A., Prakash, M., Semercigil, S. E. and Tarun, O. F. (2010). Energy dissipation through sloshing in an egg-shaped shell. *Australasian Fluid Mechanics Conference Auckland, New Zealand,* 5 -9 December 2010.

Modi, V. J. and Akinturk, A. (2002). An efficient sloshing damper for control of wind-induced instabilities. *Journal of Wind Engineering and Industrial Aerodynamics,* 90, 1907 - 1918.

Modi, V. J. and Welt, F. (1988). Damping of wind induced oscillations through liquid sloshing. *Journal of Wind Engineering and Industrial Aerodynamics,* 30, 85 - 94.

Modi, V. J., Welt, F. and Irani, M. B. (1990). On the suppression of vibrations using nutation dampers. *Journal of Wind Engineering and Industrial Aerodynamics,* 33:, 273 – 282.

Mondal, J., Nimmala, H., Abdulla, S. and Tafreshi, R. (2014). Tuned liquid dampers. *Proceeding of 3rd International Conference on Mechanical and Mechatronics,* Prague, Czech Republic, Paper No.68-1 to 68-7.

Morsy, H. (2010). A numerical study of performance of tuned liquid damper. *Master of Applied Science,* Thesis.

Murudi, M. (2001). Seismic control of structures using tuned liquid dampers. *PhD Thesis,* Department of Civil Engineering, IIT Mumbai.

Murudi, M. and Banerji, P. (2012). Effective control of earthquake response using tuned liquid dampers. *ISET Journal of Earthquake Technology*, 49, 53 – 71.

Nakayama, T. and Washizu, K. (1981). The boundary element method applied to the analysis of two-dimensional nonlinear sloshing problems. *International Journal for Numerical Methods in Engineering*, 17, 1631 – 1646.

Nanda, B. and Biswal, K. C. (2011) Application of tuned liquid damper for controlling structural vibration due to earthquake excitations. *Modern Methods and Advances in Structural Engineering and Construction*, Conference Zurich June 2011.

Olson, D. E. and Reed, D. A. (2001). A nonlinear numerical model of the sloped bottom tuned liquid damper. *Earthquake Engineering and Structural Dynamics*, 30, 731 - 743.

Paz, M. (2004). Structural dynamics theory and application. *CBS Publishers and Distributers*, New Delhi, 2004.

Reed, D., Yu, J., Yeh, H. and Gardarsson, S. (1998). Tuned liquid dampers under large amplitude excitation. *Journal of Wind Engineering and Industrial Aerodynamics*, 74, 923 -930.

Reed, D., Yu, J., Yeh, H. and Gardarsson, S. (1998). Tuned liquid dampers under large amplitude excitation. *Journal of Engineering Mechanics*, April, 405 - 413.

Reed, D., Yeh, H., Yu, J. and Gardarsson, S. (1997). An investigation of tuned liquid dampers for structural control. *University of Washington*, Seattle, WA, 98195, USA.

Ruiz, R., Lopez-Garcia, D. and Taflanidis, A. A. (2014). An innovative type of tuned liquid damper. *Tenth U. S. National Conference on Earthquake Engineering*, Alaska July 2014.

Samantha, A. and Banerji, P. (2010). Structural vibration control using modified tuned liquid dampers. *The IES Journal Part A*, Civil & Structural Engineering, 3, 14 - 27.

Sheng, D. and Hua, J. L. (2001). Characteristics of tuned liquid damper for suppressing wave induced vibration. *Proceedings of Eleventh International Offshore and Polar Engineering Conference*, Stavanger, Norway, 2001, 17 - 22.

Shrikhande M. and Agarwal P. (2006). Earthquake resistant design of structures. *Prentice Hall of India Learning Pvt. Ltd*

Sun, L. M., Fujino, Y., Pacheo, B. M. and Chaiseri, P. (1992). Modelling of tuned liquid damper (TLD). *Journal of Wind Engineering and Industrial Aerodynamics*, 44, 1883 - 1894.

Sun, L. M., Fujino, Y., Benito, M., Pacheco, B. M. and Masahiko, I. (1989) Nonlinear waves and dynamic pressures in rectangular tuned liquid damper (TLD) – simulation and experimental verification. *Structural Engineering / Earthquake Engineering*, 6, 251s - 252s.

Sun, L. M., Fujino, Y., Chaiseri, P. and Pacheco, B. M. (1995). The properties of tuned liquid dampers using a TMD analogy. *Structural Engineering and Structural Dynamics*, 24, 967 - 976.

Sung, L., Yun, C. P., Min, K., Lee., S. H., Chung, L. and Park, J. H. (2007). Real time hybrid shaking table testing method for the performance evaluation of a tuned liquid damper controlling seismic response of building structures. *Journal of Sound and Vibration*, 302, 596 - 612.

Syed, S. M., Khan, Q. Z., Tahie, F. and Ahmed, M. J. (2013). Investigation of water tank as TLD for vibration control of frame structures under seismic excitations. *Life Science Journal*, 10(7s), 1182 – 1189.

Tait, M. J. (2004) The performance of 1-D and 2-D tuned liquid dampers, PhD thesis. *The University of Western Ontario*

Tait, M. J. and El Damatty, A. A. (2007). Effectiveness of 2d tld and its numerical modelling. *Journal of Structural Engineering*, 2007, 251.

Tait, M. J., Isyumov, N. and El Damatty, A. A. (2007). Effectiveness of 2d tld and the numerical modelling. *Journal of Structural Engineering*, 133, 251 - 263.

Tait, M. J., Isyumov, N. and El Damatty, A. A. (2008). Performance of tuned liquid dampers. *Journal of Engineering Mechanics*, 134, 417 - 427.

Tamura, Y., (1995). Effectiveness of tuned liquid dampers under wind excitation. Engineering Structures, 17 – 9, 609 – 621.

Turner, M. R. (3016). Liquid sloshing in horizontally forced vessel with bottom topography. *Department of Mathematics*, University of Surrey, UK 2016.

VDC. (2012). Strong motion virtual data centre, http://strongmotioncenter.org/vdc/scripts/default.plx

Wakahara, T., Ohyama, T., Fujii, K. (1992) Suppression of wind-induced vibration of tall building using tuned liquid damper. *Journal of wind engineering and industrial Aerodynamics* 43 1-3, 1895-1906.

Yu, J. K., Wakhara, T. and Reed, D. A. (1999). A non-linear numerical model of tuned liquid damper. *Earthquake Engineering and Structural Dynamics*, 28, 671 - 686.

Yung, H. C., Wie, S. H. and Chia, H. K. (2000). Numerical simulation of the three-dimensional sloshing problem by boundary element method. *Journal of the Chinese Institute of Engineers,* 23, 321 - 330.

Xin, Y., Chen, G. and Lou, M. (2009). Seismic response control with density variable tuned liquid dampers. *Earthquake Engineering and Engineering Vibration*, 8, 537 - 546.

Xin, Y. (2006). Seismic performance of mass variable tuned liquid dampers with particles fluidization in building applications. *PhD Thesis,* University of Missouri-Rolla 2006.

Yu, J. K., Wakhara, T. and Reed, D. A. (1999). A non-linear numerical model of tuned liquid damper. *Earthquake Engineering and Structural Dynamics,* 28, 671-686.

APPENDIX A

FINITE ELEMNT FORMULATION FOR FLUID STRUCTURE INTERACTION

A.1. INTRODUCTION

Finite element for fluid structure interaction as applied to Tuned Liquid Dampers (TLD) is provided in this Appendix. FE analysis has been performed based on basic code developed by Nanda (2010) but modified suitably for the current work. FE formulation for the fluid in the tank, boundary conditions, FE elements are presented first, followed by interaction of the frame structure and the TLD tank, with a focus on 2 dimensional approximations. Important assumptions made in the formulation is also listed.

A.2. ASSUMPTIONS

Following are the assumptions made in the finite element formulation of fluid structure interaction problem.

- The liquid is considered as homogeneous, incompressible and irrotational.
- Walls of the tank are considered as rigid and hence do not deform.
- Liquid surface remains smooth during sloshing of liquid in a tank (wave breaking is absent).
- The excitation for the liquid in TLD is the response of the structure to the dynamic loading such as seismic ground motion or wind. The sloshing motion of liquid in tank in turn affects the structural response and structural response can be mitigated with proper selection of TLD dimensions.

A.3. GOVERNING EQUATION FOR LIQUID

Governing differential equation in for pressure of liquid is

$$\nabla^2 P = 0 \quad \text{on volume V of the domain} \tag{A.1}$$

$P = P(x, y, z, t)$ is the dynamic pressure of liquid.

And $\nabla^2 = \frac{\partial^2}{\partial x^2} + \frac{\partial^2}{\partial y^2} + \frac{\partial^2}{\partial z^2}$ in the Cartesian coordinate system

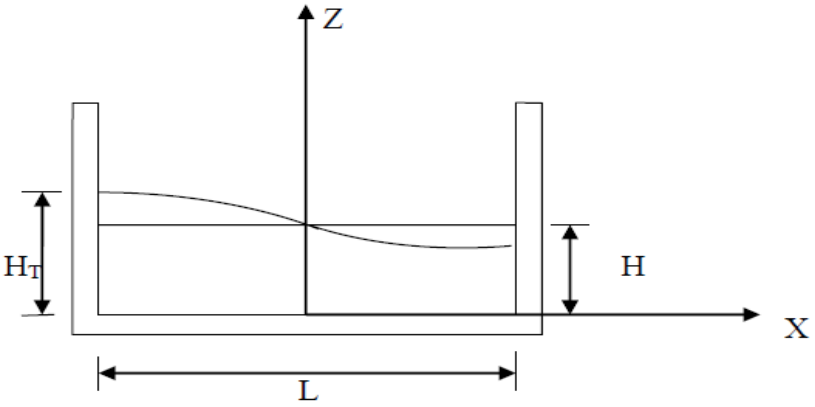

Figure A.1: Dimensions of flat bottom rectangular tank. H: Still water depth, L: Length of tank, H_T: Liquid sloshing surface level at edge

A.3..1. Boundary conditions

The liquid domain is constrained by the walls of tank at sides, base of tank at bottom and free surface at top. The dynamic conditions for liquid in a tank are applied at free surface, sides and at bottom of liquid and are described in the following section.

a) At liquid free surface:

Boundary conditions are imposed at the liquid free surface are kinematic and dynamic. Kinematic boundary conditions implies that liquid particles on the free surface at all times remain on free surface. Dynamic boundary conditions implies that the pressure on the free surface is zero. Considering small amplitude waves, the velocity term in the

Bernoulli's equation can be neglected. Thus kinematic and dynamic boundary conditions may be combined to get linearized free surface equation as:

$$\frac{\partial^2 P}{\partial t^2} + g\frac{\partial P}{\partial n} = 0 \qquad \text{(A.2)}$$

on B_f - Boundary conditions on liquid free surface area.

If free surface wave of liquid is ignored, then P = 0

b) At liquid surface interface:

$$\frac{\partial P}{\partial n} = -\rho_f \ddot{d}_n \qquad \text{(A.3)}$$

on B_s – Surface area of liquid in contact with the tank

Where, $\ddot{d}_n$ = acceleration of structure

n = outwardly drawn normal to the surface of liquid

c) At bottom of tank:

$$\frac{\partial P}{\partial n} = 0 \qquad \text{(A.4)}$$

on B_b – boundary condition at bottom of tank

A.4. FINITE ELEMENT FORMULATION

For rectangular tank, the liquid dynamic pressure 'P' is approximately given as

$$P(x, y, z, t) = \sum_{j=1}^{N} N_j(x, y, z)\, \bar{P}_j(t) \qquad \text{(A.5)}$$

Where, N_j are shape functions

$\bar{P}_j(t)$ *are* time dependent nodal pressures.

Applying divergence theorem to the residual form of governing differential equation and minimizing the energy function we get

$$\int_V \left(\frac{\partial N_i}{\partial x}\sum_1^N \frac{\partial N_j}{\partial x}\bar{P}_j + \frac{\partial N_i}{\partial y}\sum_1^N \frac{\partial N_j}{\partial y}\bar{P}_j + \frac{\partial N_i}{\partial z}\sum_1^N \frac{\partial N_j}{\partial z}\bar{P}_j\right) dV = \int_B N_i \frac{\partial P}{\partial n} ds \qquad \text{(A.6)}$$

Where B = $B_f + B_s + B_b$ are boundary conditions.

Equations (3.2), (3.3) and (3.4) are substituted in Equation (3.6) to get,

$$\int_V \left(\frac{\partial N_i}{\partial x}\sum_1^N \frac{\partial N_j}{\partial x}\bar{P}_j + \frac{\partial N_i}{\partial y}\sum_1^N \frac{\partial N_j}{\partial y}\bar{P}_j + \frac{\partial N_i}{\partial z}\sum_1^N \frac{\partial N_j}{\partial z}\bar{P}_j\right)dV = -\int_B N_i \ddot{d}_n ds - \frac{1}{g}\int_{B_f} N_j \sum_1^N N_j \ddot{\bar{P}}_j ds \quad \text{(A.7)}$$

Equation (3.7) can be reduced to get,

$$[M_f]\{\ddot{P}\} + [K_f]\{P\} = \{F_P\} \quad \text{(A.8)}$$

Elements $[M_f]$, $[K_f]$ and $\{F_P\}$ are given as,

$$M_{ij} = \frac{1}{g}\sum \int_{B_f} N_i N_j ds \quad \text{(A.9)}$$

$$K_{ij} = \sum \int_V \left[\frac{\partial N_i}{\partial x}\frac{\partial N_j}{\partial x} + \frac{\partial N_i}{\partial y}\frac{\partial N_j}{\partial y} + \frac{\partial N_i}{\partial z}\frac{\partial N_j}{\partial z}\right]dV \quad \text{(A.10)}$$

$$F_i = -\sum \int_{B_s} \rho_f N_i \ddot{d}_n ds \quad \text{(A.11)}$$

A.4.1. Two dimensional formulation

In order to reduce the complexity and computational efforts, three dimensional problem formulation can be simplified to two dimensional problem or one dimensional problem. In the present study, the motion structural frame and of liquid in a tank is in a vertical X Z plane. Therefore the analysis of structural frame and liquid in a tank is considered as two dimensional problem.

a) Liquid stiffness matrix

A two dimensional finite element analysis is used for the sloshing analysis of liquid in a rectangular tank. Domain of liquid is discretized by four node quadrilateral elements with two degree of freedom at each node.

The stiffness matrix of the liquid domain is formed by assembling element stiffness matrices.

$$[K_f] = \sum_{S=1}^{NK} K_s \quad \text{(A.12)}$$

Where, NK are number of liquid elements

K_s is element stiffness matrix written as,

$$K_s = \int_{\Omega} \left[\frac{\partial N_i}{\partial x}\frac{\partial N_j}{\partial x} + \frac{\partial N_i}{\partial z}\frac{\partial N_j}{\partial z}\right] d\Omega \tag{A.13}$$

In two dimensional field problem in Cartesian coordinate system, the dynamic pressure in a liquid element can be approximated as,

$$P_S(\mathrm{x, z, t}) = \sum_{j=1}^{4} N_j(x,z)\,\bar{P}_{js}(t) \tag{A.14}$$

Differentiating above Equation (3.14) separately with respect to x and z, we obtain the liquid pressure gradient within the s^{th} liquid element as,

$$\begin{Bmatrix} \frac{\partial \bar{P}}{\partial x} \\ \frac{\partial \bar{P}}{\partial z} \end{Bmatrix} = \begin{Bmatrix} \frac{\partial N_j}{\partial x} \\ \frac{\partial N_j}{\partial z} \end{Bmatrix} \{\bar{P}_j\} \tag{A.15}$$

The derivatives of shape functions with respect to the natural coordinates (ξ, η) are obtained from Jacobian transformation using chain rule as,

$$\begin{Bmatrix} \frac{\partial N_j}{\partial \xi} \\ \frac{\partial N_j}{\partial \eta} \end{Bmatrix} = \begin{Bmatrix} \frac{\partial x}{\partial \xi} & \frac{\partial z}{\partial \xi} \\ \frac{\partial x}{\partial \eta} & \frac{\partial z}{\partial \eta} \end{Bmatrix} \begin{Bmatrix} \frac{\partial N_j}{\partial x} \\ \frac{\partial N_j}{\partial z} \end{Bmatrix} \tag{A.16}$$

Can be written as,
$$\begin{Bmatrix} \frac{\partial N_j}{\partial \xi} \\ \frac{\partial N_j}{\partial \eta} \end{Bmatrix} = \{J_s\} \begin{Bmatrix} \frac{\partial N_j}{\partial x} \\ \frac{\partial N_j}{\partial z} \end{Bmatrix} \tag{A.17}$$

Jacobian matrix
$$\{J_s\} = \begin{Bmatrix} \frac{\partial x}{\partial \xi} & \frac{\partial z}{\partial \xi} \\ \frac{\partial x}{\partial \eta} & \frac{\partial z}{\partial \eta} \end{Bmatrix} \tag{A.18}$$

and
$$\begin{Bmatrix} \frac{\partial N_j}{\partial x} \\ \frac{\partial N_j}{\partial z} \end{Bmatrix} = \{J_s\}^{-1} \begin{Bmatrix} \frac{\partial N_j}{\partial \xi} \\ \frac{\partial N_j}{\partial \eta} \end{Bmatrix} = \{J_s\}^{-1}\, T_s(\xi, \eta) \tag{A.19}$$

Where, $\{J_s\}^{-1}$ is the inverse of Jacobian matrix and

$T_s(\xi,\eta)$ contains the derivatives of shape functions. Let

$$\begin{Bmatrix} \frac{\partial N_j}{\partial \xi} \\ \frac{\partial N_j}{\partial \eta} \end{Bmatrix} = [D] \tag{A.20}$$

Where, $[D] = \{J_s\}^{-1}\, T_s(\xi,\eta)$.

The liquid element stiffness matrix in equation (3.13) can be written as,

$$K_s = \int_\Omega \begin{bmatrix} \frac{\partial N_i}{\partial x} & \frac{\partial N_i}{\partial z} \end{bmatrix} \begin{Bmatrix} \frac{\partial N_j}{\partial x} \\ \frac{\partial N_j}{\partial z} \end{Bmatrix} d\Omega$$

Or $$K_s = \int_\Omega [D]^T\,[D]\,dx\,dz = \int_{-1}^{+1}\int_{-1}^{+1} [D]^T[D]|J_s|\,d\xi\,d\eta \tag{A.21}$$

b) Mass matrix of liquid at free surface

The liquid free surface mass matrix for the given system is formed by assembling the elements at the liquid surface as,

$$[M_f] = \sum_{t=1}^{NF} M_{ef} \tag{A.22}$$

NF is the number of liquid elements and M_{ef} is given as,

$$M_{ef} = \frac{1}{g}\int_{B_f} N_i N_j\, ds \tag{A.23}$$

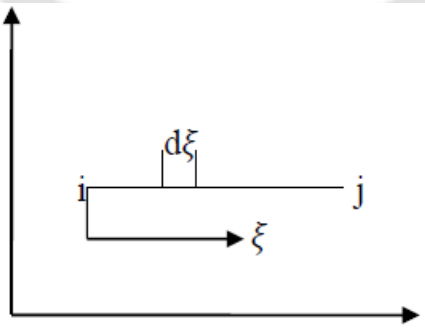

Figure A.2: Liquid free surface element in rectangular container

In the liquid free surface element, ξ is local coordinate for the free surface boundary element and L is the length of element as shown in Figure (A.2).

The shape functions of the line element at the free surface are

$$[N_j] = \left[1 - \frac{\xi}{L} \qquad \frac{\xi}{L}\right] \tag{A.24}$$

The liquid free surface matrix in equation (3.23) can be written as

$$\left[M_{ef}\right] = \frac{1}{g}\int_0^L \begin{Bmatrix} 1 - \frac{\xi}{L} \\ \frac{\xi}{L} \end{Bmatrix} \left[1 - \frac{\xi}{L} \qquad \frac{\xi}{L}\right] d\xi \tag{A.25}$$

c) Liquid load vector

The load vector for the system is

$$[\mathrm{F_f}] = \sum_{i=1}^{NL} F_{ef} \tag{A.26}$$

Where NL are the number of elements at the liquid-structure interface and element load vector F_{ef} is given by

$$F_{ef} = -\int_{B_s} \rho_f N_f \ddot{d}_n \, ds \tag{A.27}$$

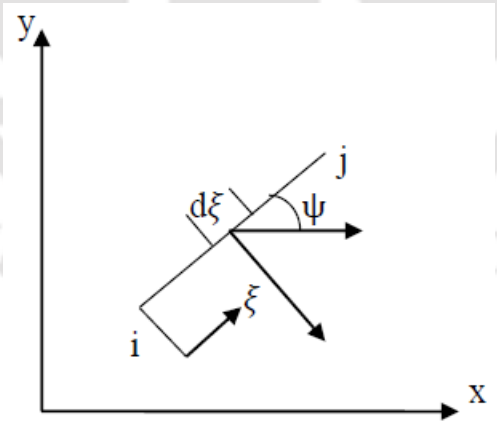

Figure A.3: Liquid-Structure interface element in rectangular tank

The liquid-structure interface is shown in the Figure A.3 and shape functions are expressed as

$$N_j = \left[1 - \frac{\xi}{L} \qquad \frac{\xi}{L}\right] \tag{A.28}$$

If $\ddot{d}_x$ is the horizontal ground acceleration in x direction, then the normal acceleration at the liquid-structure interface can be expressed as,

$$\ddot{d}_n = \ddot{d}_x \cos\psi \tag{A.29}$$

Where $\psi = tan^{-1}(x_i - x_j)/(z_i - z_j)$

Load vector in the equation (3.27) is written as,

$$F_{ef} = -\int_0^L \rho_f \begin{Bmatrix} 1 - \frac{\xi}{L} \\ \frac{\xi}{L} \end{Bmatrix} \ddot{d}_x \cos\psi \, d\xi \tag{A.30}$$

d) Forced vibration analysis of liquid

When external force is applied to the liquid, the element equation for the liquid in rigid tank, is expressed as,

$$[M_f]\{\ddot{P}\} + [K_f]\{P\} = \{F_{el}\} \tag{A.31}$$

Where $\{F_{el}\}$ is external load vector and is given as

$$\{F_{el}\} = \sum_{i=1}^{NL} F_{el}$$

And $$\{F_{el}\} = -\rho_f \int_{B_f} [N_i]^T \ddot{d}_n \, ds$$

$$= -\rho_f \ddot{d}_n \int_{-1}^{+1}\int_{-1}^{+1} [N_i]^T |J_S| \, d\zeta d\eta \tag{A.32}$$

A.4.2. Solution of forced vibration problem by using Newmark beta method

The forced vibration problem can be solved by Newmark Beta (constant acceleration) method. For the solution, displacement, velocity and acceleration at time t + Δt are also considered,

$$[M_f]^{t+\Delta t}\{\ddot{P}\}+[K_f]^{t+\Delta t}\{P\}=\{F_{el}\}^{t+\Delta t} \quad \text{(A.33)}$$

The algorithm for the scheme is given as

A. Initial calculations:

1. Formulation of global stiffness matrix K and mass matrix M of liquid
2. Initialization of P and $\ddot{P}$
3. Selection of time step Δt and parameters α' and β'

   $\alpha' \geq 0.5$ and $\beta' \geq 0.25(0.5 + \alpha')^2$

   For the present study $\alpha' = 0.5$ and $\beta' = 0.25$ are considered in the analysis
4. Calculation of coefficients for time integration

   $a_0 = \frac{1}{\beta'\Delta t^2}$; $a_1 = \frac{\alpha'}{\beta'\Delta t}$; $a_2 = \frac{1}{\beta'\Delta t}$; $a_3 = \frac{1}{2\beta'} - 1$;

   $a_4 = \frac{\alpha'}{\beta'} - 1$; $a_5 = \frac{\Delta t}{2}\left(\frac{\alpha'}{\beta'} - 2\right)$; $a_6 = \Delta t(1 - \alpha')$; $a_7 = \alpha'\Delta t$
5. Computation of effective stiffness matrix $\hat{K}$

   $\hat{K} = K + a_0 M$

B. For each time step:

1. Calculation of effective load vector

   $\hat{F}_{t+\Delta t} = F_{t+\Delta t} + M(a_0 P_t + a_2\dot{P}_t + a_3\ddot{P}_t)$
2. Solution for pressure at time t + Δt

   $\hat{K}P_{t+\Delta t} = \hat{F}_{t+\Delta t}$
3. Calculation of time derivatives of pressure (P) at time t + Δt

   $\ddot{P}_{t+\Delta t} = a_0(P_{t+\Delta t} - P_t) - a_2\dot{P}_t - a_3\ddot{P}_t$

   and

   $\dot{P}_{t+\Delta t} = \dot{P}_t + a_6\ddot{P}_t + a_7\ddot{P}_{t+\Delta t}$

A.4.3. Fundamental sloshing frequency of TLD

The fundamental sloshing frequency of a TLD, f_{TLD} can be estimated using linear wave theory as:

$$f_w = \frac{1}{2\pi}\sqrt{\frac{\pi g}{L} tanh \frac{\pi H}{L}} \quad \text{(A.34)}$$

Where, g = Acceleration due to gravity

H = Liquid/water depth at static condition

L = Length of tank in the direction of sloshing

Sloshing frequency f_{TLD} is amplitude dependent . For linearized sloshing amplitudes we take $f_{TLD} = f_w$

A.5. FLUID STRUCTURE INTERACTION MODEL

Two dimensional structural rigid frame is discretized into number of elements, as shown in Figure (A.4). Frame element has six degrees of freedom with two translations and one rotation associated with each node. The frame is assumed to have fixed base with nine number of constraints at three supports.

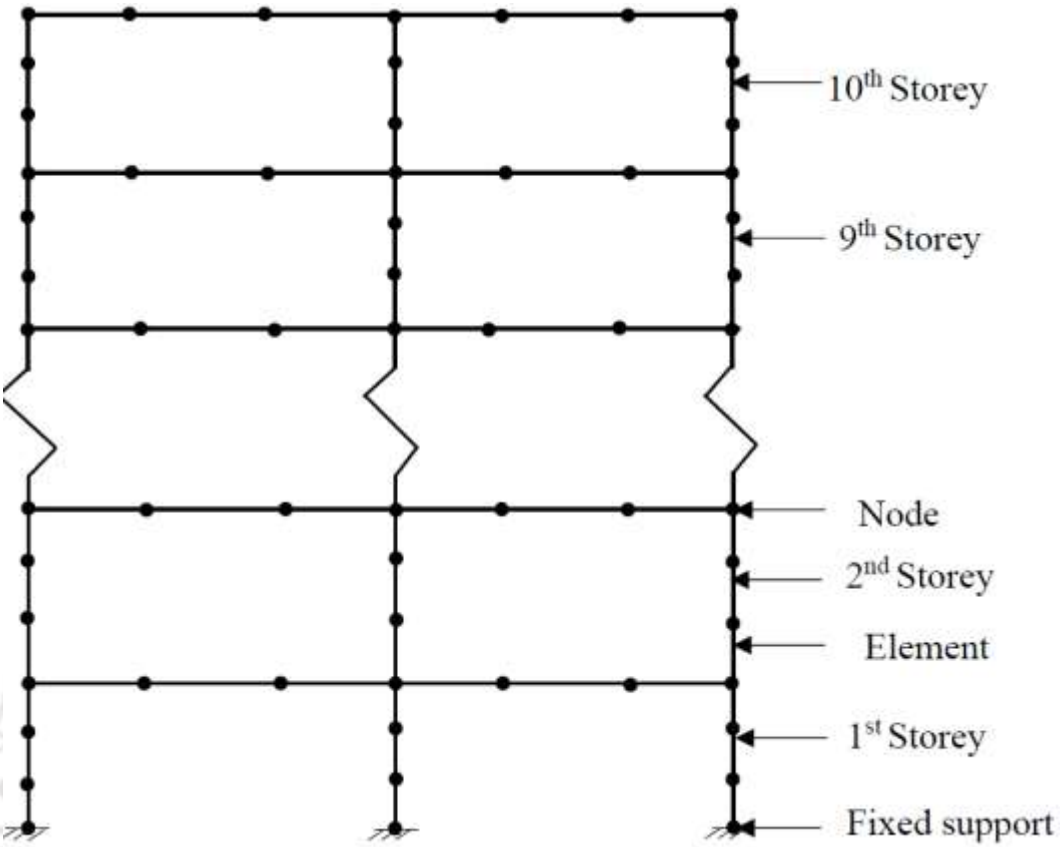

Figure A.4: Discretization of a 2D rigid frame with plane frame elements.

Equation of motion of the fluid-structure system can be written as

$$[M]\{\ddot{X}\} + [C]\{\dot{X}\} + [K]\{X\} = -[M]\{\ddot{X}_g\} + \{F_{TLD}\} \quad \text{(A.35)}$$

Where, $[M]$ is global mass matrix of frame

$[C]$ is global damping matrix of the frame and here it is assumed to be null

matrix as inherent damping of structure is neglected

$[K]$ is global stiffness matrix of the frame

$\{X\}$ is global displacement vector for all degrees of freedom

$\{\ddot{X}_g\}$ is ground acceleration vector

$\{F_{TLD}\}$ is resisting force to the structure at respective nodes offered by TLD

a) Element matrices

The element stiffness matrix for 2D frame structure is

$$[k] = \begin{bmatrix} \frac{EA}{L} & 0 & 0 & -\frac{EA}{L} & 0 & 0 \\ 0 & \frac{12EI}{L^3} & \frac{6EI}{L^2} & 0 & -\frac{12EI}{L^3} & \frac{6EI}{L^2} \\ 0 & \frac{6EI}{L^2} & \frac{4EI}{L} & 0 & -\frac{6EI}{L^2} & \frac{2EI}{L} \\ -\frac{EA}{L} & 0 & 0 & \frac{EA}{L} & 0 & 0 \\ 0 & -\frac{12EI}{L^3} & -\frac{6EI}{L^2} & 0 & \frac{12EI}{L^3} & -\frac{6EI}{L^2} \\ 0 & \frac{6EI}{L^2} & \frac{2EI}{L} & 0 & -\frac{6EI}{L^2} & \frac{4EI}{L} \end{bmatrix} \quad \text{(A.36)}$$

Where, E is Young modulus of material

A is cross sectional area of element

L is length of element

The element mass matrix for 2D frame is

$$[m] = \begin{bmatrix} 2a & 0 & 0 & a & 0 & 0 \\ 0 & 156b & 22l^2b & 0 & 54b & -13lb \\ 0 & 22l^2b & 4\,l^2b & 0 & 13lb & -3l^2b \\ a & 0 & 0 & 2\,a & 0 & 0 \\ 0 & 54b & 13lb & 0 & 156b & -22lb \\ 0 & -13lb & -3\,l^2b & 0 & -22l & -4l^2b \end{bmatrix} \quad \text{(A.37)}$$

Where, $a = \frac{\rho AL}{6}$ and $b = \frac{\rho AL}{420}$

ρ is density of the material

b) Element matrices, global coordinate system

The above matrices are for a individual frame element. A structure comprises of several number of frame elements with different orientations. Local coordinate axes would vary for each element. To assemble element matrices, all element matrices are be expressed with respect to global coordinate system. Elements are expressed in to global coordinate system with tribological transformation.

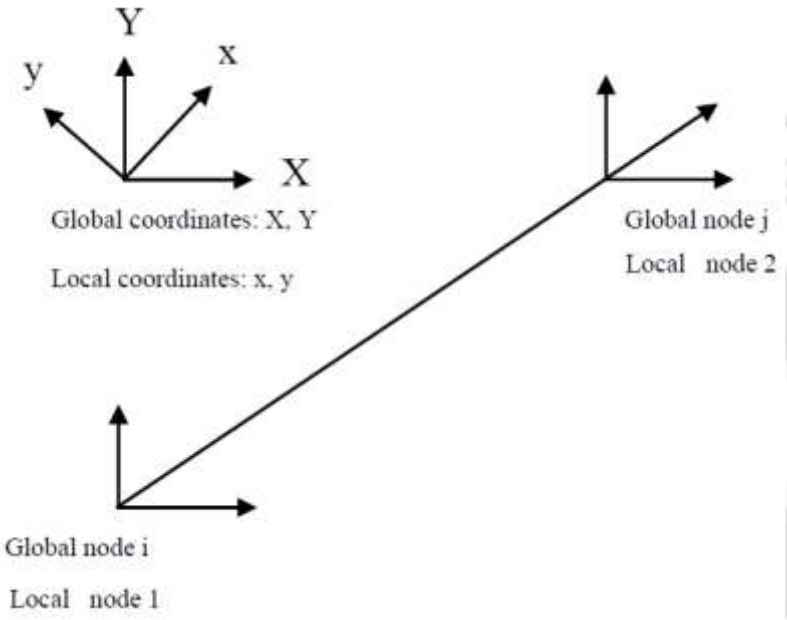

Figure A.5: Coordinate transformation for 2D frame elements

Assuming that the local nodes 1 and 2 correspond to the global nodes i and j respectively, the transformation matrix T for the frame element is

$$[T] = \begin{bmatrix} l_x & m_x & 0 & 0 & 0 & 0 \\ l_y & m_y & 0 & 0 & 0 & 0 \\ 0 & 0 & 1 & 0 & 0 & 0 \\ 0 & 0 & 0 & l_x & m_x & 0 \\ 0 & 0 & 0 & l_y & m_y & 0 \\ 0 & 0 & 0 & 0 & 0 & 1 \end{bmatrix} \quad \text{(A.38)}$$

Where, $l_x = \cos(x, X) = \cos\alpha = \frac{X_{j-} X_i}{l_e}$

$$m_x = \cos(x, Y) = \sin\alpha = \frac{Y_{j-} Y_i}{l_e}$$

$$l_y = \cos(y, X) = \cos(90+\alpha) = -\sin\alpha = -\frac{Y_{j-} Y_i}{l_e}$$

$$m_y = \cos(y, Y) = \cos\alpha = \frac{X_{j-} X_i}{l_e}$$

are direction cosines and α is the angle between x-axis and the X-X axis, as shown in the Figure A.5.

$$l_e = \sqrt{(X_{j-} X_i)^2 + (Y_{j-} Y_i)^2}$$

is the length of element

Using the transformation matrix T, the element matrices for the frame element in the global coordinate system become

$$K_e = T^T k\, T$$

$$M_e = T^T m\, T$$

c) Application of boundary conditions

A node in a plane frame element has two translations and one rotation as degrees freedom. At the fixed support, translations and rotations restrained which act as boundary conditions. Boundary conditions are imposed on the structure by eliminating the corresponding rows and columns in the stiffness and mass matrix.

A.6. FORCED VIBRATION ANALYSIS OF INTERACTION PROBLEM

The equation of motion is coupled one containing number of independent variables. These equations can be made uncoupled into set of differential equations in which each equation contains only one variable. For this we can express the displacement $\{X\}$ in terms of natural modes of system without damping as:

$$\{X\} = \Phi\, \{q\} \qquad \text{(A.39)}$$

Where, Φ = Normalized modal matrix

Substituting equation (3.38) in equation (3.34) we get

$$[M]\Phi\{\ddot{q}\} + [C]\Phi\{\dot{q}\} + [K]\Phi\{q\} = \{F_e\} - \{F_{TLD}\} \quad \text{(A.40)}$$

Pre-multiplying by Φ^T gives

$$[M]\Phi\{\ddot{q}\} + \Phi^T[C]\Phi\{\dot{q}\} + \Phi^T[K]\Phi\{q\} = \Phi^T\{F_e\} - \Phi^T\{F_{TLD}\}$$

$$\hat{M}\{\ddot{q}\} + \hat{C}\{\dot{q}\} + \hat{K}\{q\} = P(t) \quad \text{(A.41)}$$

Where, $\hat{M}$ is modal mass matrix

$\hat{C}$ is modal damping matrix

$\hat{K}$ is modal stiffness matrix

$P(t)$ is modal force vector

q *is* displacement in normal coordinate system

$\hat{M}$ and $\hat{K}$ are diagonal mass matrix and stiffness matrix respectively. and $\hat{C}$ is diagonal matrix for classically damped system. For a classically damped system the equation (3.40) can be uncoupled into set of differential equations as

$$\left.\begin{array}{l} \hat{M}(1,1).\ddot{q}(1) + \hat{C}(1,1).\dot{q}(1) + \hat{K}(1,1).q(1) = \mathrm{P}(1) \\ \hat{M}(2,2).\ddot{q}(2) + \hat{C}(2,2).\dot{q}(2) + \hat{K}(2,2).q(1) = \mathrm{P}(2) \\ - \\ \hat{M}(\mathrm{n},\mathrm{n}).\ddot{q}(\mathrm{n}) + \hat{C}(\mathrm{n},\mathrm{n}).\dot{q}(\mathrm{n}) + \hat{K}(\mathrm{n},\mathrm{n}).q(\mathrm{n}) = \mathrm{P}(n) \end{array}\right\} \quad \text{(A.42)}$$

Solution of each set of equations can be determined using Duhamel's integral. Displacements in absolute coordinate system can be calculated from normal coordinates system as,

$$\{X\} = \Phi^T\{q\} \quad \text{(A.43)}$$

A.6.1. Numerical evaluation using Duhamel's integral

This integral method can be used to determine the response of single degree of freedom (SDOF) system under general type of excitations (harmonic or random). The total response of damped SDOF system subjected to an arbitrary loading can be expressed as

$$X(t) = e^{-\xi\omega_n t}\left(x_0 cos\omega_D t + \frac{u_0 + X_0\,\xi\omega_n}{\omega_D} sin\omega_D t\right) \qquad (A.44)$$

Assuming $x_0 = 0$, and $u_0 = F_t(\tau)d\tau/M_s$ and substituting t for t-τ in equation (A.43) and integrating this equation over the entire loading duration results in

$$X(t) = \frac{1}{M_s\omega_D}\int_0^t F_t(\tau)\, e^{-\xi\omega_n(t-\tau)} sin\omega_D(t-\tau)d\tau \qquad (A.45)$$

Where F_t is sum of external excitations and TLD sloshing force. $X(t)$ in the equation (A.44) is the response of a damped system using Duhamel's integral. Displacement is calculated by numerical integration of above equation. Using trigonometric relationship

$sin\omega(t - \tau) = sin\omega t.cos\omega\tau - cos\omega t.sin\omega\tau$, the displacement can be determined as,

$$X(t) = \frac{e^{-\xi\omega_n t}}{M_s\omega_D}\{A_D(t)sin\omega_D t - B_D(t)cos\omega_D t\} \qquad (A.46)$$

Where A_D and B_D are determined as,

$$A_D(t_i) = A_D(t_{i-1}) + \int_{t_{i-1}}^{t_i} F_t(\tau)\, e^{\xi\omega_n\tau} cos(\omega_D\tau)d\tau \qquad (A.47)$$

$$B_D(t_i) = B_D(t_{i-1}) + \int_{t_{i-1}}^{t_i} F_t(\tau)\, e^{\xi\omega_n\tau} sin(\omega_D\tau)d\tau \qquad (A.48)$$

Considering a linear piecewise loading function, the forcing function $F_t(\tau)$ can be approximated as:

$$F_t(\tau) = F_t(t_{i-1}) + \frac{\Delta F_i}{\Delta t_i}(\tau - t_{i-1}), \qquad t_{i-1} \le \tau \le t_i \qquad \text{(A.49)}$$

Where, $$\Delta F_i = F_t(t_i) - F_t(t_{i-1}) \qquad \text{(A.50)}$$

$$F_t(t_i) = F_e(t_i) + F_{TLD}(t_i) \qquad \text{(A.51)}$$

$$\Delta t_i = t_i - t_{i-1} \qquad \text{(A.52)}$$

In Equations A.47 and A.48, $A_D(t_i)$ and $B_D(t_i)$ can be evaluated from:

$$A_D(t_i) = A_D(t_{i-1}) + \left(F_t(t_{i-1}) - t_{i-1}\frac{\Delta F_i}{\Delta t_i}\right) I_1 + \frac{\Delta F_i}{\Delta t_i} I4 \qquad \text{(A.53)}$$

$$B_D(t_i) = B_D(t_{i-1}) + \left(F_t(t_{i-1}) - t_{i-1}\frac{\Delta F_i}{\Delta t_i}\right) I_2 + \frac{\Delta F_i}{\Delta t_i} I_3 \qquad \text{(A.54)}$$

Where the integrals I_1, I_2, I_3 and I_4 are evaluated as follows:

$$I_1 = \int_{t_{i-1}}^{t_i} e^{\xi\omega_n\tau} \cos\omega_D \tau d\tau = \frac{e^{\xi\omega_n\tau}}{(\xi\omega_n)^2+\omega_D{}^2}(\xi\omega_n \cos\omega_D\tau + wD\sin\omega_D\tau)\Big|_{t_{i-1}}^{t_i} \qquad \text{(A.55)}$$

$$I_2 = \int_{t_{i-1}}^{t_i} e^{\xi\omega_n\tau} \sin\omega_D \tau d\tau = \frac{e^{\xi\omega_n\tau}}{(\xi\omega_n)^2+\omega_D{}^2}(\xi\omega_n \sin\omega_D\tau + \omega_D \cos\omega_D\tau)\Big|_{t_{i-1}}^{t_i} \qquad \text{(3.56)}$$

$$I_3 = \int_{t_{i-1}}^{t_i} \tau e^{\xi\omega_n\tau} \sin\omega_D \tau d\tau = \tau - \frac{\xi\omega_n}{(\xi\omega_n)^2+\omega_D{}^2} I_2 + \frac{\omega_D}{(\xi\omega_n)^2+\omega_D{}^2} I_1\Big|_{t_{i-1}}^{t_i} \qquad \text{(A.57)}$$

$$I_4 = \int_{t_{i-1}}^{t_i} \tau e^{\xi\omega_n\tau} \cos\omega_D \tau d\tau = (\tau - \frac{\xi\omega_n}{(\xi\omega_n)^2+\omega_D{}^2})I_1 - \frac{\omega_D}{(\xi\omega_n)^2+\omega_D{}^2} I_2\Big|_{t_{i-1}}^{t_i} \qquad \text{(A.58)}$$

The substitution of equation (3.49) and (3.50) into equation (3.45), displacement at time t_i is given as,

$$X(t_i) = \frac{e^{-\xi\omega_n t}}{M_s\omega_D}\{A_D(t_i)\sin\omega_D t_i - B_D(t_i)\cos\omega_D t_i\} \qquad \text{(A.59)}$$

The derivative of the above equation with respect to time t_i gives the velocity at time t_i as,

$$\text{V}(t_i = \frac{e^{-\xi\omega_n t}}{M_s\omega_D}\{(B_D\omega_D - A_D e\omega_n)\sin\omega_D t_i - (A_D\omega_D - B_D e\omega_n)\cos\omega_D t_i\} \qquad \text{(A.60)}$$

APPENDIX B

SAMPLE CALCULATIONS

B.1. FREE VIBRATION ANALYSSIS OF 2D RC STRUCTURAL FRAME BY STADD PRO SOFTWARE

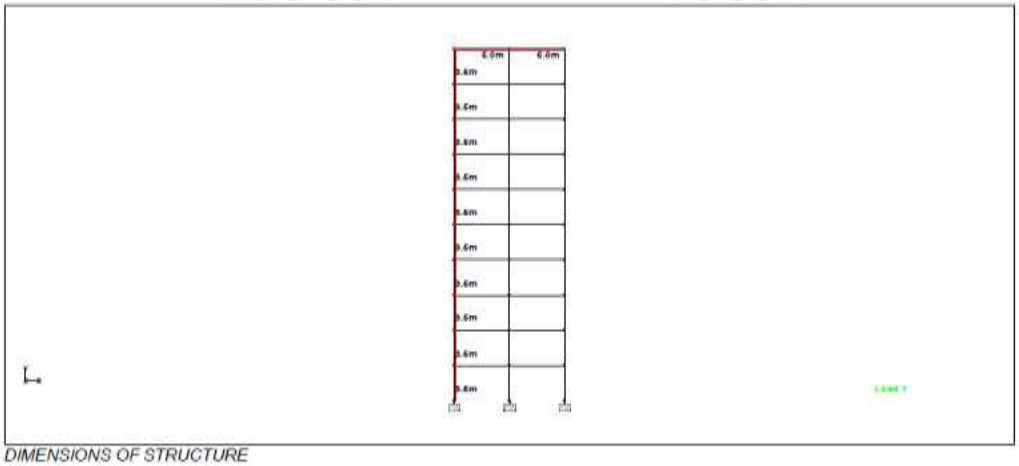

DIMENSIONS OF STRUCTURE

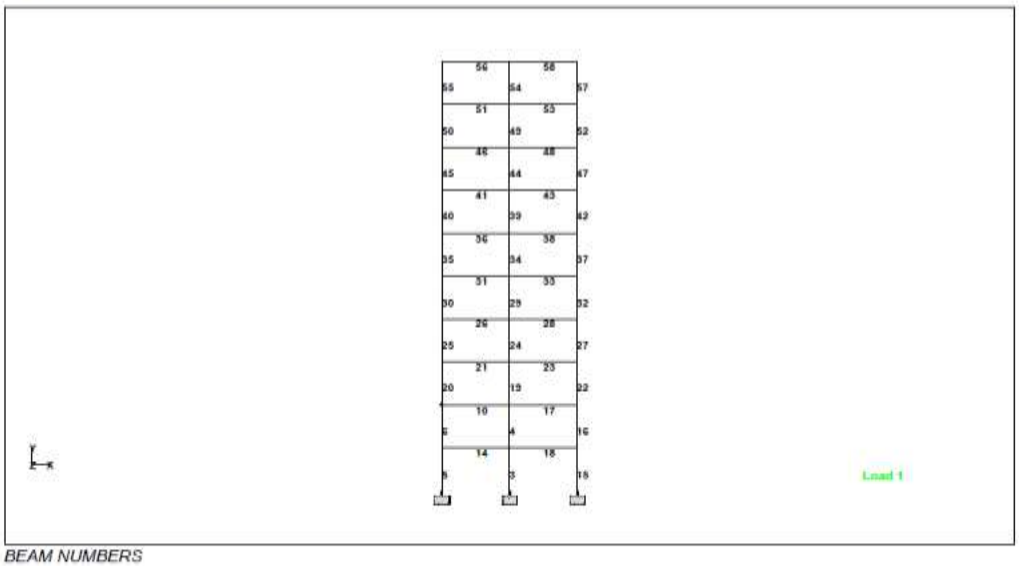

BEAM NUMBERS

Section Properties

Prop	Section	Area (mm^2)	I_{yy} (mm^4)	I_{zz} (mm^4)	J (mm^4)	Material
1	Rect 0.40x0.25	100E+3	521E+6	1.33E+9	1.27E+9	CONCRETE
2	Rect 0.25x0.45	112E+3	1.9E+9	586E+6	1.53E+9	CONCRETE

Supports

Node	X (kN/mm)	Y (kN/mm)	Z (kN/mm)	rX (kN-m/deg)	rY (kN-m/deg)	rZ (kN-m/deg)
33	Fixed	Fixed	Fixed	Fixed	Fixed	Fixed
34	Fixed	Fixed	Fixed	Fixed	Fixed	Fixed
36	Fixed	Fixed	Fixed	Fixed	Fixed	Fixed

Primary Load Cases

Number	Name	Type
1	DEAD LOAD + LIVE LOAD	None

1 DEAD LOAD + LIVE LOAD : Node Loads

Node	FX (kN)	FY (kN)	FZ (kN)	MX (kN-m)	MY (kN-m)	MZ (kN-m)
8	-	-12.500	-	-	-	-
	-12.500	-	-	-	-	-
21	-	-12.500	-	-	-	-
	-12.500	-	-	-	-	-
35	-	-12.500	-	-	-	-
	-12.500	-	-	-	-	-
37	-	-12.500	-	-	-	-
	-12.500	-	-	-	-	-
39	-	-12.500	-	-	-	-
	-12.500	-	-	-	-	-
40	-	-12.500	-	-	-	-
	-12.500	-	-	-	-	-
42	-	-12.500	-	-	-	-
	-12.500	-	-	-	-	-
43	-	-12.500	-	-	-	-
	-12.500	-	-	-	-	-
45	-	-12.500	-	-	-	-
	-12.500	-	-	-	-	-
46	-	-12.500	-	-	-	-
	-12.500	-	-	-	-	-
48	-	-12.500	-	-	-	-
	-12.500	-	-	-	-	-
49	-	-12.500	-	-	-	-
	-12.500	-	-	-	-	-
51	-	-12.500	-	-	-	-
	-12.500	-	-	-	-	-
52	-	-12.500	-	-	-	-
	-12.500	-	-	-	-	-
54	-	-12.500	-	-	-	-
	-12.500	-	-	-	-	-
55	-	-12.500	-	-	-	-
	-12.500	-	-	-	-	-
57	-	-12.500	-	-	-	-
	-12.500	-	-	-	-	-

1 DEAD LOAD + LIVE LOAD : Node Loads Cont...

Node	FX (kN)	FY (kN)	FZ (kN)	MX (kN-m)	MY (kN-m)	MZ (kN-m)
58	-	-12.500	-	-	-	-
	-12.500	-	-	-	-	-
60	-	-12.500	-	-	-	-
	-12.500	-	-	-	-	-
61	-	-12.500	-	-	-	-
	-12.500	-	-	-	-	-

1 DEAD LOAD + LIVE LOAD : Beam Loads

Beam	Type	Direction	Fa	Da (m)	Fb	Db	Ecc. (m)
10	UNI kN/m	GY	-17.500	-	-	-	-
	UNI kN/m	GY	-12.500	-	-	-	-
	UNI kN/m	GX	-12.500	-	-	-	-
	UNI kN/m	GX	-17.500	-	-	-	-
14	UNI kN/m	GY	-17.500	-	-	-	-
	UNI kN/m	GY	-12.500	-	-	-	-
	UNI kN/m	GX	-17.500	-	-	-	-
	UNI kN/m	GX	-12.500	-	-	-	-
17	UNI kN/m	GY	-17.500	-	-	-	-
	UNI kN/m	GY	-12.500	-	-	-	-
	UNI kN/m	GX	-17.500	-	-	-	-
	UNI kN/m	GX	-12.500	-	-	-	-
18	UNI kN/m	GY	-17.500	-	-	-	-
	UNI kN/m	GY	-12.500	-	-	-	-
	UNI kN/m	GX	-12.500	-	-	-	-
	UNI kN/m	GX	-17.500	-	-	-	-
21	UNI kN/m	GY	-17.500	-	-	-	-
	UNI kN/m	GY	-12.500	-	-	-	-
	UNI kN/m	GX	-12.500	-	-	-	-
	UNI kN/m	GX	-17.500	-	-	-	-
23	UNI kN/m	GY	-12.500	-	-	-	-
	UNI kN/m	GY	-17.500	-	-	-	-
	UNI kN/m	GX	-17.500	-	-	-	-
	UNI kN/m	GX	-12.500	-	-	-	-
26	UNI kN/m	GY	-17.500	-	-	-	-
	UNI kN/m	GY	-12.500	-	-	-	-
	UNI kN/m	GX	-17.500	-	-	-	-
	UNI kN/m	GX	-12.500	-	-	-	-
28	UNI kN/m	GY	-12.500	-	-	-	-
	UNI kN/m	GY	-17.500	-	-	-	-
	UNI kN/m	GX	-12.500	-	-	-	-
	UNI kN/m	GX	-17.500	-	-	-	-
31	UNI kN/m	GY	-12.500	-	-	-	-
	UNI kN/m	GY	-17.500	-	-	-	-
	UNI kN/m	GX	-12.500	-	-	-	-
	UNI kN/m	GX	-17.500	-	-	-	-
33	UNI kN/m	GY	-17.500	-	-	-	-

1 DEAD LOAD + LIVE LOAD : Beam Loads Cont...

Beam	Type		Direction	Fa	Da (m)	Fb	Db	Ecc. (m)
33	UNI	kN/m	GY	-12.500	-	-	-	-
	UNI	kN/m	GX	-17.500	-	-	-	-
	UNI	kN/m	GX	-12.500	-	-	-	-
36	UNI	kN/m	GY	-12.500	-	-	-	-
	UNI	kN/m	GY	-17.500	-	-	-	-
	UNI	kN/m	GX	-12.500	-	-	-	-
	UNI	kN/m	GX	-17.500	-	-	-	-
38	UNI	kN/m	GY	-17.500	-	-	-	-
	UNI	kN/m	GY	-12.500	-	-	-	-
	UNI	kN/m	GX	-17.500	-	-	-	-
	UNI	kN/m	GX	-12.500	-	-	-	-
41	UNI	kN/m	GY	-12.500	-	-	-	-
	UNI	kN/m	GY	-17.500	-	-	-	-
	UNI	kN/m	GX	-17.500	-	-	-	-
	UNI	kN/m	GX	-12.500	-	-	-	-
43	UNI	kN/m	GY	-17.500	-	-	-	-
	UNI	kN/m	GY	-12.500	-	-	-	-
	UNI	kN/m	GX	-12.500	-	-	-	-
	UNI	kN/m	GX	-17.500	-	-	-	-
46	UNI	kN/m	GY	-12.500	-	-	-	-
	UNI	kN/m	GY	-17.500	-	-	-	-
	UNI	kN/m	GX	-17.500	-	-	-	-
	UNI	kN/m	GX	-12.500	-	-	-	-
48	UNI	kN/m	GY	-12.500	-	-	-	-
	UNI	kN/m	GY	-17.500	-	-	-	-
	UNI	kN/m	GX	-12.500	-	-	-	-
	UNI	kN/m	GX	-17.500	-	-	-	-
51	UNI	kN/m	GY	-12.500	-	-	-	-
	UNI	kN/m	GY	-17.500	-	-	-	-
	UNI	kN/m	GX	-17.500	-	-	-	-
	UNI	kN/m	GX	-12.500	-	-	-	-
53	UNI	kN/m	GY	-17.500	-	-	-	-
	UNI	kN/m	GY	-12.500	-	-	-	-
	UNI	kN/m	GX	-12.500	-	-	-	-
	UNI	kN/m	GX	-17.500	-	-	-	-
56	UNI	kN/m	GY	-12.500	-	-	-	-
	UNI	kN/m	GY	-17.500	-	-	-	-
	UNI	kN/m	GX	-12.500	-	-	-	-
	UNI	kN/m	GX	-17.500	-	-	-	-
58	UNI	kN/m	GY	-12.500	-	-	-	-
	UNI	kN/m	GY	-17.500	-	-	-	-
	UNI	kN/m	GX	-17.500	-	-	-	-
	UNI	kN/m	GX	-12.500	-	-	-	-

1 DEAD LOAD + LIVE LOAD : Selfweight

Direction	Factor	Assigned Geometry
Y	-1.000	ALL

Calculated Modal Frequencies & Mass Participations

Mode	Frequency (Hz)	Period (sec)	Participation X (%)	Participation Y (%)	Participation Z (%)	Type
1	0.382	2.619	80.369	0.000	0.000	Elastic
2	1.180	0.847	10.336	0.000	0.000	Elastic
3	2.089	0.479	3.751	0.000	0.000	Elastic
4	3.092	0.323	2.073	0.000	0.000	Elastic
5	4.226	0.237	1.316	0.000	0.000	Elastic
6	5.223	0.191	0.000	67.786	0.000	Elastic
7	0.000	1E+6	0.000	0.000	0.000	Missing Mass

B.2. DIMENSIONS OF EQUIVALENT FLAT BOTTOM TLD FOR CENTRAL SLOPE TLD (XIN'S APPROACH)

B.2.1. TLD with central slope of (θ) = 12.5°

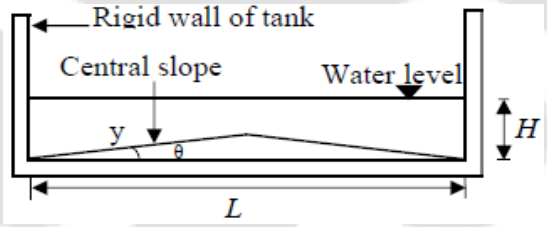

Figure B.1. Elevation of TLD

The of TLD as stated earlier are; depth of liquid (H) = 0.20 m, Length of TLD (L) = 1.72 m and width of TLD (B) =1.00 m.

From the Figure B.1 of TLD with central slope θ , wetting length of TLD with central slope on one side of centre of TLD is

$$y = \frac{L/2}{Cos(\theta)} \tag{B.1}$$

Net wetting length for central slope of is

$$L' = 2y \tag{B.2}$$

$\therefore$ For $\theta = 12.5^{o}$, $L' = 1.761$ m

$\therefore$ Equivalent length of flat bottom TLD $L' = 1.761$ m

Width of equivalent flat bottom TLD is determined from expression

$$B' = \frac{V_w}{H'L'} \tag{B.3}$$

Where $(H' = H)$ and V_w is volume of water or liquid in TLD

$\therefore$ $B' = 0.976$ m

B.3. TLD WITH CENTRAL SLOPE OF (Θ) = 14°

The of TLD as stated earlier are; depth of liquid (H) = 0.2235 m, Length of TLD (L) = 1.72 m and width of TLD (B) =1.00 m.

From the Figure of TLD with central slope θ , wetting length of TLD with central slope on one side of centre of TLD is

$$y = \frac{L/2}{Cos(\theta)}$$

Net wetting length for central slope of is

$$L' = 2y$$

$\therefore$ For $\theta = 14^{o}$, $L' = 1.772$ m

$\therefore$ Equivalent length of flat bottom TLD $L' = 1.772$ m

Width of equivalent flat bottom TLD is determined from expression

$$B' = \frac{V_w}{H'L'}$$

Where $(H' = H)$ and V_w is volume of water or liquid in TLD

$\therefore \quad B' = 0.970$ m

B.3.1. Reduction in volume of liquid due to application of central slope of 14º at bottom of TLD

Volume of liquid/water in a flat bottom TLD (V) = LBH (B.4)

$= 0.384 m^3$

Height of central slope at midpoint of TLD (y'') = $L/2\ tan(14)$ (B.5)

$= 0.214$ m

Reduction in volume of liquid in a TLD due central slope of 14º

$$(V') = \tfrac{1}{2}(Ly'')B \quad \text{(B.6)}$$

$= 0.180\ m^3$

Percent reduction in volume of liquid (VR) or (MR) = $(V'/V)100$ (B.7)

$= 47.96$ %

B.4. TLD WITH DUAL TRIANGULAR SLOPES OF (Θ) = 20º

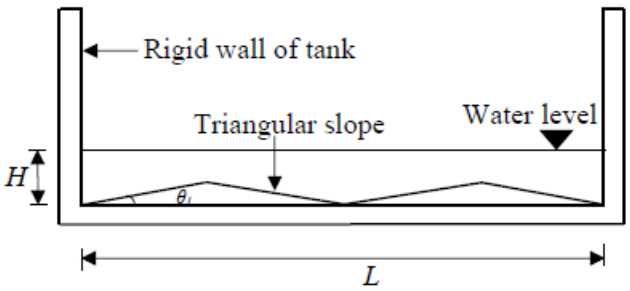

Figure B.2. Elevation of TLD

The of TLD as stated earlier are; Depth of liquid (H) = 0.2235 m, Length of TLD (L) = 1.72 m and Width of TLD (B) =1.00 m.

From the Figure B.2 of TLD with central slope θ_1, wetting length of TLD with dual triangular slope at bottom of TLD is

$$y_1 = \frac{L/4}{Cos(\theta_1)} \tag{B.8}$$

Net wetting length for dual triangular slopes of is

$$L' = 4y_1 \tag{B.9}$$

$\therefore$ For $\theta_1 = 20^o$, $L' = 1.830$ m

$\therefore$ Equivalent length of flat bottom TLD $L' = 1.830\ m$

Width of equivalent flat bottom TLD is determined from expression

$$B' = \frac{V_w}{H'L'}$$

Where ($H' = H$) and V_w is volume of water or liquid in TLD

$\therefore$ $B' = 0.939$ m

B.4.1. Reduction in volume of liquid due to application of dual triangular slopes of 20º at bottom of TLD

Volume of liquid/water in a flat bottom TLD (V) = LBH

$= 0.384 m^3$

Height of central slope at midpoint of TLD (y'') = $L/4\ tan(20)$ (B.10)

$= 0.156$ m

Reduction in volume of liquid in a TLD due dual triangular slopes of 20º

$$(V') = 2\,(\tfrac{1}{2}(L'\,y'')B) \qquad \text{(B.11)}$$

$$= 0.134\ \text{m}^3$$

Percent reduction in volume of liquid (VR) or (MR) = $(V'/V)100$

$$= 35.01\ \%$$

B.5. DIMENSIONS OF EQUIVALENT FLAT BOTTOM TLD FOR END SLOPE (GARDARSSON'S APPROACH)

B.5.1. TLD with end slope of (α) = 30°

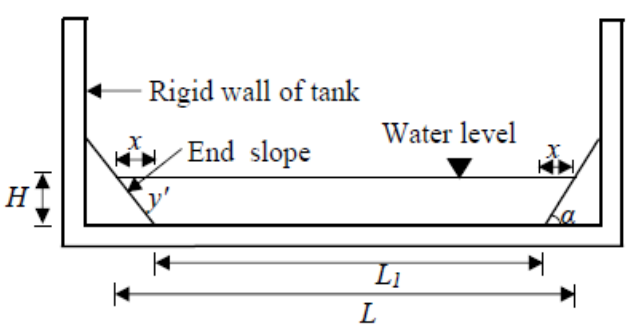

Figure B.3. Elevation of TLD

Data: Depth of liquid /water in TLD (H) = 0.20 m

Length of TLD (L) = 1.72 m

Width of THD (B) = 1.00 m

Horizontal projection of sloping length on one end of TLD bottom

$$x = \frac{H}{\tan(30)} \qquad \text{(B.12)}$$

$$\therefore \quad x = 0.3461\ \text{m}$$

Net horizontal projection of sloping length on both ends of TLD at bottom

$2x$ = 0.6928 m

Shape parameter s

$$s = \frac{2x}{L} \tag{B.13}$$

$\therefore \quad s$ = 0.4024 m

Sloshing frequency of liquid in a box/flat shaped TLD

$$f_b = \sqrt{\frac{\pi g}{L}} \tanh \frac{\pi H}{L} \tag{B.14}$$

$\therefore \quad f_b$ = 2.5038 rad/sec

Sloshing frequency (f) of liquid in a TLD with end slope at bottom is determined from the geometric curve (plot of f / f_b vs s) as shown in Figure .

and $$\frac{f}{f_b} = 0.4024$$

$\therefore \quad f$ = 2.4274 rad/sec

Length of equivalent flat bottom TLD (L') is calculated from expression

$$f = \sqrt{\frac{\pi g}{L'}} \tanh \frac{\pi H}{L'} \tag{B.15}$$

$\therefore \quad L'$ = 1.776 m

Width of equivalent flat bottom TLD is determined from expression

$$B' = \frac{V_w}{H' L'}$$

Where ($H' = H$) and V_w is volume of water or liquid in TLD

$\therefore \quad B'$ = 0.773 m

B.6. TLD WITH END SLOPE OF 15°

Data: Depth of liquid /water in TLD (H) = 0.2235 m (Figure B.3)

Length of TLD (L) = 1.72 m

Width of THD (B) = 1.00 m

Horizontal projection of sloping length on one end of TLD bottom

$$x = \frac{H}{\tan(15)}$$

$$\frac{f}{f_b} = 0.786$$

$$\therefore \quad x = 0.834 \text{ m}$$

Net horizontal projection of sloping length on both ends of TLD at bottom

$$2x = 1.668 \text{ m}$$

Shape parameter s

$$s = \frac{2x}{L}$$

$$\therefore \quad s = 0.969 \text{ m}$$

Sloshing frequency of liquid in a box/flat shaped TLD

$$f_b = \sqrt{\frac{\pi g}{L}} \tanh \frac{\pi H}{L}$$

$$\therefore \quad f_b = 2.633 \text{ rad/sec}$$

Sloshing frequency (f) of liquid in a TLD with end slope at bottom is determined from the geometric curve (plot of f / f_b vs s) as shown in Figure .

and $$\frac{f}{f_b} = 0.786$$

$$\therefore \quad f = 2.075 \text{ rad/sec}$$

Length of equivalent flat bottom TLD (L') is calculated from expression

$$f = \sqrt{\frac{\pi g}{L'}} \tanh \frac{\pi H}{L'}$$

$$\therefore \quad L' = 2.205 \text{ m}$$

Width of equivalent flat bottom TLD is determined from expression

$$B' = \frac{V_w}{H'L'}$$

Where $(H' = H)$ and V_w is volume of water or liquid in TLD

$$\therefore \quad B' = 0.401 \text{ m}$$

B.6.1. Reduction in volume of liquid due to application of central slope of 15º at bottom of TLD

Volume of liquid/water in a flat bottom TLD $(V) = LBH$

$$= 0.384 \text{m}^3$$

Reduction in volume of liquid in a TLD due end slope slope of 15º

$$(V') = 2 (\tfrac{1}{2} xH)B)$$

$$= 0.186 \text{ m}^3$$

Percent reduction in volume of liquid (VR) or $(MR) = (V'/V)100$

$$= 48.49 \%$$

B.7. TLD WITH END SLOPE OF 15° (XIN'S APPROACH)

The of TLD as stated earlier are; depth of liquid (H) = 0.2235 m, Length of TLD (L) = 1.72 m and width of TLD (B) =1.00 m.

From the Figure of TLD with end slope α , wetting length of TLD with end slope on one side of bottom of TLD is

$$y' = \frac{H}{Sin(\alpha)} \tag{B.16}$$

$\therefore \quad y' = 0.863$ m

Horizontal distance of TLD at bottom (L_1) = 0.052 m

Equivalent length of flat bottom TLD L'

$$L' = L_1 + 2y' \tag{B.17}$$

$\therefore$ For $\alpha = 15^o$, $\quad L' = 1.782$ m

Width of equivalent flat bottom TLD is determined from expression

$$B' = \frac{V_w}{H' L'}$$

Where ($H' = H$) and V_w is volume of water or liquid in TLD

$\therefore \quad B' = 0.515$ m

B.8. DIMENSIONS OF EQUIVALENT FLAT BOTTOM TLD FOR COMBINATION OF CENTRAL SLOPE AND END SLOPE AT BOTTOM

B.8.1. TLD with central slope (θ) = 5º and end slope (α) = 25º

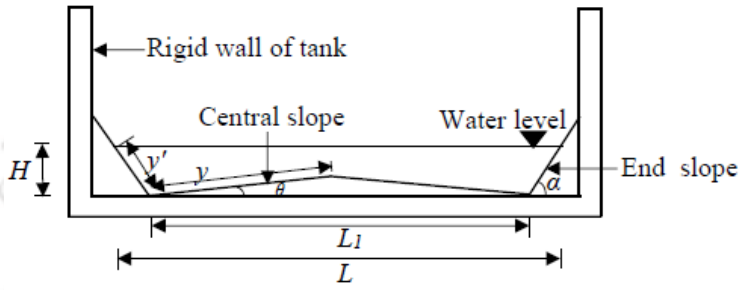

Figure B.4. Elevation of TLD

Data: Length of TLD (L) = 1.72 m

Depth of liquid /water in TLD (H) = 0.2235 m

Width of HD (B) = 1.00 m

Central slope angle (θ) = 5º

End slope angle (α) = 25º

From Figure

The wetting length of TLD with end slope at one side is

$$y' = \frac{H}{Sin(\alpha)} \tag{B.18}$$

$\therefore$ y' = 0.528 m

Distance between end slope at two sides of bottom of TLD (L_1)

$$L_1 = L - 2\frac{H}{\tan(\alpha)} \tag{B.19}$$

$\therefore\ L_1 = 0.761$ m

Wetting length of TLD with central slope on one side centre of TLD is

$$y = \frac{L_1 / 2}{Cos(\theta)} \qquad \text{(B.20)}$$

$\therefore\quad y = 0.381$ m

Wetting length due end slope and central triangular slope (L')

$$L' = 2y + 2y' \qquad \text{(B.21)}$$

$\therefore\ L' = 1.820$ m

Width of equivalent flat bottom TLD is determined from expression

$$B' = \frac{V_w}{H' L'}$$

Where ($H' = H$) and V_w is volume of water or liquid in TLD

$\therefore\ B' = 0.491$ m

B.8.2. Reduction in volume of liquid due to application of central slope of 5º and end slope of 25º at bottom of TLD

Volume of liquid/water in a flat bottom TLD (V) = LBH

$= 0.384\text{m}^3$

Horizontal projection of end slope (x)

$$x = \frac{H}{\tan(\alpha)}$$

$= 0.479$ m

Height of central slope at centre (y'') = $L_1/2\tan(5)$

= 0.033 m

Reduction in volume of liquid in a TLD due end slope of 25º and central slope of 5º

$$(V') = 2\,(\tfrac{1}{2}xH)B) + (\tfrac{1}{2}(L_1y'')B \qquad \text{(B.22)}$$

$$= 0.119\ m^3$$

Percent reduction in volume of liquid (*VR*) or (*MR*) = (*V'/V*)100

= 31.14 %

B.9. EVALUATING DIMENSIONS OF EQUIVALENT FLAT BOTTOM TLD FOR COMBINATION OF DUAL TRIANGULAR SLOPES AND END SLOPE AT BOTTOM

B.9.1. TLD with combination of dual triangular slopes of (θ_1) = 5º and end slope of (α) = 25º at bottom

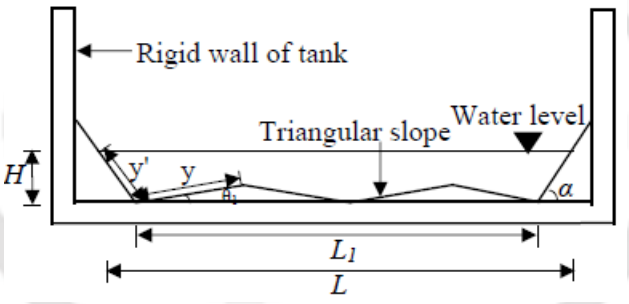

Figure B.5. Elevation of TLD

Data: Length of TLD (*L*) = 1.72 m

Width of TLD (*B*) = 1.00 m

Depth of liquid /water in TLD (*H*) = 0.2235 m

Dual triangular slope angle (θ_1) = 5º

End slope angle (α) = 25º

The wetting length of TLD with end slope at one side is

$$y' = \frac{H}{Sin(\alpha)} \qquad \text{(B.23)}$$

$\therefore$ y' = 0.528 m

Distance between end slope at two sides of bottom of TLD (L_1)

$$L_1 = L - 2\frac{H}{\tan(\alpha)} \qquad \text{(B.24)}$$

$\therefore$ L_1 = 0.761 m

Wetting length of TLD with central slope on one side centre of TLD is

$$y = \frac{L_1 / 4}{Cos(\theta_1)}$$

$\therefore$ y = 0.190 m

Wetting length due end slope and central triangular slope (L')

$$L' = 4y + 2y' \qquad \text{(B.25)}$$

$\therefore$ L' = 1.829 m

Width of equivalent flat bottom TLD is determined from expression

$$B' = \frac{V_w}{H'L'}$$

Where ($H' = H$) and V_w is volume of water or liquid in TLD

$\therefore$ B' = 0.646 m

B.9.2. Reduction in volume of liquid due to application of end slope of 25º and dual triangular slopes of 5º at bottom of TLD

Volume of liquid/water in a flat bottom TLD(V) = LBH

= 0.384m^3

Horizontal projection of end slope (x)

$$x = \frac{H}{\tan(\alpha)}$$

$$= 0.479 \text{ m}$$

Height of central slope at centre $(y'') = L_1/4\tan(5)$

$$= 0.016 \text{ m}$$

Reduction in volume of liquid in a TLD due end slope of 25º and central slope of 5º

$$(V') = 2\,(\tfrac{1}{2}xH)B) + 2(\tfrac{1}{2}(L_1 y'')B \qquad \text{(B.26)}$$

$$= 0.113 \text{ m}^3$$

Percent reduction in volume of liquid (VR) or (MR) $= (V'/V)100$

$$= 29.42\ \%$$

Note: Since water (density = 1000 kg/m^3) is used as a liquid in the analysis, the percent reduction in volume of liquid is taken as percent reduction in mass of liquid.

APPENDIX C

TYPICAL TIME HISTORY PLOTS OF STRUCTURE WITH AND WITHOUT TLD

C.1. CHAPTER 3 SAMPLE FIGURES

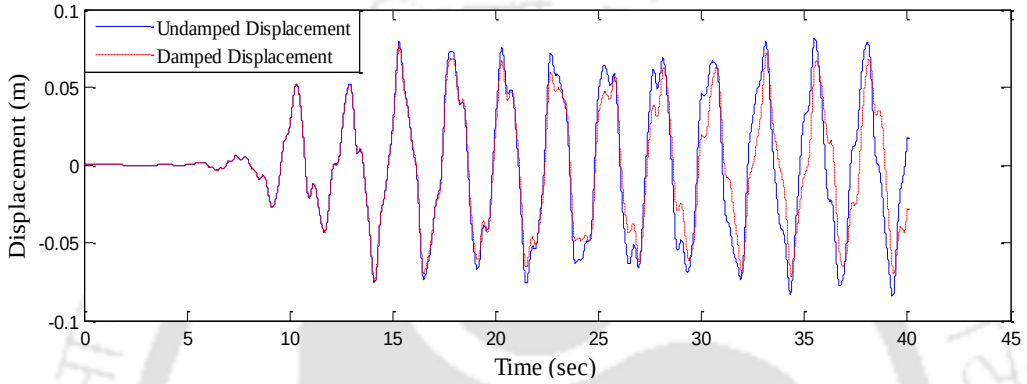

Figure C.1. Response of structure with 5º central sloped TLD to Loma Prieta earthquake

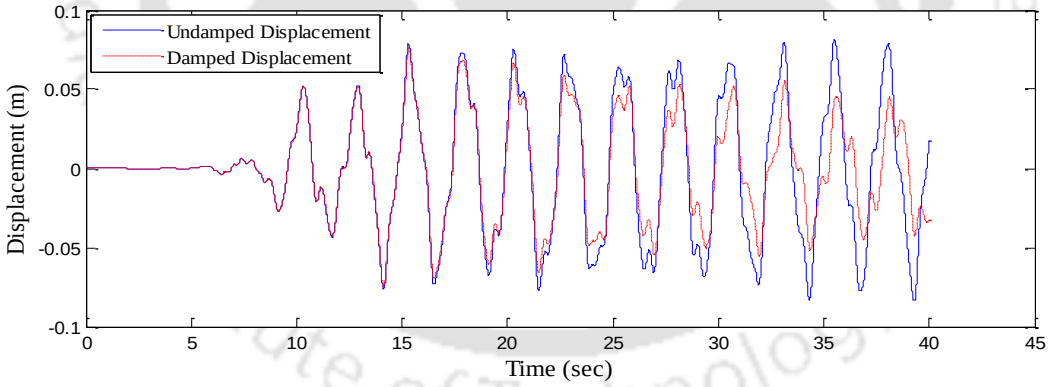

Figure C.2. Response of structure with 14º central sloped TLD to Loma earthquake

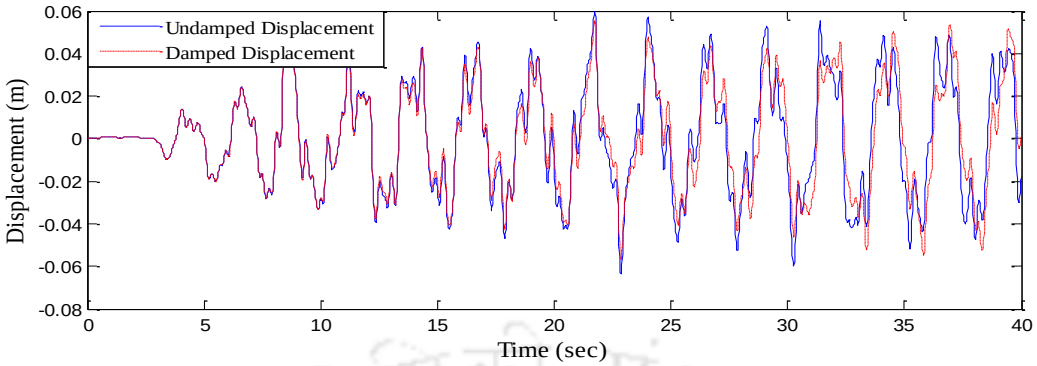

Figure C.3. Response of structure with 5º central sloped TLD to Northridge earthquake

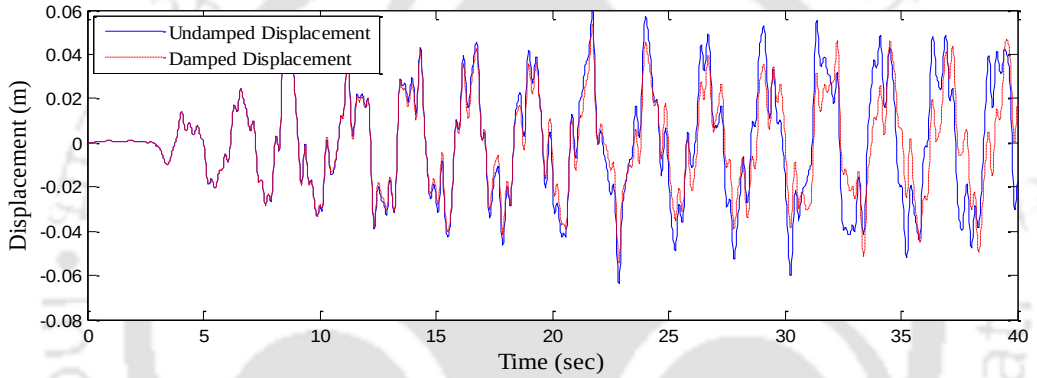

Figure C.4. Response of structure with 14º central sloped TLD to Northridge earthquake

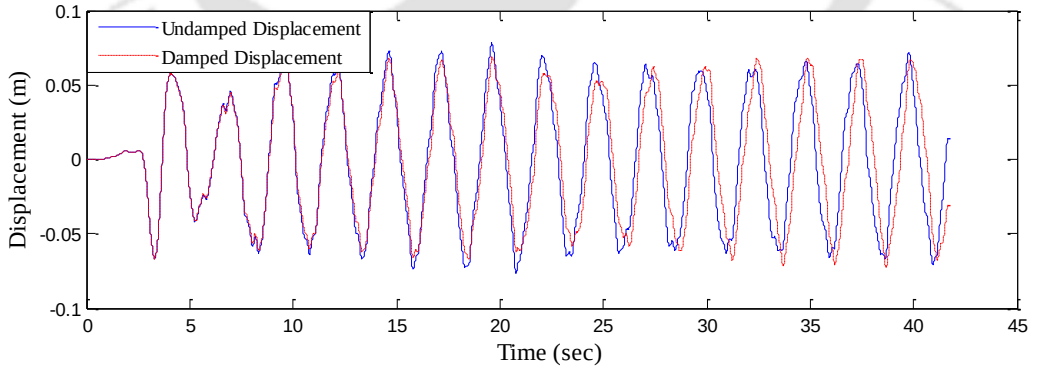

Figure C.5. Response of structure with 5º central sloped TLD to San Fernando earthquake

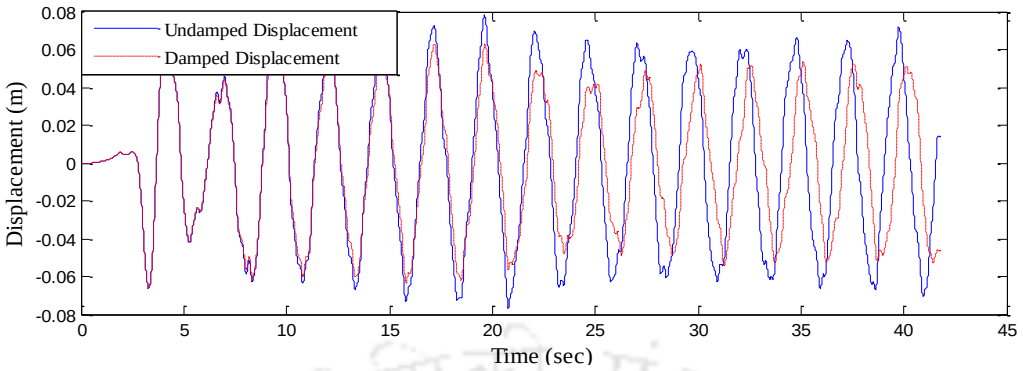

Figure C.6. Response of structure with 14º central sloped TLD to San Fernando earthquake

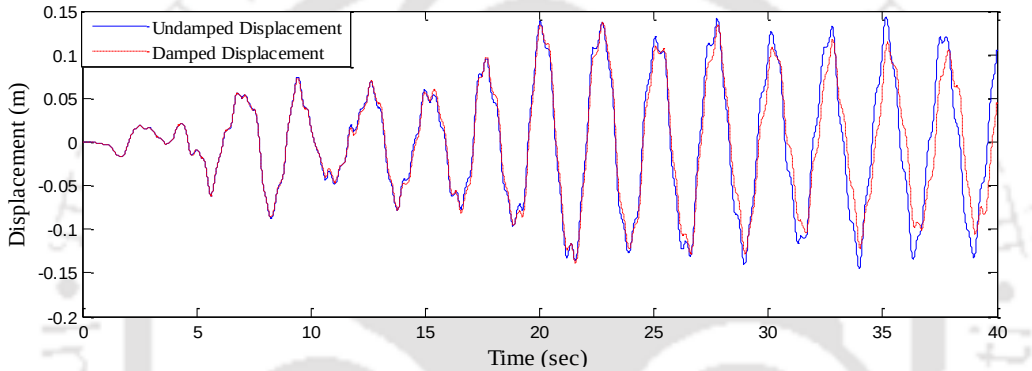

Figure C.7. Response of structure with 5º central sloped TLD to IS time history

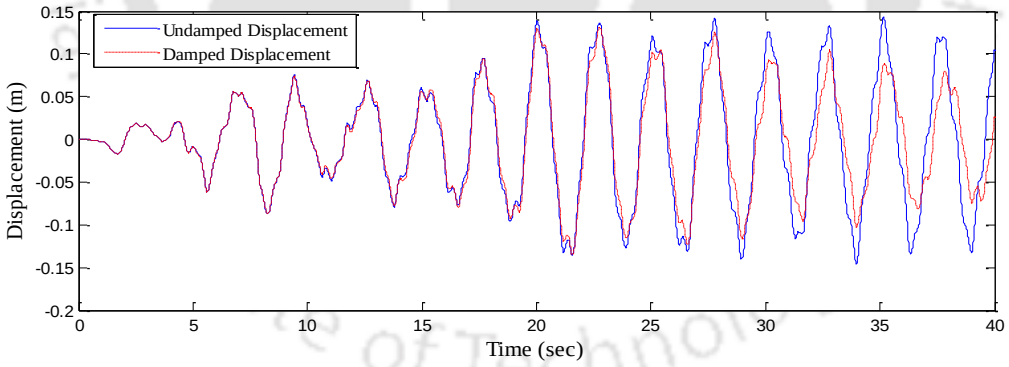

Figure C.8. Response of structure with 14º central sloped TLD to IS time history

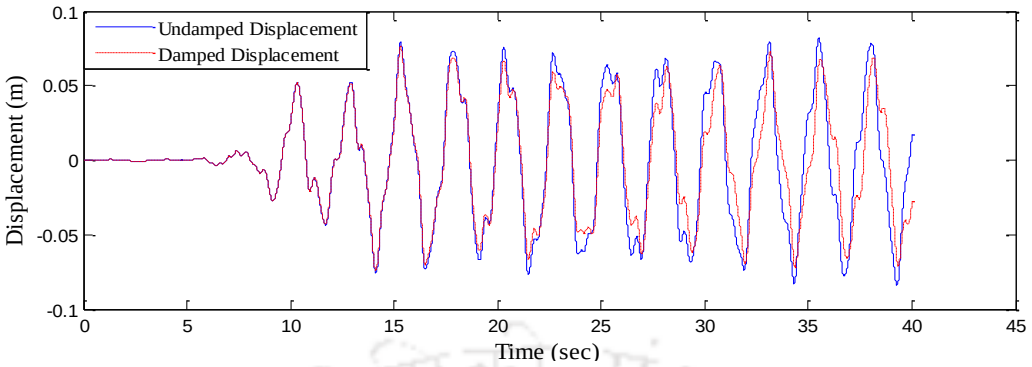

Figure C.9. Response of structure with 5º dual triangular sloped TLD to Loma Prieta earthquake

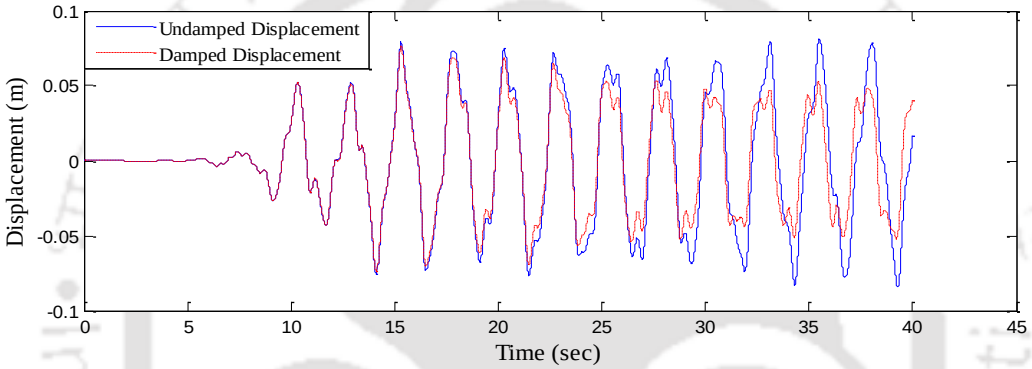

Figure C.10. Response of structure with 25º dual triangular sloped TLD to Loma Prieta earthquake

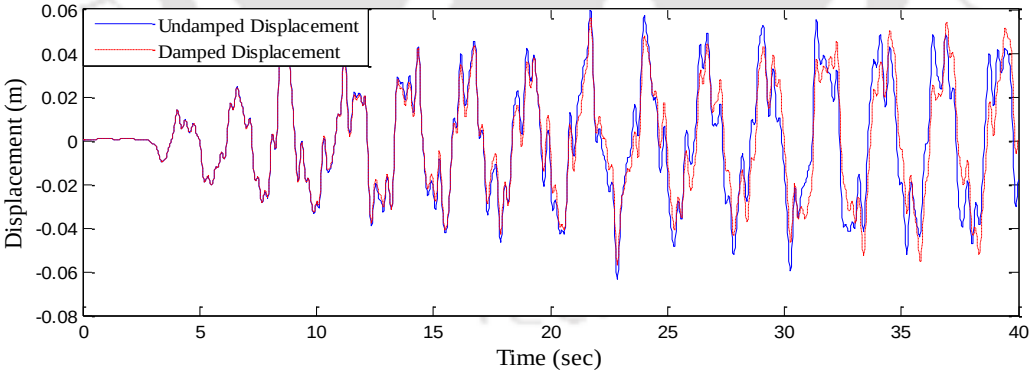

Figure C.11. Response of structure with 5º dual triangular sloped TLD to Northridge earthquake

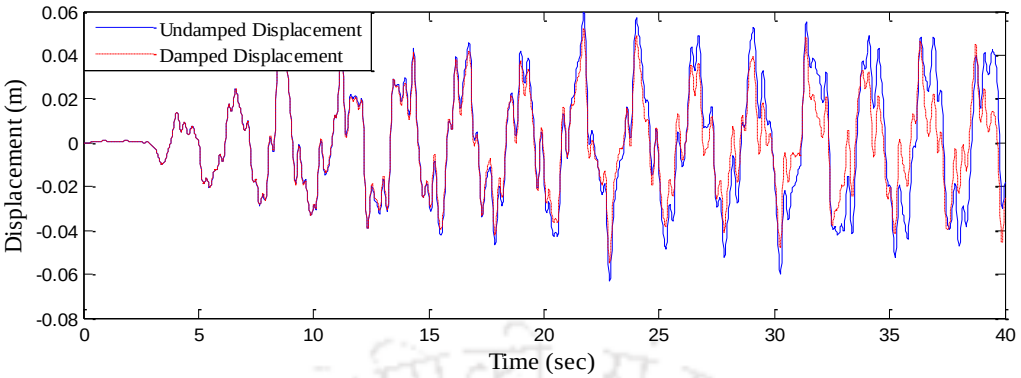

Figure C.12. Response of structure with 25º dual triangular sloped TLD to Northridge earthquake

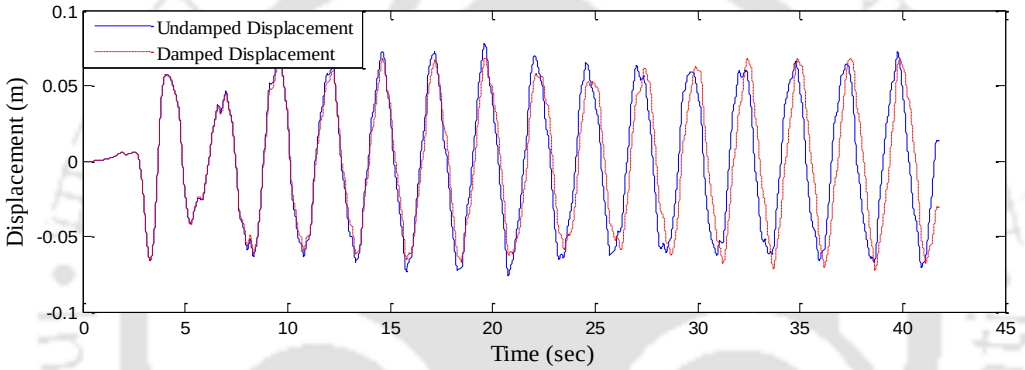

Figure C.13. Response of structure with 5º dual triangular sloped TLD to San Fernando earthquake

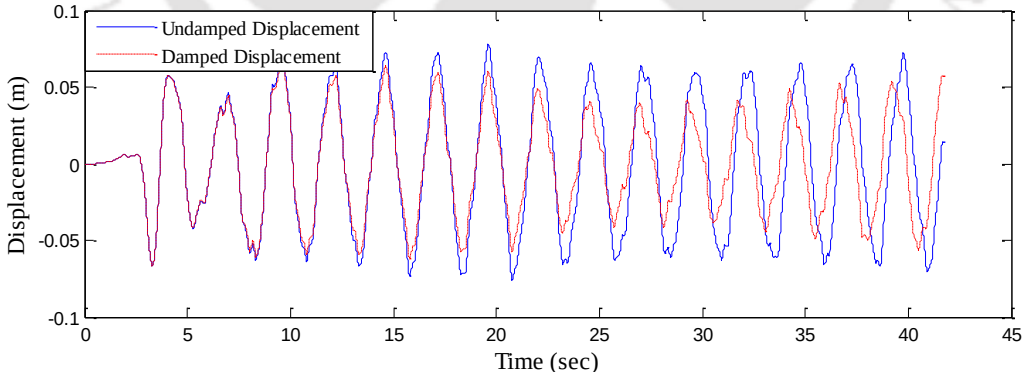

Figure C.14. Response of structure with 25º dual triangular sloped TLD ton San Fernando earthquake

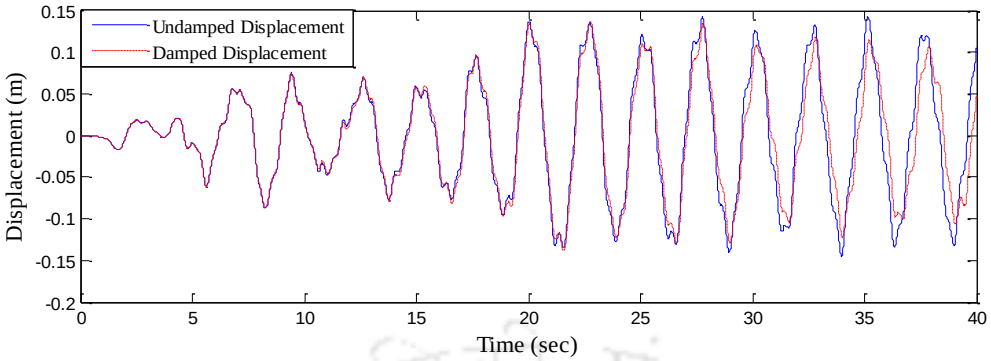

Figure C.15. Response of structure with 5º dual triangular sloped TLD to IS time history

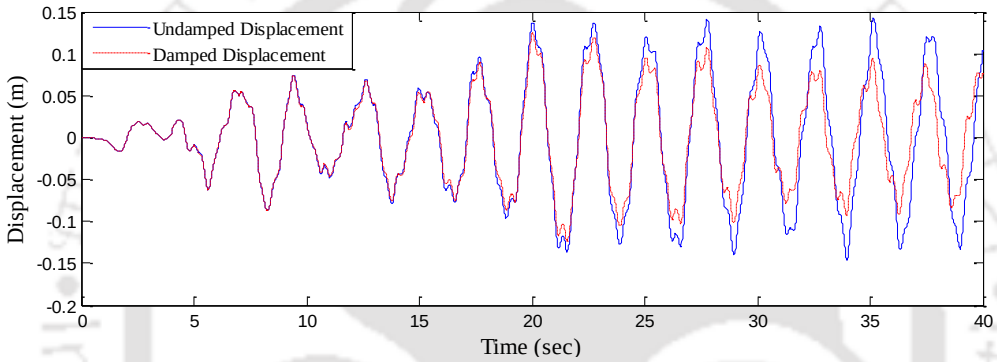

Figure C.16. Response of structure with 25º dual triangular sloped TLD to IS time history

C.2. CHAPTER 4 SAMPLE FIGURES

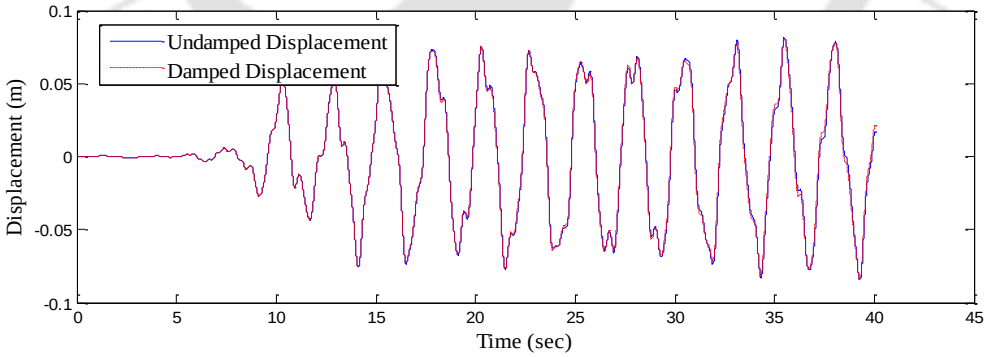

Figure C.17. Response of structure with 15º sloped TLD to Loma Prieta earthquake

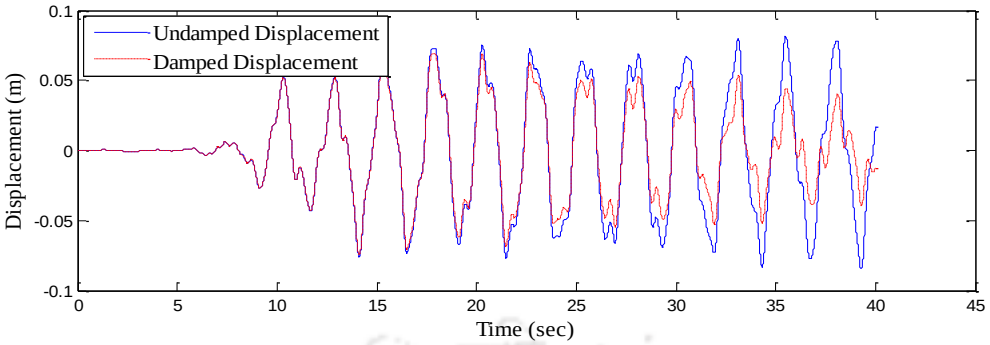

Figure C.18. Response of structure with 30º sloped TLD to Loma Prieta earthquake

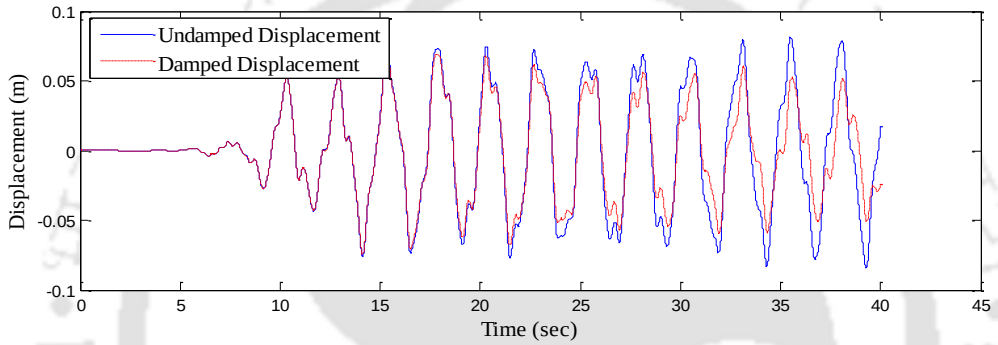

Figure C.19. Response of structure with 35º sloped TLD to Loma Prieta earthquake

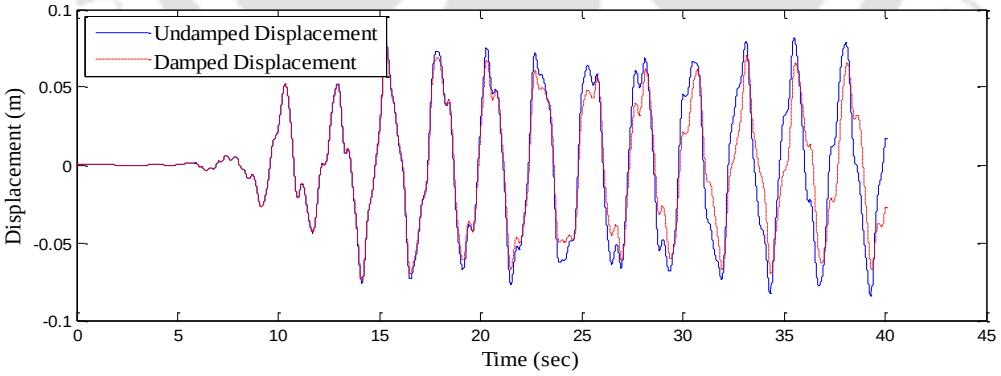

Figure C.20. Response of structure with 50º sloped TLD to Loma Prieta earthquake

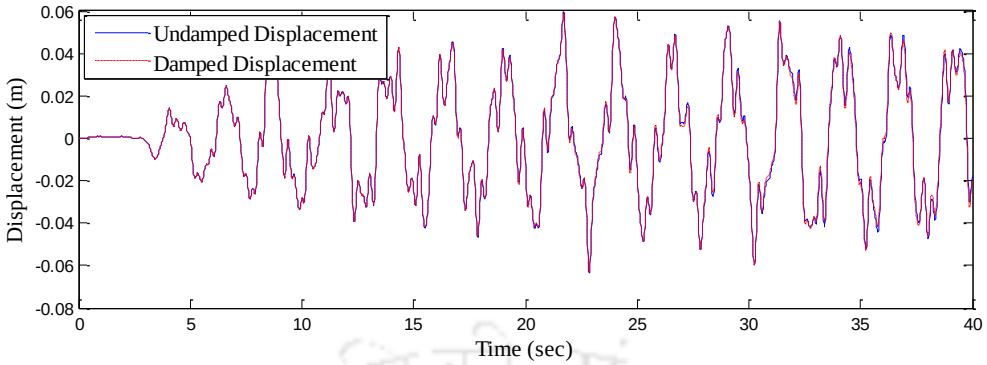

Figure C.21. Response of structure with 15º sloped TLD to Northridge earthquake

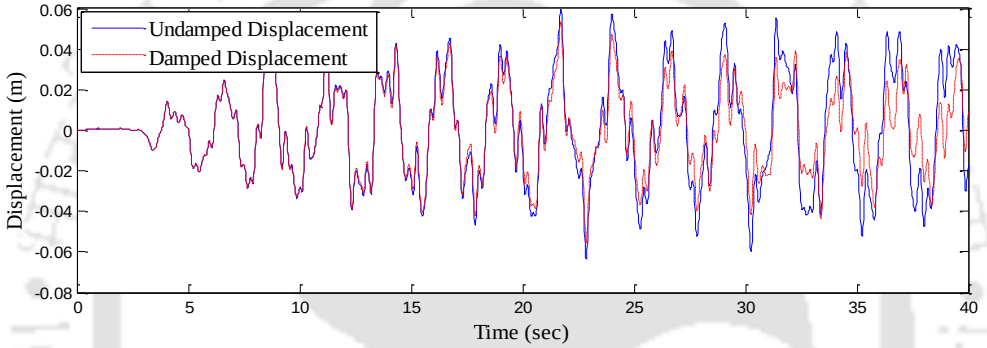

Figure C.22. Response of structure with 30º sloped TLD to Northridge earthquake

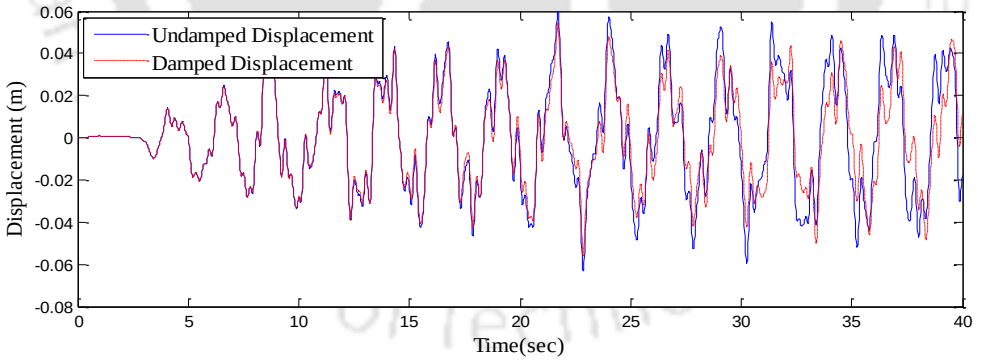

Figure C.23. Response of structure with 35º sloped TLD to Northridge earthquake

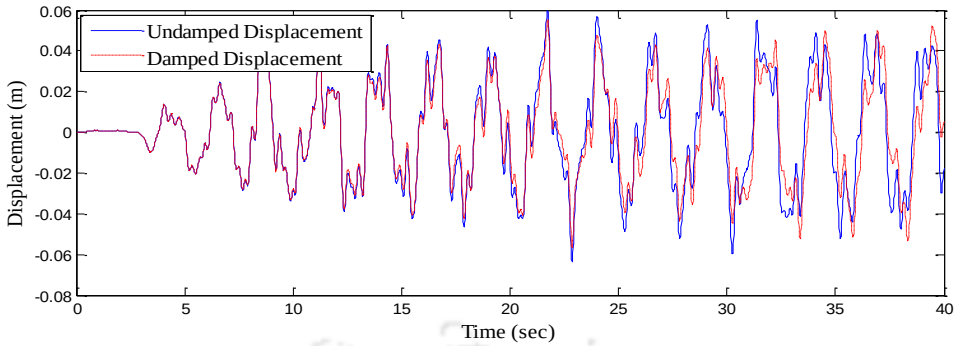

Figure C.24. Response of structure with 50º sloped TLD to Northridge earthquake

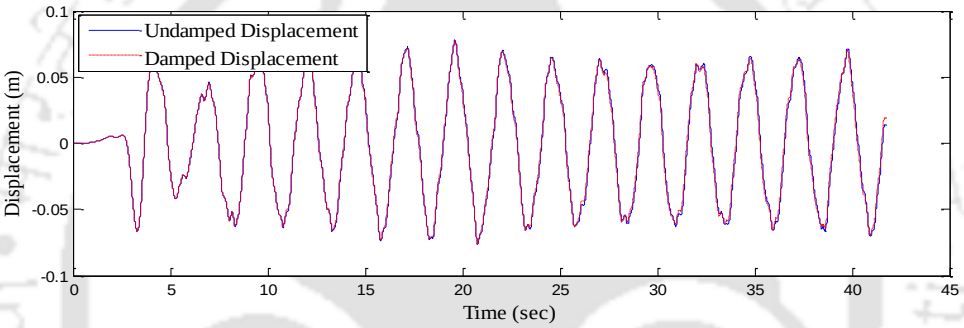

Figure C.25. Response of structure with 15º sloped TLD to San Fernando earthquake

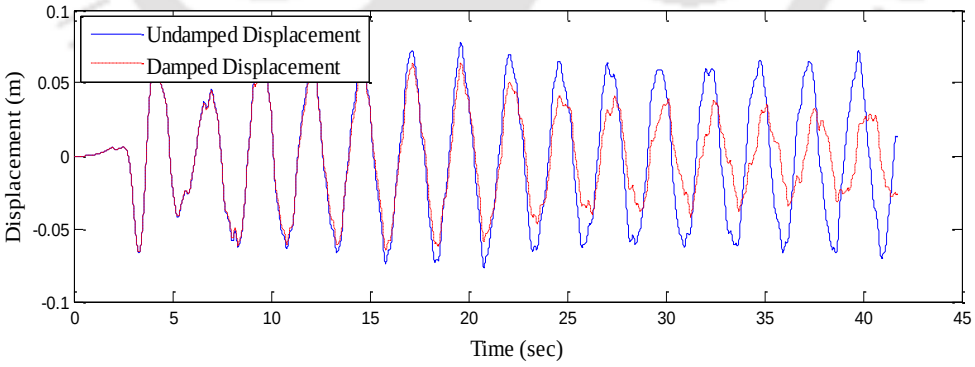

Figure C.26. Response of structure with 30º sloped TLD to San Fernando earthquake

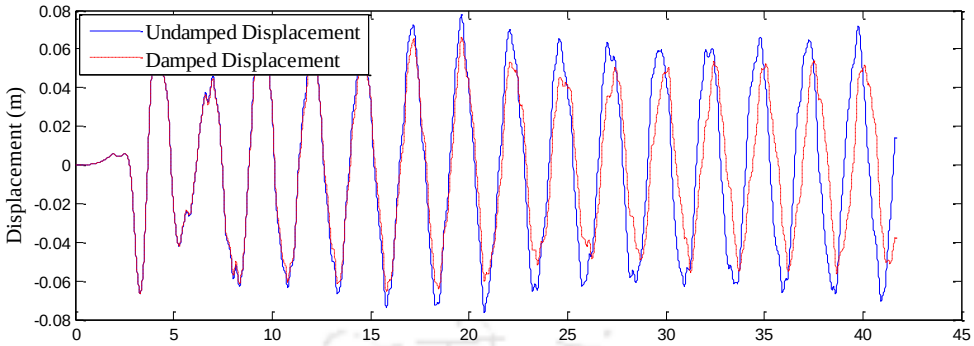

Figure C.27. Response of structure with 35º sloped TLD to San Fernando earthquake

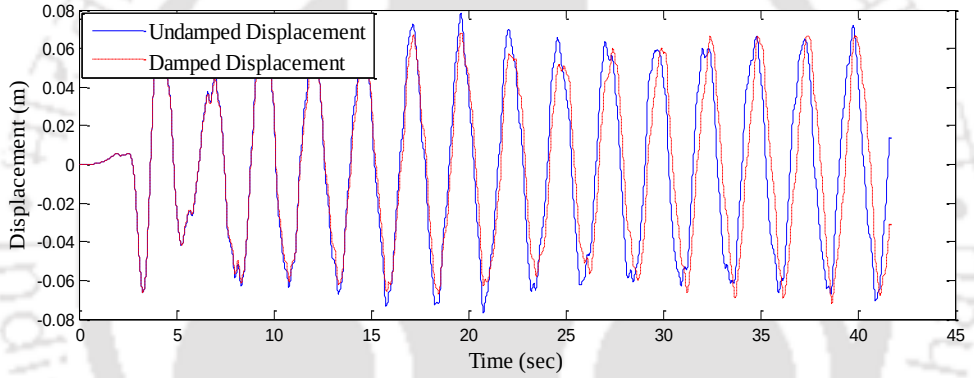

Figure C.28. Response of structure with 50º sloped TLD to San Fernando earthquake

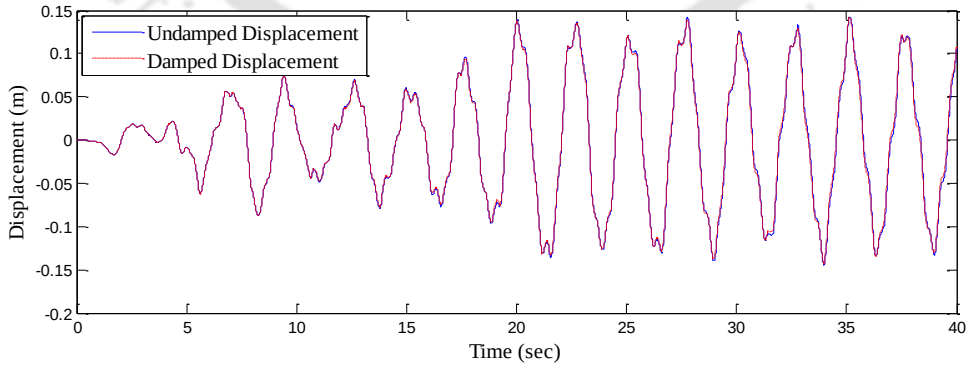

Figure C.29. Response of structure with 15º sloped TLD to IS time history

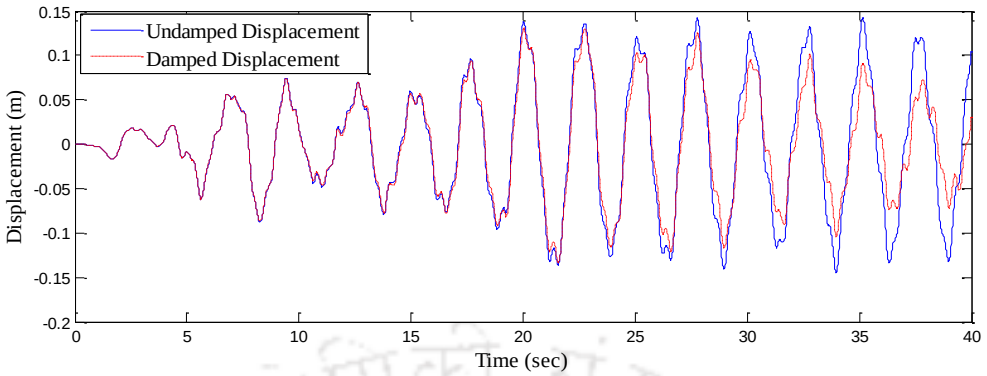

Figure C.30. Response of structure with 30º sloped TLD to IS time history

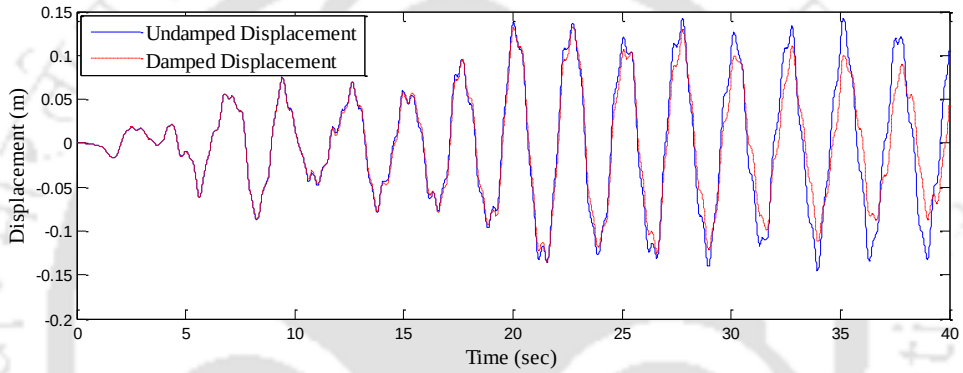

Figure C.31. Response of structure with 35º sloped TLD to IS time history

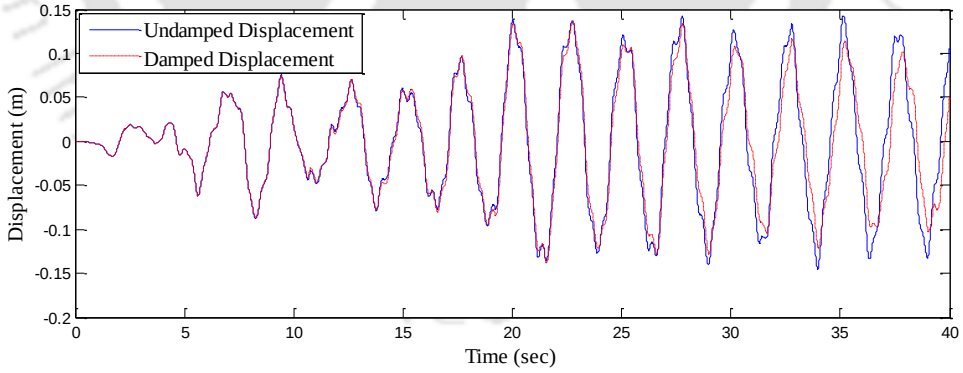

Figure C.32. Response of structure with 50º sloped TLD to IS time history

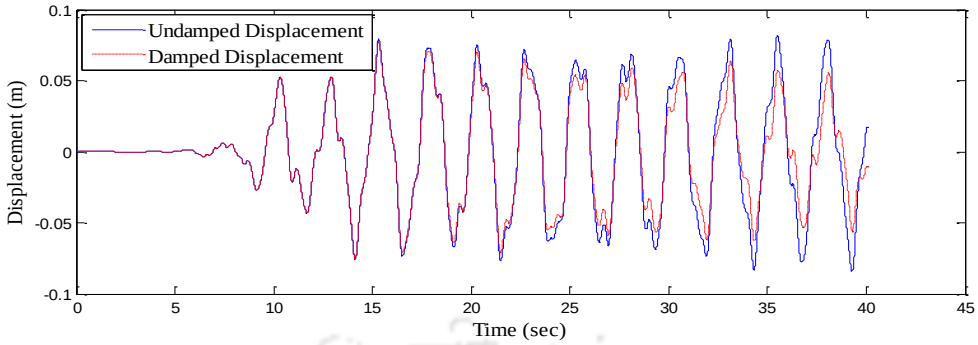

Figure C.33. Response of structure with 15º sloped TLD to Loma Prieta earthquake

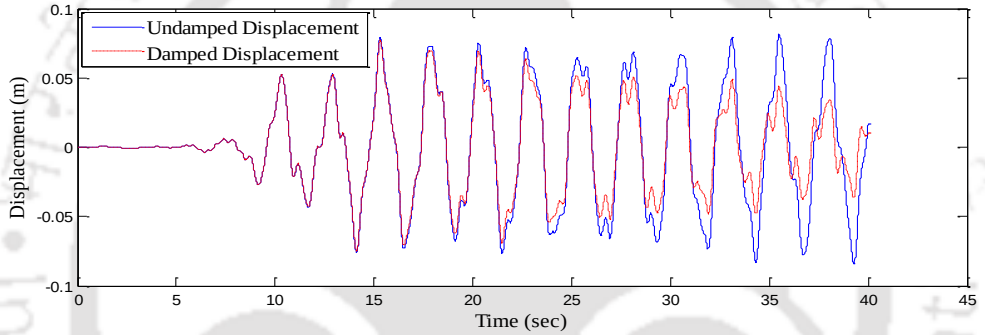

Figure C.34. Response of structure with 30º sloped TLD to Loma Prieta earthquake

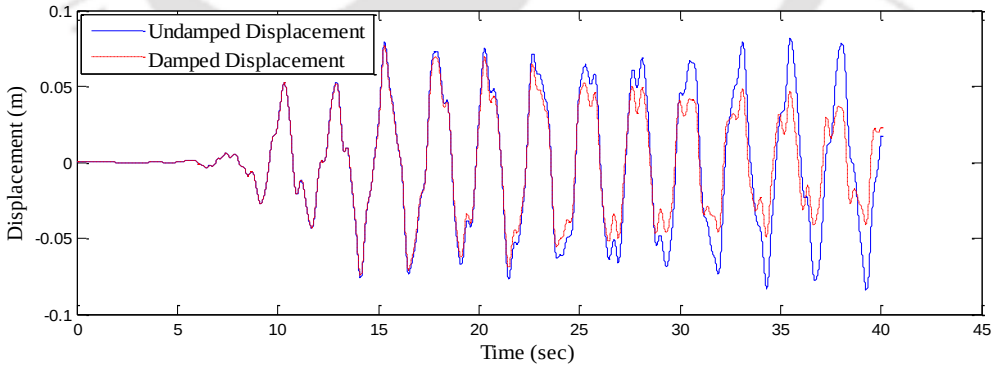

Figure C.35. Response of structure with 35º sloped TLD to Loma Prieta earthquake

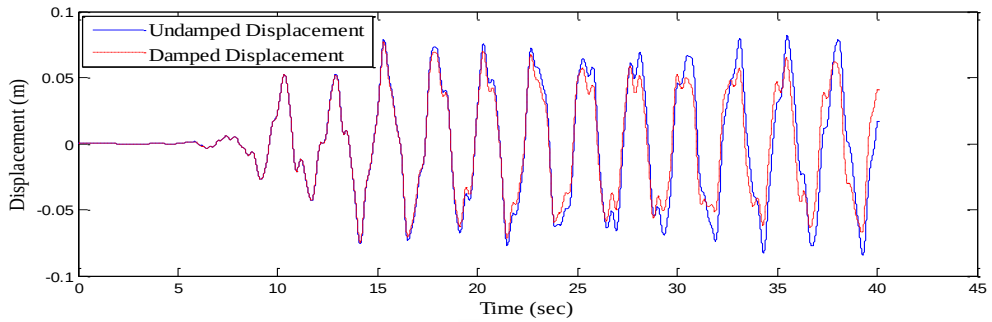

Figure C.36. Response of structure with 50º sloped TLD to Loma Prieta earthquake

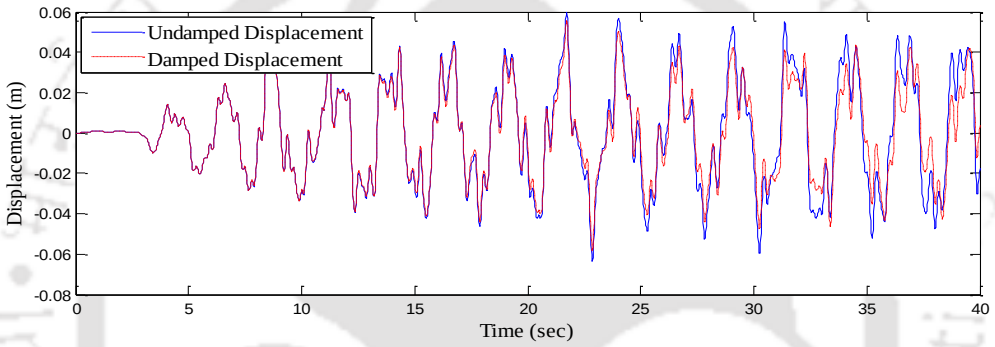

Figure C.37. Response of structure with 15º sloped TLD to Northridge earthquake

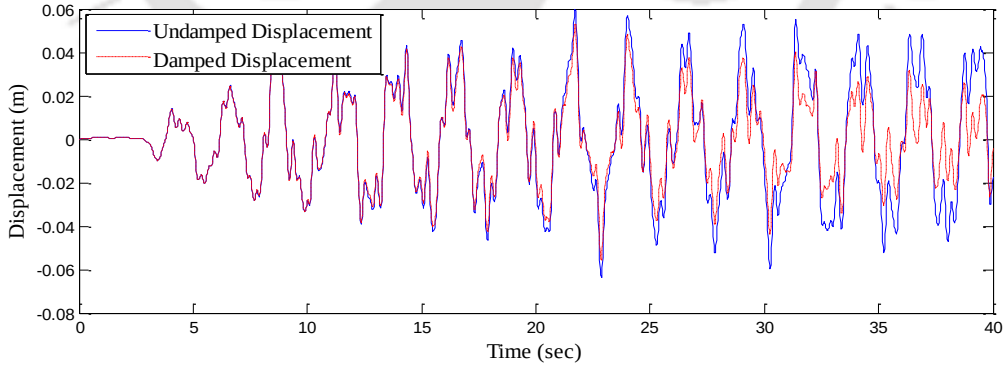

Figure C.38. Response of structure with 30º sloped TLD to Northridge earthquake

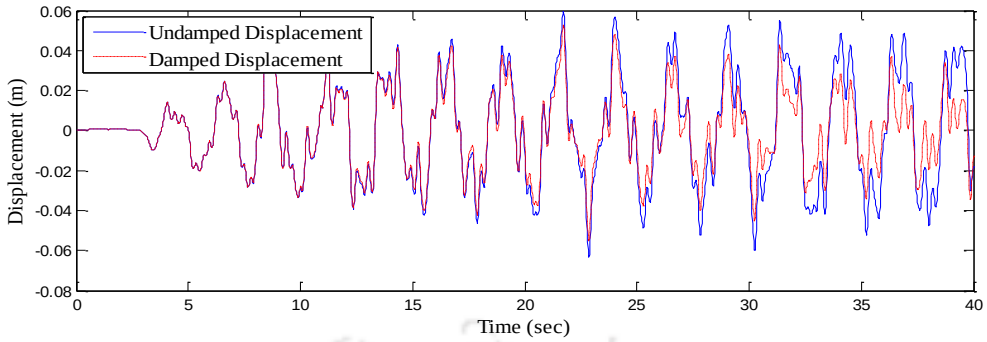

Figure C.39. Response of structure with 35º sloped TLD to Northridge earthquake

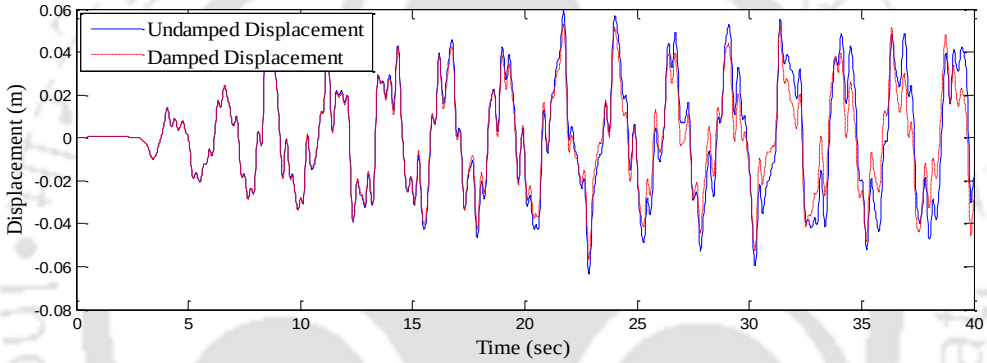

Figure C.40. Response of structure with 50º sloped TLD to Northridge earthquake

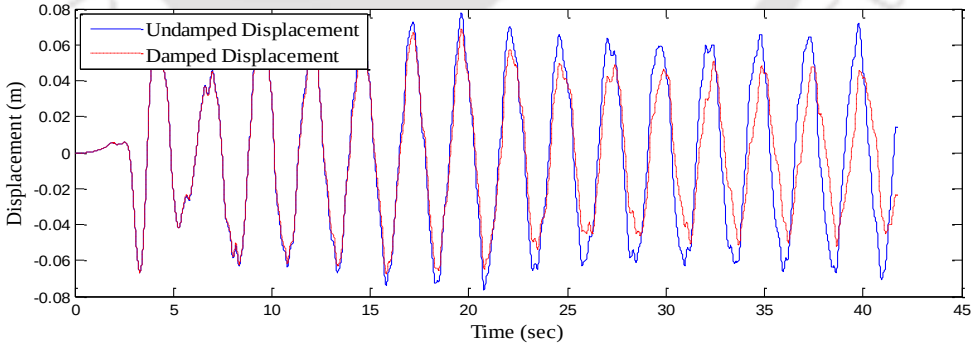

Figure C.41. Response of structure with 15º sloped TLD to San Fernando ground motion

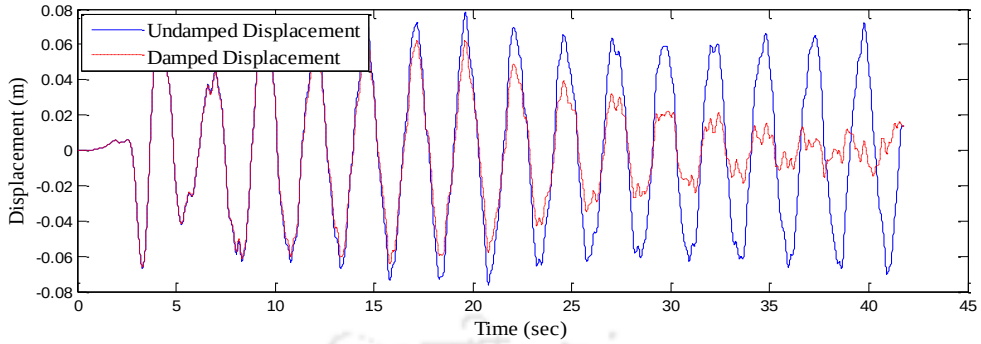

Figure C.42. Response of structure with 30º sloped TLD to San Fernando earthquake

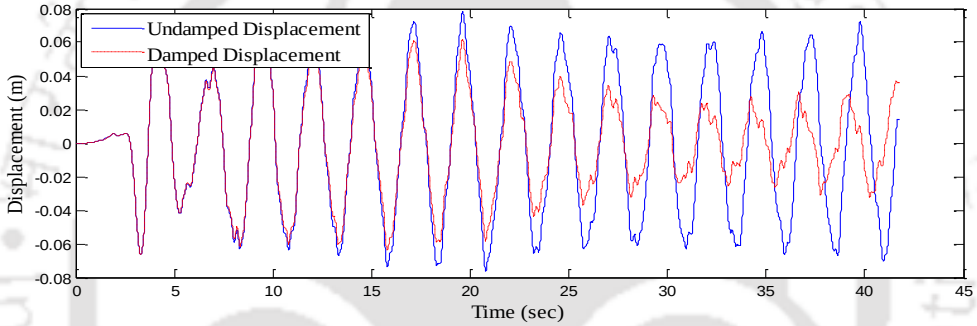

Figure C.43. Response of structure with 35º sloped TLD to San Fernando earthquake

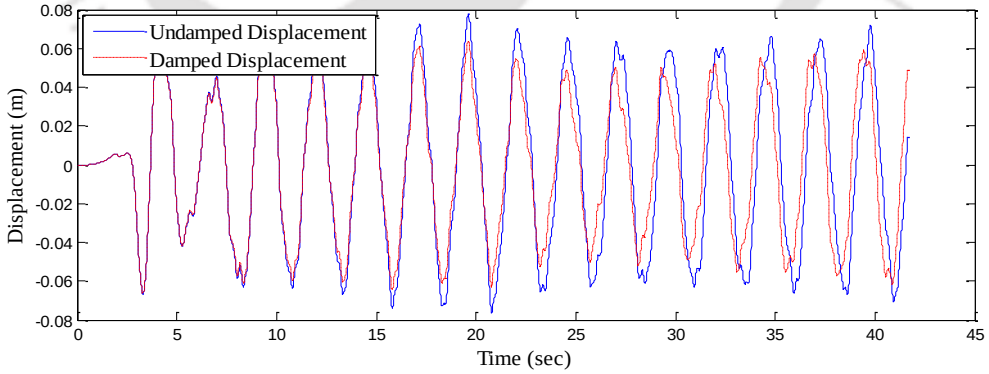

Figure C.44. Response of structure with 50º sloped TLD to San Fernando earthquake

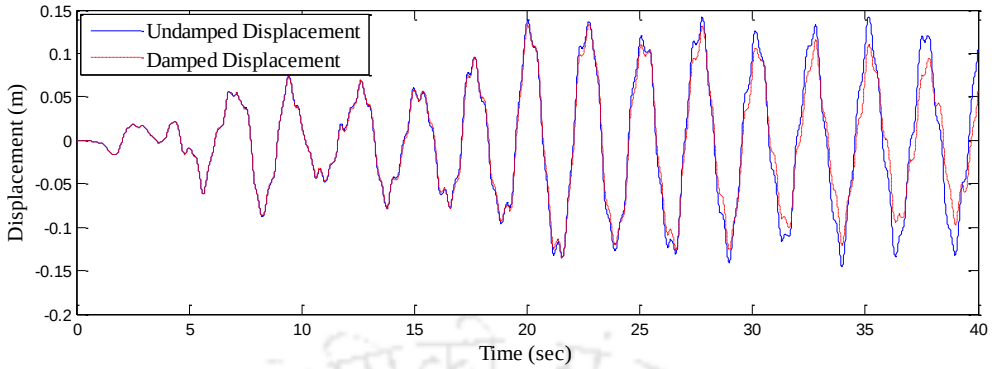

Figure C.45. Response of structure with 15° sloped TLD to IS time history

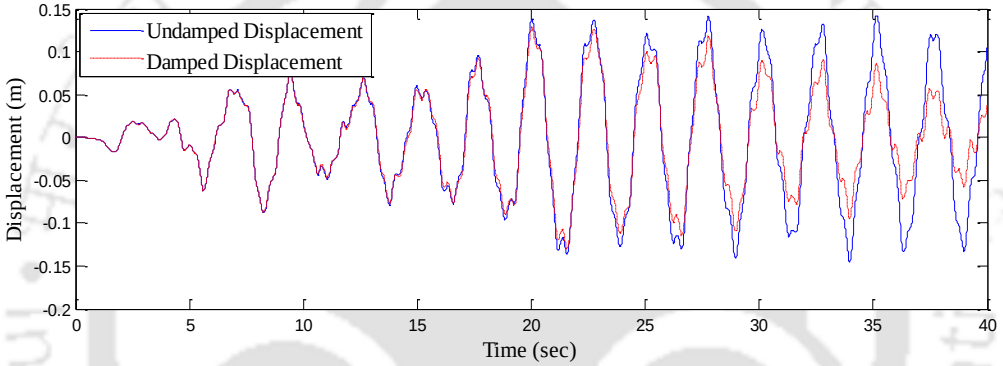

Figure C.46. Response of structure with 30° sloped TLD to IS time history

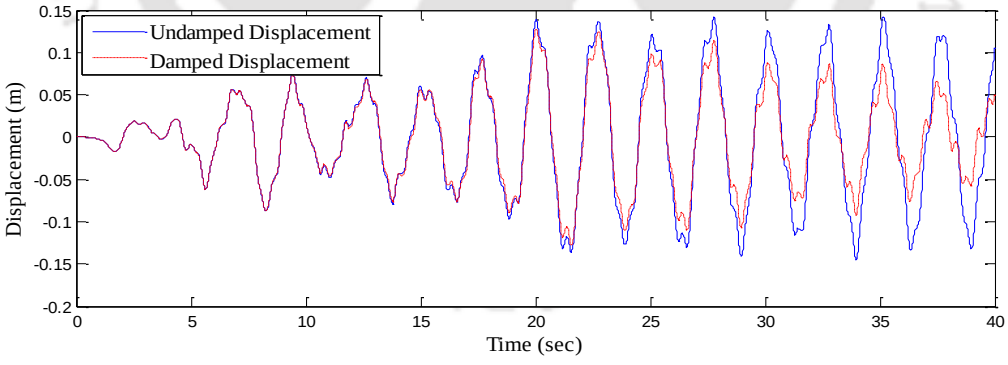

Figure C.47. Response of structure with 35° sloped TLD to IS time history

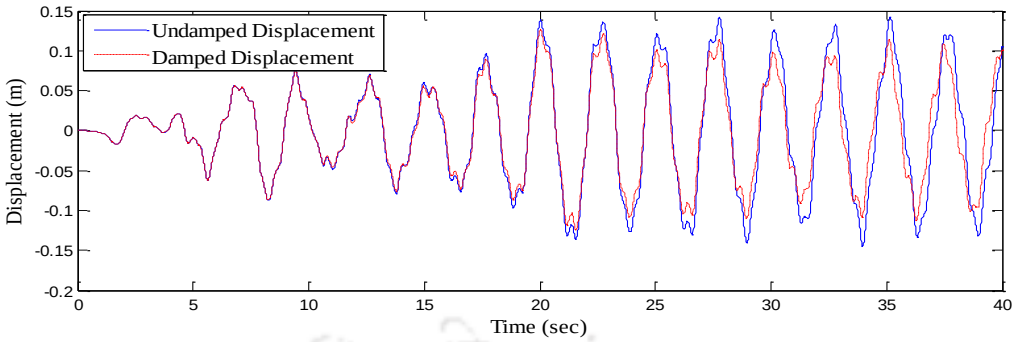

Figure C.48. Response of structure with 50º sloped TLD to IS time history

C.3. CHAPTER 5 SAMPLE FIGURES

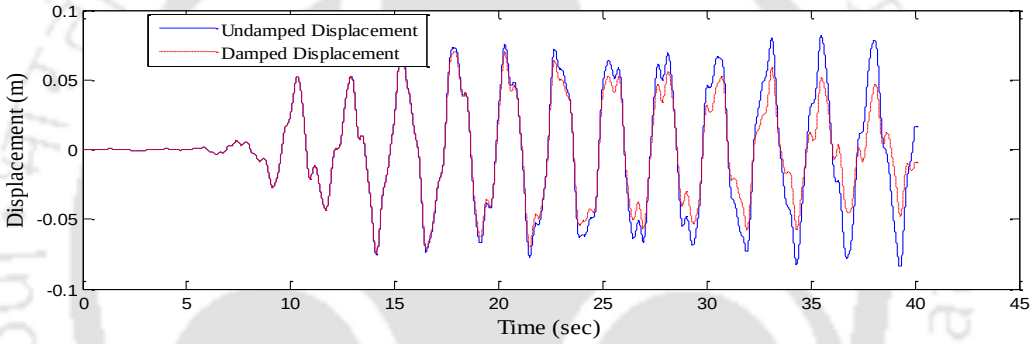

Figure C.49. Response of structure with 20º end slope and 5º central slope TLD subjected to Loma Prieta earthquake

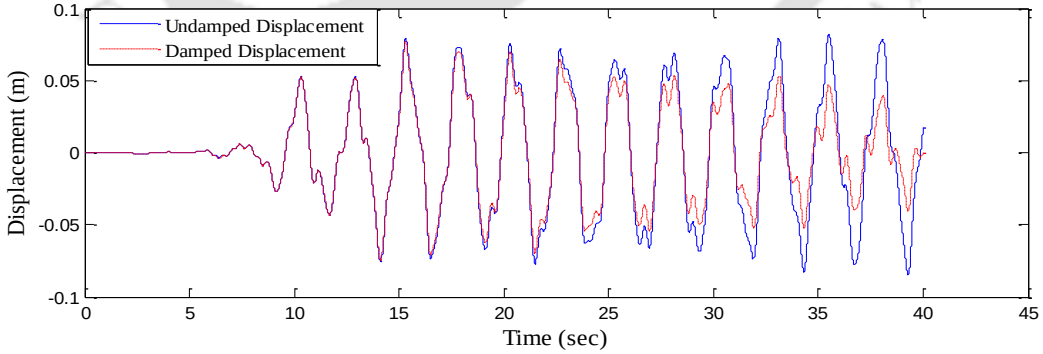

Figure C.50. Response of structure with 25º end slope and 5º central slope TLD subjected to Loma Prieta earthquake

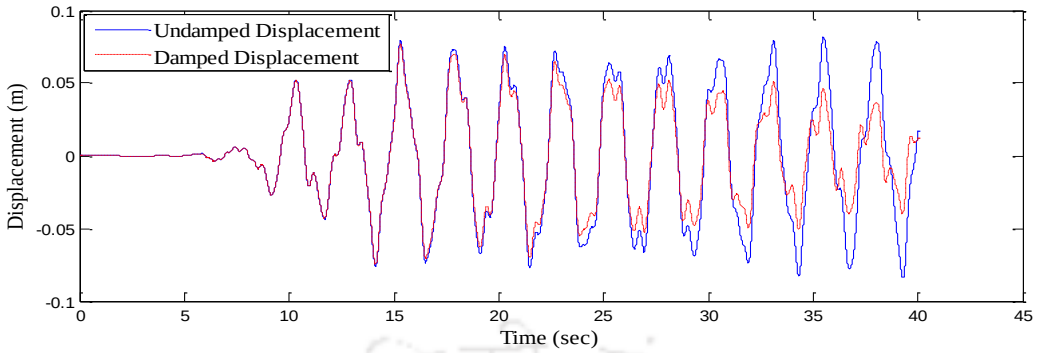

Figure C.51. Response of structure with 30º end slope and 5º central slope TLD subjected to Loma Prieta earthquake

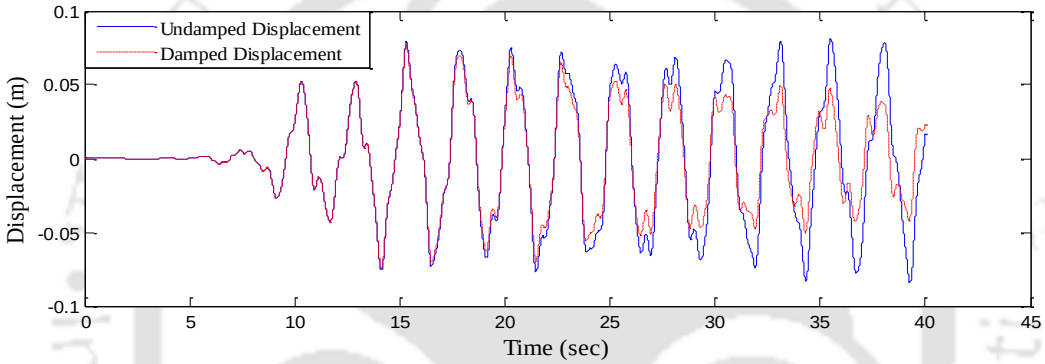

Figure C.52. Response of structure with 35º end slope and 5º central slope TLD subjected to Loma Prieta earthquake

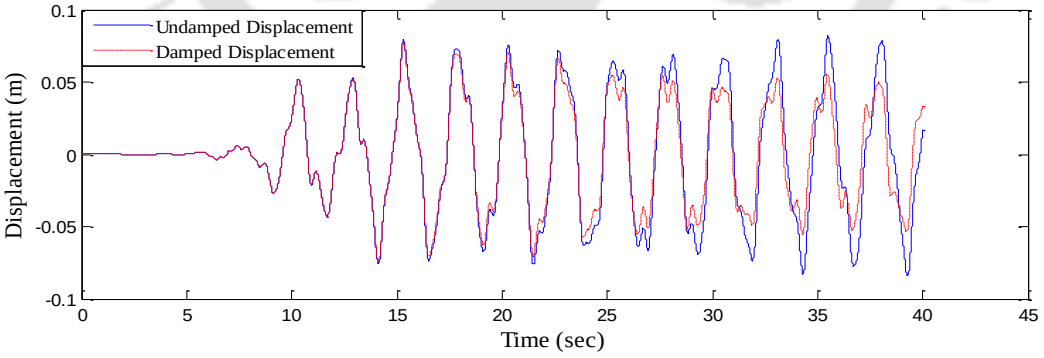

Figure C.53. Response of structure with 40º end slope and 5º central slope TLD subjected to Loma Prieta earthquake

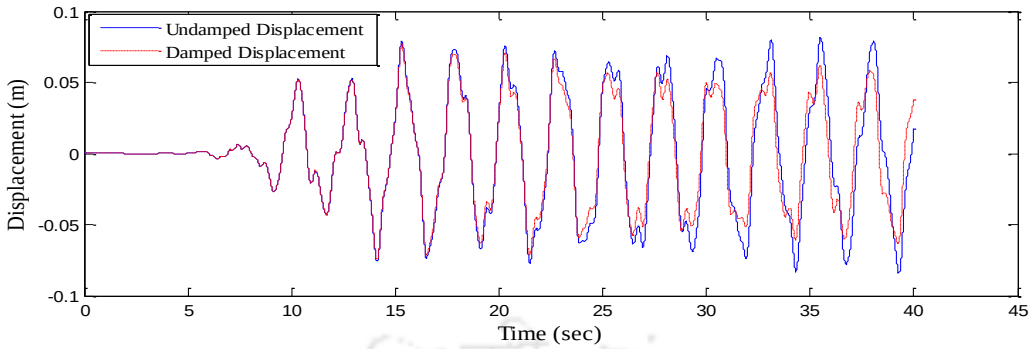

Figure C.54. Response of structure with 45º end slope and 5º central slope TLD subjected to Loma Prieta earthquake

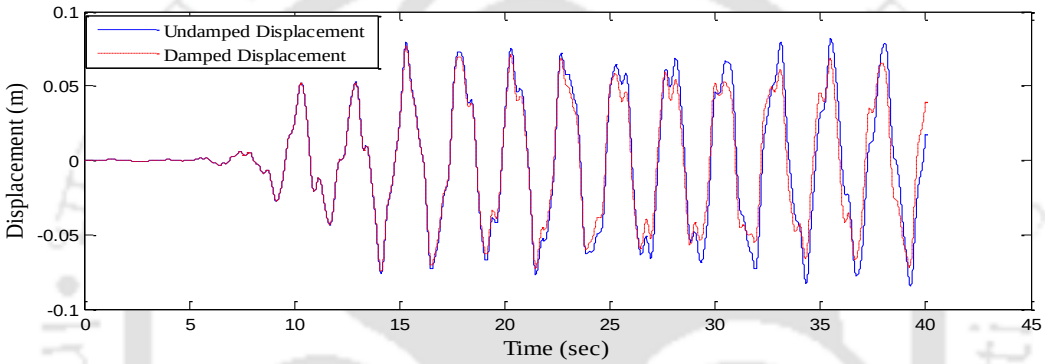

Figure C.55. Response of structure with 50º end slope and 5º central slope TLD subjected to Loma Prieta earthquake

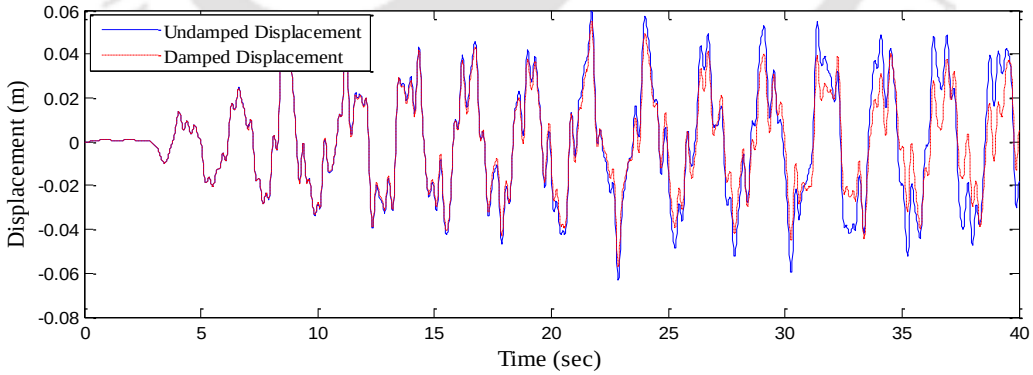

Figure C.56. Response of structure with 20º end slope and 5º central slope TLD subjected to Northridge earthquake

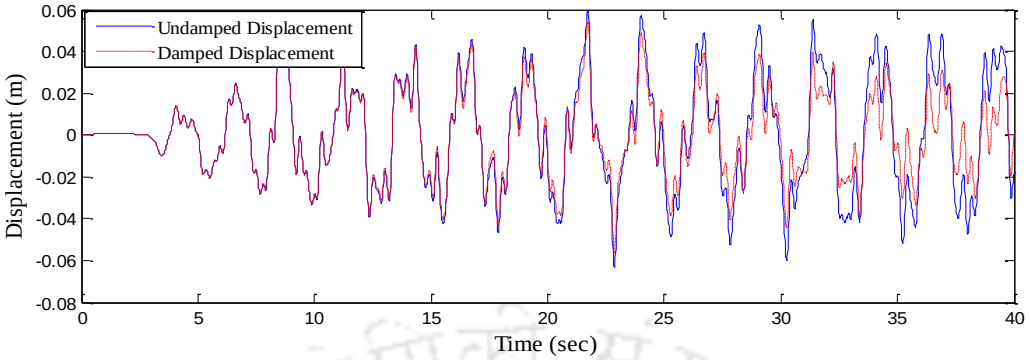

Figure C.57. Response of structure with 25º end slope and 5º central slope TLD subjected to Northridge earthquake

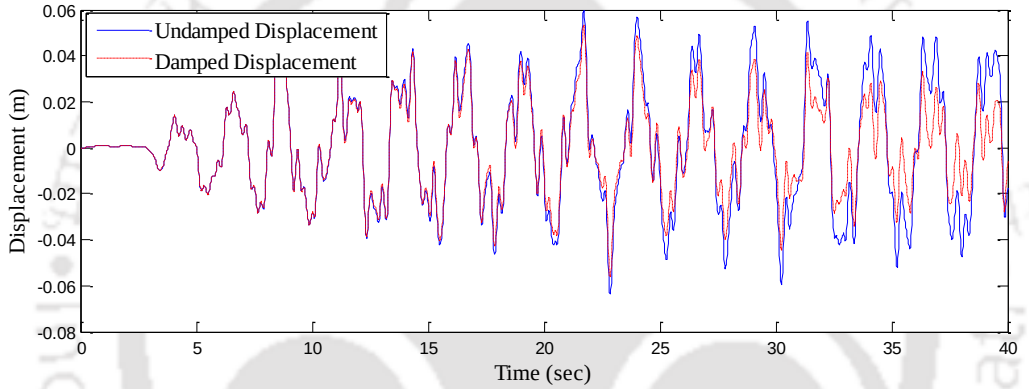

Figure C.58. Response of structure with 30º end slope and 5º central slope TLD subjected to Northridge earthquake

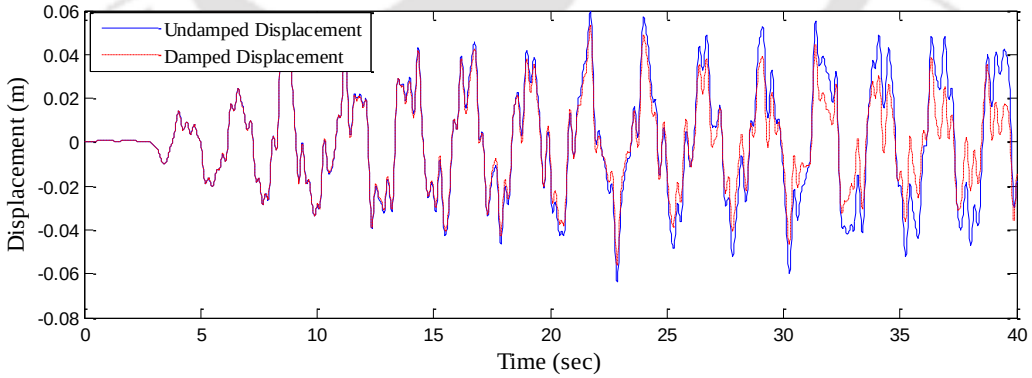

Figure C.59. Response of structure with 35º end slope and 5º central slope TLD subjected to Northridge earthquake

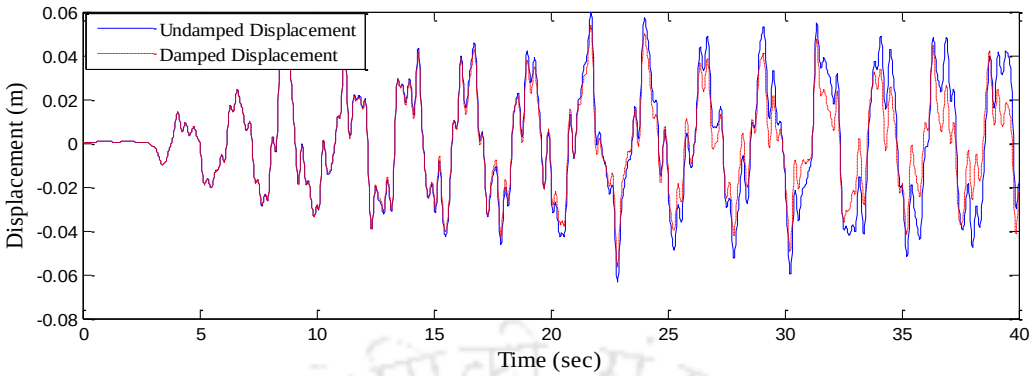

Figure C.60. Response of structure with 40º end slope and 5º central slope TLD subjected to Northridge earthquake

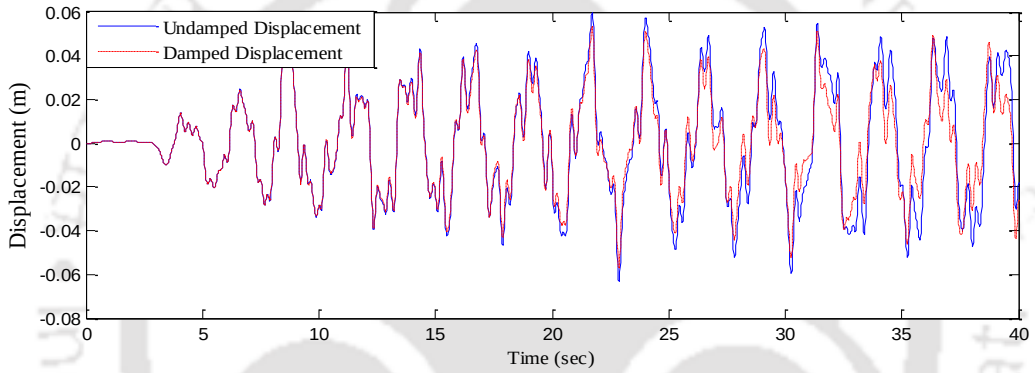

Figure C.61. Response of structure with 45º end slope and 5º central slope TLD subjected to Northridge earthquake

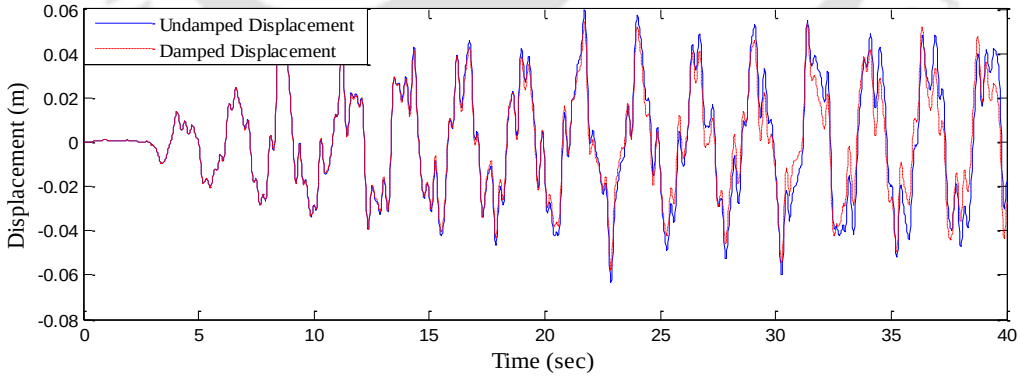

Figure C.62. Response of structure with 50º end slope and 5º central slope TLD subjected to Northridge earthquake

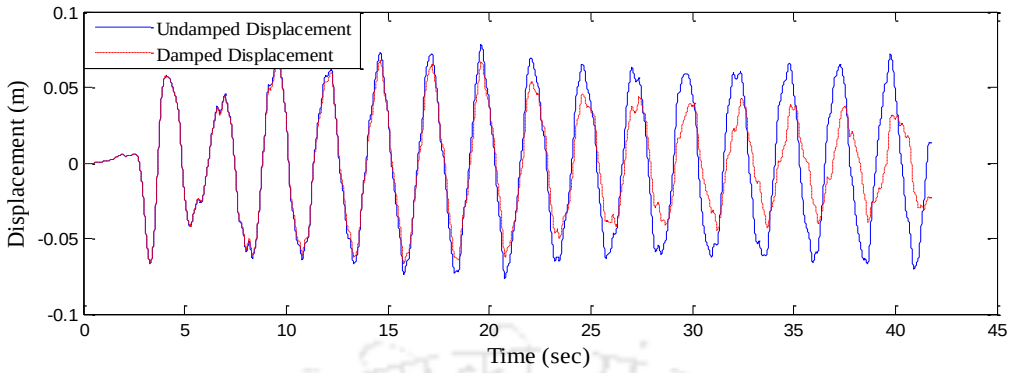

Figure C.63. Response of structure with 20º end slope and 5º central slope TLD subjected to San Fernando earthquake

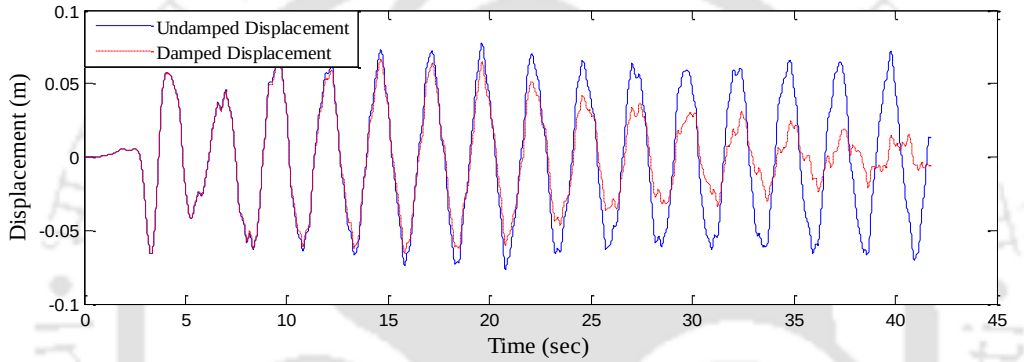

Figure C.64. Response of structure with 25º end slope and 5º central slope TLD subjected to San Fernando earthquake

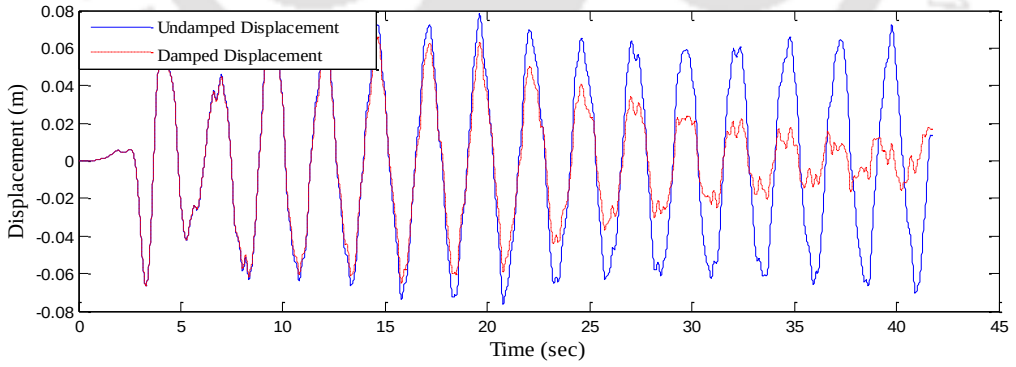

Figure C.65. Response of structure with 30º end slope and 5º central slope TLD subjected to San Fernando earthquake

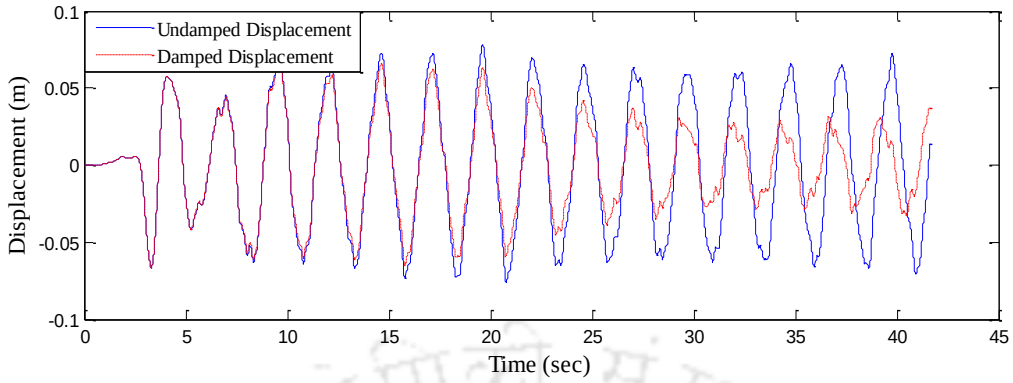

Figure C.66. Response of structure with 35º end slope and 5º central slope TLD subjected to San Fernando earthquake

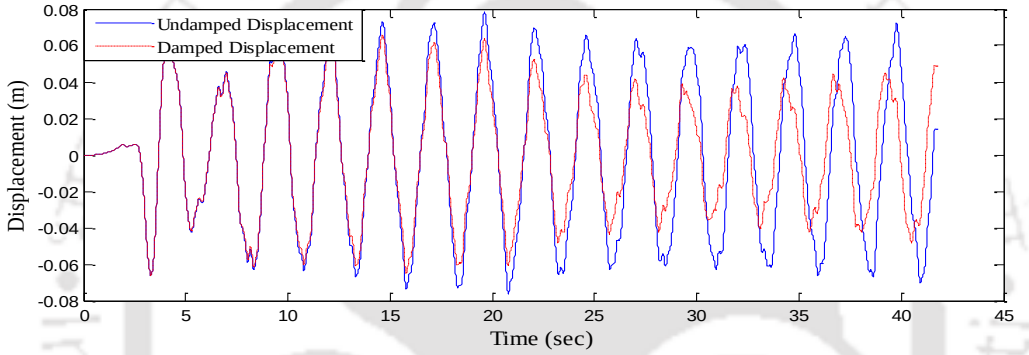

Figure C.67. Response of structure with 40º end slope and 5º central slope TLD subjected to San Fernando earthquake

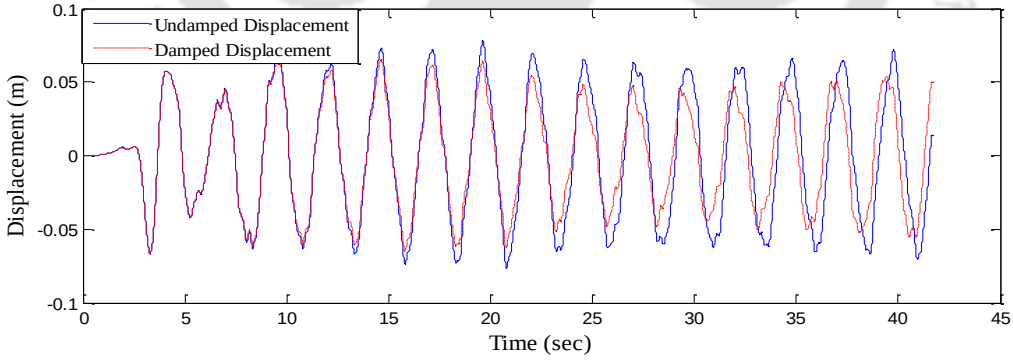

Figure C.68. Response of structure with 45º end slope and 5º central slope TLD subjected to San Fernando earthquake

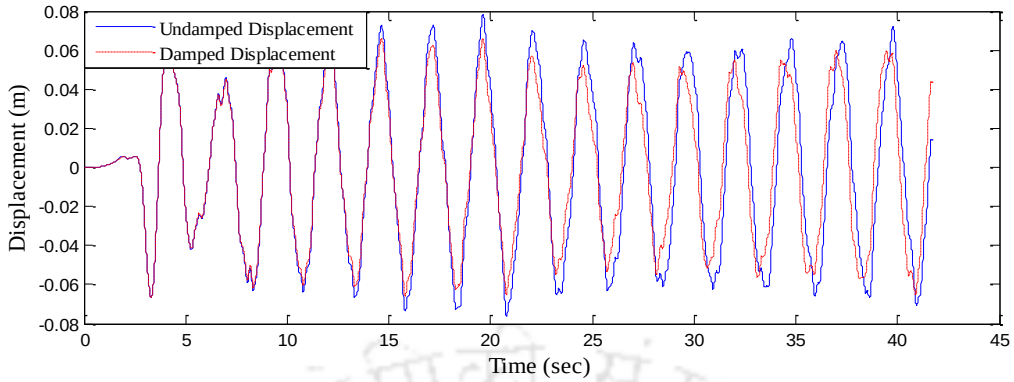

Figure C.69. Response of structure with 50º end slope and 5º central slope TLD subjected to San Fernando earthquake

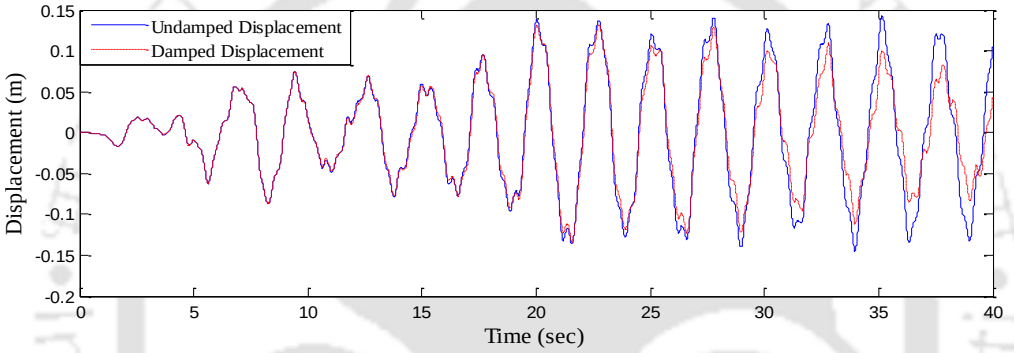

Figure C.70. Response of structure with 20º end slope and 5º central slope TLD subjected to IS compatible time history

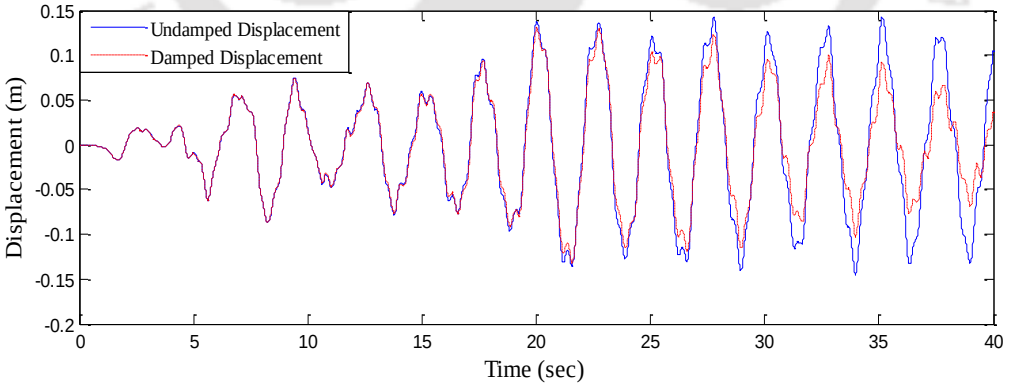

Figure C.71. Response of structure with 25º end slope and 5º central slope TLD subjected to IS compatible time history

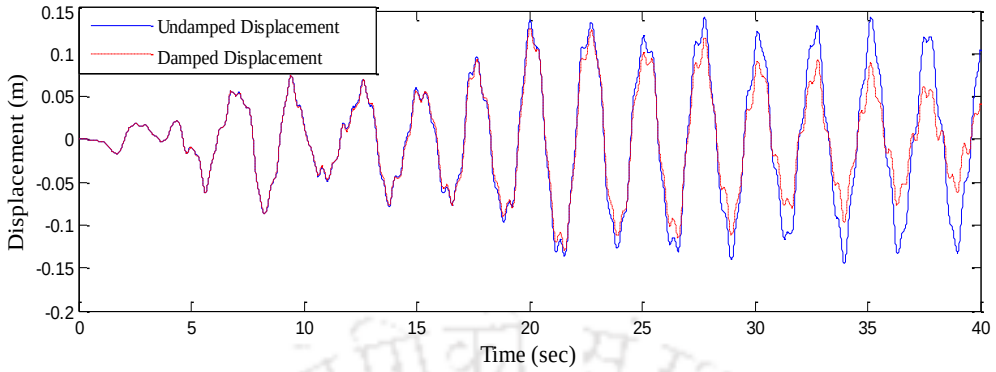

Figure C.72. Response of structure with 30º end slope and 5º central slope TLD subjected to IS compatible time history

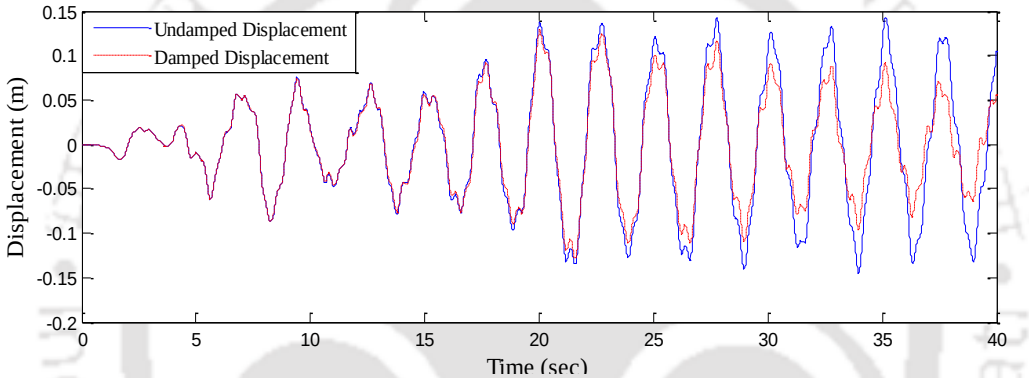

Figure C.73. Response of structure with 35º end slope and 5º central slope TLD subjected to IS compatible time history

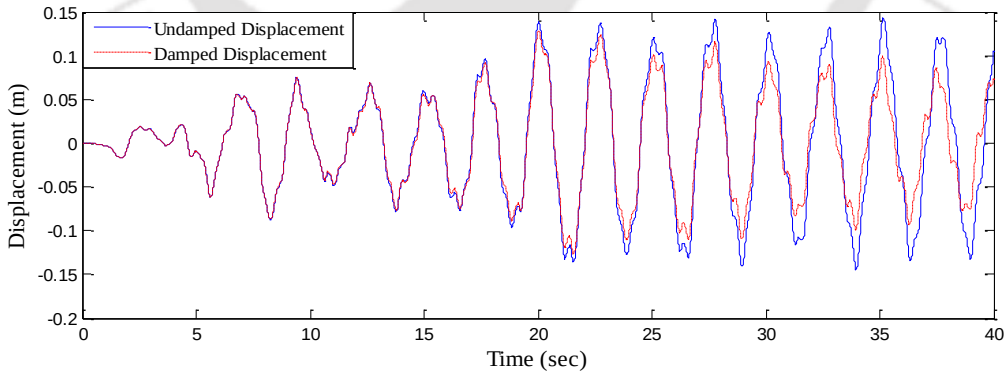

Figure C.74. Response of structure with 40º end slope and 5º central slope TLD subjected to IS compatible time history

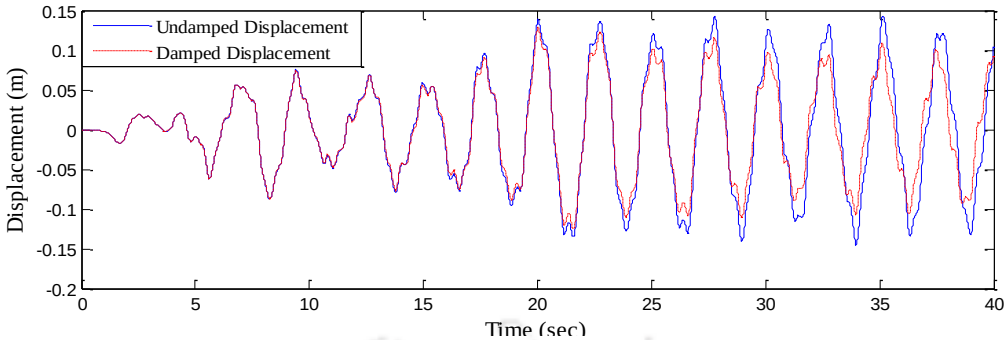

Figure C.75. Response of structure with 45º end slope and 5º central slope TLD subjected to IS compatible time history

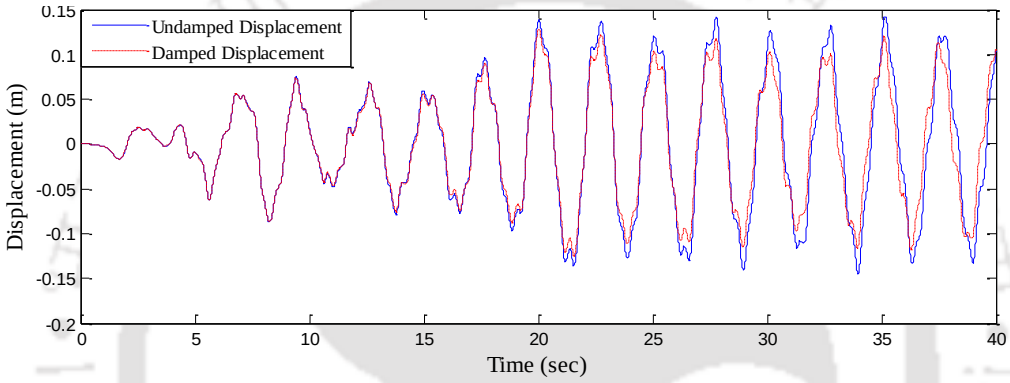

Figure C.76. Response of structure with 50º end slope and 5º central slope TLD subjected to IS compatible time history

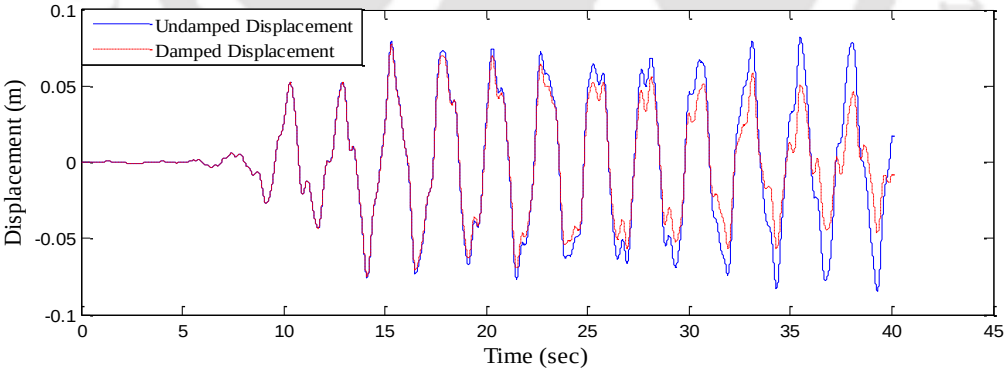

Figure C.77. Response of structure with 20º end slope and 5º dual triangular slope TLD subjected to Loma Prieta earthquake

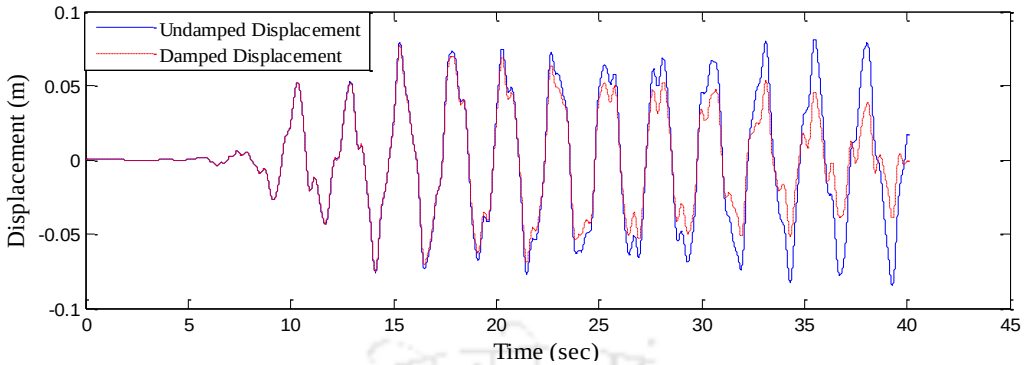

Figure C.78. Response of structure with 25º end slope and 5º dual triangular slope TLD subjected to Loma Prieta earthquake

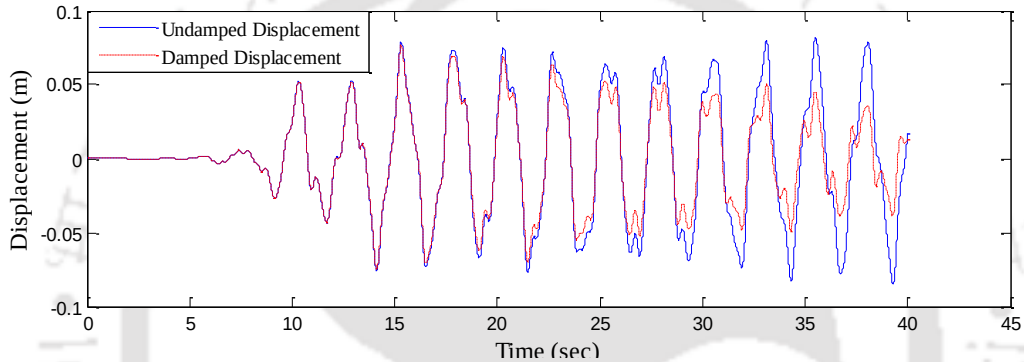

Figure C.79. Response of structure with 30º end slope and 5º dual triangular slope TLD subjected to Loma Prieta earthquake

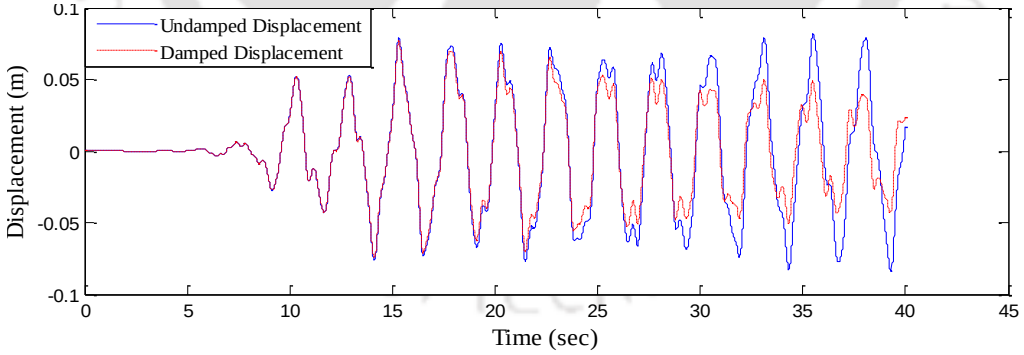

Figure C.80. Response of structure with 35º end slope and 5º dual triangular slope TLD subjected to Loma Prieta earthquake

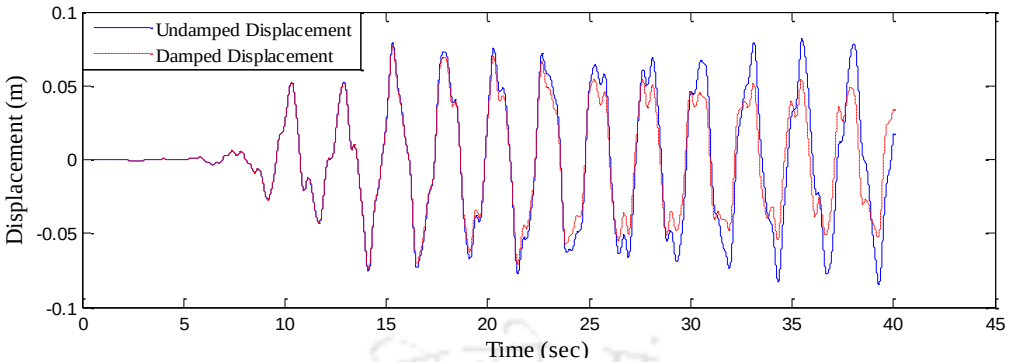

Figure C.81. Response of structure with 40º end slope and 5º dual triangular slope TLD subjected to Loma Prieta earthquake

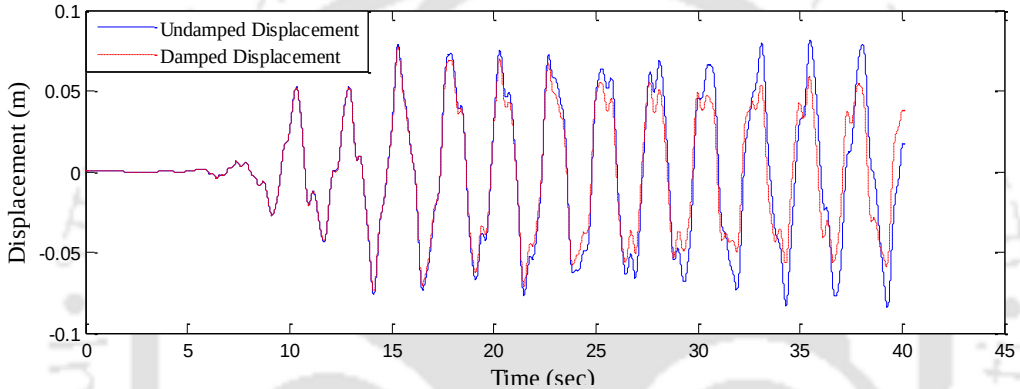

Figure C.82. Response of structure with 45º end slope and 5º dual triangular slope TLD subjected to Loma Prieta earthquake

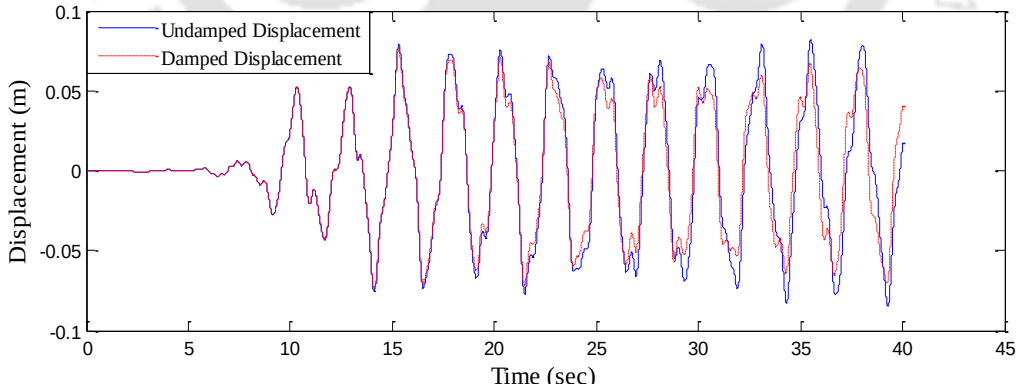

Figure C.83. Response of structure with 50º end slope and 5º dual triangular slope TLD subjected to Loma Prieta earthquake

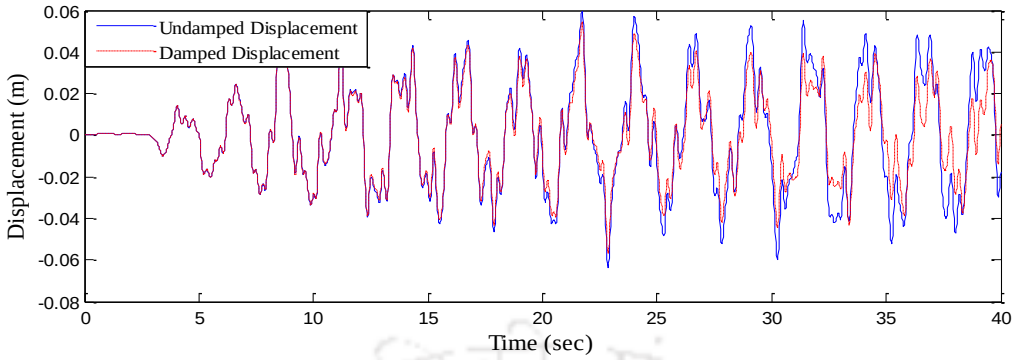

Figure C.84. Response of structure with 20º end slope and 5º dual triangular slope TLD subjected to Northridge earthquake

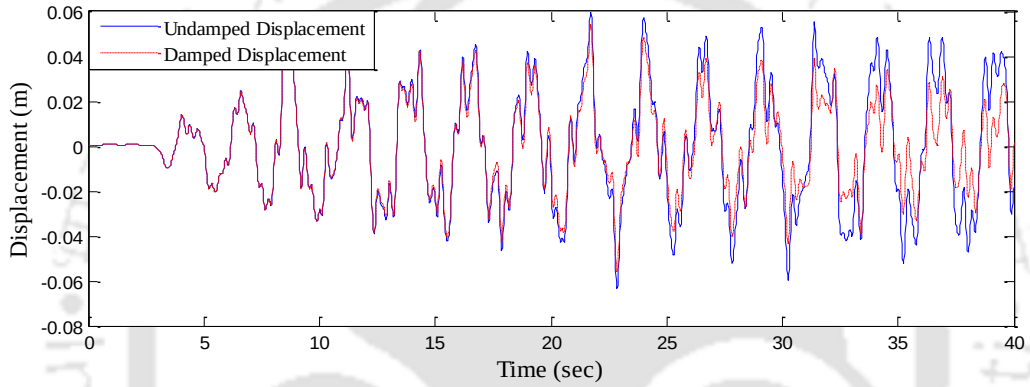

Figure C.85. Response of structure with 25º end slope and 5º dual triangular slope TLD subjected to Northridge earthquake

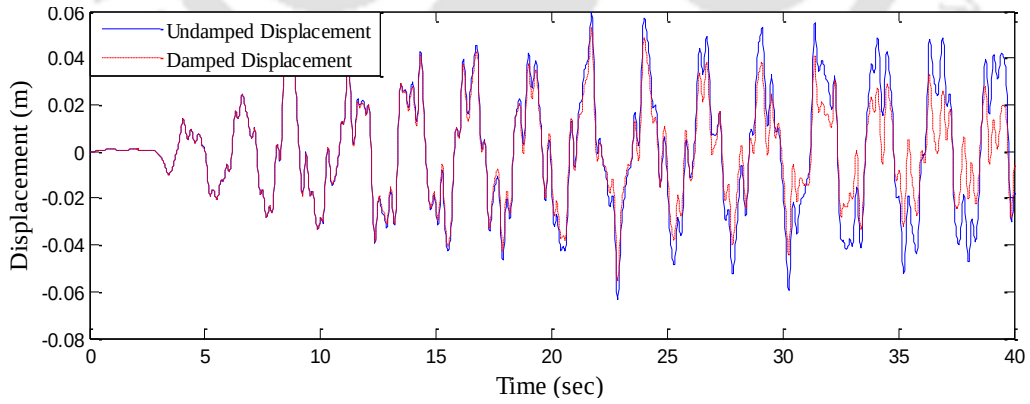

Figure C.86. Response of structure with 30º end slope and 5º dual triangular slope TLD subjected to Northridge earthquake

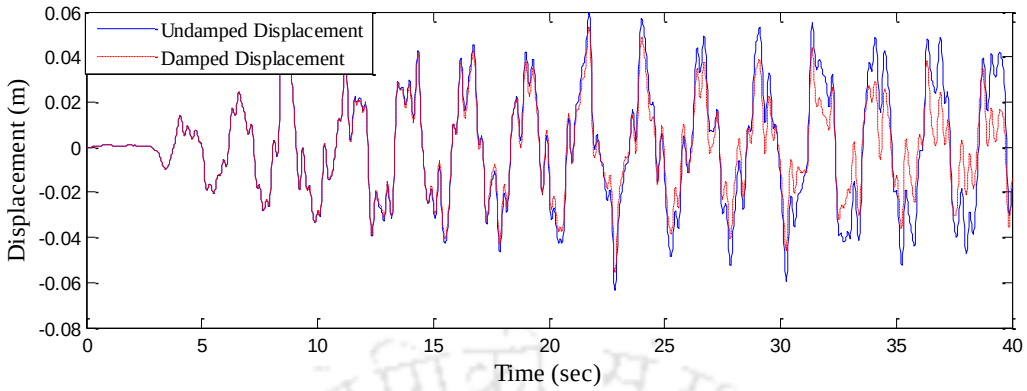

Figure C.87. Response of structure with 35º end slope and 5º dual triangular slope TLD subjected to Northridge earthquake

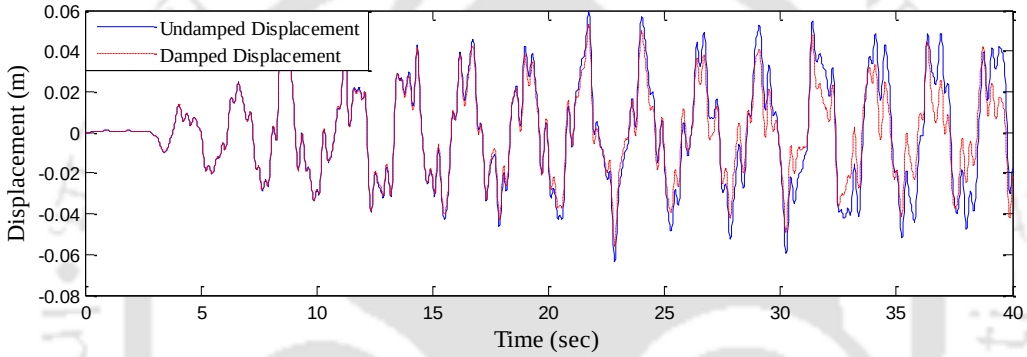

Figure C.88. Response of structure with 40º end slope and 5º dual triangular slope TLD subjected to Northridge earthquake

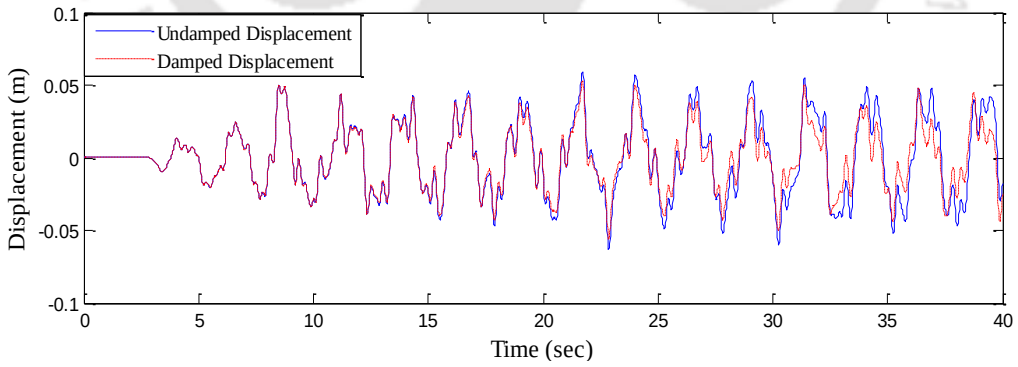

Figure C.89. Response of structure with 45º end slope and 5º dual triangular slope TLD subjected to Northridge earthquake

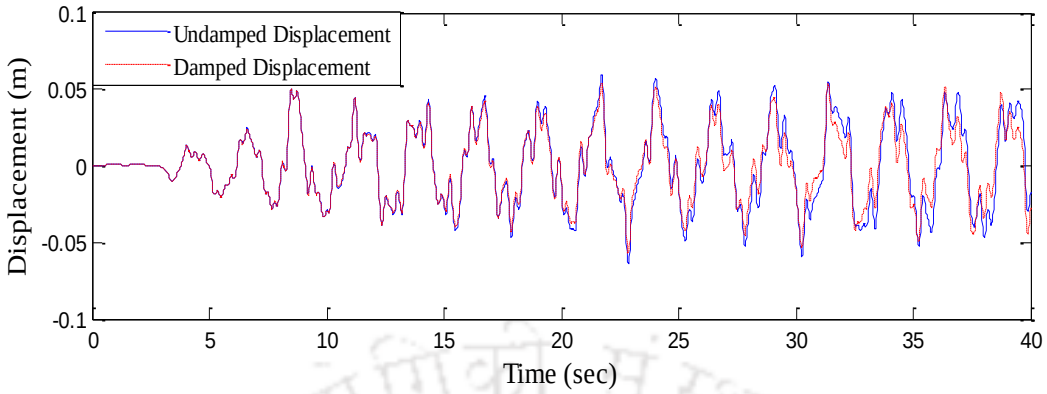

Figure C.90. Response of structure with 50º end slope and 5º dual triangular slope TLD subjected to Northridge earthquake

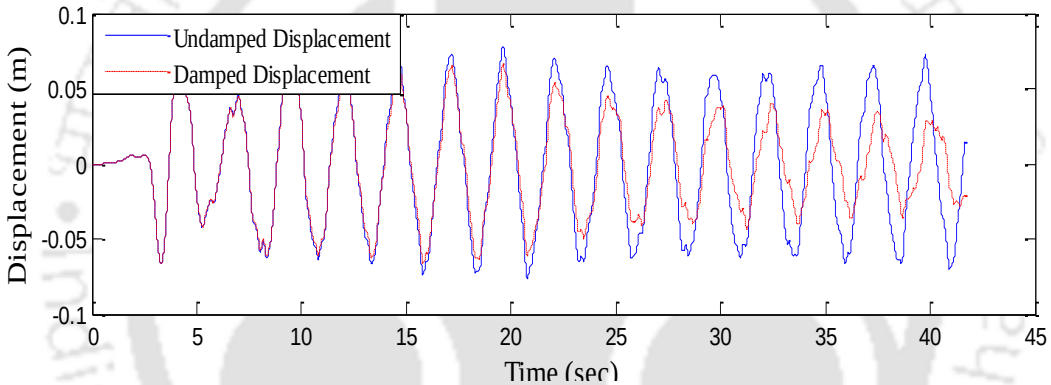

Figure C.91. Response of structure with 20º end slope and 5º dual triangular slope TLD subjected to San Fernando earthquake

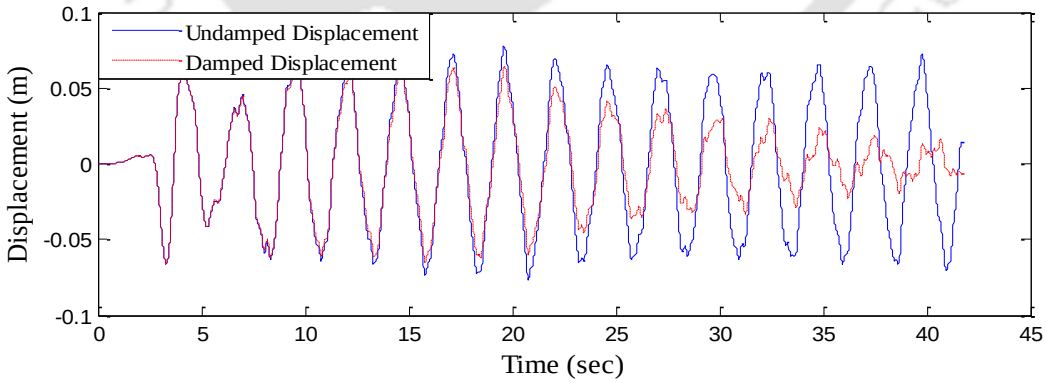

Figure C.92. Response of structure with 25º end slope and 5º dual triangular slope TLD subjected to San Fernando earthquake

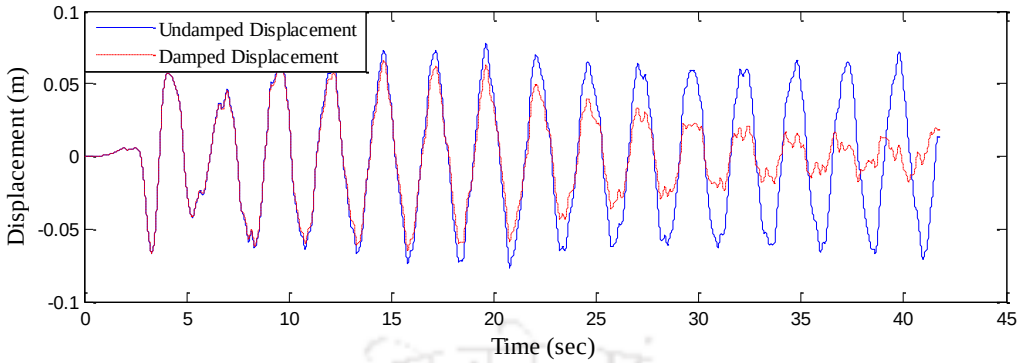

Figure C.93. Response of structure with 30º end slope and 5º dual triangular slope TLD subjected to San Fernando earthquake

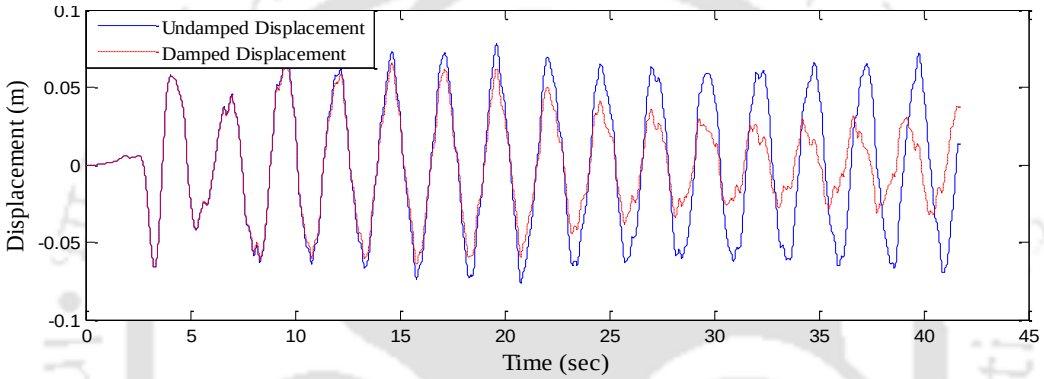

Figure C.94. Response of structure with 35º end slope and 5º dual triangular slope TLD subjected to San Fernando earthquake

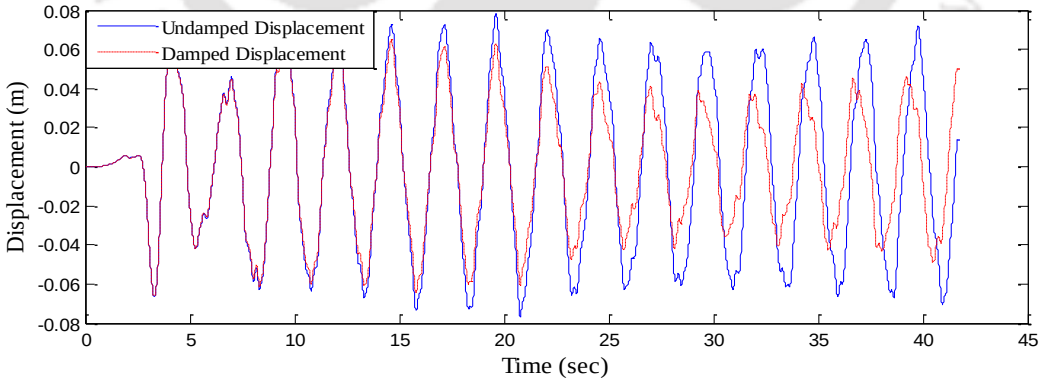

Figure C.95. Response of structure with 40º end slope and 5º dual triangular slope TLD subjected to San Fernando earthquake

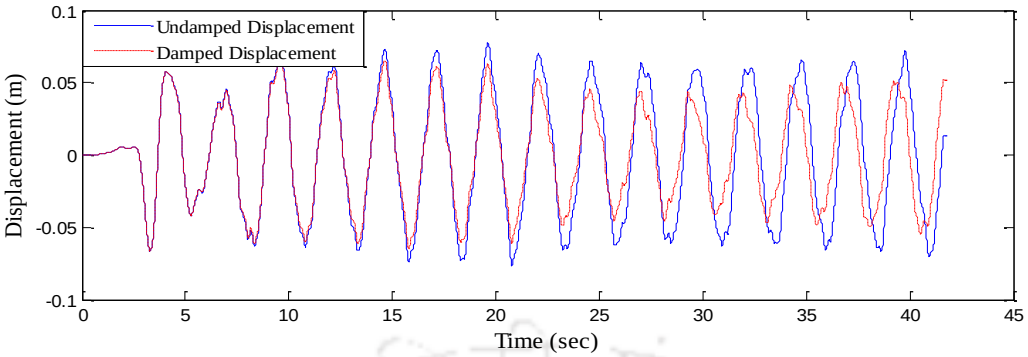

Figure C.96. Response of structure with 45º end slope and 5º dual triangular slope TLD subjected to San Fernando earthquake

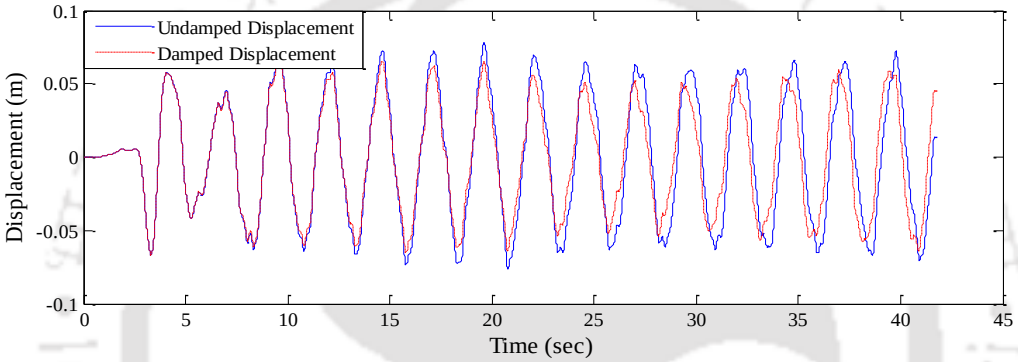

Figure C.97. Response of structure with 50º end slope and 5º dual triangular slope TLD subjected to San Fernando earthquake

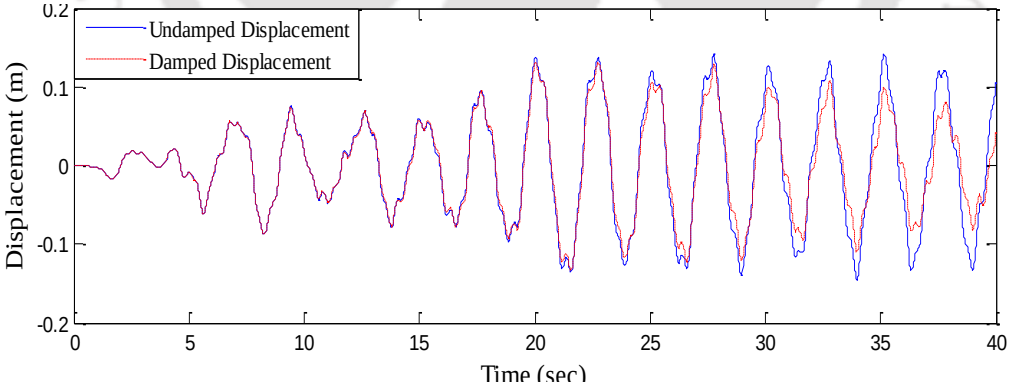

Figure C.98. Response of structure with 20º end slope and 5º dual triangular slope TLD subjected to IS compatible time history

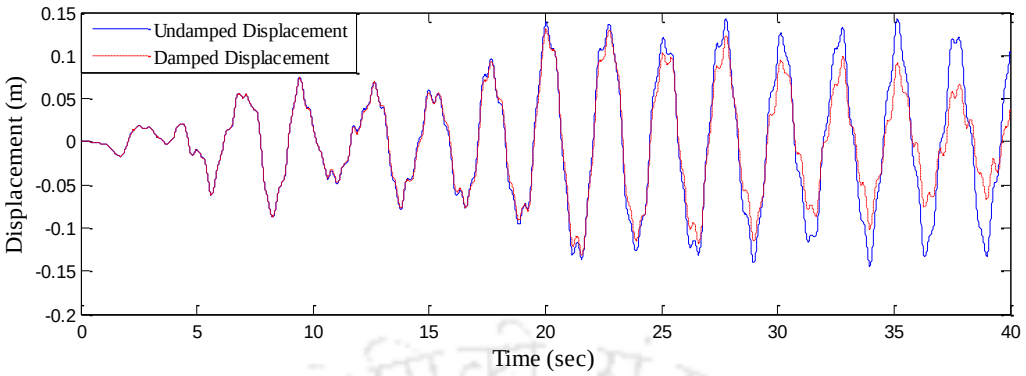

Figure C.99. Response of structure with 25º end slope and 5º dual triangular slope TLD subjected to IS compatible time history

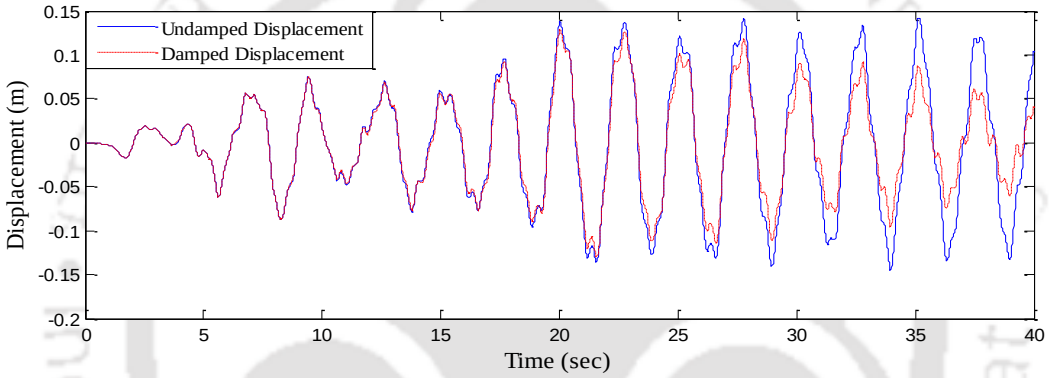

Figure C.100. Response of structure with 30º end slope and 5º dual triangular slope TLD subjected to IS compatible time history

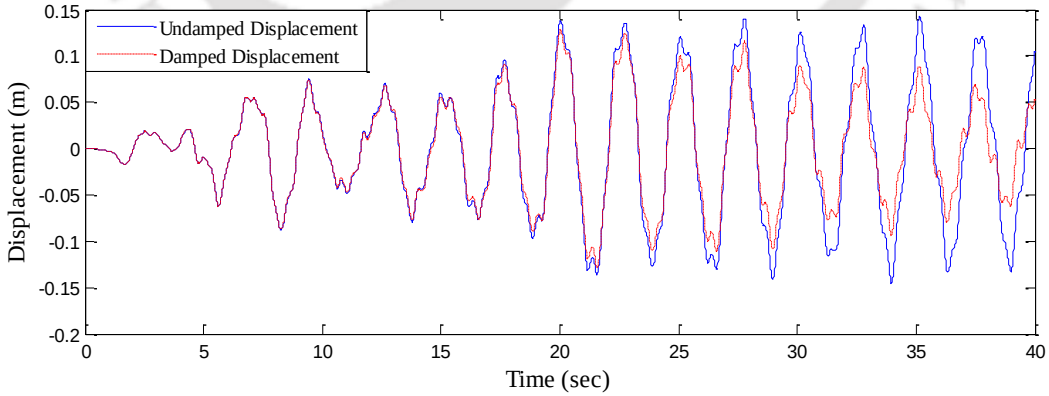

Figure C.101. Response of structure with 35º end slope and 5º dual triangular slope TLD subjected to IS compatible time history

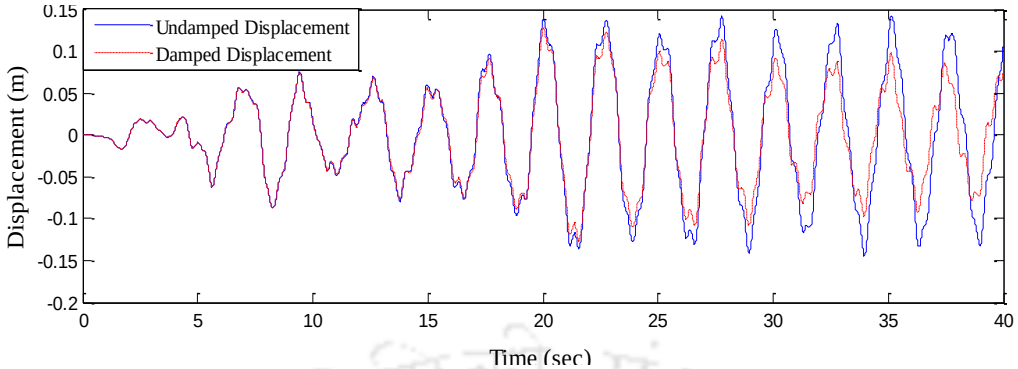

Figure C.102. Response of structure with 40º end slope and 5º dual triangular slope TLD subjected to IS compatible time history

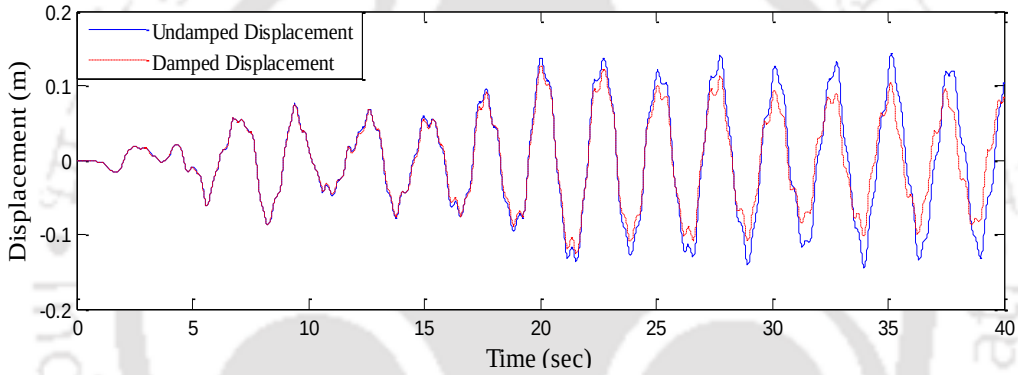

Figure C.103. Response of structure with 45º end slope and 5º dual triangular slope TLD subjected to IS compatible time history

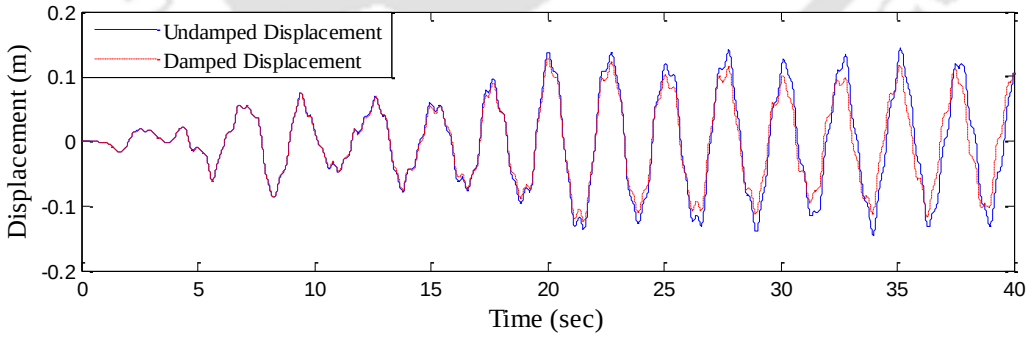

Figure C.104. Response of structure with 50º end slope and 5º dual triangular slope TLD subjected to IS compatible time histor

APPENDIX D

DYNAMIC ANALYSIS USING HARMONIC INPUT

D.1. INTRODUCTION

In this appendix, FE analysis of RC frame with TLD having end slope at the bottom, subjected to harmonic excitation at the base of structure is presented. The analysis is done with converting sloped bottom TLD in to equivalent flat bottom TLD following the approaches *viz.* Gardarsson (2006) and Xin (2001).

D.2. RESPONSE OF STRUCTURE WITH TLD (GARDARSSON'S APPROACH)

The dimensions of equivalent bottom TLD are evaluated from the sloshing frequency of liquid in sloped bottom tank, determined from plot of f/f_b verses the shape factor '*s*' as stated in Section 4.2.1. As there seems to be influence of slope on response, analysis with different slopes is performed with angles 15-50º. The dimensions of equivalent flat bottom tank and corresponding tuning ratios are shown in Table D.1. The results of dynamic analysis are presented in the form of time history of undamped displacement and damped displacement due to application of TLD at roof level of structure (for slope of 15º, 30º and 45º TLDs, see Figure D.1–D.3). From Figure D.4 and Table D.1 it has been seen that the displacement response of structure reduces with increases of end slope angle of TLD of around 30º. The effectiveness of TLD has seen to be reduced for the end slope angle of TLD above 30º. The optimum angle of end slope is observed to be around 30.5º (see Figure D.4).

D.3. RESPONSE STRUCTURE WITH TLD (XIN'S APPROACH)

In this approach the dimensions of equivalent flat bottom TLD are evaluated from the sloshing frequency of liquid in sloped bottom tank, determined from the wetting length (see Section 4.2.2). The dimensions of equivalent flat bottom TLD, tuning ratio and liquid volume reduction are shown in Table D.2. The results of dynamic analysis of structure subjected to harmonic excitation at the base are presented in the form of plots of undamped displacement and damped displacement with application of TLD verse time (for slope of 15º, 30º and 45º TLDs, see Figure D.5–D.7). From Table D.2 and Figure D.8 it can be seen that the displacement reduction of structure increases with the amount of end slope angle of around 30º. The effectiveness of TLD thereafter seen to be reducing for the higher angles of slope. An optimum angle of end slope is observed to be around 29.5º (see Figure D.8).

Table D.1. Effect of slope angle of TLD on response reduction of structure (Gardarsson's approach)

Sr. No.	Slope (º)	Equivalent flat bottom TLD		Displacement reduction (%)		*MR* (%)
		Length (m)	Width (m)	Flat bottom TLD	Sloped bottom TLD	
1	15	2.20	0.40	30.84	03.7	48.49
2	20	1.94	0.55	30.84	14.57	35.69
3	25	1.84	0.67	30.84	32.27	27.86
4	30	1.80	0.74	30.84	36.71	22.50
5	35	1.77	0.76	30.84	34.30	18.55
6	40	1.75	0.82	30.84	33.47	15.47
7	45	1.74	0.85	30.84	31.81	12.98
8	50	1.73	0.88	30.84	30.90	10.90

Table D.2. Effect of slope angle of TLD on response reduction of structure (Xin's approach)

Sr. No.	Slope (º)	Equivalent flat bottom TLD		Displacement reduction (%)		*MR* (%)
		Length (m)	Width (m)	Flat bottom TLD	Slope bottom TLD	
1	15	1.78	0.51	30.84	17.32	48.46
2	20	1.79	0.61	30.84	31.35	35.69
3	25	1.81	0.65	30.84	33.74	27.86
4	30	1.83	0.72	30.84	35.28	22.45
5	35	1.86	0.75	30.84	33.89	18.55
6	40	1.88	0.77	30.84	31.05	15.48
7	45	1.90	0.78	30.84	27.28	12.98
8	50	1.92	0.79	30.84	23.31	10.90

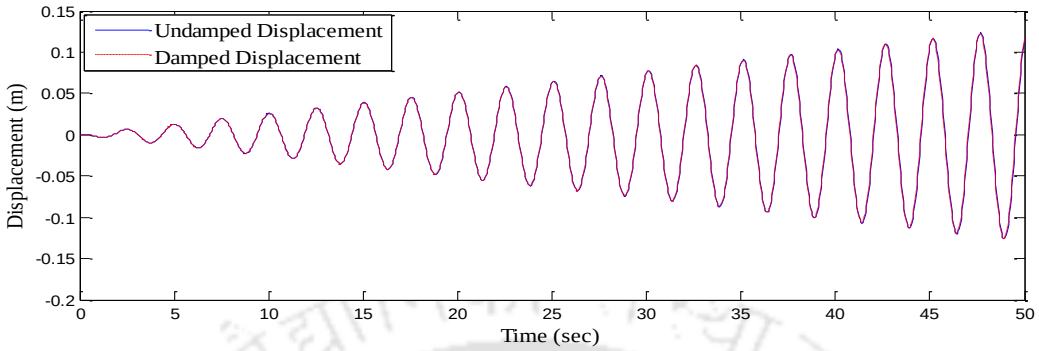

Figure D.1. Response of structure with 15º sloped TLD subjected to harmonic motion

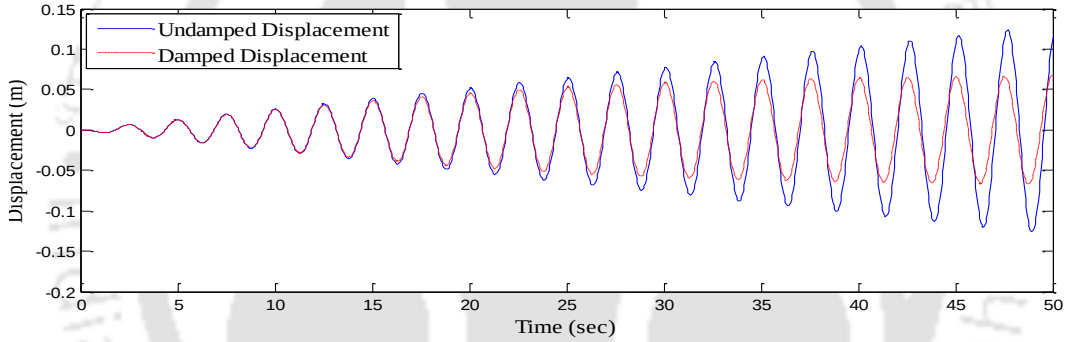

Figure D.2. Response of structure with 30 º sloped TLD subjected to harmonic motion

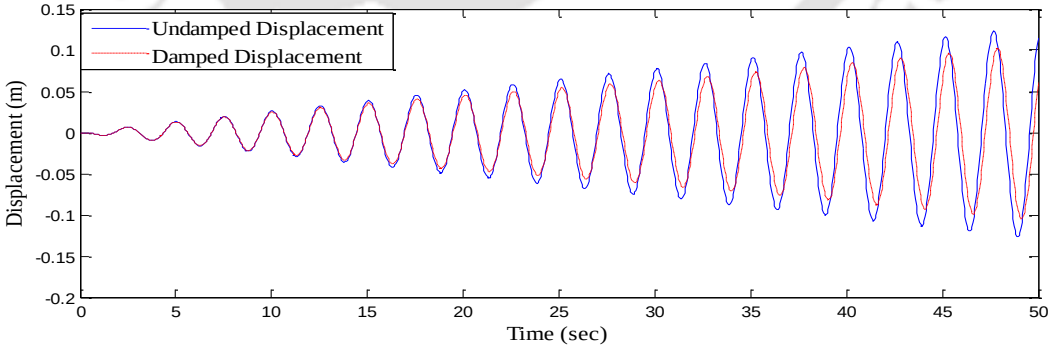

Figure D.3. Response of structure with 45º sloped TLD subjected to harmonic motion

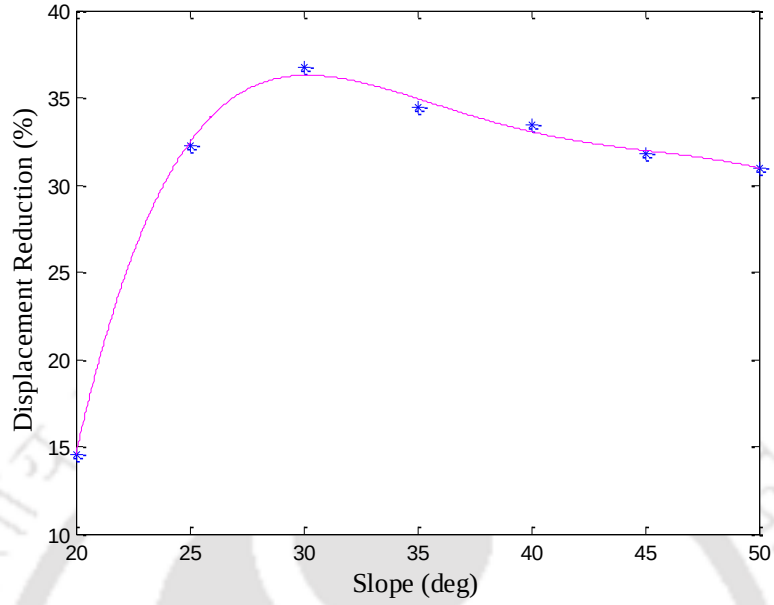

Figure D.4. Variation of reduction in displacement of structure with slope of TLD (Gardarsson's approach)

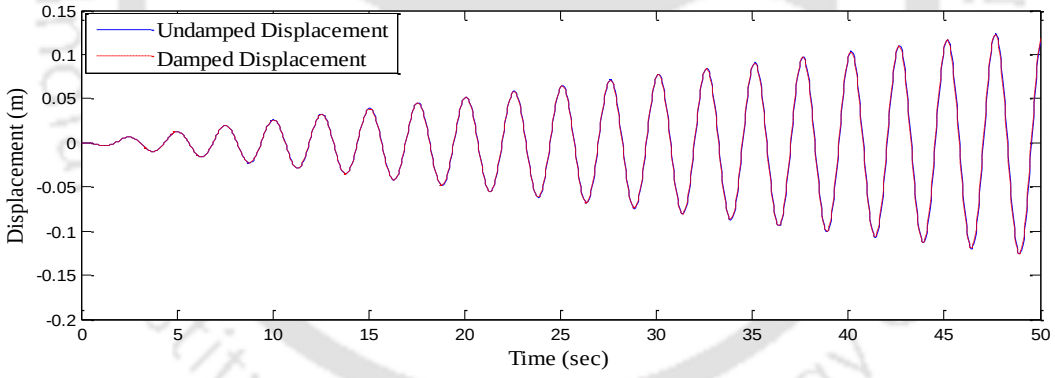

Figure D.5. Response of structure with 15º sloped TLD subjected to harmonic motion

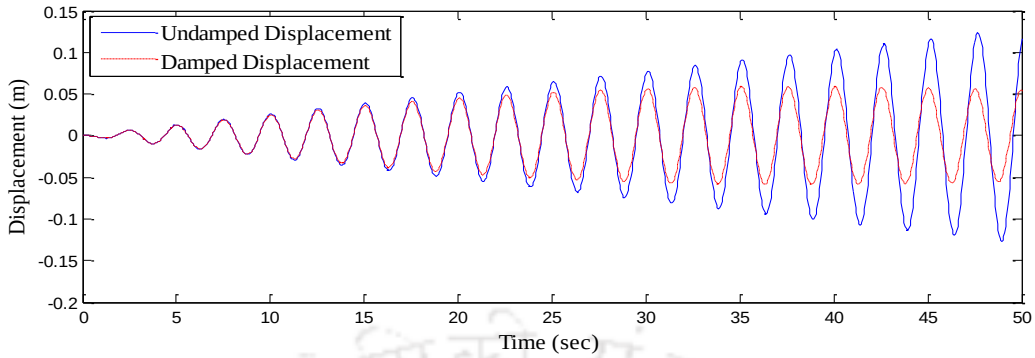

Figure D.6. Response of structure with 30º sloped TLD subjected to harmonic motion

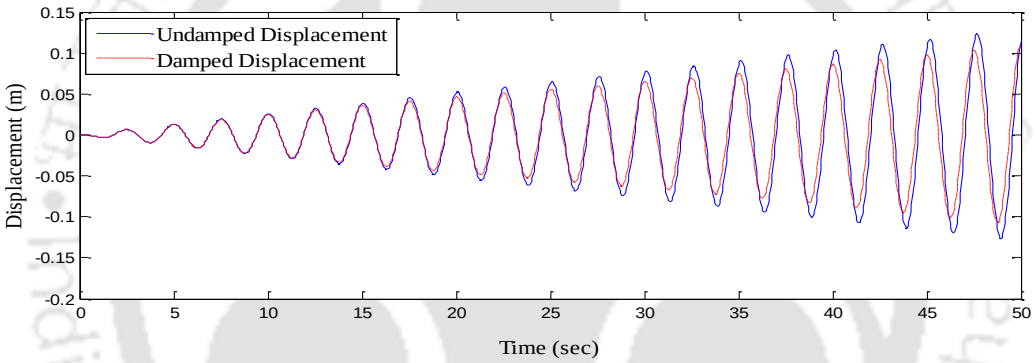

Figure D.7. Response of structure with 45º sloped TLD subjected to harmonic motion

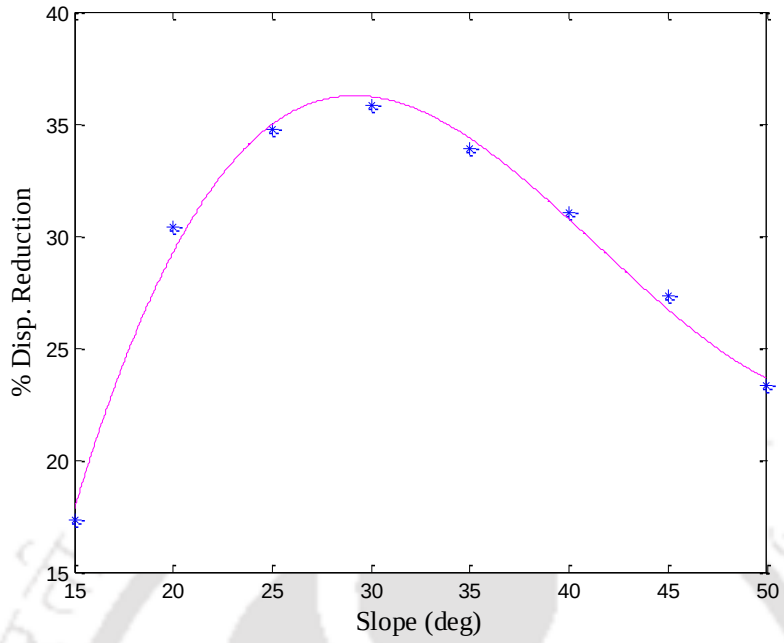

Figure D.8.Variation of reduction in displacement of structure with slope of TLD (Xin's approach)

APPENDIX E

FORMULATION OF TLD EQUATIONS

The rectangular TLD has a length *2a* or *L* and width *b* or *B* and still liquid depth *h* or *H*. It is subjected to lateral base excitation, x_s, identical to structure's excitation at top. The equation of motion of liquid in TLD can be defined in terms of surface motion. Strong earthquake ground motion generally results in large amplitude TLD excitation and wave breaking effect should be included. The formulation suggested by Sul et. al (1992) is given as

$$\frac{\partial \eta}{\partial t} + h\sigma \frac{\partial (\phi u)}{\partial x} = 0 \qquad \text{(E.1)}$$

$$\frac{\partial \eta}{\partial t} + (1 - T_H^2)u\frac{\partial u}{\partial x} + C_{fr}^2 gh\sigma\phi \frac{\partial^2 \eta}{\partial x^2}\frac{\partial \eta}{\partial x} = -C_{da}\lambda u - \ddot{x}_s \qquad \text{(E.2)}$$

where the dependent variables are *η(x, t)* and *u(x, η, t)*. They indicate the free elevation above still liquid level and horizontal free surface liquid particle velocity respectively. The horizontal acceleration of TLD base, which is identical to structure's acceleration at top, is $\ddot{x}_s$ and g is gravitational acceleration.

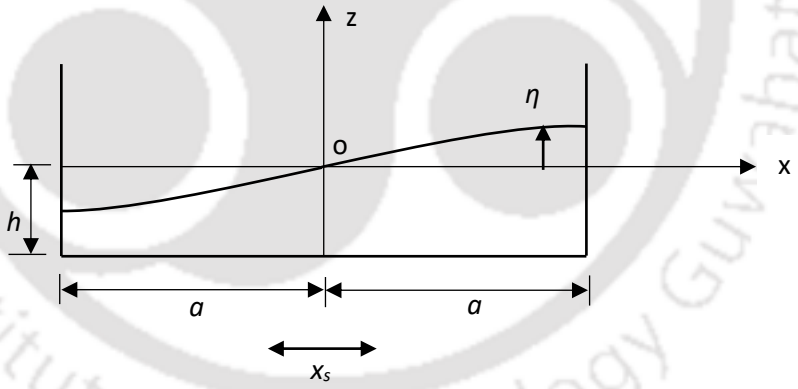

Equation (E.1) represents is the integrated form of continuity equation of liquid and equation (E.2) is derived from two-dimensional Navier-Stocks equation. The parameters in equation (E.1) are given as

$$\sigma = \tanh kh/kh \quad \phi = \tanh k(h + \eta)/\tanh kh \quad T_H = \tanh k(h + \eta) \qquad \text{(E.3)}$$

Where k is the wave number. The λ in equation (4) is damping parameter which accounts for effect of boundary layer and can be given semi-analytically as

$$\lambda = \frac{1}{(\eta+h)}\frac{1}{\sqrt{2}}\sqrt{\omega_l \nu}\left[1 + \left(\frac{2h}{b}\right) + s\right] \quad \text{(E.4)}$$

in which ω_l is the fundamental linear sloshing frequency of liquid in tank, ν is kinematic viscosity and s is surface contamination factor and can be taken as unity. The fundamental sloshing frequency is given as

$$\omega_l = \sqrt{\frac{\Pi g}{2a}}\tanh(\Pi \Delta) \quad \text{(E.5)}$$

where Δ is the ratio of *h to 2a* called depth ratio.

The coefficients C_{fr} and C_{da} in equation (4) are included to modify the liquid wave velocity and damping respectively when waves are unstable (η > h) and break. Values of these coefficients are taken as unity when wave do not break. C_{fr} is found empirically as 1.05 (Sun 1992) and C_{da} has a value dependent on amplitude $(x_s)_{max}$ of motion of structure top and is given as

$$C_{da} = 0.57\sqrt{\frac{h^2\omega_l}{av}}(x_s)_{max} \quad \text{(E.6)}$$

By solving equations (E.1) and (E.2) simultaneously for η_n and neglecting higher order terms and shear stresses along the bottom of tank, a reasonable estimation og shear force F at the base of TLD is given by following equation:

$$F = \frac{\rho g b}{2}[(\eta_n + h)^2 - (\eta_0 + h)^2] \quad \text{(E.7)}$$

where ρ is mass density of liquid b is width of tank and η_n and η_o are free surface elevations at right and lift walls respectively of the TLD.

APPENDIX F

LIST OF ABBREVIATIONS

2D	Two dimensional
BEM	Boundary element method
DL	Dead load
DR	Displacement reduction
DVTLD	Density variable tuned liquid damper
FE	Finite elements
IRIS	Incorporated Research Institutions for Seismology
IS	Indian standard
LL	Live load
MDOF	Multi degree of freedom
MR	Mass reduction
MTLD	Multiple/Modified tuned liquid dampers
NSD	Non-linear stiffness damping
PGA	Peak ground acceleration
RC	Reinforced concrete
RHSTTM	Real time hybrid sloshing table testing method
RMS	Root mean square
RTHS	Real time hybrid system
SDOF	Single degree of freedom system
SPH	Smoothened particle hydrodynamics

TLD	Tuned liquid damper
TLD-FR	Tuned liquid damper floating roof
TMD	Tuned mass damper
TR	Tuning ratio

LIST OF PUBLICATIONS

- Patil, G. R., Singh, K. D. and Nanda, B. (2017). Application of sloped bottom tuned liquid damper for controlling dynamic response of buildings, *13th International Conference on Vibration Problems*. IIT Guwahati, India.

- Patil, G. R., Singh, K. D. and Nanda, B. (2018). Performance of TLD with different slope profiles utilized to mitigate dynamic response of structure, *11th Structural Engineering Convention*, Jadavpur University, Kolkata, India